

**Some pages of this thesis may have been removed for copyright restrictions.**

If you have discovered material in Aston Research Explorer which is unlawful e.g. breaches copyright, (either yours or that of a third party) or any other law, including but not limited to those relating to patent, trademark, confidentiality, data protection, obscenity, defamation, libel, then please read our [Takedown policy](#) and contact the service immediately ([openaccess@aston.ac.uk](mailto:openaccess@aston.ac.uk))

"COMPUTER ANALYSIS OF LARGE CIVIL ENGINEERING  
STRUCTURES"

KENNETH HUGH MADELEY BRAY

A THESIS SUBMITTED FOR THE DEGREE OF  
DOCTOR OF PHILOSOPHY

DEPARTMENT OF CIVIL ENGINEERING  
THE UNIVERSITY OF ASTON IN BIRMINGHAM

27. June 72 163208.

APRIL 1973

## SUMMARY

The finite element method is now well established among engineers as being an extremely useful tool in the analysis of problems with complicated boundary conditions. One aim of this thesis has been to produce a set of computer algorithms capable of efficiently analysing complex three dimensional structures.

This set of algorithms has been designed to permit much versatility. Provisions such as the use of only those parts of the system which are relevant to a given analysis and the facility to extend the system by the addition of new elements are incorporated. Five element types have been programmed, these are, prismatic members, rectangular plates, triangular plates and curved plates.

The 'in and out of plane' stiffness matrices for a curved plate element are derived using the finite element technique. The performance of this type of element is compared with two other theoretical solutions as well as with a set of independent experimental observations. Additional experimental work was then carried out by the author to further evaluate the acceptability of this element.

Finally the analysis of two large civil engineering structures, the shell of an electrical precipitator and a concrete bridge, are presented to investigate the performance of the algorithms. Comparisons are made between the computer time, core store requirements and the accuracy of the analysis, for the proposed system and those of another program.

### ACKNOWLEDGEMENTS

The author would like to thank his tutor, Professor K. I. Majid, for his help and encouragement during the last four years. His thanks are also due to Dr. D. Just for his advice and availability for discussion. Thanks also go to Mr. Walter Parsons and his team of technicians as well as the staff of both the University Computer Centre and the Atlas Computer Laboratory.

In the preparation of this thesis the author would like to express his appreciation to both Miss Christine Horton and Miss Jenny Baker for typing the manuscript as well as Miss Pat Sage for tracing the diagrams.

Finally the author is indebted to the Science Research Council for their financial support.



## CONTENTS

	Page
SUMMARY	i
ACKNOWLEDGEMENTS	ii
CONTENTS	iii
NOTATION	vii
CHAPTER 1	INTRODUCTION
1.1	The finite element method 1
1.2	The matrix displacement method 5
1.3	Topic covered by this thesis 8
1.4	Storage and solution of the equations forming the stiffness matrix of a structure 10
1.5	Historical review of the finite element method 17
1.6	Scope of work 23
CHAPTER 2	INITIAL CONSIDERATIONS
2.1	Introduction 26
2.2	Storage of the stiffness matrix 26
2.3	Methods of forming the overall stiffness matrix 27
2.4	The composition of the stiffness matrix 28
2.5	The joint data 30
2.6	The subdivision of the stiffness matrix 31
2.7	The generation of the Diagonal Address Sequence 33
CHAPTER 3	THE OVERALL STIFFNESS MATRIX
3.1	Introduction 39
3.2	Tridiagonal co-ordination 39
3.3	The organisation of data 44
3.4	Sub-block positioning 47

3.5	Direct construction of sub-blocks	52
3.6	The computation of the force and stress matrices of an element	61
3.7	Sub-division of the stiffness matrix prior to solution	62
CHAPTER 4	ELEMENT PACKAGES	
4.1	Introduction	65
4.2	Auxiliary subroutines	65
4.2.1	Subroutine Joint Group	65
4.2.2	Subroutine Standardise	68
4.2.3	Subroutine Read Load Vector	68
4.2.4	Subroutine Discomdiv	68
4.2.5	Subroutine Print Deflection Vector	71
4.3	General description of element packages	71
4.4	Rectangular plate package	74
4.4.1	General considerations	74
4.4.2	Rectangular plate forces	76
4.4.3	Rectangular plate stresses	81
4.4.4	Direct evaluation of the $\underline{A}' \underline{k} \underline{A}$ contribution	81
4.5	Triangular plate package	88
4.5.1	General considerations	88
4.5.2	Triangular plate stresses	94
4.5.3	Direct evaluation of the $\underline{A}' \underline{k} \underline{A}$ contribution	94
4.6	Prismatic member package	102
4.6.1	General considerations	102
4.6.2	Member forces	109
4.6.3	Direct evaluation of the $\underline{A}' \underline{k} \underline{A}$ contribution	109

CHAPTER 5	FORMATION OF THE STIFFNESS MATRICES FOR A CURVED PLATE ELEMENT	
5.1	Introduction	119
5.2	The out of plane displacement function	119
5.3	The out of plane stress and strain matrices	127
5.4	The out of plane element stiffness matrix	136
5.5	The in plane displacement function	144
5.6	The in plane stress and strain matrices	146
5.7	The in plane element stiffness matrix	151
5.8	The out of plane displacement transformation matrix	156
5.9	The in plane displacement transformation matrix	159
CHAPTER 6	CURVED PLATE PROGRAMMING	
6.1	Introduction	166
6.2	General Considerations	166
6.3	Curved plate stresses	168
6.4	Direct evaluation of the $\underline{A}' \underline{k} \underline{A}$ contributions	168
CHAPTER 7	COMPUTER TESTS ON THE CURVED PLATE ELEMENT	
7.1	Introduction	179
7.2	Testing the out of plane element stiffness matrix	179
7.3	Testing the in plane element stiffness matrix	184
7.4	Investigation into the effect of mesh refine- ment on the computed deflections	184
7.5	Comparison between theoretical results and previous experimental work	191

CHAPTER 8	EXPERIMENTAL CURVED PLATE TESTS	
8.1	Introduction	198
8.2	Material of the plates	198
8.3	Control tests	199
8.4	Preliminary considerations	199
8.5	Testing the plates	205
8.6	Comparison between experimental and theoretical results	211
CHAPTER 9	THE ANALYSIS OF LARGE STRUCTURES	
9.1	Introduction	219
9.2	The electrical precipitator shell	219
9.3	Analysis of the shell	219
9.4	Results of the shell analysis	223
9.5	Analysis of the road bridge	226
9.6	Results of the bridge analysis	232
CHAPTER 10	GENERAL CONCLUSIONS	234
REFERENCES		249

## NOTATION

$\underline{A}$	Displacement transformation matrix
$\underline{A}_{0,I}$	Out of plane, in plane displacement transformation matrix for a plate
$\underline{A}_f$	Displacement transformation matrix for a frame
$\underline{B}$	Strain matrix
$\underline{D}$	Elasticity matrix
DAS	Diagonal address sequence array
E	Young's modulus of elasticity
$\underline{f}$	General displacement vector for a finite element
$\underline{G}$	Decomposition matrix
GJ	Torsional stiffness of a prismatic member
$I_{r,q,qr}$	Second moment of area about R,Q axes and the product moment of inertia
$\underline{K}$	Overall stiffness matrix
$\underline{K}_{i,i}$	Stiffness matrix for elements connected to joints lying wholly in joint group i
$\underline{K}_{i,i+1}$	Stiffness matrix for elements connected to joints lying in joint group i and i+1
$\underline{L}$	Load matrix
$L_{P,Q,R}$	Direction cosines
$M_{P,Q,R}$	Direction cosines
$\underline{N}$	Identity matrix containing general functions of position within a finite element
$N_{P,Q,R}$	Direction cosines
$\underline{P}$	Vector containing the forces acting at the nodes of a finite element
P,Q,R	Local element axes

$P_{ca,cb}$	Length of the rigid portion at the ends of a prismatic member
$Q_{c,s}$	Offsets in the Q direction for a prismatic member
$R_{c,s}$	Offsets in the R direction for a prismatic member
$R$	Outer radius of a curved plate
$S_{q,r}$	Shear in the Q and R directions for a prismatic member
$T$	Torque
$X,Y,Z$	Global reference axes
$\underline{X}$	Displacement vector
$\underline{Z}$	Nodal displacement vector for a finite element
$\underline{Z}_{0,I}$	Nodal displacement vector for out of plane and in plane plate displacements
$a_1-a_{12}$	Constants of a displacement function
$a$	Rectangular plane dimension in the P direction
$b$	Rectangular plate dimension in the Q direction
$f_{1,2}$	Rectangular plate stresses
$\underline{G}_{i,j}$	Term within the $\underline{G}$ matrix at row i column j
$h,i,j,p,l,m$	Arbitrary joint numbers
$\underline{k}$	Finite element stiffness matrix
$p,q,r,\theta_p,\theta_q,\theta_r$	Local degrees of freedom
$t$	Plate thickness
$x,y,z,\theta_x,\theta_y,\theta_z$	Global degrees of freedom
$\alpha,\beta,\gamma$	Intermediate transformation axes
$\mu$	Poisson's ratio
$\underline{\sigma}_{0,I}$	Out of plane, in plane stress matrix
$\sigma_{x,y} \quad \tau_{xy}$	Stress components
$\underline{\epsilon}$	Strain at a point in a finite element

$\underline{\varepsilon}_0$

Initial strains at a point in a finite element

$\underline{\delta}$

Nodal displacements of a finite element

## CHAPTER 1

### INTRODUCTION

#### (1.1) The finite element method

Conventional engineering structures can be considered to consist of individual structural elements interconnected at a discrete number of nodes. If the force-displacement relationships for the individual elements are known then it is possible to derive the properties and study the behaviour of the complete structure. In an elastic continuum, however, there are an infinite number of interconnecting points, consequently an alternative approach has to be adopted.

The concept of finite elements, suggested by Turner et al.<sup>(1)</sup>, may be used to discretize such a problem in the following manner:

- (i) The continuum is separated by imaginary lines or surfaces into a number of 'finite elements';
- (ii) The elements are assumed to be interconnected at a discrete number of nodal points situated on their boundaries. The displacements of these nodal points will be the unknown parameters;
- (iii) A function is chosen to define uniquely the state of displacement within each 'finite element' in terms of its nodal displacements;
- (iv) The displacement function now defines uniquely the state of strain within an element in terms of the nodal displacements. These strains, together with any initial strains and the elastic properties of the material will define the state of stress throughout the element, and hence, also on its boundaries;
- (v) A system of forces concentrated at the nodes and equilibrating the boundary stresses and any distributed loads is determined, resulting in a stiffness relationship.

This approach introduces two significant approximations. Firstly, since it is difficult to ensure that the chosen displacement function



will satisfy the requirement of displacement continuity between adjacent elements, the compatibility conditions on such lines may be violated. Secondly, by concentrating the equivalent forces at the nodes overall equilibrium conditions are satisfied, however, local violations of equilibrium conditions within each element will usually arise.

The mathematical derivation of the characteristics of a 'finite element' will now be presented.

A typical finite element,  $e$ , is defined by nodes 1, 2, 3, ...  $n$ ., and straight line boundaries. Let the displacements at any point within the element be defined by:

$$\{\underline{f}\} = \underline{N}\{\underline{\delta}\}^e = [N_1 \ N_2 \ N_3 \ \dots \ N_n] \{\delta_1 \ \delta_2 \ \delta_3 \ \dots \ \delta_n\} \quad (1.1)$$

where  $\{\underline{f}\}$  is the displacement vector,  $\underline{N}$  contains general functions of the position and  $\{\underline{\delta}\}^e$  represents a listing of nodal displacements for a particular element.

With displacements known at all points within the element the strains at any point may be determined. These will always result in a relationship which may be written in matrix notation as:

$$\{\underline{\epsilon}\} = \underline{B}\{\underline{\delta}\}^e \quad \dots \quad (1.2)$$

The material within the element boundaries may be subjected to initial strains denoted by  $\{\underline{\epsilon}_0\}$ . The stresses will be caused by the difference between the actual and initial strains. Assuming general elastic behaviour, the relationship between stresses and strains will be linear and of the form

$$\{\underline{\sigma}\} = \underline{D}(\{\underline{\epsilon}\} - \{\underline{\epsilon}_0\}) \quad \dots \quad (1.3)$$

where  $\underline{D}$  is the elasticity matrix containing the appropriate material properties.

If the nodal forces, which are statically equivalent to the boundary stresses and distributed loads on the element, are defined as:

$$\{\underline{P}\}^e = \{P_1 \ P_2 \ P_3 \ \dots \ P_i \ \dots \ P_n\} \quad \dots \quad (1.4)$$

Each of the forces  $\{p_i\}$  must contain the same number of components as the corresponding nodal displacements  $\{\delta_i\}$  and be ordered in the appropriate corresponding directions.

The distributed loads  $\{\underline{p}\}$  are defined as those acting on a unit volume of material within the element with directions corresponding to those of the displacements  $\{\underline{f}\}$  at that point.

It is now essential that the nodal forces are made statically equivalent to the actual boundary stresses and distributed loads. The simplest procedure is to impose a virtual nodal displacement and to equate the external and internal work done by the various forces and stresses during that displacement. Let such a virtual displacement be  $\{\underline{\delta}^*\}^e$  at the nodes. This results by equations (1.1) and (1.2), in the displacements and strains within the element equal to

$$\{\underline{f}^*\} = \underline{N}\{\underline{\delta}^*\}^e \quad \text{and} \quad \{\underline{\epsilon}^*\} = \underline{B}\{\underline{\delta}^*\}^e \quad \dots \quad (1.5)$$

respectively.

The work done by the forces is equal to the sum of the products of the individual force components and corresponding displacements, this can be expressed in matrix form as:

$$(\{\underline{\delta}^*\}^e)^T \cdot \{\underline{P}\}^e \quad \dots \quad (1.6)$$

Similarly, the internal work per unit volume done by the stresses and distributed forces is

$$\{\underline{\epsilon}^*\}^T \{\underline{\sigma}\} - \{\underline{f}^*\}^T \{\underline{p}\} \quad \dots \quad (1.7)$$

or

$$(\{\underline{\delta}^*\}^e)^T (\underline{B}^T \{\underline{\sigma}\} - \underline{N}^T \{\underline{p}\}) \quad \dots \quad (1.8)$$

Equating the external work with the total internal work obtained by integrating over the volume of the element the following expression is obtained:

$$(\{\underline{\delta}^*\}^e)^T \{\underline{P}\}^e = (\{\underline{\delta}^*\}^e)^T \left( \int \underline{B}^T \{\underline{\sigma}\} d(\text{vol}) - \int \underline{N}^T \{\underline{p}\} d(\text{vol}) \right) \quad (1.9)$$

As this relationship is valid for any value of the virtual displacement, the equality of the multipliers must exist. On substitution of equations (1.2) and (1.3) we have, therefore,

$$\{\underline{P}\}^e = \left( \int \underline{B}^T \underline{D} \underline{B} d(\text{vol}) \right) \{\underline{\delta}\}^e - \int \underline{B}^T \underline{D} \{\underline{\epsilon}_0\} d(\text{vol}) - \int \underline{N}^T \{\underline{p}\} d(\text{vol}) \quad (1.10)$$

This relationship is one typical of characteristics of any structural element. In general form it is usually expressed as:

$$\{\underline{f}\} = \underline{k} \{\underline{\delta}\} + \{\underline{P}\}_p + \{\underline{P}\}_{\epsilon_0}$$

The stiffness matrix becomes

$$\underline{k}^e = \int \underline{B}^T \underline{D} \underline{B} d(\text{vol}) \quad \dots \quad (1.11)$$

Nodal forces due to distributed loads are

$$\{\underline{P}\}_p^e = - \int \underline{N}^T \{\underline{p}\} d(\text{vol}) \quad \dots \quad (1.12)$$

and those due to initial strains are

$$\{\underline{P}\}_{\epsilon_0}^e = - \int \underline{B}^T \underline{D} \{\underline{\epsilon}_0\} d(\text{vol}) \quad \dots \quad (1.13)$$

## (1.2) The matrix displacement method

Two types of analysis stem from the finite element idealisation. The matrix force and the matrix displacement method. The force method considers the forces in the structure as unknowns whereas the displacement method solves for displacements. The force method was formerly more attractive to the engineer as less work was involved in its solution, but, special redundant forces have to be selected before the analysis and consequently the process is not as fully automated as the displacement method. The matrix displacement method which is the more applicable of the two to the finite element method will now be described in detail.

Consider, for example, a member element. A set of forces can be found at either node which equilibrate the stress throughout the beam and are related to the nodal displacements by the equation,

$$\underline{P} = \underline{k} \underline{Z} \quad \dots (1.14)$$

where  $\underline{P}$ , the element forces acting at the nodes, is a column vector.

For an assembly of  $n$  elements this will take the form

$$\underline{P} = \{\underline{P}_1, \underline{P}_2, \underline{P}_3 \dots \underline{P}_n\}$$

$\underline{Z}$  is the nodal displacement vector corresponding to the force vector.

Thus:

$$\underline{Z} = \{\underline{Z}_1, \underline{Z}_2, \underline{Z}_3 \dots \underline{Z}_n\}$$

The  $\underline{k}$  matrix is defined as the element stiffness matrix. The presence of a unique stiffness matrix is shown by the presence of slope deflection equations. The matrix will be square and symmetrical due to the theorems of Maxwell and Betti.

These individual stiffnesses are assembled in the following manner. For convenience the displacement matrix of the total structure is defined relative to some arbitrary reference axes,  $X, Y, Z$  and given by the column

vector:-

$$\underline{X} = \{\underline{X}_1, \underline{X}_2 \dots \underline{X}_j \dots \underline{X}_n\}$$

for a structure containing n joints, where  $\underline{X}_j$  is a submatrix of the form:-

$$\underline{X}_j = \{x_j, y_j, z_j, \theta_{xj}, \theta_{yj}, \theta_{zj}\}$$

The six elements of  $\underline{X}_j$  correspond to the possible degrees of freedom, both translational and rotational, at joint j. It is now possible to relate the element displacements to the joint displacements by the equation:-

$$\underline{Z} = \underline{A} \underline{X} \dots (1.15)$$

The  $\underline{A}$  matrix is known as the displacement transformation matrix. Its elements are constants referring to the cosine of the angle between the various element and reference axes. A load vector, equivalent to the joint displacement vector, is defined as:-

$$\underline{L} = \{\underline{L}_1, \underline{L}_2, \underline{L}_3, \dots \underline{L}_j \dots \underline{L}_n\}$$

where, at joint j for instance, the submatrix  $\underline{L}_j$  is a vector of forces and moments taking the form:-

$$\underline{L}_j = \{X_j, Y_j, Z_j, M_{xj}, M_{yj}, M_{zj}\}$$

The principle of virtual work states that, for a structure in equilibrium, the applied virtual work is equal to the internal virtual work, hence:-

$$\underline{X}^T \underline{L} = \underline{Z}^T \underline{P} \dots (1.16)$$

From equations (1.15) and (1.16) it is clear that,

$$\underline{L} = \underline{A}^T \underline{P} \dots (1.17)$$

But from equations (1.14) and (1.15),

$$\underline{P} = \underline{k} \underline{A} \underline{X} \quad \dots (1.18)$$

hence, from equations (1.17) and (1.18)

$$\underline{L} = \underline{A}^T \underline{k} \underline{A} \underline{X} \quad \dots (1.19)$$

Equation (1.19) relates the applied forces of the structure to its displacements and can be rewritten as:-

$$\underline{L} = \underline{K} \underline{X} \quad \dots (1.20)$$

Hence K is the overall stiffness matrix of the structure and,

$$\underline{K} = \underline{A}^T \underline{k} \underline{A} \quad \dots (1.21)$$

This method was derived using the concept of virtual work and it is evident that the basic equations of elasticity are not violated. Strain-displacement, stress-strain, and equilibrium equations within each element are represented by equation (1.14). Although this equation also includes continuity of displacement (and hence strain) for this element, overall compatibility is achieved by the 'uniqueness' of the displacement vector X. Equation (1.17) is, in fact, the overall equilibrium equation for the structure at each joint.

The K matrix is the overall stiffness matrix of a structure as a free body, hence L, the load matrix, constitutes a system of forces, both imposed and reactive, in equilibrium acting on all the joints of the structure. Even if all these forces were known, which would not be true of the reactive forces in the general case, six of the equations (in a three dimensional structure), in equation (1.20) would be linearly dependent. This is overcome by specifying the displacements at the reactions to be zero. Hence the corresponding rows and columns in the K and L matrices disappear and the overall stiffness matrix becomes nonsingular, thus allowing inversion.

It is now possible, if the stiffnesses of the individual elements and

the geometry of the structure are known, to solve the equation:-

$$\underline{X} = \underline{K}^{-1} \underline{L} \quad \dots (1.22)$$

and proceed to find the forces throughout the structure using equation (1.18).

### (1.3) Topics covered by this thesis

The work undertaken by the author may be divided into two parts, firstly that of programming and system development and secondly, the derivation and verification of the in and out of plane element stiffness matrices of an annular segment. Each of these topics is now briefly discussed.

One specific application of computers to structural problems is the analysis of really large three dimensional structures. A considerable amount of sophisticated programming is required to handle the large matrices involved. Consequently there has been a tendency to develop a large number of programs each appropriate to a single problem, rather than one general program capable of handling a variety of problems. One such general program originally written by Jennings and Majid<sup>(2)</sup> to analyse space frames made use of sparse matrix techniques<sup>(3)</sup>. This program was extended by Williamson<sup>(4)</sup> to include rectangular plate elements and then further extended by Craig<sup>(5)</sup> to include triangular elements. Inevitably this piecemeal approach to programming leads to inefficiencies, furthermore recent analyses using this extended program had not provided satisfactory results.

It was therefore decided that part of the work would include the writing and development of a general program with the capability of analysing complex three dimensional structures. Such structures could consist of a variety of elements which would include prismatic members, rectangular, triangular and curved plates. The resulting program should not only be versatile, but also easy to use and update. To achieve this it was necessary

to consider the following objectives:

- (a) The system should be 'open ended' allowing extensions to the system library by the addition of new structural elements;
- (b) Such extensions should be carried out by the addition of new subroutines which would not involve any fundamental changes to the system. The program structure would necessitate the writer of a new element's subroutines only to be familiar with a general element subroutine specification.
- (c) The system should be efficient in the use of computer time as well as the available core and backing stores;
- (d) The system should be flexible, compiling only the subroutines relevant to a given analysis;
- (e) In the interests of practicality the required data should not be cumbersome or confusing.

The element stiffness matrices of prismatic members and rectangular and triangular plates are well documented<sup>(2,6,5)</sup>. One type of element which would be useful and which cannot easily be simulated by other element types is a curved or annular element. An example of the use of such an element is the analysis of elevated roadways which require curved structures at complex interchanges. The increased flexibility of the longer outer edge of such an element gives rise to stress and deflection characteristics which are very different from those obtained with right bridge decks. Despite the popularity of this type of structure comparatively little research work appears to have been done in this field, the most notable exception being that by Coull and Das<sup>(7)</sup>.

In their paper Coull and Das present an 'exact' solution for the analysis of isotropic curved bridge decks subjected to concentrated loads. The deflected form is expressed as a Fourier series in the spanwise direction, the coefficients being functions of the radial direction only. The loads are expressed as a corresponding series, thereby allowing the incorporation of the concentrated loads as a discontinuity in the shear force along the



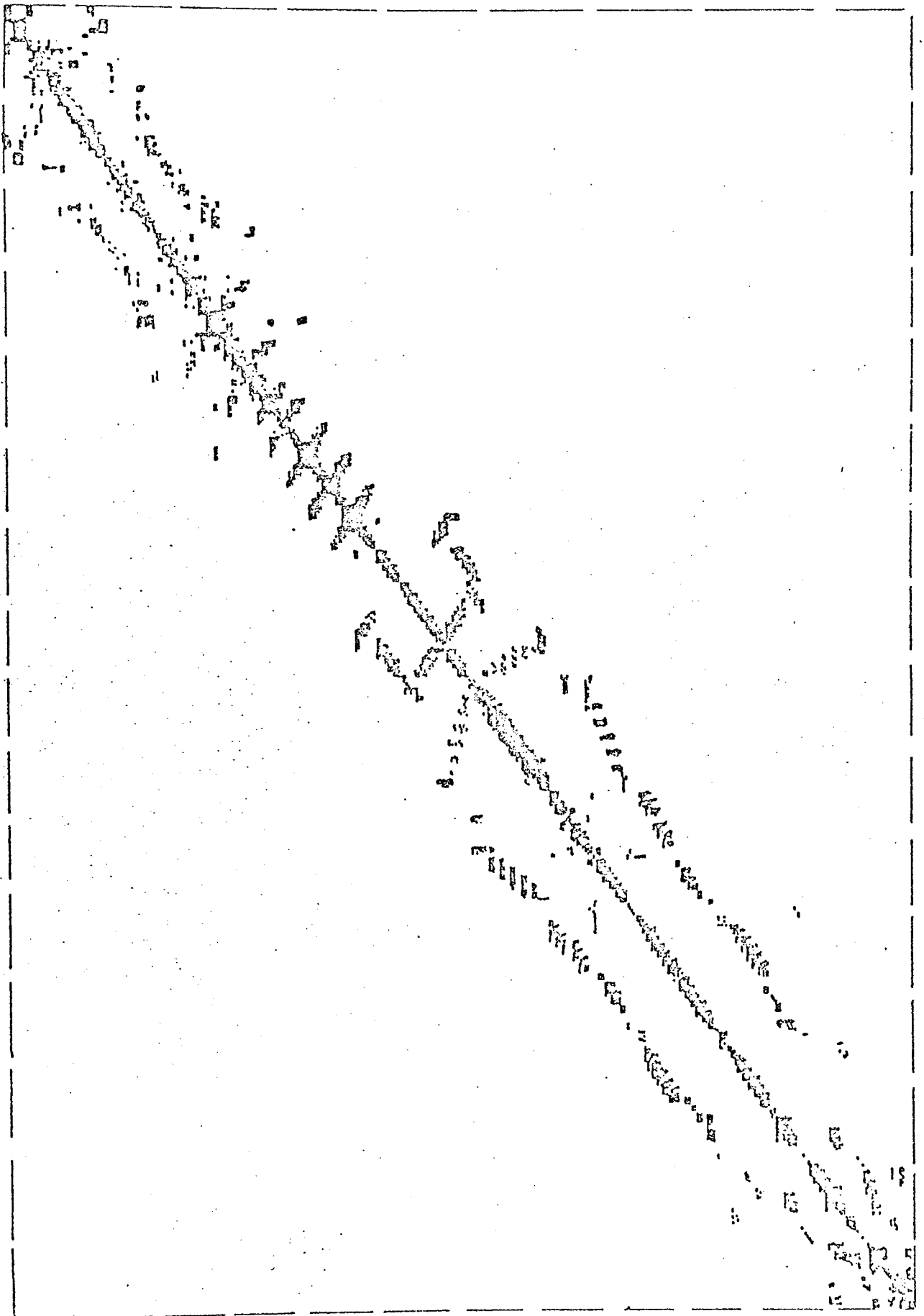
load line. Tests are conducted on two models in order that a comparison can be made between theoretical and experimental values of deflection and moment. This comparison indicates that although the solution has been expressed in the form of an infinite Fourier series, convergence is rapid and three terms are adequate to give accurate results. This form of solution has an advantage over purely numerical solutions, using a grid analogy or finite element techniques, in that the computational difficulties do not multiply as the number of terms is increased to achieve better accuracy. It does not, however, have the flexibility of the numerical solutions. The requirement that the curved bridge deck is radially supported without provision for such items as edge stiffening means that the type of structure analysed by Coull and Das would be used only infrequently. Their paper, therefore, presents work which may be used as a yardstick to test the accuracy of such numerical approaches as the grillage or finite element methods. In such schemes the continuous slab is replaced by a series of elements connected at a discrete number of nodes.

It was therefore decided that the author should derive element stiffness matrices for an annular segment by employing the finite element approach. Furthermore the element should be included into the program system and be compared with experimental results obtained both by the author and by Coull and Das<sup>(7)</sup>.

#### (1.4) Storage and solution of the equations forming the stiffness matrix of a structure

The methods of storage and solution of the overall stiffness matrix adopted by the author are both due to Jennings and Tuff<sup>(8)</sup>. Comprehensive details will, however, be given in this chapter as frequent reference to both techniques is made throughout this thesis.

The non-zero terms of the stiffness matrix of a large structure are shown in figure 1.1. Clearly a method of storage which takes into account



THE NON ZERO ELEMENTS OF THE STIFFNESS MATRIX OF A LARGE STRUCTURE

FIGURE 1.1

such properties as the sparseness and symmetry of the non zero terms is essential. The scheme adopted is one which stores for each row all the terms from the first non zero element up to the leading diagonal. The reasons for selecting this method are given in Chapter 2. At this stage it is relevant only to give a description of the technique.

This method of storage is admissible because when a direct elimination technique is used to solve the equations then zero elements before the first non-zero element on a row will always remain zero. This is provided that there is no row or column interchange. A storage scheme therefore need only retain elements between the first non-zero and the diagonal element of each row. Figure 1.2 shows an enlarged part of the stiffness matrix given in figure 1.1. Here it can be seen that this technique will usually involve the storage of some zero elements; this is acceptable as the efficiency of the solution is dependent upon the layout as well as the amount of store used.

Each of the rows is stored consecutively in a unidimensional array, an address sequence is used to locate the position of the diagonal elements within the array. An example of this is now given:

$$\begin{bmatrix} 1.5 & & & & & & & & & & & \\ 0.2 & 1.2 & & & & & & & & & & \\ -1.1 & 0.0 & 2.2 & & & & & & & & & \\ 0.0 & 0.0 & 5.1 & 10.6 & & & & & & & & \\ 0.0 & 0.0 & 0.0 & 0.0 & 2.6 & & & & & & & \\ 0.0 & 0.0 & -1.2 & 0.0 & 0.0 & 6.1 & & & & & & \end{bmatrix} \quad \text{SYMMETRIC}$$

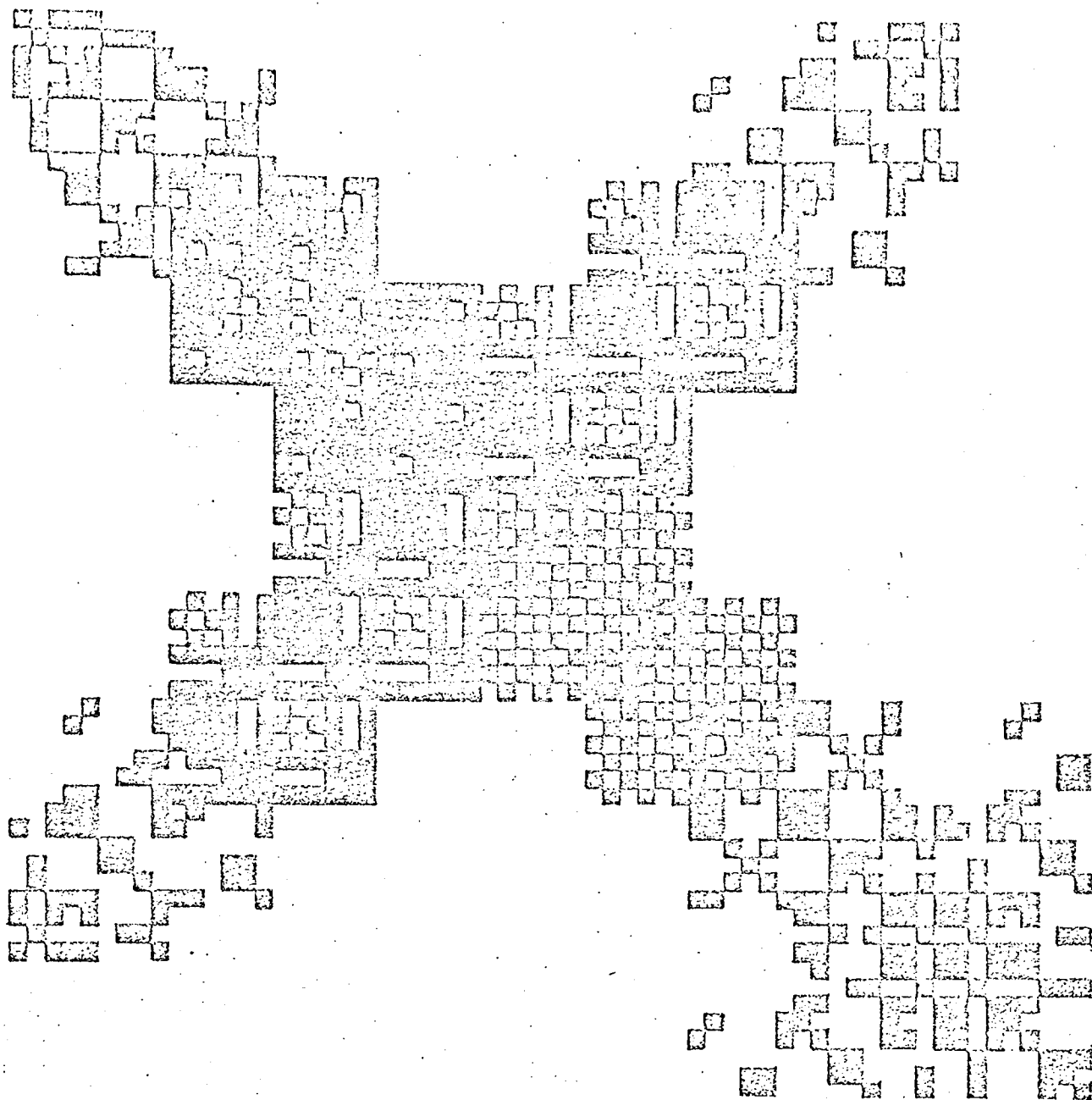
This matrix would be stored in the computer as:

(a) The main sequence

1.5 0.2 1.2 -1.1 0.0 2.2 5.1 10.6 2.6 -1.2 0.0 0.0 6.1

(b) The diagonal address sequence (DAS)

1 3 6 8 9 13



AN ENLARGED PORTION OF THE STIFFNESS MATRIX GIVEN IN FIGURE 1.1

FIGURE 1.2

Here it can be seen that the third element in the address sequence stores 6 and the sixth element of the main sequence stores the diagonal element of the third row, namely 2.2. Generally if the diagonal address sequence is stored in array DAS, then element  $(i,j)$  is stored in the main sequence at location  $DAS(i) - i + j$ .

The application of this technique to matrices such as the one shown in figure 1.1 results in significant savings of store. The sheer size of these matrices, however, still precludes their complete storage in core at one time. It is therefore essential that the matrix is split up and use is made of backing store facilities. This can be achieved by putting an integral number of consecutive rows into a unit such that any two units may be contained within the available core store at the same time. The diagonal address sequence is used to obtain the maximum number of rows that can fit into each unit. Simply the largest  $DAS(i)$  which is less than half the available core store will define the number of rows which may be put into the first unit.

A very wide range of numerical methods exist for the solution of linear simultaneous equations, both direct and indirect methods are available. In general the direct methods are preferred for structural analysis since the programming of these is simpler and they are more easily adapted for the simultaneous analysis of a number of loading systems. The two principal direct methods are Gaussian elimination and the Choleski triangular factorisation. When these schemes are to be used with backing store facilities then the form of elimination best suited is the Choleski triangular factorisation. This is because it requires no other storage facilities than that available for the left hand side coefficients. Jennings and Tuff<sup>(8)</sup> present details of how the Cholesky method may be used in conjunction with the units of the stiffness matrix mentioned previously. Details of this scheme are now presented.

The set of simultaneous equations in matrix form are:

$$\underline{K} \underline{X} = \underline{L} \quad \dots (1.23)$$

Any positive definite matrix has a unique decomposition of the form

$$\underline{K} = \underline{G} \underline{G}^T \quad \dots (1.24)$$

where  $\underline{G}$  is the lower triangle matrix with positive diagonal elements.

Substitution of equation (1.24) into equation (1.23) yields

$$\underline{G} \underline{G}^T \underline{X} = \underline{L} \quad \dots (1.25)$$

$$\text{if } \underline{G} \underline{Y} = \underline{L} \quad \dots (1.26)$$

Then  $\underline{Y}$  may be obtained from equation (1.26) after which the back substitution process can be carried out on the equation

$$\underline{G}^T \underline{X} = \underline{Y} \quad \dots (1.27)$$

The elements of the  $\underline{G}$  matrix may be formed from the  $\underline{K}$  matrix in the following manner

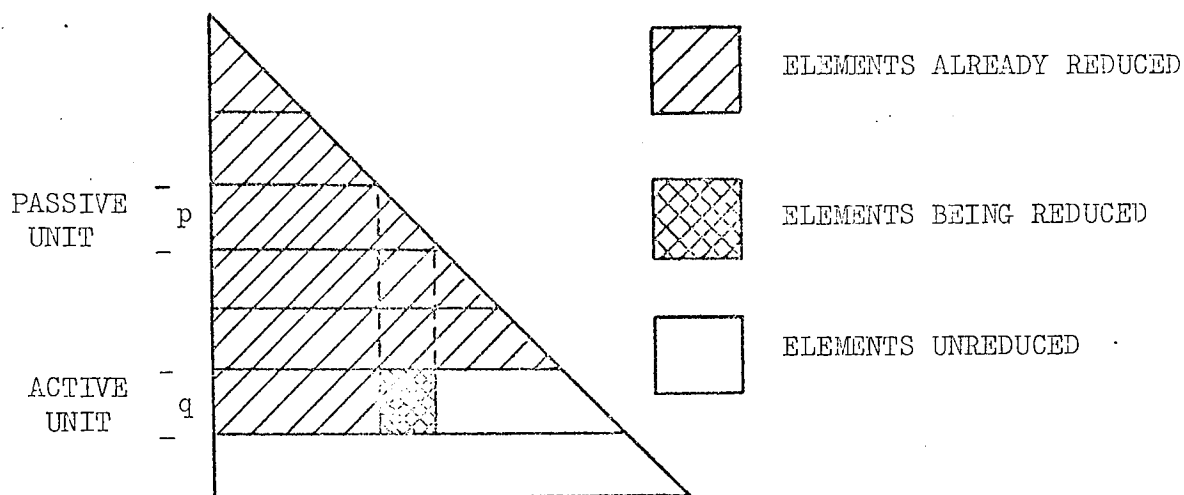
(1) for on diagonal elements ( $i=j$ )

$$g_{ii} = \sqrt{\left( K_{ii} - \sum_{l=1}^{l=j-1} g_{il}^2 \right)} \quad \dots (1.28)$$

(2) for lower triangle off diagonal elements ( $j < i$ )

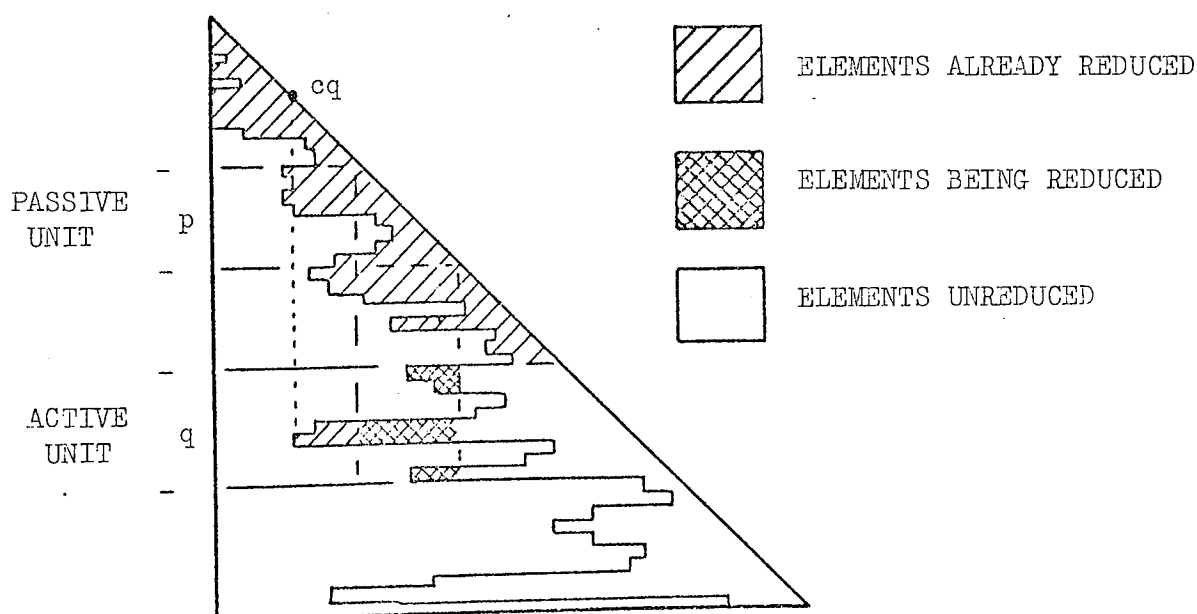
$$g_{ij} = \left( K_{ij} - \sum_{l=1}^{l=j-1} g_{il} \cdot g_{jl} \right) / g_{jj} \quad \dots (1.29)$$

It can be seen from equations (1.28) and (1.29) that to form any coefficient  $g_{ij}$  only rows  $i$  and  $j$  of the main sequence need to be in the core store. The unit which contains row  $i$  is known as the active unit and that which contains row  $j$  as the passive unit. When the active and passive units indicated in figure 1.3 are in the core store then the reduction



THE TERMS COMPRISING THE LOWER TRIANGLE OF A FULLY POPULATED MATRIX

FIGURE 1.3



THE NON ZERO TERMS COMPRISING THE LOWER TRIANGLE OF A MATRIX

FIGURE 1.4

process will progress in the manner indicated in the figure. It may also be seen from the figure that the determination of the coefficients  $g_{ij}$  within an active unit, require the previous determination of the coefficients of  $G$  within the passive unit, as well as the area of the active unit preceding the area of coefficients to be determined. The procedure may be expressed in a general manner as follows. If unit  $q$  is the active unit, all previous units having been reduced, then to perform the reductions for a dense matrix it would be necessary to call in passive units in turn from 1 to  $q-1$ . The final operation is one in which the active and passive unit can be considered to coincide.

When the storage scheme discussed previously is adopted it is not necessary to call in all the preceding passive units if the area of reduction lies entirely to the left of the stored unit. The method of determination of the first passive unit required by an active unit is to inspect the column corresponding to the first stored element in each of the rows comprising the active unit. The selection of the least of these, this corresponds to  $cq$  in figure 1.4, yields the first passive unit to be used. This is illustrated in figure 1.4 where all the elements in active segment  $q$  which may be reduced using passive segment  $p$  are indicated.

#### (1.5) Historical review of the finite element method

Since its formulation less than two decades ago the finite element method, in conjunction with the matrix displacement method, has emerged as a powerful tool available to the engineer for the analysis of complex structures.

Livesley<sup>(9,10)</sup> was one of the first to adapt the matrix displacement method for the computational analysis of bare frameworks. At about the same time, 1954, Argyris<sup>(11)</sup> comprehensively formulated the matrix force and displacement method. He showed that each method stemmed from either the concepts of virtual work or complementary virtual work. He also



derived a stiffness matrix for a rectangular plate element for 'in plane' action. This was done by assuming linear distribution of displacements in the plate and imposing unit displacements at each corner. The unit displacement theorem states that:

$$P_L = \int e_L^T s \, dv$$

where  $P_L$  is the appropriate force corresponding to the displacement. Thus by adding the stiffnesses for each imposed deflection it was possible to build up an eight by eight stiffness matrix for the plate. This method is analogous to that of using a displacement function.

Two years later Turner et al<sup>(1)</sup> laid the foundations of the finite element technique by deriving stiffness matrices for various spar, rib and cover plate elements. An 'in plane' stiffness matrix was derived for a triangular element by assuming a constant strain pattern over the element. They showed that this assumption led to a linear distribution of displacement in the element. To equilibriate the nodal forces to the stresses, the basic patterns that could be expected were considered and the forces were obtained by direct equilibrium.

Clough<sup>(12)</sup> extended the idea of assumed stress and corresponding node displacement patterns to derive stiffness matrices for both rectangular and triangular elements.

The finite element method was next extended to cover out of plane or bending action. Previously, for in plane stiffnesses, two translational degrees of freedom had been considered for each node. Melosh<sup>(13)</sup> derived a stiffness matrix for the bending of a rectangular plate <sup>Joint</sup> having one translational and two rotational degrees of freedom. The translational displacement  $w$ , perpendicular to the plane of the plate, was taken to vary as a cubic polynomial over the length. For the  $P$  direction

$$w = A_3 p^3 + A_2 p^2 + A_1 p + A_0$$

The constants  $A_0 - A_3$  can be evaluated by making this function equal to the nodal deflections and rotations at each corner. The strain energy for the plate can be calculated by differentiating the polynomial and integrating the resulting terms over the appropriate area.

By this time definite methods of derivation of the stiffness matrix were being formulated and these were reviewed by Gallagher<sup>(14)</sup> to be:-

- (i) Inversion of a flexibility matrix<sup>(15)</sup>;
- (ii) Direct formulation<sup>(1)</sup>;
- (iii) From virtual work or the unit displacement theorem<sup>(11)</sup>.

Although the inter-relation of some derivations was noticed and, in fact, gave the same results for stiffnesses of particular elements, the actual implications of the basic assumptions were not appreciated.

The majority of elements formed by one or other of these methods were known to converge to a satisfactory result as their subdivision was refined, but the extent of the accuracy that could be expected was not yet defined. Melosh<sup>(16)</sup> was the first to tackle this problem. Errors could be classified as those involved in the structural idealization, the computation, or the finite element itself. In the investigation of the finite element errors he showed that solutions obtained using extremum variational theorems of elasticity could be bounded between upper and lower limits. Using a displacement function he showed the approximation to be minimizing the potential energy of the system and hence forming a lower bound. He concluded that, as long as the structural idealization was not redefined on subdivision, monotonic convergence would exist although not necessarily to the correct solution. He stated that the displacement function must satisfy the following requirements if such convergence was to be achieved.

- (i) Strains must be continuous over the element
- (ii) Inter-element displacement continuity must exist

(iii) Functions must be expressible in such a form that the linear elasticity condition is satisfied

(iv) They should exhibit monotonic convergence

(v) Rigid body movements should not cause straining.

Irons<sup>(17)</sup> relaxes Melosh's requirements for convergence and accuracy by proposing that, for elements in bending,

(i) They must be able to exhibit all rigid body movements

(ii) They must have a continuous displacement within and across interfaces in deflection and slope

(iii) They must be able to represent constant stress.

The last proposal, an additional one to those proposed by Melosh, can be substantiated by the fact that an infinite subdivision implies constant stresses in the limit.

Fraeijs de Veubeke<sup>(15,18)</sup> proved upper and lower limits to exist for equilibrium and displacement models but, while agreeing with Melosh's requirements, thought that different element patterns might cause convergence to an erroneous answer. He also pointed out the difficulty in forming a stiffness matrix from an equilibrium model (i.e. by inverting a flexibility matrix) which will include all possible rigid body deformations.

Zienkiewicz<sup>(19)</sup> formulated a stiffness matrix for out of plane bending in a rectangular element. He assumed the vertical displacement  $w$  to vary throughout the element as the polynomial:

$$w = A_1 + A_2 p + A_3 q + A_4 p^2 + A_5 pq + A_6 q^2 + A_7 p^3 + A_8 p^2 q + A_9 pq^2 + A_{10} q^3 + A_{11} p^3 q + A_{12} pq^3$$

The twelve constants  $A_1$ - $A_{12}$  which correspond to the rigid body movements can be evaluated in a similar manner to that employed by Melosh. Along the edge where  $p$  or  $q$  is a constant the deflection will vary as a cubic. The slopes will vary as a quadratic. It can be seen that both the matrices of Melosh<sup>(13)</sup> and Zienkiewicz will conform for vertical displacements but not slope along their interfaces. In spite of this, both matrices provide good

results.

The finite element method developed along these lines until the mid sixties when the concept of isoparametric elements was introduced by Irons<sup>(20)</sup>. In his paper Irons puts forward the idea that instead of using many simple elements it would be better to use a few complicated ones. Such an element would not have an explicit stiffness matrix, instead the stiffness matrix of each of a set of elements would be obtained by numerical integration of a general displacement function. Irons states that the pioneer work was done by Taig and is presented in an unpublished report<sup>(21)</sup>. Taig's quadrilateral elements were the first powerful series of elements whose higher members have curved edges about which certain convergence theorems may be derived.

Irons presented a comprehensive paper<sup>(22)</sup> in 1966 where he argued the case for numerical integration applied to finite element techniques. In that paper he suggests that engineers are restricting themselves to trivial problems by using analytical integration. Consequently, he suggests, finite element techniques will only begin to reveal their full potential when research workers are freed from the time consuming effort of deducing new matrices afresh for each new problem. His exposition takes the form of a series of examples comprising plane elements with curved edges, solid elements with curved edges and faces, and linear elements with orthogonal displacement functions. These are described with applications to plane stress, torsion and solid elasticity.

The isoparametric concept developed rapidly and in 1968 Irons and Zienkiewicz presented a paper<sup>(23)</sup> on this topic. Their group concentrated on improvement of element characteristics and automation of input. The characteristics of isoparametric elements are inherently superior to those of simple finite elements. This is because, as has been frequently demonstrated, for a given total number of degrees of freedom in a structure the accuracy is increased for larger elements which have a greater number of

degrees of freedom. Large simple elements, however, will not always follow the boundaries of the structure, a problem which may be overcome by the use of suitable isoparametric elements.

Irons and Zienkiewicz summarise the necessary steps for the formulation of an isoparametric element in the following way. The most important being the definition of a 'parent' element with an appropriate displacement function. This function describes the variations of the unknowns within the element in terms of the appropriate nodal values. Once such a function has been determined the calculation of the element stiffness matrix follows standard rules. There are two conditions which the displacement function has to satisfy, namely:

- (i) Compatibility of the unknowns across inter-element boundaries;
- (ii) The constant strain criterion requiring the displacement function to be such that constant states of strain can be exactly reproduced.

Once such a 'parent' element has been defined then the stiffness matrix of its curvilinear derivative may be determined. Each derivative originates from a different type of parent element. If the displacement functions are based on the parent element definition then not only will the compatibility of displacements be satisfied on element interfaces but an original fit of these surfaces will be ensured. Similarly if constant strain conditions were obeyed by the original parent functions this will be preserved in the distorted elements.

The integration of the element properties is carried out numerically using a number of Gauss points in each co-ordinate direction. Integration is simplified as at the boundaries constant values of the curvilinear co-ordinates occur. Irons and Zienkiewicz found that three to five Gauss point divisions were adequate in most cases.

The finite element method has therefore split into two main areas, isoparametric, and explicit derivation of the stiffness matrix. Although there is overlap in as much as isoparametric elements can do, at the price of

computer time, all the element types that explicit derivation is capable of, there are many applications in civil engineering for which one or the other is better suited. It is probable, however, that in the future isoparametric elements will receive more attention as their potential has yet to be fully exploited.

#### (1.6) Scope of work

An outline of the topics covered in this thesis has already been given in section 1.3 of the current chapter. The way in which this work was carried out is now discussed.

A large part of the thesis is devoted to details of the computer system, the objectives of which have been stated in section 1.3. The attainment of these objectives necessitated the development of the system from its earliest stages. A prerequisite of designing such a system is the selection of the most suitable techniques for the formation, storage and inversion of the overall stiffness matrix. These initial considerations, some of which have been discussed in section 1.4 are further dealt with in Chapter Two.

The composition of the overall stiffness matrix of a structure is investigated in some detail in Chapter Three. In this chapter the positioning of the sets of terms contributed by a finite element to the stiffness matrix is discussed. The storage of these terms using the technique selected as the most suitable is also detailed. The program has to be capable of analysing large structures, consequently the whole stiffness matrix would often be too big to be constructed at once. The way in which the contributions of sets of terms of some finite elements appear in different constructional units of the stiffness matrix is also discussed in Chapter Three. Once the stiffness matrix is constructed the next step is the solution of these equations. This must be done in a piecemeal manner, the way in which the matrix is subdivided for this is also detailed in Chapter Three.

Chapter Four describes how each of the finite elements immediately

available to the author has been programmed for the system. Such elements comprise rectangular plates, triangular plates and prismatic members. There is some programming which is independent of the element type, the subroutines comprising this set are known as auxiliary subroutines and are also detailed in Chapter Four.

The theory for the author's own element, a plate circularly curved in plan, follows in Chapter Five. Here both in and out of plane action is considered and an explicit element stiffness matrix is derived for each case. The necessary displacement transformation matrices are also derived at this stage. This type of explicit derivation was used in preference to an isoparametric approach. It is the author's opinion that where feasible an ordinary finite element should be used in preference to an isoparametric one. This is because there is significantly less computation required to evaluate the stiffness matrix of a simple element. There is no clear dividing line, however, at which one can say that a 'once and for all' explicit integration should be carried out. In the author's retrospective opinion the curved plate is probably the most complicated element which should be attempted by this explicit method. The fact that the other elements adopted for the system also relied on this explicit approach is not significant. The system is capable of analysing structures which have been subdivided into both isoparametric and explicit elements.

Once the theoretical work had been completed it could then be programmed to form an element package for the system. The method in which this was done is presented in Chapter Six.

The programming of the curved plate theoretical work was a complicated step. It was therefore important to ensure that the program was working free of all error before any investigations into the usefulness of the element could be conducted. This is done in Chapter Seven where, once the program has been rigorously checked, an investigation is made into the effect of mesh refinement. In addition a comparison is made between previous

experimental work and a theoretical series solution for this type of element.

A description of the author's experimental work follows in Chapter Eight. Here the author's tests are described in detail. A comparison is made between the experimental results and the theoretical results obtained by using the theory and programming developed in earlier chapters.

Chapter Nine contains descriptions of the application of the system to analyse two large structures, an electrical precipitator shell and a skew road bridge formed by two concrete box sections. In each case the results obtained have been compared with analyses carried out by other methods. Comparisons are also made between the amount of computer time and store required by these other methods and that used by the author's system.



## CHAPTER 2

### INITIAL CONSIDERATIONS

#### (2.1) Introduction

Recently the matrix displacement method has become a powerful tool for the practising engineer. The basis of this method is the formation and inversion of the overall stiffness matrix of a complete structure. Such a matrix has several intrinsic properties, it is square, symmetrical and sparse, often with the non-zero elements grouped around the leading diagonal. These properties influence the method of construction as well as the method of storage.

The size of the stiffness matrix prohibits its construction in one stage, consequently a piecemeal approach has to be adopted. This necessitates the subdivision of the overall stiffness matrix into discrete parts and the subsequent construction of these parts. In order that the stiffness contributions may be correctly positioned within the matrix it is necessary to form a skeletal representation of the matrix. Such a representation is based upon the unsuppressed degrees of freedom of the joints comprising the structure and the interconnectivity of these joints.

#### (2.2) Storage of the stiffness matrix

A sparse storage scheme <sup>(3)</sup> is especially applicable when the non-zero elements are randomly distributed. In the case of a matrix which is to be constructed directly, and with the properties listed previously, a more suitable method of storage would be a band matrix technique <sup>(24)</sup>.

Since it is difficult to maintain a constant band width except in the case of regular structures, such as multi-storey frames, the use of a fixed band width method results in a large

number of zero elements being wastefully stored. An improvement on the fixed band width approach is to use a variable band width scheme. In this method, storage for each row commences with the first non-zero element and continues up to, and includes, the leading diagonal element. Easy access to any element is facilitated by storing the address location of the leading diagonal element. Details of this scheme are given in reference (8) and summarized in Chapter 1. It is, therefore, sufficient to mention that each row of the lower triangle is stored sequentially within a unidimensional array. The efficiency of the scheme can be further improved by grouping the non-zero elements around the leading diagonal. Such a grouping is achieved by employing a technique similar to tridiagonalisation, where nodes in any group (i) are connected to each other, or to those in groups (i - 1) or (i + 1).

### (2.3) Methods of forming the overall stiffness matrix

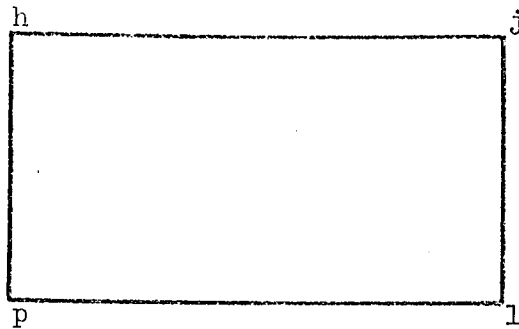
The overall stiffness matrix of a structure can be constructed by several methods. Advocates of the isoparametric, numerical integration, techniques construct the stiffness matrix directly by considering each structural element in turn. This method is extremely flexible since the actual stiffness matrix of an element is never expressed explicitly. A disadvantage, however, is that in order to construct the stiffness matrix the process of numerical integration has to be repeated for each element, naturally this increases the computation time.

Conversely, it is both possible, and efficient, to express the contribution of a structural element to the stiffness matrix explicitly, and then construct this matrix either by considering each joint, or each structural element. The nodal approach has the advantage that an entire row of the stiffness matrix, or several rows corresponding to a given joint, may be constructed in

isolation. Once this has been done the results may be sent to a backing store, thus releasing the locations in the core store for the contributions of the next joint. One drawback of this method is that the data associated with each joint has to be preserved for inspection until the last joint has been dealt with. In the proposed system the overall stiffness matrix for each structural element is constructed directly into the overall stiffness matrix for the whole structure. This offers greater flexibility when new structural elements are introduced. Furthermore the contributions to the stiffness matrix by an element, as well as the force and stress matrices of that element, may be evaluated sequentially since much the same information is required in each case.

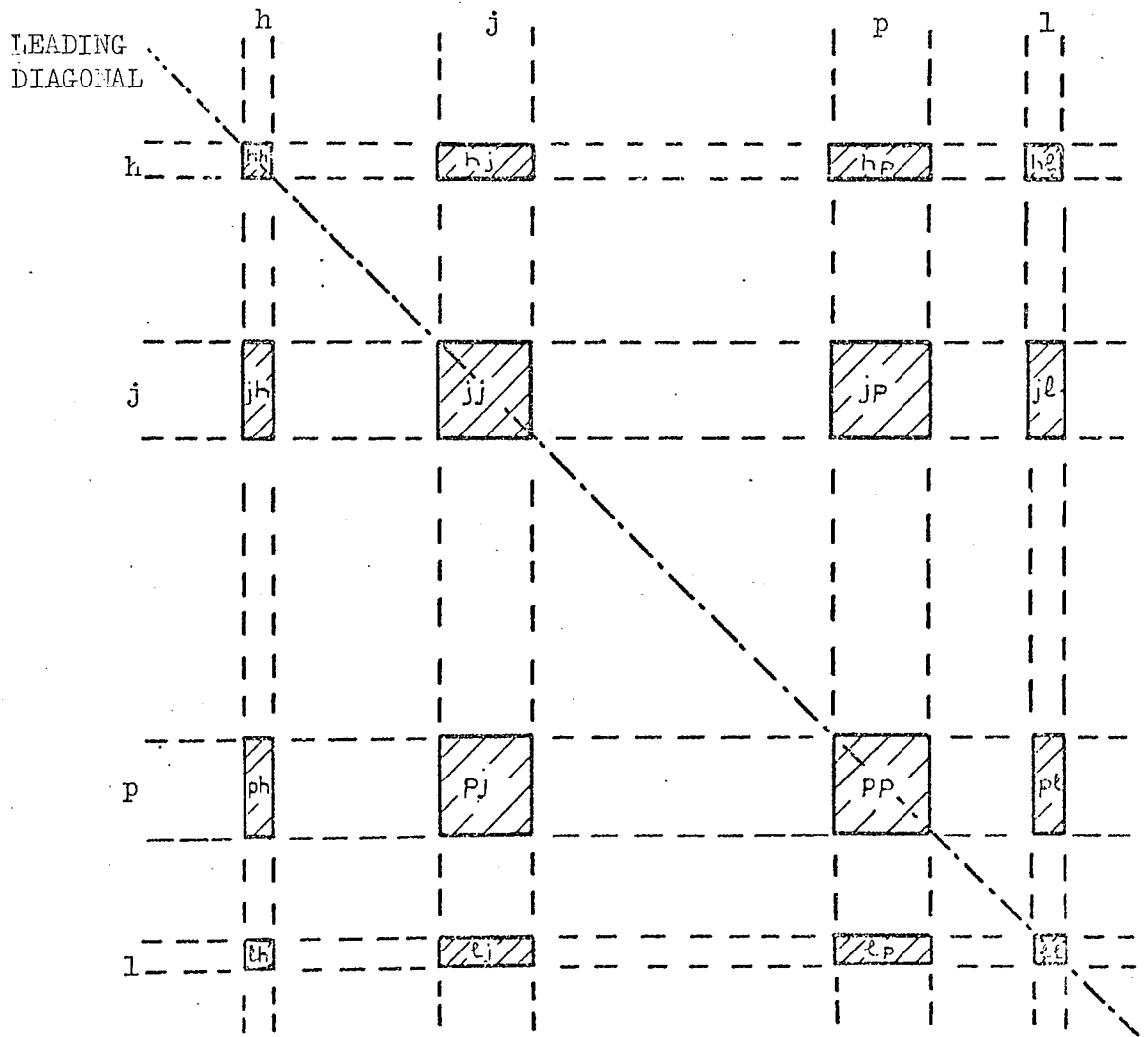
#### (2.4) The composition of the stiffness matrix

As mentioned previously, the stiffness matrix is formed by evaluating in turn the contributions due to each finite element forming the structure. The number and position of each element's contribution is dependent on the number of joints which connect it to the structure, and the arbitrary numbers assigned to those joints. Figure 2.1 illustrates this by showing the sets of terms contributed to the stiffness matrix by a plate, connected by four joints  $h, j, p, l$ . Each joint will contribute as many rows and columns as it has unsuppressed degrees of freedom. The intersection of such rows and columns gives the location of the contributions which are shown shaded in figure 2.1b, and will be referred to as sub-blocks. It is noticed that the four noded rectangle of figure 2.1a, contributes sixteen sub-blocks to the stiffness matrix shown in figure 2.1b. Clearly the number of sub-blocks contributed by an element with  $n$  joints will be  $n^2$ . The number of terms comprising a given sub-block is dependant upon the unsuppressed degrees of freedom of the two joints



ARBITRARY NUMBERS REPRESENTED BY  $h, j, p, l$  ARE GIVEN TO EACH JOINT OF THE STRUCTURAL ELEMENT

FIGURE 2.1a



IN THIS EXAMPLE  $h < j < p < l$  NUMERICALLY.

THE SIXTEEN SUB-BLOCKS FORMED BY THE FOUR JOINTS OF A RECTANGULAR PLATE

FIGURE 2.1b

FIGURE 2.1

forming that sub-block. Consequently if these joints each have six unsupressed degrees of freedom the maximum number of terms will be thirty six. For instance if joint p (see figure 2.1) has five degrees of freedom, and h has three, then the sub-blocks hp and ph will each comprise fifteen terms. Sub-blocks occurring on the leading diagonal will be square as each is associated with a single joint. Finally, since a joint <sup>may</sup> ~~will~~ often connect more than one element to the structure, the eventual value of any sub-block will be the summation of several contributions.

#### (2.5) The joint data

Certain items of information are independant of the types of finite elements comprising the structure. Every joint, for instance, requires seven facts to be stored. These are, the reference number of the joint, the three joint co-ordinates, a code number indicating which of the six possible degrees of freedom of the joint have not been supressed, the LJ value, (this is the joint with the lowest reference number which is directly connected to the joint in question), and the total number of degrees of freedom for that joint. All except the last of these items are input data.

The six degrees of freedom  $X, Y, Z, \theta_x, \theta_y, \theta_z$  are represented by a six figure integer. Each digit is either a one, for an existing degree of freedom, or a zero for a supressed degree of freedom. Thus a joint in a space frame will be represented by the integer 111111. If this joint were to be restrained in the Y direction, for example, then the integer representation becomes 101111. In this manner any type of boundary condition may be specified. This representation is referred to as 'the degrees of freedom of a joint in expanded form'. Frequently it is necessary to add the degrees of freedom for several joints. In order to expedite this operation the unsupressed degrees of freedom of each joint are summated and stored. For instance 101111

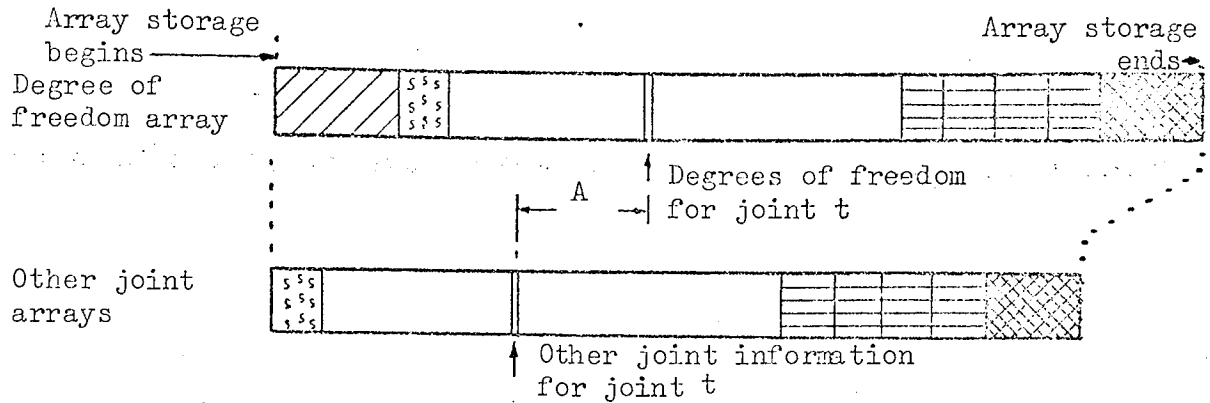
is stored as 5. This representation of the degrees of freedom is known as 'the summated value'.

For reasons given in the following text not all joints will have the same amount of information stored. For instance, when considering joint group (i), the joints lying in group (i - 1) but connected to joints in group (i), will have only their degrees of freedom stored. Consequently the arrays storing the degrees of freedom will be out of step with those storing the rest of the joint data and it will be necessary to calculate this discrepancy. The items of data relating to joints in group (i + 1) but not required at this stage are also stored in these arrays and will be needed when constructing the stiffness matrix of group (i + 1). It is thus necessary to move such data items from the end to the beginning of their arrays. After which the rest of the joint information relating to the group is input. Since this follows sequentially only discarded data is overwritten. This is illustrated in figure 2.2 where it is shown that after considering joint group (i), all the data for joints in group (i + 1) which are connected to group (i) as well as the degrees of freedom of joints in group (i) connected to group (i + 1) are moved to the beginning of the relevant arrays.

#### (2.6) The subdivision of the stiffness matrix

One of the most limiting factors in computing is the amount of core storage available. The stiffness matrix of a small structure, even when stored in one of the economical manners described earlier, is of significant size. Clearly, if the complete stiffness matrix cannot be kept in the core during its formation then it must be formed in a piecemeal manner. This necessitates the division of the structure into joint groups. An example of this is shown in

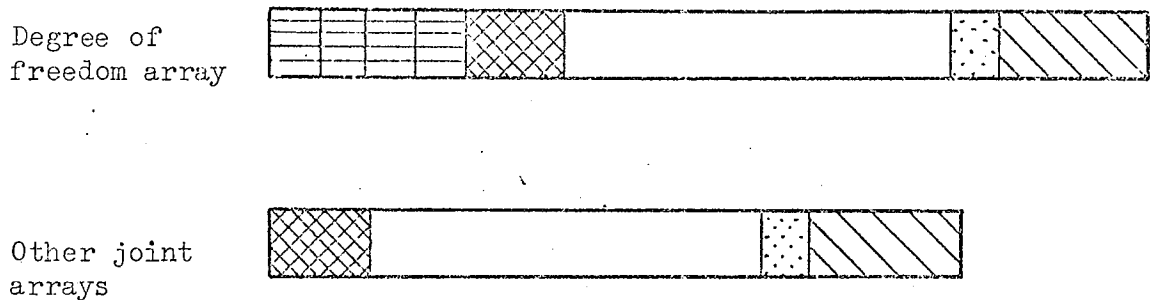
# JOINT ARRAYS FOR GROUP(i)



'A' is the offset between the two array schemes

t is an arbitrary joint in joint group i

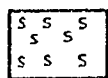
# JOINT ARRAYS FOR GROUP(i+1)



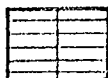
JOINTS WHOLLY WITHIN THE RELEVANT GROUP



JOINTS IN GROUP(i-1) AND CONNECTED TO GROUP(i)



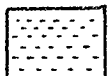
JOINTS IN GROUP(i) AND CONNECTED TO GROUP(i-1)



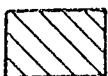
JOINTS IN GROUP(i) AND CONNECTED TO GROUP(i+1)



JOINTS IN GROUP(i+1) AND CONNECTED TO GROUP(i)



JOINTS IN GROUP(i+1) AND CONNECTED TO GROUP(i+2)



JOINTS IN GROUP(i+2) AND CONNECTED TO GROUP(i+1)

FIGURE 2.2

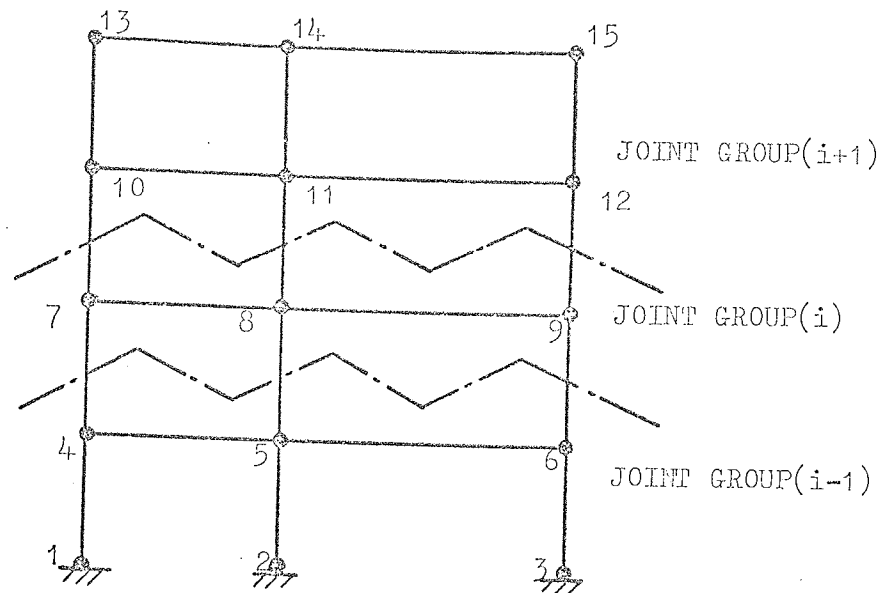
figure 2.3, for a plane frame comprising fifteen joints which are split up into three joint groups. In this structure the joints in a given group ( $i$ ) are only connected by structural elements to joints in the previous group ( $i - 1$ ), and joints in the next group ( $i + 1$ ). The stiffness matrix (figure 2.4) will then be tridiagonal. This tridiagonalisation scheme has two main advantages. Firstly the resulting grouping around the leading diagonal reduces the number of zero elements requiring storage. This is particularly the case when the variable band width scheme is adopted for the storage of the stiffness matrix. Secondly, only that information specifically required for constructing the stiffness matrix of a given joint group need be held in the core store.

The information required for this purpose when considering any joint group ( $i$ ), may thus be explicitly expressed by three sets of data. These are the joint data for all joints in group ( $i$ ), the joint data for those joints in group ( $i + 1$ ) which are connected to joints in group ( $i$ ), and the degrees of freedom of joints in group ( $i - 1$ ) connected to joints in group ( $i$ ). Figure 2.5 shows the area ABEDC in which the stiffness matrix for group ( $i$ ) will lie. Contributions within the rectangle ABDC are formed by elements crossing from group ( $i - 1$ ) to group ( $i$ ). Contributions to the triangle BED are formed by all the sub-blocks of elements lying wholly within group ( $i$ ) and some of the sub-blocks of the elements which cross from group ( $i$ ) to ( $i + 1$ ). These contributions are detailed in the figure.

#### (2.7) The generation of the Diagonal Address Sequence

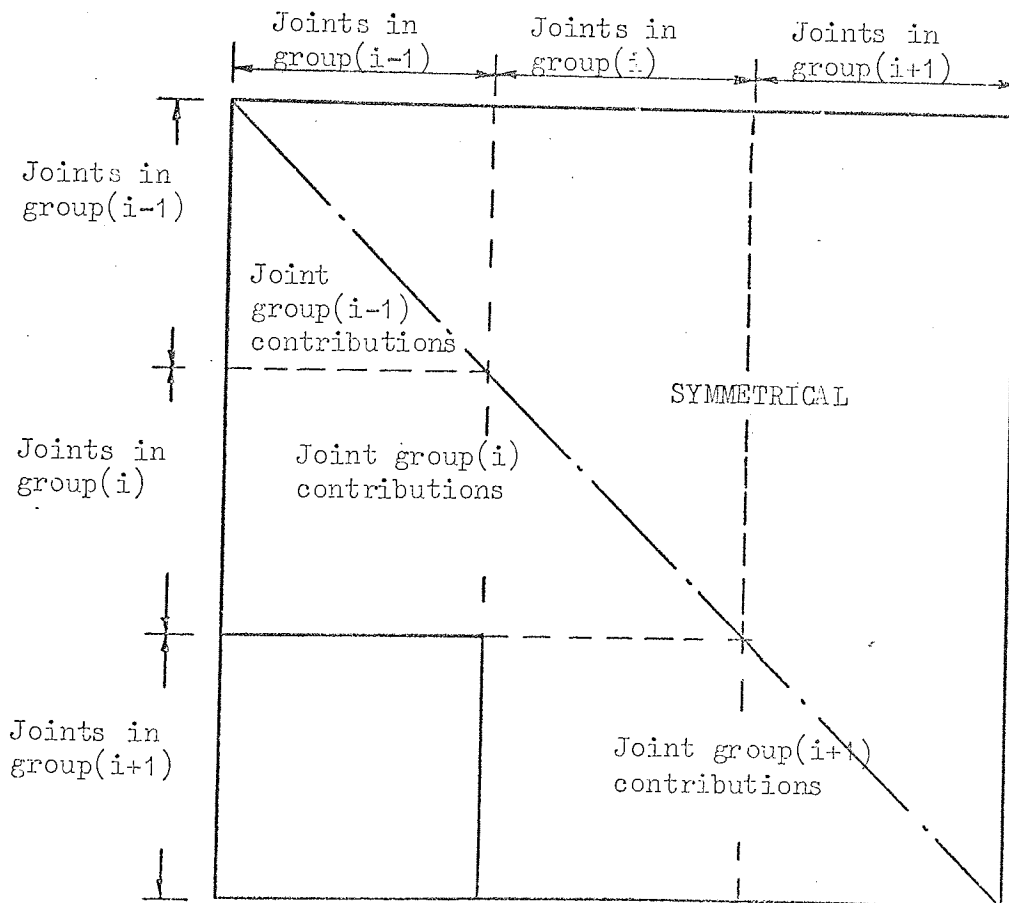
One of the most important operations at this stage is the interpretation of the joint information to form a skeletal representation of the stiffness matrix. This is done by forming the Diagonal Address





STRUCTURE COMPRISING FIFTEEN JOINTS WHICH HAVE BEEN DIVIDED INTO THREE JOINT GROUPS

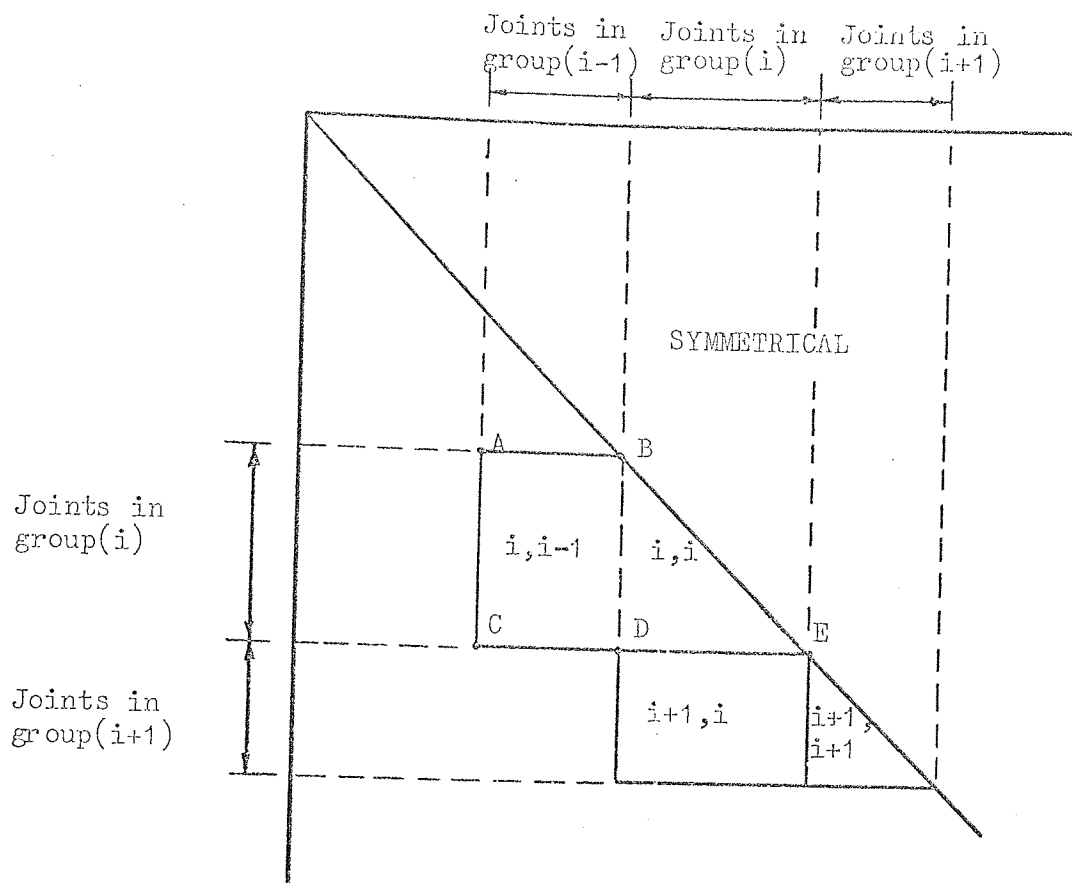
FIGURE 2.3



OVERALL STIFFNESS MATRIX FOR THE STRUCTURE SHOWN IN FIGURE 2.3

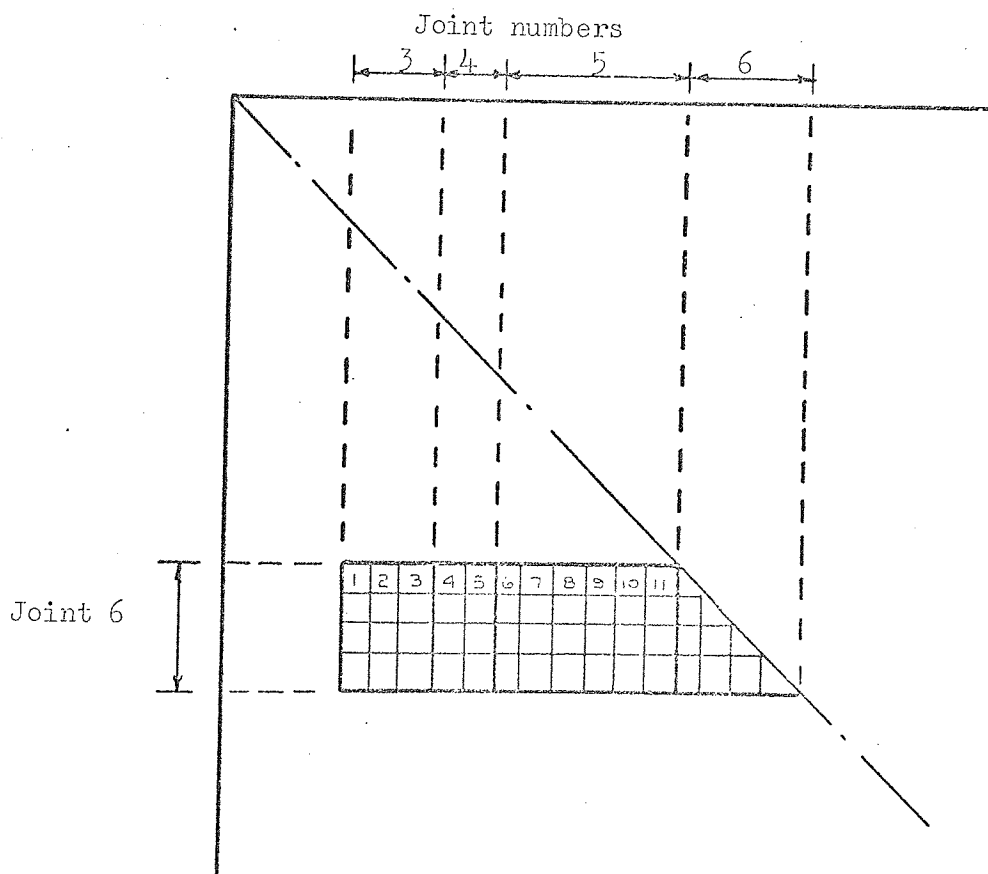
SHOWING THE TRIDIAGONAL NATURE OF THE STIFFNESS MATRIX

FIGURE 2.4



PART OF THE STIFFNESS MATRIX OF A STRUCTURE SHOWING HOW THE CONTRIBUTIONS FROM ONE GROUP MAY BE SPLIT INTO TWO PARTS

FIGURE 2.5



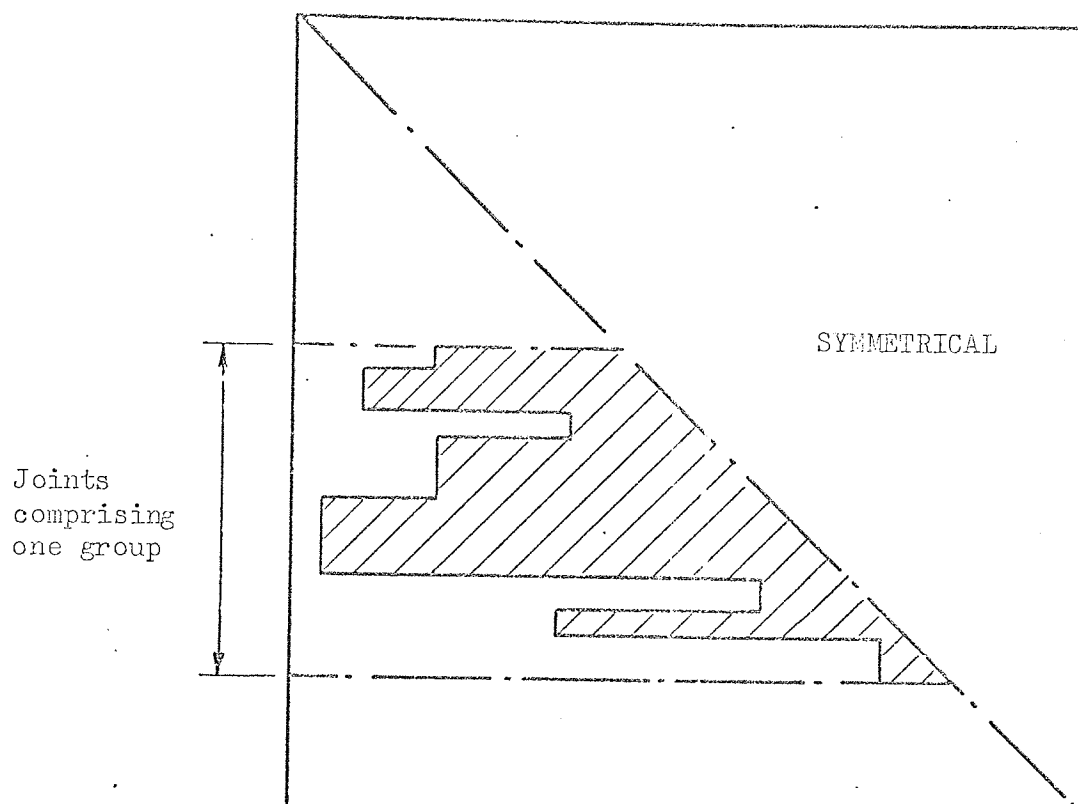
IF JOINT 6 HAS AN LJ VALUE OF 3 AND THE DEGREES OF FREEDOM OF JOINTS 3, 4 AND 5 ARE AS INDICATED THEN THE INTERVAL FOR JOINT 6 IS 11

FIGURE 2.6

Sequence, (DAS) array, for each joint group prior to the construction of the stiffness matrix of that group.

For each joint  $j$ , the LJ value, corresponding to the lowest column number, indicates the position of the first sub-block contributing to the rows of that joint, and thus defines the commencement of storage for those rows. If the degrees of freedom are summated sequentially from LJ up to  $j - 1$  then this summation is known as the 'interval' for the rows corresponding to joint  $j$ . This is illustrated in figure 2.6, where joint 3 is the lowest joint connected to joint 6 in a structure. The interval for joint 6 will be the sum of the degrees of freedom of joints 3, 4 and 5. The storage required for the first of this set of rows is the interval plus one, which is 12 for the joint illustrated in the figure, for the second row the storage is the interval plus two. The step up increases by one for each row until all the unsupressed degrees of freedom of the joint in question have been accounted for. This operation is carried out sequentially for each joint comprising the group.

The storage requirement for each row is retained in the DAS array. In figure 2.7, the elements of the stiffness matrix of a joint group which require storage are shown shaded. Whilst the DAS array for the whole structure is eventually constructed and stored in the core, the stiffness matrix for each group is constructed individually, and then stored on a backing unit. This releases the core locations for the stiffness matrix of the next joint group. It is thus necessary to know the position of the DAS element relating to the last row of the previous joint group. This allows the DAS elements for a group to be related to the first DAS element in that group, thus permitting the stiffness matrix for each group to be constructed as an independant quantity.



THE SHADED AREA SHOWS THE ACTUAL STORAGE REQUIREMENTS FOR ONE JOINT GROUP. FOR EACH JOINT COMPRISING THE GROUP STORAGE COMMENCES AT THE LJ VALUE AND CONTINUES UP TO THE LEADING DIAGONAL.

FIGURE 2.7

This information will be used to facilitate the positioning of the stiffness contributions of individual structural elements within the overall stiffness matrix of a structure.

## CHAPTER 3

### THE OVERALL STIFFNESS MATRIX

#### (3.1) Introduction

It was stated earlier that the construction of the stiffness matrix was to be carried out by considering individual elements rather than discrete rows of the matrix. This is implemented by dealing with each of the element types in turn.

In order that the stiffness contribution of each element of a given type contributing to the joint group in question may be evaluated, it is essential that the following points are considered:

- (1) Which of the element's sub-blocks contribute to the group stiffness matrix?
- (2) What are the properties and what is the orientation of the element?
- (3) What is the position of each of the contributing sub-blocks within the stiffness matrix of the group?

Once these facts have been determined, then each of the contributing sub-blocks may be evaluated directly into the storage array. At that stage the force and stress matrices of the element may also be computed.

After all the element types have been considered in this manner the stiffness matrix for the group is complete. The remaining operation, at that stage, is the subdivision of the group matrix into blocks suitable to the requirements of the inversion process.

#### (3.2) Tridiagonal co-ordination

From the study of the tridiagonal process it is clear that when considering joint group (i) a structural element will conform to one of the three modes listed overleaf.

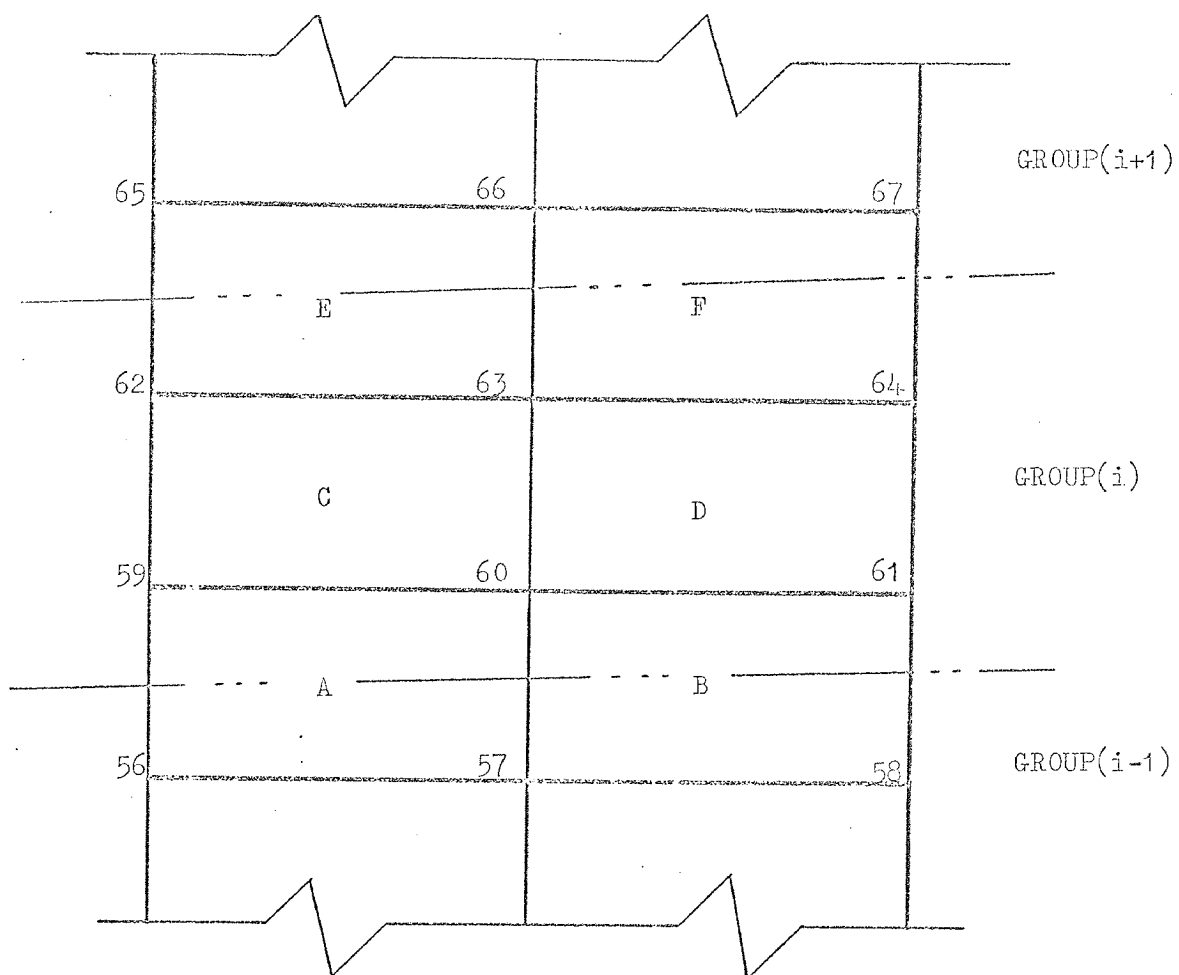
(a) Mode 1. The element is connected to the structure by joints which lie in both groups  $(i - 1)$  and  $(i)$ .

(b) Mode 2. The element is connected to the structure by joints which lie wholly in group  $(i)$ .

(c) Mode 3. The element is connected to the structure by joints which lie in both groups  $(i)$  and  $(i + 1)$ .

Elements conforming to either Mode 1 or Mode 3 contribute to the stiffness matrices of more than one group. Consequently, it is essential to be able to predict which of an element's sub-blocks occur within a given group. Clearly all the sub-blocks defined by rows corresponding to joints in group  $(i)$  will lie in that group. It is thus necessary to know which joints connect an element to a given joint group.

Tridiagonalisation imposes the restriction that lower numbered joints lie in lower numbered groups. Figure 3.1 illustrates this with the joint numbering shown. Here it is noticed that joints 59 to 64 are in group  $(i)$  while joints with lower or higher numbers lie in group  $(i - 1)$  or  $(i + 1)$  respectively. In the case of members this information is enough to allow the construction of the stiffness matrix contributions. This is attributable to the fact that a member is only connected to two joints, and when it crosses a group boundary the lower numbered joint must always lie in the lower numbered group. A triangular plate has three joints, and when such a plate crosses a group boundary either one or two of the joints will lie in the lower numbered group. One way of defining the orientation is to input a parameter in addition to the plate properties indicating which of the two cases exist. This permits triangular plates crossing the same boundary to have different sub-block contributions. In the case where this generality is not required, then one parameter defining the state of all triangular plates could be used.



WHEN CONSIDERING GROUP(i):

PLATES A AND B CONFORM TO MODE 1

PLATES C AND D CONFORM TO MODE 2

PLATES E AND F CONFORM TO MODE 3

THE NUMBERING TECHNIQUE USED ILLUSTRATES THAT LOWER NUMBERED JOINTS  
APPEAR IN LOWER NUMBERED GROUPS

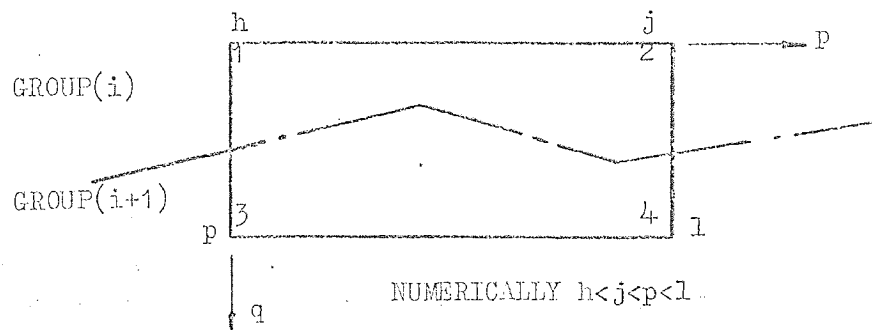
FIGURE 3.1



When a rectangular plate crosses a group boundary, it may be assumed that it is split by the boundary so that two joints lie in one group and two in the other. Figure 3.2 illustrates this point: consider the plate shown in figure 3.2a joints h and j lie in group (i), joints p and l in group (i + 1). The sub-block contribution to the lower triangle of the stiffness matrix for both groups (i) and (i + 1) due to this rectangular plate is shown in figure 3.2b. There are two triangular sub-blocks and one rectangular sub-block contributing to the lower numbered joint group, this may be known as Area 1. Five rectangular and two triangular sub-blocks contribute to the higher numbered group, this may be known as Area 2. These Areas are shown in figure 3.2c. It is therefore necessary to define Areas 1 and 2 for each element type so that the sub-block contributions may be known.

The position of such sub-blocks within the stiffness matrix is also required, and this is dependent upon the arbitrary numbers assigned to the element's joints. The local axes P, Q, R of each element are defined by its corner or end numbers. For the rectangular plate in figure 3.2a corners 1 to 2 define the positive P axis, and corners 1 to 3 the positive Q axis. The direction of the R axis is now implied. It is in terms of these corner numbers that the general sub-blocks are expressed. If the corner numbers can be related to the joint numbers then the sub-block positions will be defined. This may conveniently be done by having the lowest corner number connected to the lowest joint, a process which is continued so that the highest corner number is connected to the highest numbered joint.

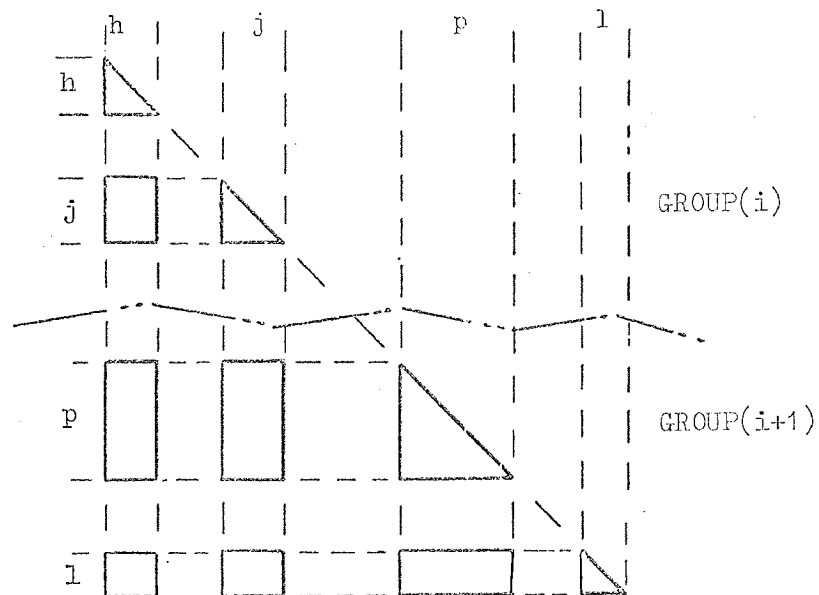
Figure 3.1 shows two plates A and B which both conform to Mode 1 when considering group (i). During the construction of the stiffness matrix for group (i) both of these plates contribute their Area 2 sub-blocks to this matrix. Plates C and D in the same figure belong to



RECTANGULAR PLATE SPLIT BY A GROUP BOUNDARY SHOWING THAT THE TWO LOWER  
NUMBERED JOINTS LIE IN THE LOWER NUMBERED GROUP.

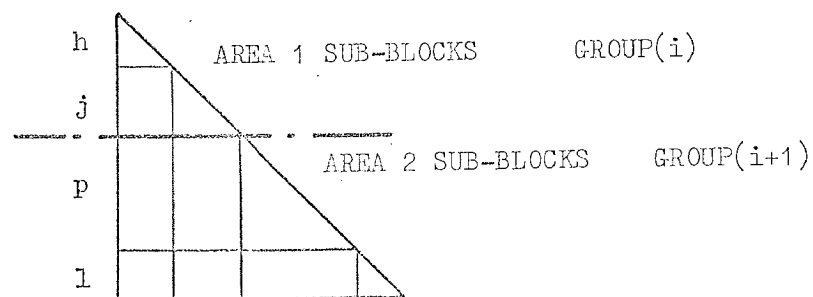
THE LOCAL PLATE AXES ARE ALSO SHOWN

FIGURE 3.2a



ORIENTATION OF THE SUB-BLOCKS FOR A RECTANGULAR PLATE WITH JOINT  
NUMBERING AS SHOWN IN FIGURE 3.2a

FIGURE 3.2b



SUB-BLOCKS GROUPED SO AS TO ILLUSTRATE AREAS 1 AND 2

FIGURE 3.2c

FIGURE 3.2

Mode 2 when considering group (i), and contribute their Area 1 and Area 2 sub-blocks to the stiffness matrix of that group. In the case of Plates E and F both of these conform to Mode 3, and thus contribute their Area 1 sub-blocks to the stiffness matrix. The action necessary in a co-ordination subroutine for each of the three Modes is given in figure 3.3.

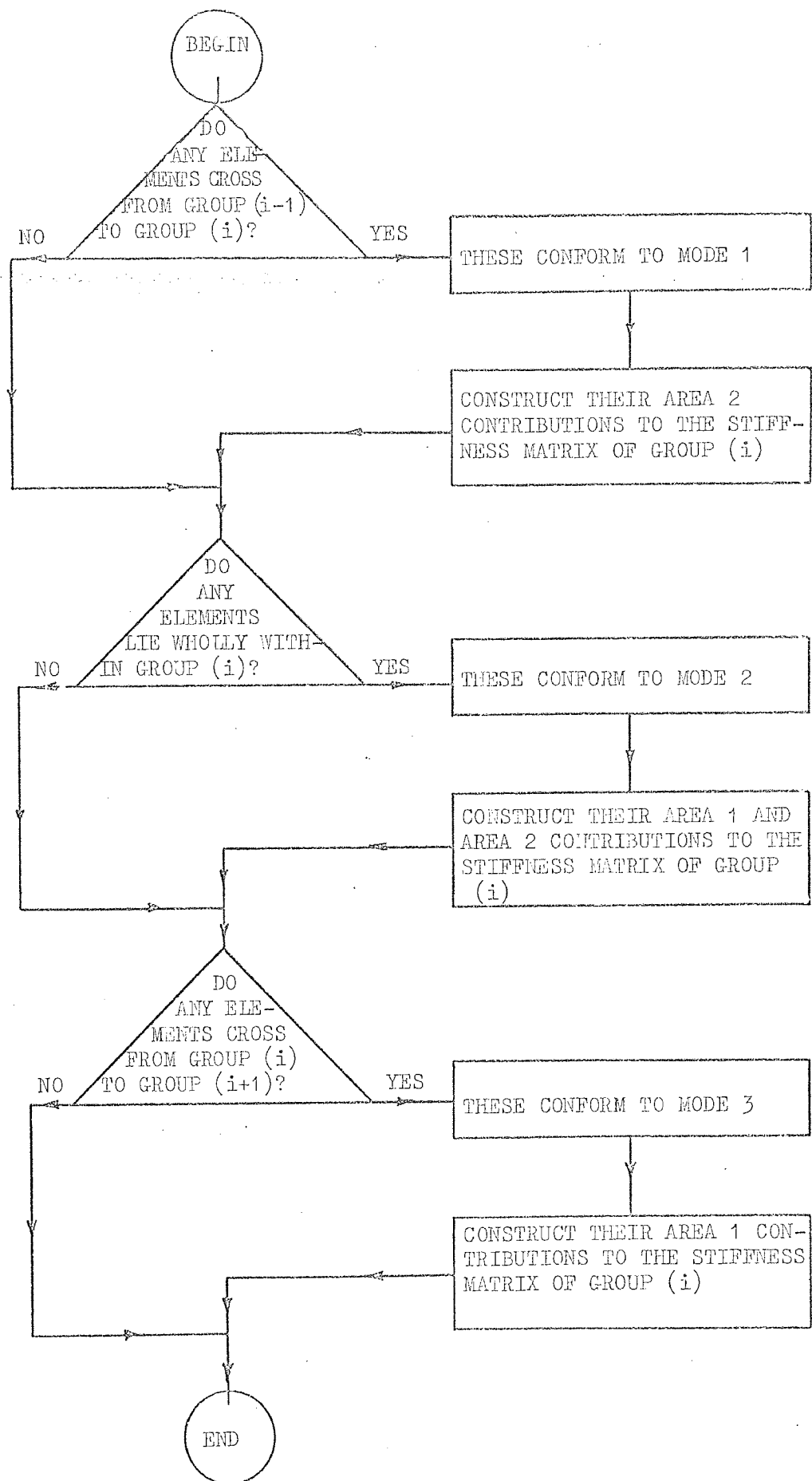
### (3.3) The organisation of data

In the case of some simpler elements, such as prismatic members or rectangular plates, the construction of the overall stiffness matrix may be carried out explicitly. This is because it is possible to evaluate directly the element's stiffness contributions. In more complicated cases, an example of which is the out of plane element stiffness matrix of a curved plate, it is necessary to use general variables for the overall stiffness contributions. The actual computation of these terms has to be carried out as a separate operation. The calculated values are then assigned to the general variables mentioned above. To avoid duplication of the calculation, which would be necessary for elements falling into Mode 1 and Mode 3, the values are stored on a disc backing unit.

Information relating to the element under construction is always kept at the beginning of relevant arrays, such locations are called the 'active areas' of the arrays.

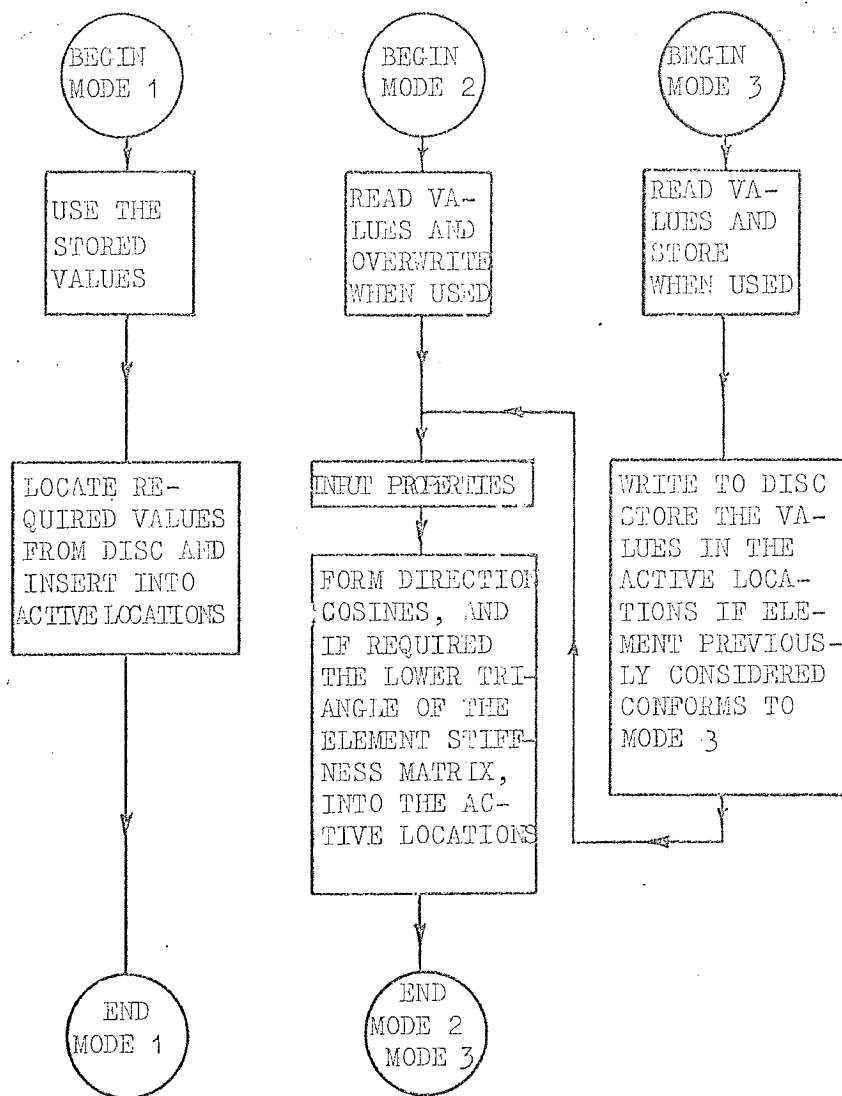
The way in which the data for a given group is used is dependent upon the mode to which the element conforms for the group under consideration. The action taken for each of the three modes is now discussed in conjunction with figures 3.3 and 3.4.

When the stiffness matrix for the first group is under consideration, no elements will conform to Mode 1. Thereafter elements in this classification will have already contributed their Area 1 sub-



FLOW DIAGRAM SHOWING THE METHOD OF SELECTING THE MODE TO WHICH ELEMENTS CONNECTED TO GROUP (i) CONFORM. EACH ELEMENT TYPE IS CONSIDERED IN THIS MANNER

FIGURE 3.3



ACTION INITIATED REGARDING COMPUTATION OF PARAMETERS AND INPUT OF PROPERTIES  
FOR EACH OF THE THREE MODES

FIGURE 3.4

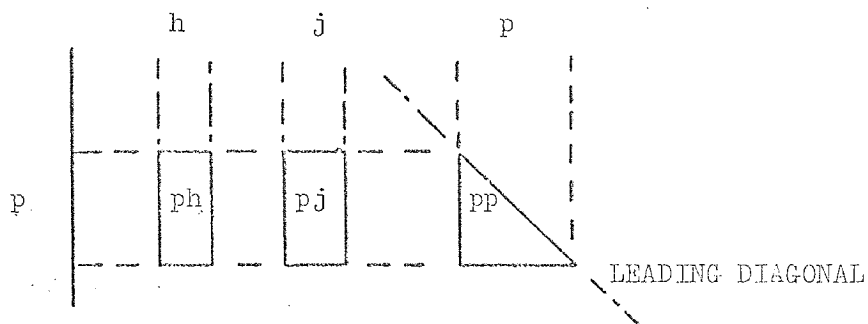
blocks to the previous group, thus only their Area 2 sub-blocks contribute to the group being considered. Since their Area 1 contribution has already been evaluated all relevant properties will have been input and computed. These must now be located in the storage area and copied into the active areas of the relevant arrays. Such an operation is referred to in the flow diagrams shown in figures 3.3 and 3.4.

Both Area 1 and Area 2 sub-blocks of an element conforming to Mode 2 will contribute to the stiffness matrix of the group under construction. As all the sub-blocks will be evaluated there is no need to retain the element's properties, which are read and computed directly into the active array areas. Once all of a given element's contributions have been made, the properties of the next element may be stored in the active areas, thus overwriting the previous information.

Elements comprising Mode 3 only contribute their Area 1 sub-blocks. These elements form Mode 1 for the next group. Most of the details required for Area 2 are also needed for the construction of Area 1. Consequently once Area 1 has been constructed these properties are transferred from the active areas in readiness for the next group.

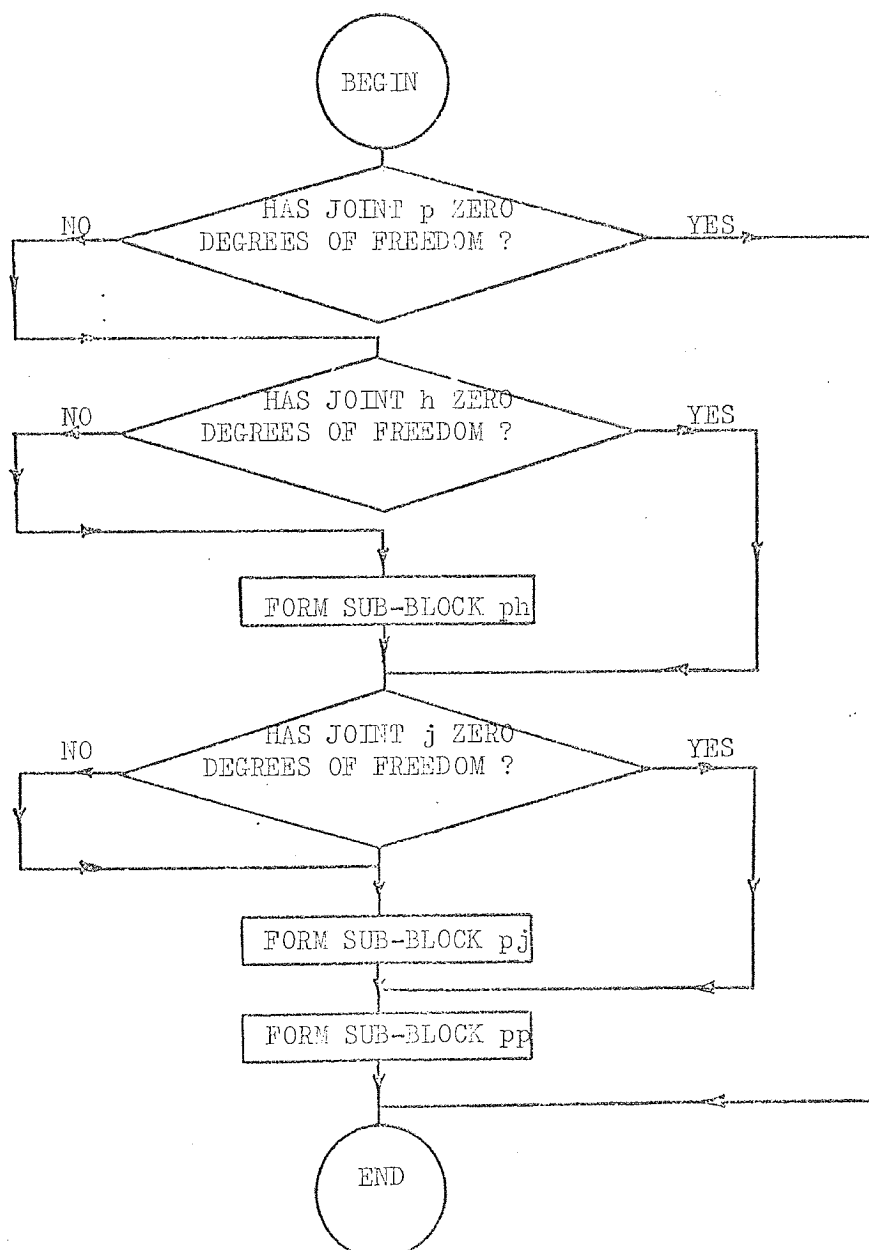
#### (3.4) Sub-block positioning

It was explained previously that the sub-blocks contributed by an element could be divided into two distinct areas, these have been called Area 1 and Area 2, figure 3.2 shows both of these. For reasons mentioned above it is necessary to be able to construct each area independently. The joint numbering technique adopted ensures that the sub-blocks comprising each of these Areas are known. These sub-blocks may be considered in any order. Figure 3.5 shows the three sub-blocks



PART OF THE STIFFNESS MATRIX CONTRIBUTIONS, SHOWN IN FIGURE 3.2  
 SHOWING THE POSITIONS OF THREE SUB-BLOCKS CONTRIBUTED BY ONE ELEMENT  
 TO THE SET OF ROWS CORRESPONDING TO THE DEGREES OF FREEDOM OF JOINT  $p$ .

FIGURE 3.5



DETERMINATION OF THE EXISTANCE OF SUB-BLOCK OCCURANCE

FIGURE 3.6

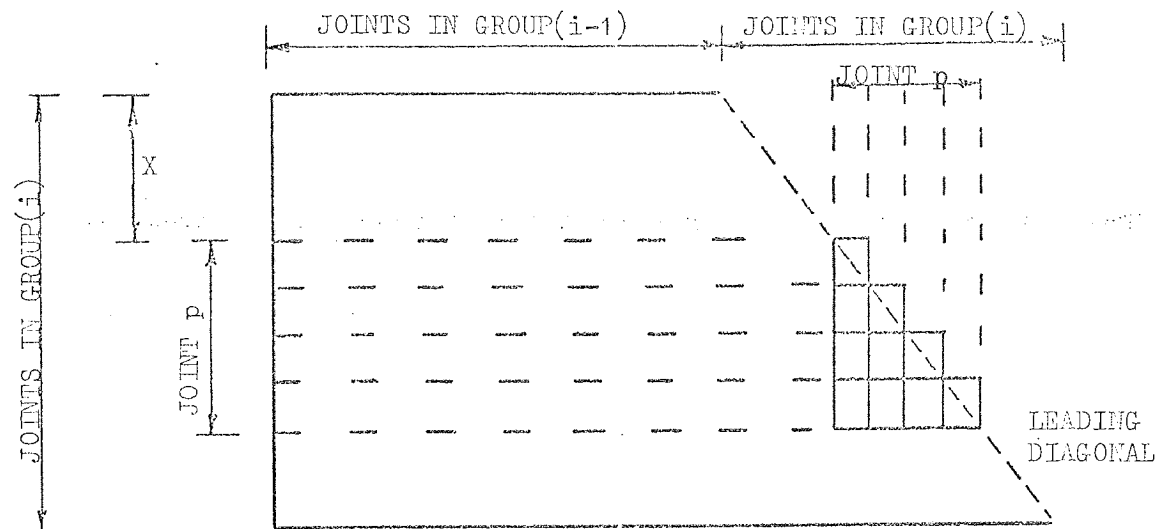
corresponding to the rows defined by joint  $p$  in figure 3.2. A flow diagram shown in figure 3.6 illustrates the operations necessary prior to the construction of each of these sub-blocks. If joint  $p$  has zero degrees of freedom then none of the sub-blocks exist. If  $p$  and  $h$  have non-zero degrees of freedom then the rectangular sub-block  $ph$  shown in figure 3.5 needs to be constructed. Similarly, if joints  $j$  and  $p$  have non-zero degrees of freedom, then rectangular sub-block  $pj$  will contribute terms. Finally, if joint  $p$  has at least one non-suppressed degree of freedom then triangular sub-block  $pp$  also shown in figure 3.5, will require construction.

Once the existence of a given sub-block has been established, then before it can be constructed into the stiffness matrix, details concerning its position must be computed. Rectangular and triangular sub-blocks require slightly different sets of information, consequently each of the types will be considered individually.

A triangular sub-block is the lower triangle of a rectangular sub-block which has its leading diagonal coincidental with the leading diagonal of the stiffness matrix. Figure 3.7 illustrates such a sub-block. It is relevant to note that for a sub-block to lie on the leading diagonal both its columns and rows are formed by the same joint, in the case of the example in figure 3.7 this is joint  $p$ . To construct such a sub-block it is necessary to have access to three facts, namely: the degrees of freedom of the joint forming the sub-block in both summed and expanded form, and the number of rows of the stiffness matrix of the group which precede the first row of the sub-block. This latter value is marked  $X$  in figure 3.7 and is obtained by adding the degrees of freedom of all the previous joints in that group.

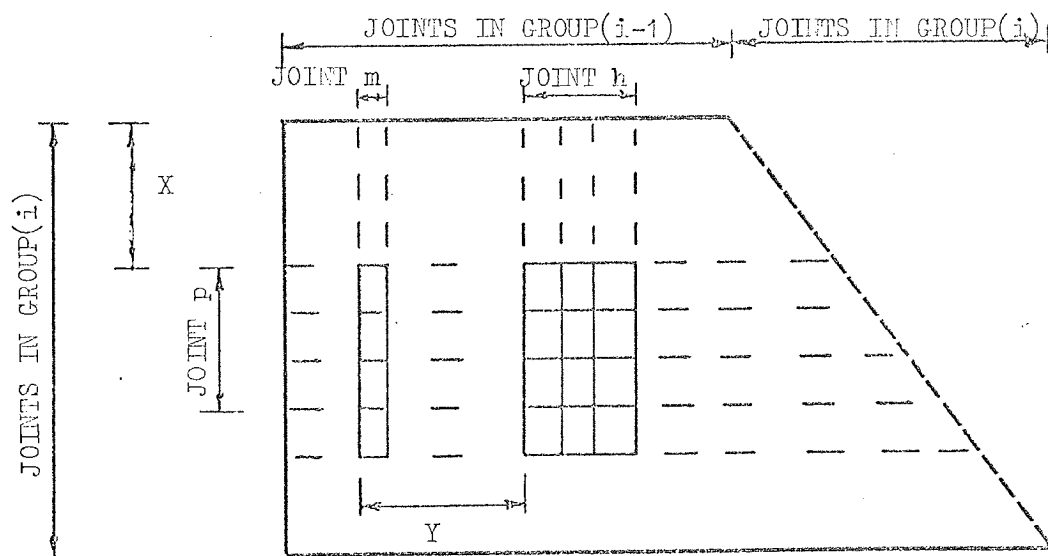
At this stage it is also useful to evaluate the total degrees of freedom for the whole structure up to the joint forming the sub-block. Since all the joints form a triangular sub-block every joint will be





PART OF THE STIFFNESS MATRIX RELATING TO GROUP(i) SHOWING THE POSITION OF THE TERMS FORMING A TRIANGULAR SUB-BLOCK DUE TO AN ELEMENT CONNECTED TO JOINT p

FIGURE 3.7



PART OF THE STIFFNESS MATRIX RELATING TO GROUP(i) SHOWING THE POSITION OF THE TERMS FORMING A RECTANGULAR SUB-BLOCK( $p_h$ ) DUE TO AN ELEMENT CONNECTED TO JOINTS p AND h. JOINT m IS THE LOWEST NUMBERED JOINT CONNECTED TO JOINT p BY A STRUCTURAL ELEMENT

FIGURE 3.8

considered, hence the displacements for each joint may be located in the displacement vector. This enables the multiplication of the stress and force matrices of an element and the relevant part of the displacement vector to be carried out.

A rectangular sub-block is formed by the intersection of rows and columns attributable to different joints. When considering group (i) the joint forming the set of columns may lie in either group (i) or (i + 1), while the joint forming the set of rows always lies in group (i). Figure 3.8 illustrates the position of a rectangular sub-block formed by joint p and h. The construction of such a sub-block requires the computation of six quantities. The first four of these are the degrees of freedom of both joints forming the sub-block in summated and expanded form. The fifth is the number of rows in the stiffness matrix for the joint group, prior to the first row of the sub-block. This is obtained in a similar manner to that adopted in the case of a triangular sub-block and is shown in figure 3.8 by the value X. In this manner the position of the first row of the sub-block within the stiffness matrix is located. Finally the sixth parameter fixes the position of the first column of the sub-block. This is expressed as the number of columns requiring storage on the row, prior to the first contribution of the sub-block in question.

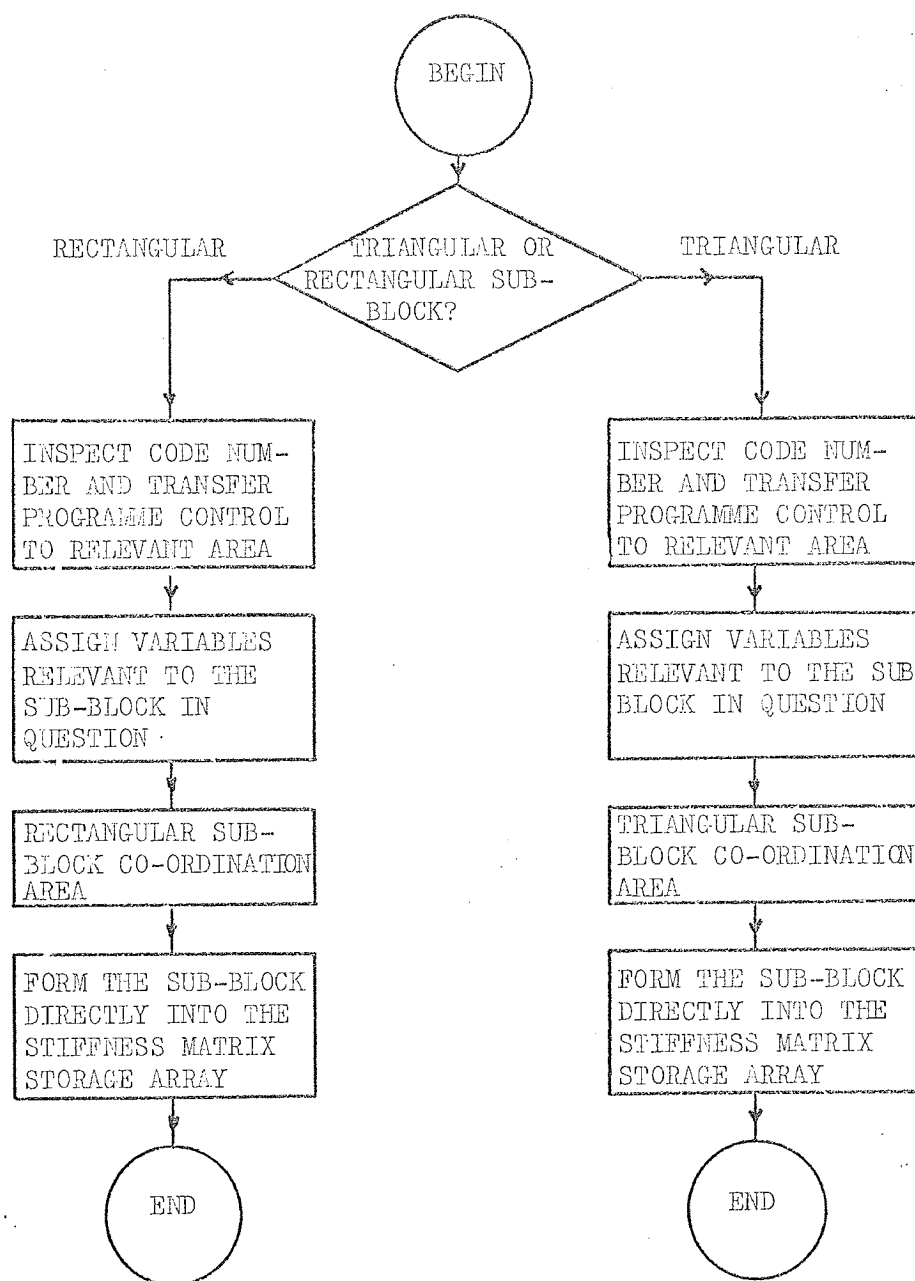
Storage of a set of rows corresponding to a given joint begins at the first non-zero contribution which is given by the joint's LJ value. For joint p this is shown by m in figure 3.8. The first contribution of the sub-block ph starts Y locations away from LJ, where Y is the sum of the degrees of freedom of joints m to h - 1. Once X and Y have been computed the position of a rectangular sub-block within a group stiffness matrix is known.

### (3.5) Direct construction of sub-blocks

When the existence of a sub-block has been confirmed, (see figure 3.6) and the parameters necessary for its construction have been evaluated, (see figures 3.7 and 3.8) it is then possible to construct the sub-block directly into the storage array for the stiffness matrix of that group. In order that this may be carried out, it is necessary, prior to the programming stage, to have available the stiffness contribution  $\underline{A'kA}$  of each term comprising the sub-block. This multiplication expresses the total sub-block contribution due to any element of the given type. To reduce programming effort, the sub-blocks of a given element are not presented separately. Instead, a single sub-block which can be transformed to each one of the individual sub-blocks of that element is prepared and used in the program. Consequently once the identity of a sub-block is defined by means of a code value its variables are assigned, and its construction may proceed.

In figure 3.9 the construction method for a sub-block is outlined. The steps taken when constructing a rectangular sub-block being different from those taken when forming a triangular sub-block. It is also essential to know which one of the sub-blocks of the given type is to be constructed. Figure 3.2b shows that a rectangular plate contributes a total of six rectangular and four triangular sub-blocks to the lower triangle of the stiffness matrix. Once such distinctions have been made, the assignments mentioned previously may be carried out.

In order that the construction may proceed the locations of the storage positions for the sub-block terms, as well as the ability to select the non-suppressed terms, need to be available. It has been explained with reference to figures 3.7 and 3.8 how the values X and

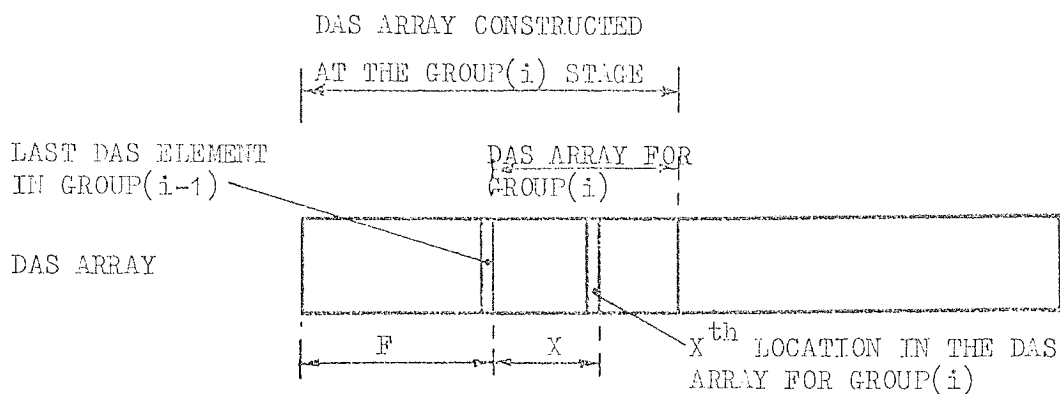


MACROSCOPIC FLOW DIAGRAM SHOWING THE METHOD ADOPTED TO CONSTRUCT A SUB-BLOCK

FIGURE 3.9

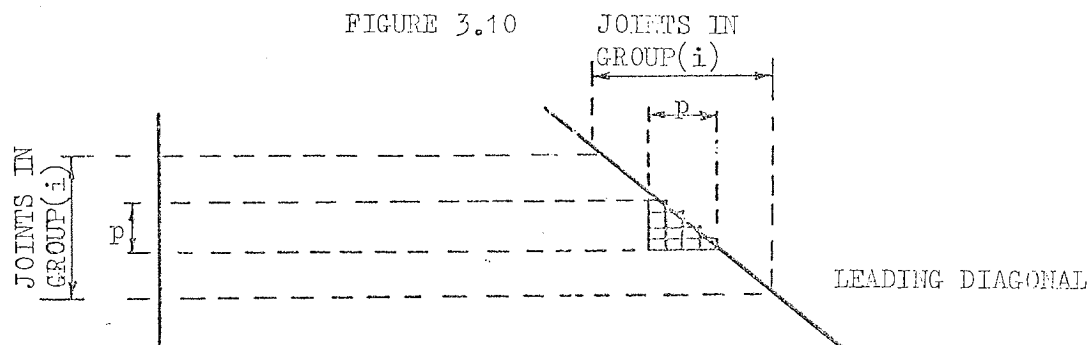
Y were obtained. It will now be shown with reference to figure 3.10, 3.11 and 3.12 how these quantities are used in conjunction with the stiffness matrix storage array for a given group. Figure 3.10 gives a schematic representation of the DAS array for a structure. The array stores the locations of the leading diagonal terms of the stiffness matrix. When group (i) is being considered, only that part of the DAS array for joints lying in groups prior to group (i + 1) will have been constructed. An address location of any leading diagonal element, given in the DAS array, will be relative to the entire structure. Since storage of the stiffness matrix in the core is for one group at a time, the value of the DAS elements used must be adjusted. If the last DAS element for group (i - 1) is the  $F^{\text{th}}$  (see figure 3.10) then all values relating to group (i) should be reduced by the quantity stored in DAS (F). This is illustrated for the case of a triangular sub-block in figure 3.11. The first term of this triangular sub-block occurs on row (X + 1) of the stiffness matrix of group (i), and the location in the DAS array which will reference this leading diagonal term is given by (F + X + 1). The address location for the same element within an array storing only the stiffness matrix of group (i) will be given by  $\text{DAS (F + X + 1)} - \text{DAS (F)}$ . The addresses of the remaining terms forming the triangular sub-block are computed in a similar manner, and shown in figure 3.12.

When considering a rectangular sub-block, as shown in figure 3.13, the address location of the leading diagonal element occurring on the row prior to that holding the first row of the sub-block is given by  $\text{DAS (X + F)} - \text{DAS (F)}$ , this is once again for the array holding only the stiffness matrix of group (i). The first term contributed by the sub-block is stored (Y + 1) locations after the leading diagonal element, consequently its address is  $\text{DAS (F + X)} + \text{Y} + 1 - \text{DAS (F)}$ .



F REPRESENTS THE NUMBER OF DEGREES OF FREEDOM IN THE STRUCTURE PRIOR TO GROUP(i)

SCHEMATIC DIAGRAM OF THE DAS ARRAY FOR A COMPLETE STRUCTURE WHEN CONSIDERING GROUP(i)



PART OF THE STIFFNESS MATRIX FOR GROUP(i) SHOWING THE ON DIAGONAL TRIANGULAR SUB-BLOCK FORMED AT JOINT p

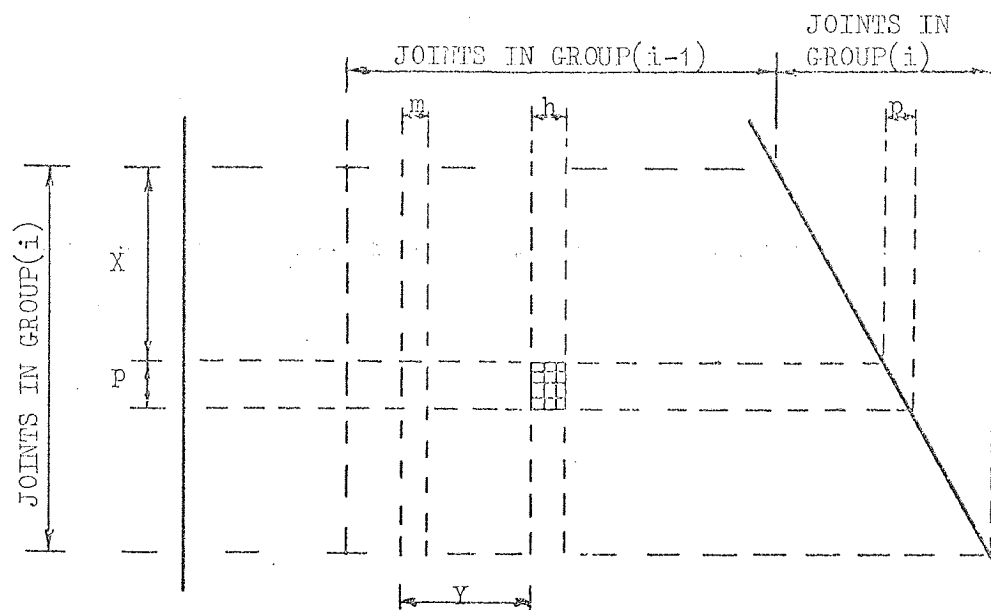
FIGURE 3.11

DAS(Z+1) -DAS(F)			
DAS(Z+2) -1-DAS(F)	DAS(Z+2) -DAS(F)		
DAS(Z+3) -2-DAS(F)	DAS(Z+3) -1-DAS(F)	DAS(Z+3) -DAS(F)	
DAS(Z+4) -3-DAS(F)	DAS(Z+4) -2-DAS(F)	DAS(Z+4) -1-DAS(F)	DAS(Z+4) -DAS(F)

WHERE  $Z=X+F$

STORAGE LOCATIONS OF THE TRIANGULAR SUB-BLOCK pp WITHIN AN ARRAY  
STORING THE STIFFNESS MATRIX FOR GROUP(i)

FIGURE 3.12



PART OF THE STIFFNESS MATRIX FOR GROUP(i) SHOWING THE RECTANGULAR SUB-BLOCK FORMED AT JOINTS p AND h. JOINT m IS THE LOWEST NUMBERED JOINT CONNECTED BY A STRUCTURAL ELEMENT TO JOINT p

FIGURE 3.13

DAS(Z) +Y+1 -DAS(F)	DAS(Z) +Y+2 -DAS(F)	DAS(Z) +Y+3 -DAS(F)
DAS(Z+1) +Y+1 -DAS(F)	DAS(Z+1) +Y+2 -DAS(F)	DAS(Z+1) +Y+3 -DAS(F)
DAS(Z+2) +Y+1 -DAS(F)	DAS(Z+2) +Y+2 -DAS(F)	DAS(Z+2) +Y+3 -DAS(F)
DAS(Z+3) +Y+1 -DAS(F)	DAS(Z+3) +Y+2 -DAS(F)	DAS(Z+3) +Y+3 -DAS(F)

Where  $Z = X + F$

STORAGE LOCATIONS OF THE RECTANGULAR SUB-BLOCK ph WITHIN AN ARRAY STORING THE STIFFNESS MATRIX FOR GROUP(i)

FIGURE 3.14

The addresses of the other terms are similarly computed and are shown in figure 3.14.

The remaining operations are the selection and direct evaluation of the terms comprising the sub-block under construction. Such terms correspond to unsuppressed degrees of freedom. The degrees of freedom in expanded form, for the joint, or joints forming the sub-block are used to select such terms. Figure 3.15 illustrates the technique developed for numbering each of the degrees of freedom. A joint requires six code values if no movements are restrained. When a degree of freedom is suppressed then its code value is deleted, consequently the number of significant code values is given by the summated degrees of freedom of the joint. Such code representations are illustrated in figure 3.16 where eight different types of joint condition, together with their associated code values, are shown. These codes are used to generate reference co-ordinates and hence permit the location of specific terms within the sub-blocks. Figure 3.17 shows all the reference co-ordinates for a rectangular sub-block, and figure 3.18 shows the similar arrangement for a triangular sub-block.

The method of selecting the reference co-ordinates of the unsuppressed terms is now explained in conjunction with the example illustrated in figures 3.7 and 3.8. If the four unsuppressed degrees of freedom of joint p and the three of joint h are as shown in figure 3.19, then the code arrays are those illustrated in the same figure. The rectangular sub-block ph is shown in figure 3.20 and the triangular sub-block pp in figure 3.21, both these show the reference co-ordinates of the unsuppressed terms. The method of generating these reference co-ordinates, when constructing the sub-block row by row, is to hold the code value for a given row and consider the code value of



DEGREE OF FREEDOM	X	Y	Z	$\theta_x$	$\theta_y$	$\theta_z$
CODE VALUE	1	2	3	4	5	6

THE CODE VALUES ASSIGNED TO EACH DEGREE OF FREEDOM OF ANY JOINT

FIGURE 3.15

JOINT	DEGREE OF FREEDOM					
	X	Y	Z	$\theta_x$	$\theta_y$	$\theta_z$
A	1	1	1	0	0	0
B	1	1	0	0	0	1
C	0	0	0	0	0	0
D	1	1	0	0	0	0
E	1	0	0	0	0	0
F	0	0	0	1	0	0
G	0	0	0	0	0	1
H	1	1	1	1	1	1

JOINT	CODE VALUE STORAGE ARRAY					
	1	2	3	4	5	6
A	1	2	3			
B	1	2	6			
C						
D	1	2				
E	1					
F	4					
G	6					
H	1	2	3	4	5	6



DENOTES A NON-SIGNIFICANT  
STORAGE LOCATION

EIGHT OF THE POSSIBLE DEGREES OF FREEDOM OF A JOINT. EACH WITH ITS  
ASSOCIATED SIX LOCATION CODE STORAGE ARRAY

FIGURE 3.16

	X	Y	Z	$\theta_x$	$\theta_y$	$\theta_z$
X	1,1	1,2	1,3	1,4	1,5	1,6
Y	2,1	2,2	2,3	2,4	2,5	2,6
Z	3,1	3,2	3,3	3,4	3,5	3,6
$\theta_x$	4,1	4,2	4,3	4,4	4,5	4,6
$\theta_y$	5,1	5,2	5,3	5,4	5,5	5,6
$\theta_z$	6,1	6,2	6,3	6,4	6,5	6,6

A RECTANGULAR SUB-BLOCK SHOWING THE REFERENCE CO-ORDINATES OF EACH TERM

FIGURE 3.17

	X	Y	Z	$\theta_x$	$\theta_y$	$\theta_z$
X	1,1					
Y	2,1	2,2				
Z	3,1	3,2	3,3			
$\theta_x$	4,1	4,2	4,3	4,4		
$\theta_y$	5,1	5,2	5,3	5,4	5,5	
$\theta_z$	6,1	6,2	6,3	6,4	6,5	6,6

A TRIANGULAR SUB-BLOCK SHOWING THE REFERENCE CO-ORDINATES OF EACH TERM

FIGURE 3.18

JOINT	DEGREE OF FREEDOM					
	X	Y	Z	$0_x$	$0_y$	$0_z$
p	1	1	1	0	0	1
h	0	0	1	1	1	0

JOINT	CODE VALUE STORAGE ARRAY					
	1	2	3	4	5	6
p	1	2	3	6		
h	3	4	5			

EXPANDED DEGREES OF FREEDOM OF JOINTS p AND h AND THEIR ASSOCIATED CODE ARRAYS

FIGURE 3.19

1,3	1,4	1,5
2,3	2,4	2,5
3,3	3,4	3,5
6,3	6,4	6,5

RECTANGULAR SUB-BLOCK  $ph$  SHOWING THE NON-SUPRESSED REFERENCE CO-ORDINATES

FIGURE 3.20

1,1			
2,1	2,2		
3,1	3,2	3,3	
6,1	6,2	6,3	6,6

TRIANGULAR SUB-BLOCK  $pp$  SHOWING THE NON-SUPRESSED REFERENCE CO-ORDINATES

FIGURE 3.21

each column in conjunction with this row value. For instance in figure 3.20 the first row value is 1, the three column values are 3, 4, and 5, thus co-ordinates (1, 3), (1, 4) and (1, 5) are generated. A triangular sub-block is a special case of this method. It is constructed in the same way except that when the column code exceeds the row code, then the row under consideration will have been completely formed. Figure 3.21 illustrates such reference co-ordinates.

The remaining step is to relate each of the thirty-six expressions comprising the general sub-block to its reference co-ordinate. This may be done by labelling each expression in accordance with its co-ordinate. When a co-ordinate is generated, during the construction of a sub-block, the program control transfers to the required expression which is evaluated. Once this evaluation is completed, program control is returned and the next co-ordinate is calculated. This process continues until all the non-suppressed terms have been formed. Since each sub-block is constructed individually this process never requires more than two six element arrays to generate the reference co-ordinates.

### (3.6) The computation of the force and stress matrices of an element

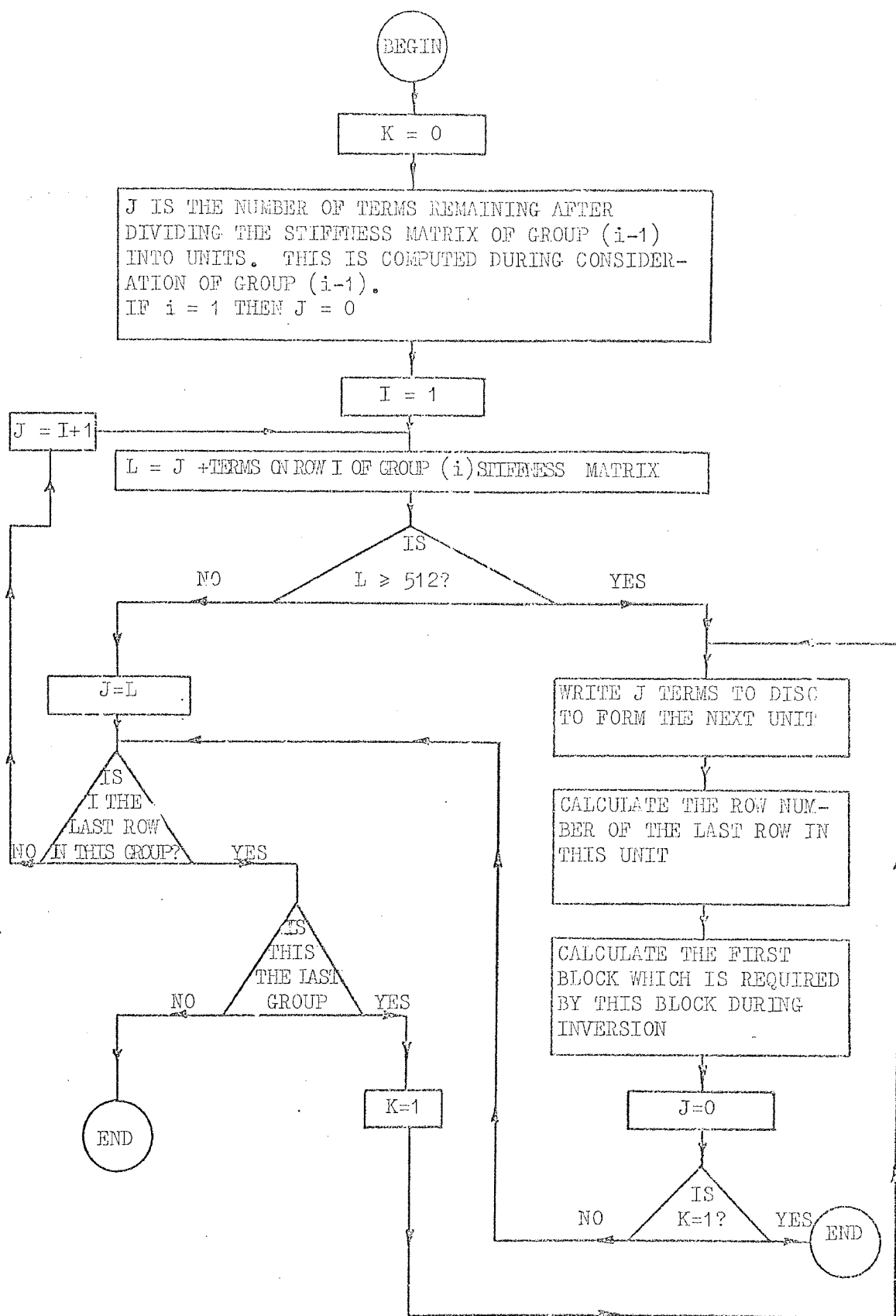
To permit the computation of the forces and stresses in a finite element it is necessary to form the kA and DBA matrix for that element. Since such elements are considered individually when calculating the overall stiffness matrix, it is convenient to form these matrices at the same time. Elements which cross a group boundary fall into both Modes 1 and 3, and it is only when they are being considered in the Mode 1 stage that enough information exists to construct their force and stress matrices. A technique similar to that employed in the formation of the stiffness matrix is used. Before

the programming stage the stress and force matrices are formed in general terms. When  $n$  joints connect the element to the structure a total of  $n$  blocks exist. Every block has a fixed number of rows, and a maximum of six columns each of which correspond to an unsuppressed degree of freedom. An additional more abstract block is expressed, to which the original  $n$  blocks are related. This block is then used for the evaluation of each of the  $n$  blocks in a similar manner to that employed by the general sub-block during the construction of an element's contributions to the stiffness matrix.

Once the blocks for one element are completed they are transferred to a disc file, thus releasing the core locations. Later, during the evaluation of element forces and stresses these  $kA$  and  $DBA$  blocks are returned to core, for each element in turn, and multiplied by the relevant displacements, thus yielding the forces and stresses within that element.

### (3.7) Subdivision of the stiffness matrix prior to solution

It was stated in the introduction that the solution technique adopted employs a method which operates on one unit of the stiffness matrix at a time. Each unit contains an integral number of rows and comprises not more than a specified number of terms. In the case of the Atlas computer, which was used by the author, the unit was limited to 512 terms, thus permitting the use of 'rapid' transfers between the disc and core stores. It is necessary, therefore, to subdivide the stiffness matrix of each group into these units prior to its transfer to the backing store. The stiffness matrix for a group is unlikely to form an exact number of units. For this reason, some terms of the stiffness matrix of one group may have to be considered with some of those in the succeeding group. Figure 3.22 shows by means of a simplified flow diagram the manner in which this is achieved. The



SIMPLIFIED FLOW DIAGRAM SHOWING HOW THE STIFFNESS MATRIX OF JOINT GROUP (i) IS  
SPLIT INTO UNITS SUITABLE FOR INVERSION

FIGURE 3.22

number of terms in successive rows are summated until the total exceeds 512. If this occurs when the  $n$ th row is included in the counting process, then that row is left to form part of the next unit, and  $(n - 1)$  rows are transferred to the backing store. The index number of the last row just transferred is preserved, together with the index number of the first passive unit with which the current unit is associated. These latter index values are required by the solution routine.

When the stiffness matrix of the last group has been considered in this way then the overall stiffness matrix of the entire structure has been computed and is ready for inversion.

## CHAPTER 4

### ELEMENT PACKAGES

#### (4.1) Introduction

To ensure that the program is flexible, requiring little change whenever a new element is introduced, it was decided that each finite element would have its own independent set of subroutines. Such a set of subroutines being known as that element's subroutine package. In addition to these packages the system would also comprise a set of auxiliary subroutines. The auxiliary subroutines are responsible for such operations as: the manipulation of the joint data to form the DAS array; the splitting up of group stiffness matrices into units ready for inversion; the assimilation of the load data; the inversion of the stiffness matrix and finally the outputting of the deflections.

Input to an element package takes two forms: the DAS array generated in the auxiliary package, and element details read from the data within the relevant element package. Output from element packages is in the form of additions to the overall stiffness matrix and element forces and stresses.

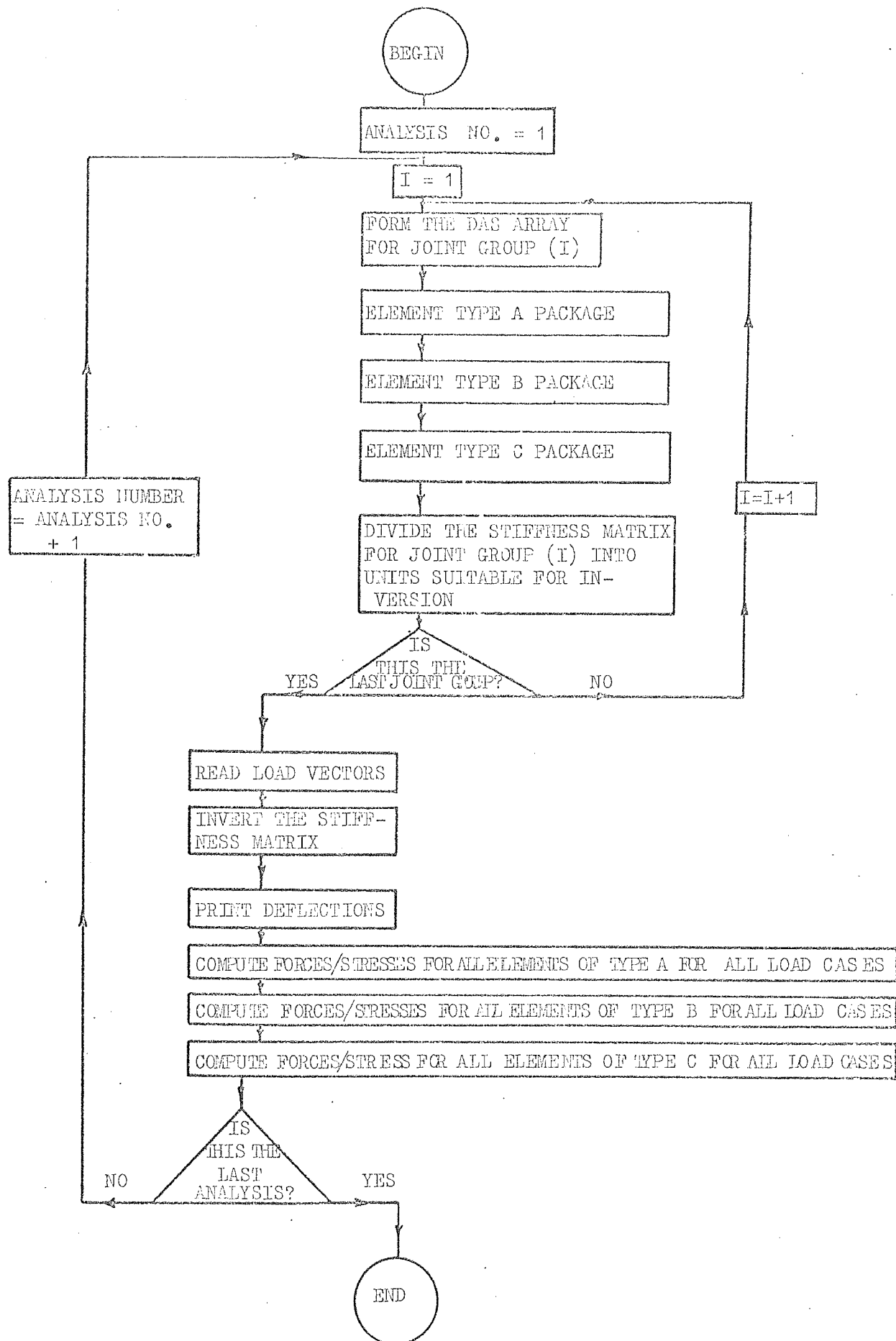
The sequence of operations, illustrated in figure 4.1 shows how packages for three elements A, B and C interconnect with the auxiliary subroutines to form the program.

#### (4.2) Auxiliary subroutines

The modes of operation of the five main subroutines comprising the auxiliary package will now be detailed.

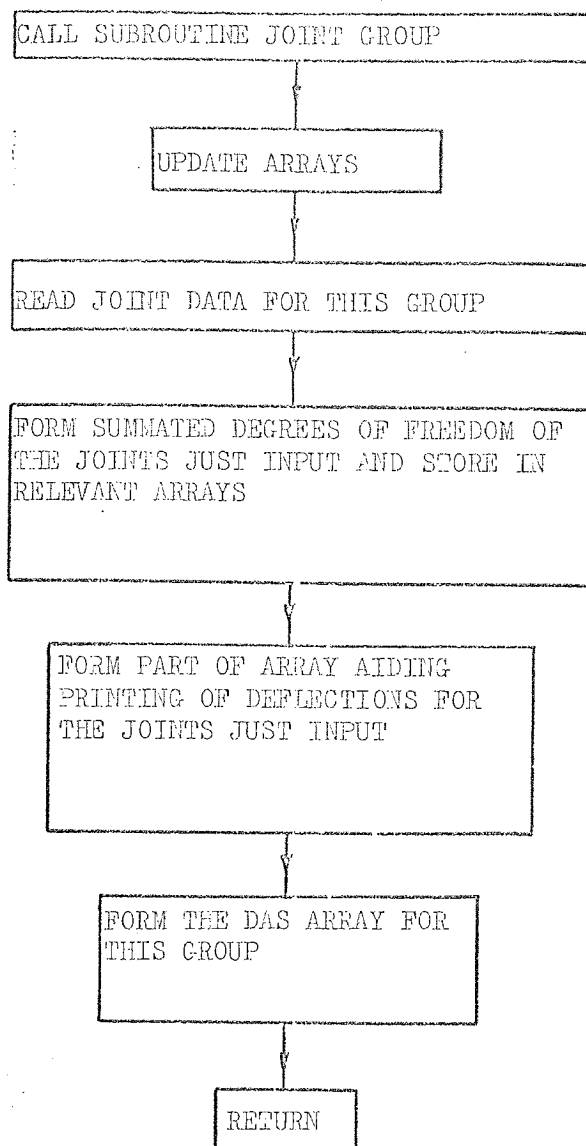
(4.2.1) Subroutine Joint Group. This is responsible for the assimilation of the joint information and the formation of the resulting DAS array. The manner in which such operations are carried out has already been described (see chapter 2). Figure 4.2 shows by means of a simplified





SEQUENCE OF CALLS

FIGURE 4.1



SEQUENCE OF OPERATIONS WITHIN SUBROUTINE JOINT GROUP

FIGURE 4.2

JOINT NUMBER	DEGREE OF FREEDOM					
	X	Y	Z	$\theta_x$	$\theta_y$	$\theta_z$
1	1	2	3	4	5	6
2	7	8	9	10	11	12
3	13	14	15	16	17	18
$\vdots$	$\vdots$	$\vdots$	$\vdots$	$\vdots$	$\vdots$	$\vdots$
$i$	$6*i-5$	$6*i-4$	$6*i-3$	$6*i-2$	$6*i-1$	$6*i$

CODE NUMBERS FOR THE SUPPRESSED DEGREES OF FREEDOM

FIGURE 4.3

1	2	3	4	5	6	7	9
---	---	---	---	---	---	---	---

CODE ARRAY

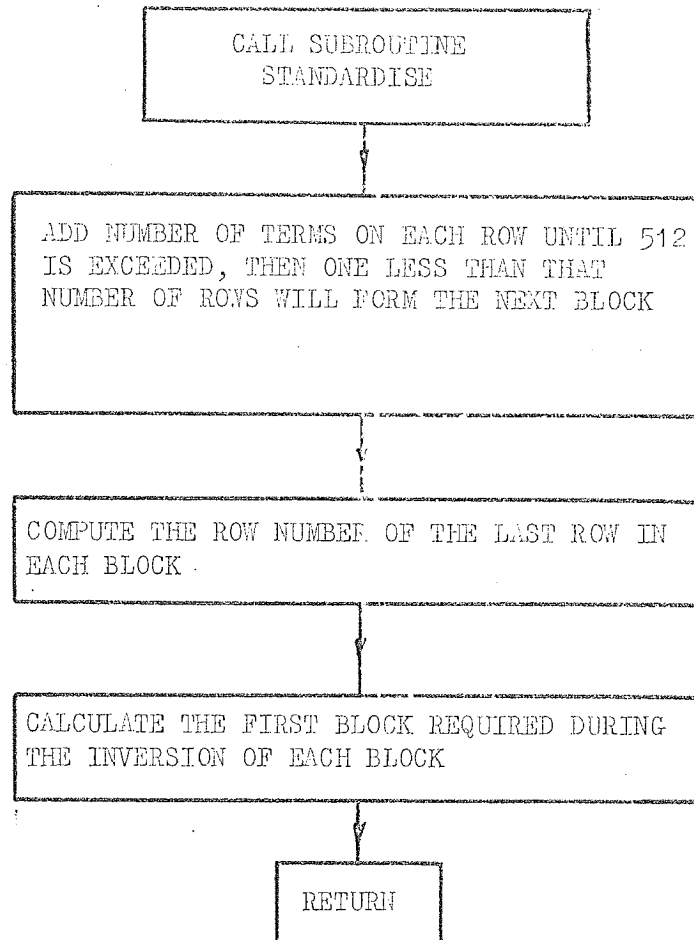
FIGURE 4.4

flow diagram the sequence in which the operations are performed. There is one further step carried out by this subroutine; this is the preparation of an array which, when used in conjunction with the joint displacements, permits the satisfactory printing of those displacements. Suppressed degrees of freedom are ignored when displacements are calculated, consequently the displacements of all unsuppressed movements appear as a continuous string of values. The array to be generated stores a unique code value for each suppressed degree of freedom. Code values for all degrees of freedom are shown in figure 4.3 and those corresponding to relevant suppressed movements are selected to form the array. If joint 1 in figure 4.3 had all its movements suppressed and joint 2 had its X and Z translations suppressed, then the stored code numbers relating to these two joints would be those shown in figure 4.4. This technique will not usually involve the storage of a large number of code values.

(4.2.2) Subroutine Standardise. When the stiffness matrix for one group has been completely constructed, it is split up into units which are compatible with those required for inversion. The method adopted has been described in chapter 2. A simplified flow diagram illustrating the technique is given in figure 4.5.

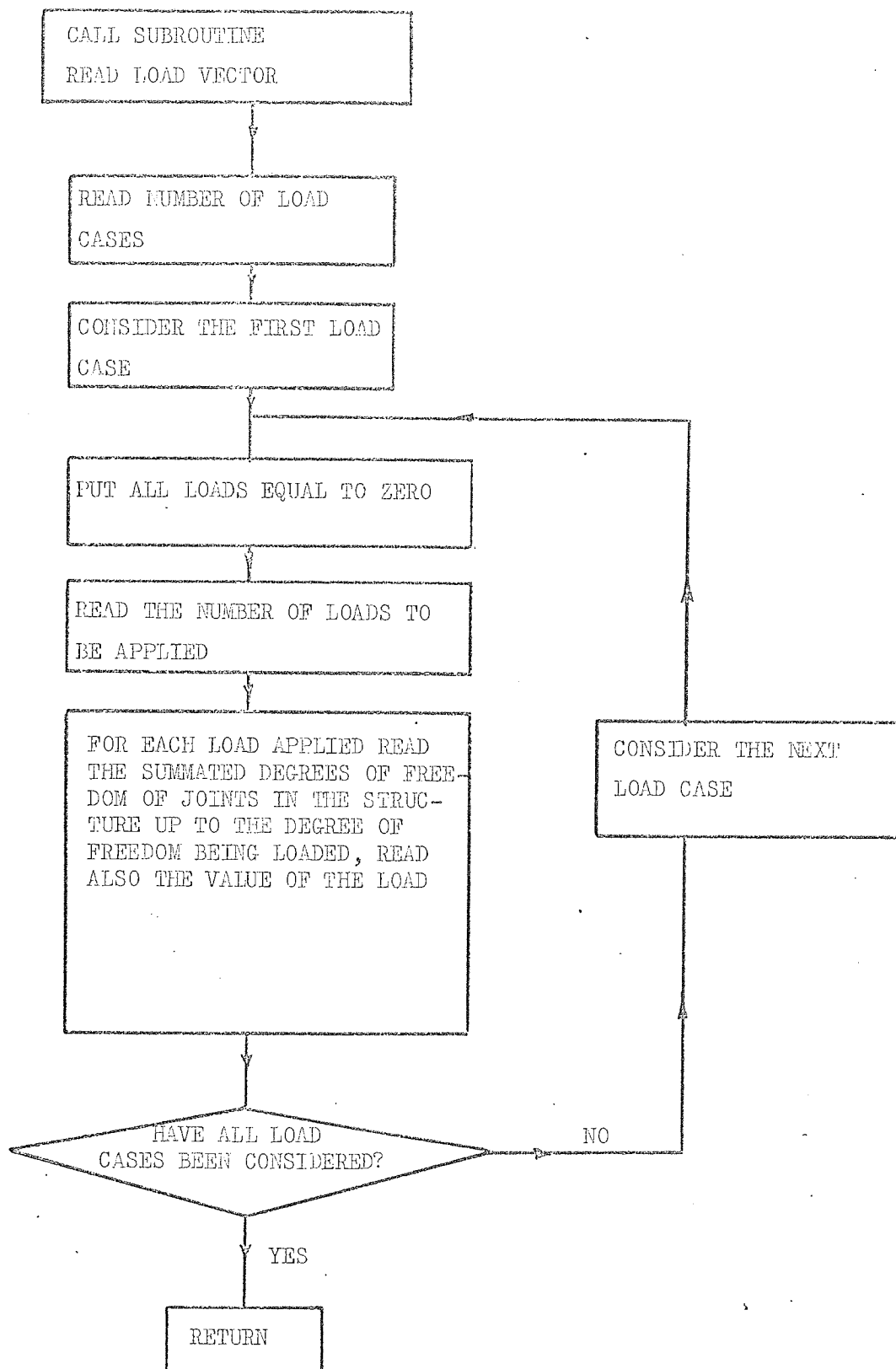
(4.2.3) Subroutine Read Load Vector. This assimilates the load vector for each load case, several of which may be considered in the same analysis. Any combination of the unsuppressed degrees of freedom may be loaded. The position of a load within the relevant storage array is given by the summation of the degrees of freedom up to, and including, the degree of freedom at which the load is applied. The macroscopic flow diagram for this subroutine given in figure 4.6 indicates that initially all degrees of freedom are assumed to have zero load applied. As a load is read its value replaces the relevant zero in the array.

(4.2.4) Subroutine Discomdiv. This solves the equation



SEQUENCE OF OPERATIONS WITHIN SUBROUTINE STANDARDISE

FIGURE 4.5



SEQUENCE OF OPERATIONS WITHIN SUBROUTINE READ LOAD VECTOR

FIGURE 4.6

$$\underline{X} = \underline{K}^{-1} \underline{L}$$

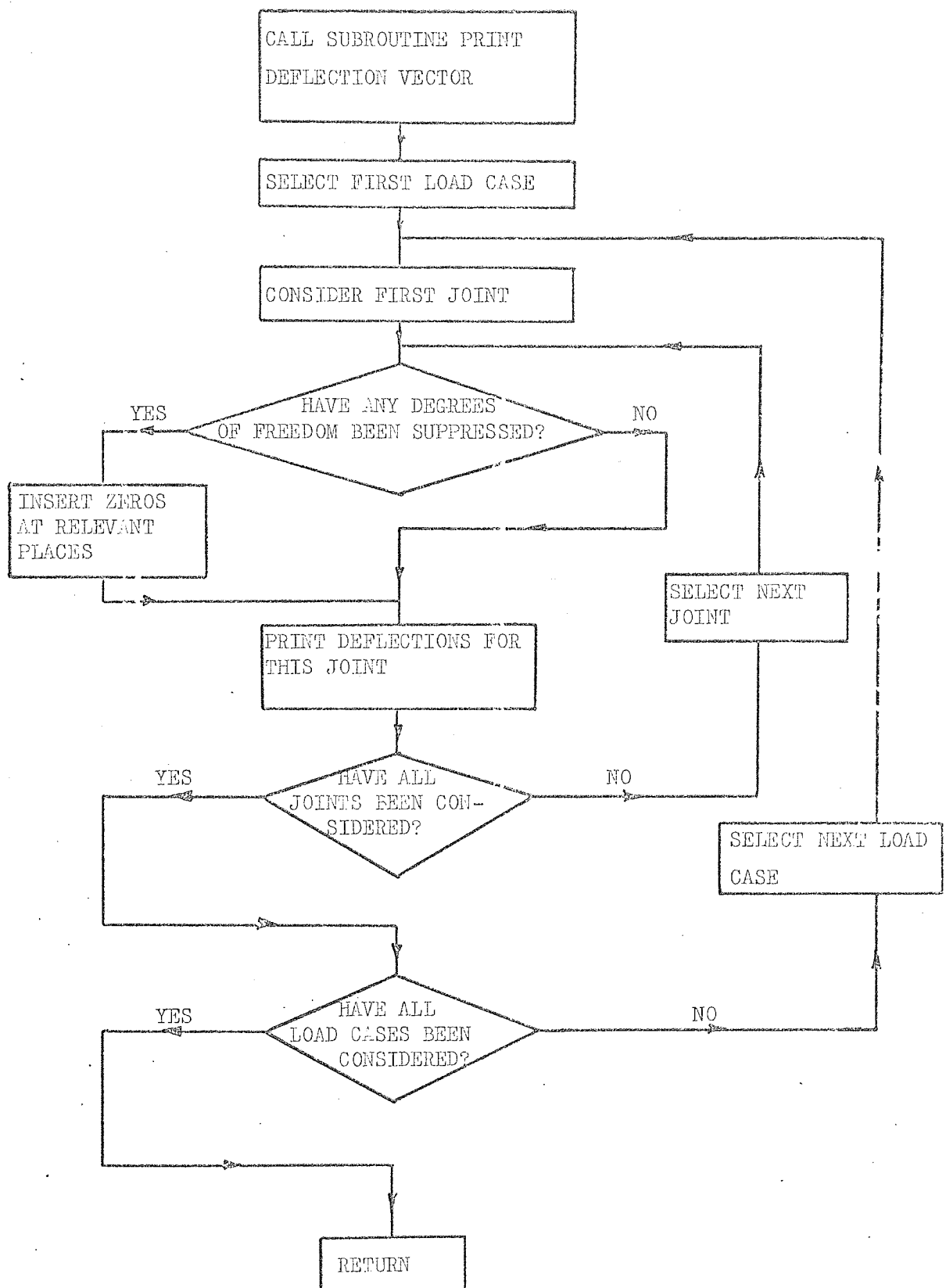
using the Choleski method (25). The subroutine written by Jennings and Tuff<sup>(8,26)</sup> is detailed in chapter 1.

(4.2.5) Subroutine Print Deflection Vector. Once the deflection vectors have been computed by Discomdiv only the printing of these vectors remains. So that the displacements may be easily interpreted it is desirable to print zero displacements where possible movements have been suppressed. This is done by considering the deflection vectors in conjunction with the code array generated in Joint Group. The manner in which this is done is illustrated by a simple flow diagram in figure 4.7.

#### (4.3) General description of element packages

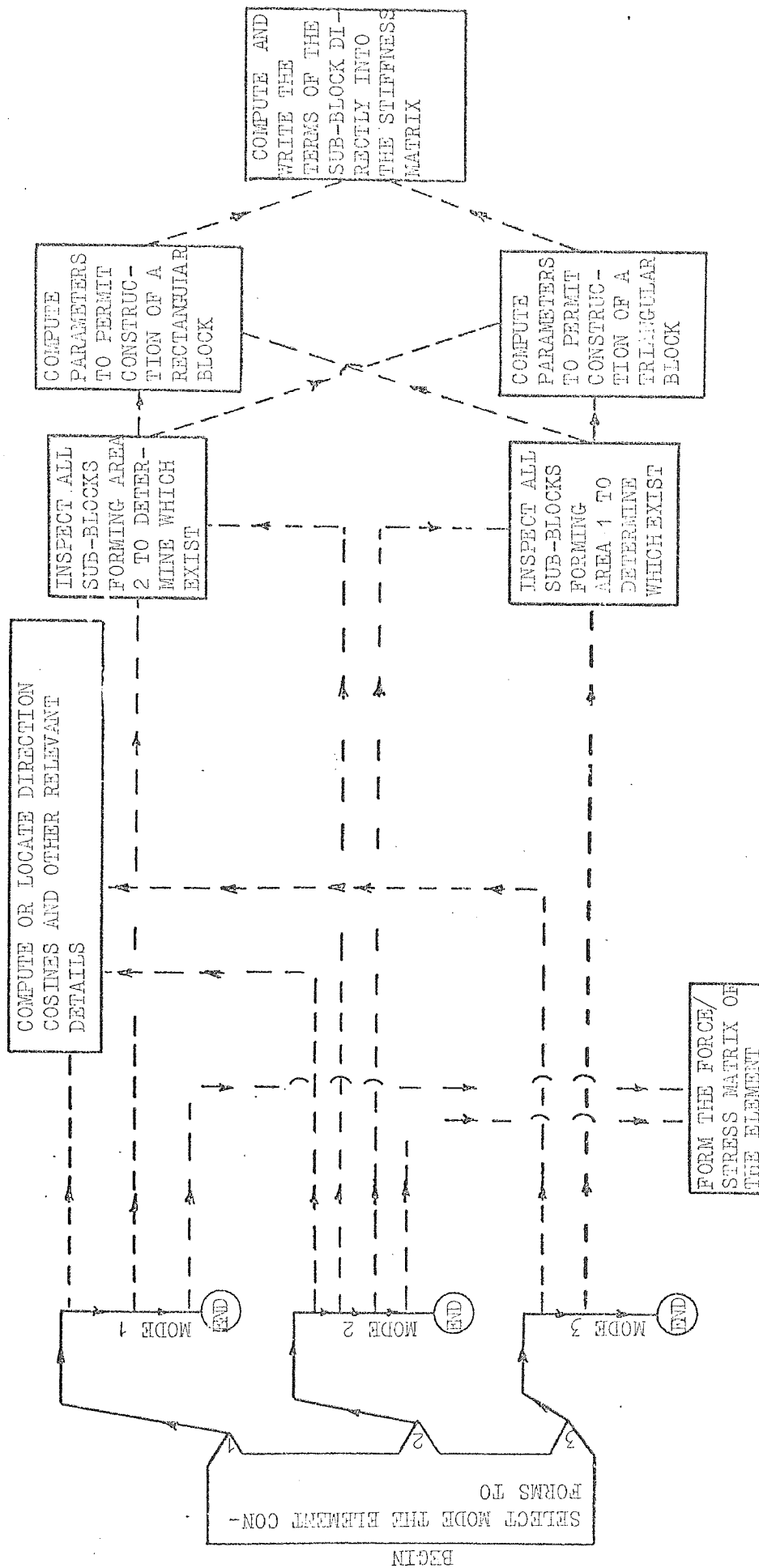
The co-ordinating subroutine of an element package is entered by the program during the construction of the stiffness matrix of each joint group. Such a subroutine has three main sequences of calls, illustrated in figure 4.8, each corresponding to a different Mode (see chapter 3). In figure 4.8 the dotted lines indicate reversible paths, the arrow denoting the outward path, the return always being made along the same path.

For each joint group the elements of a given type, which contribute terms to the stiffness matrix of that joint group, are handled in an order dependent upon the Mode to which they conform. Area 1 and Area 2 sub-blocks (see chapter 3) may occur independently in different modes, consequently it is essential to construct these Areas individually. Access to one of the Area subroutines results in tests being made on the degrees of freedom of the joints forming the sub-blocks in question. Figure 4.8 shows that after such tests have been completed control is transferred to either of two subroutines, depending whether the sub-block is rectangular or triangular. It is at this stage that the parameters required to position the sub-blocks within the stiffness matrix storage array are computed. Once this has been



SEQUENCE OF OPERATIONS WITHIN SUBROUTINE PRINT DEFLECTION VECTOR

FIGURE 4.7



STRUCTURE OF THE SUBROUTINE CALLS

FIGURE 4.8



carried out direct construction of the terms may take place. This occurs in a 'write' subroutine where the non-suppressed contributions are evaluated within their storage positions. When all the sub-blocks for the element forming the Area have been constructed then, depending upon the Mode, the sub-blocks forming the other Area may be constructed.

Figure 4.8 shows additional action is taken during some Modes. For example the stress and force matrices are constructed during the Mode 1 and 2 stage. All the elements of a given type contributing to the stiffness matrix of the joint group are treated in the manner defined by their Mode and illustrated in figure 4.8.

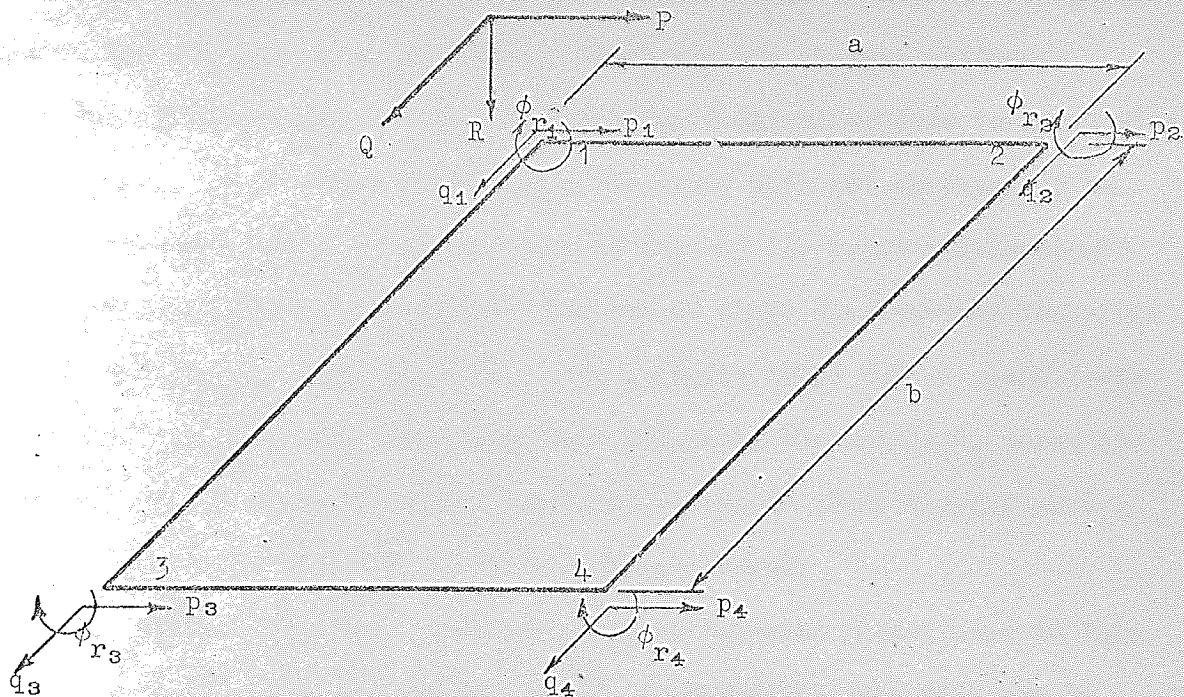
Other element types occurring within the joint group have their stiffness contributions evaluated by their own 'element package' in this manner.

In the following text the individual element packages for rectangular plates, triangular plates and prismatic members are detailed.

#### (4.4) Rectangular plate package

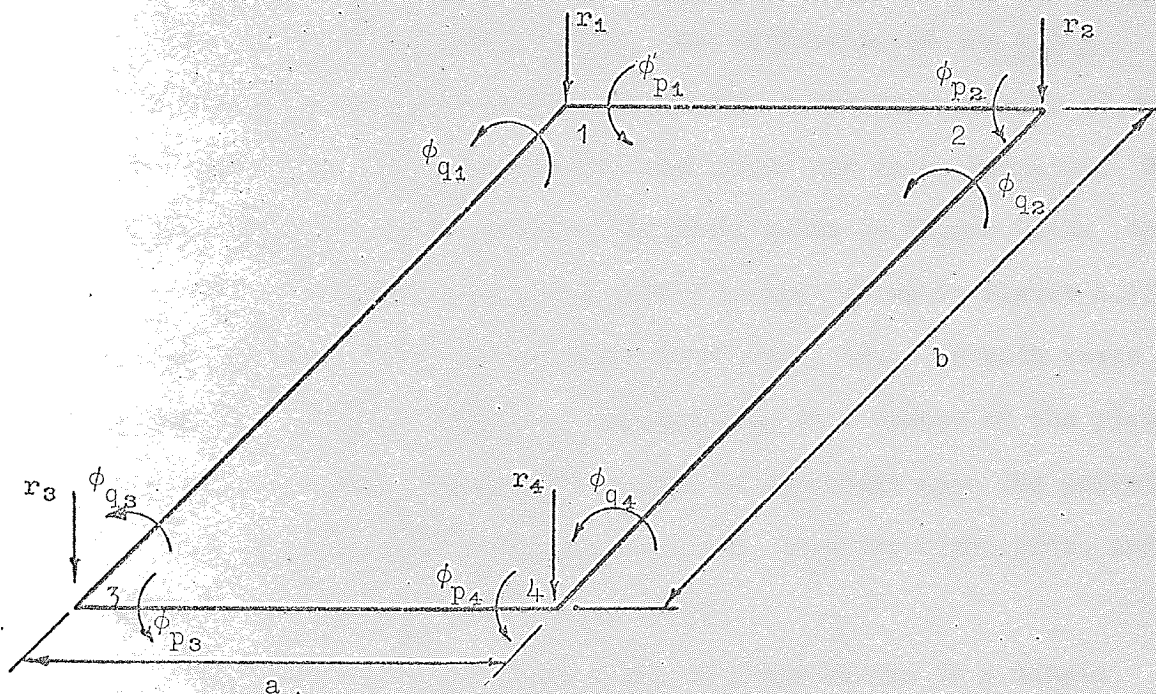
(4.4.1) General Considerations. Consider a rectangular plate, such as the one illustrated in figure 4.9. Under the influence of in plane forces each of the corners experience three displacements. Namely two translations in the P and Q directions, and one rotation about the R axis. These displacements are shown in figure 4.9a. It is usual to <sup>ignore</sup> ~~suppress~~ the in plane rotation of a corner, thus  $\phi_r$  in the figure is always zero. Consequently it is not included in the formulation of the in plane stiffness matrix for such a plate. The translations p and q at each corner, also illustrated in the figure, are therefore the only in plane displacements considered.

There are three further displacements at each corner, these are illustrated in figure 4.9b, and are caused by the action of out of plane forces on the plate. Such displacements are known as the out of plane displacements and comprise two rotations and one translation.



IN PLANE DISPLACEMENTS

FIGURE 4.9a



OUT OF PLANE DISPLACEMENTS

FIGURE 4.9b

FIGURE 4.9

These translations and rotations at each corner of a plate are parallel to the local axes of the plate. Similarly the element stiffness matrices relate forces and moments acting in these directions to local displacements. As elements comprising a structure will not necessarily be similarly orientated, it is essential to express the local displacements in terms of global displacements. The out of plane displacement transformation matrix  $\underline{A}_0$ , shown in figure 4.10, converts these out of plane local displacements to global displacements. Similarly the matrix  $\underline{A}_1$  shown in figure 4.11, performs the same operation for the in plane displacements. Both of these matrices only show the non-zero terms.

The element stiffness matrices for a rectangular plate, used in this work are those given by Zienkiewicz<sup>(19)</sup>, consequently they will not be explicitly detailed in this text. Reference, however, is made to terms within these matrices.

(4.4.2) Rectangular plate forces. The evaluation of the  $\underline{k} \underline{A} \underline{X}$  multiplication for one plate yields the forces at the four corners of that plate, consequently the  $\underline{k} \underline{A}$  matrix for each plate has to be computed. When this multiplication is performed for the plate shown in figure 4.12a then the layout of the resulting in plane matrix is that shown in figure 4.12b, and the out of plane matrix is as shown in figure 4.12c. In both cases four blocks are generated each one corresponding to a corner of the plate and having six columns. The number of rows is dependent upon the potential forces, thus the in plane blocks, figure 4.12b, comprise eight rows, and the out of plane, figure 4.12c, twelve rows.

It is possible to relate each of the in plane blocks to a single general block, which is shown in figure 4.13a. This block comprises direction cosines and general variables A to P. The allocation of in plane stiffness terms to these variables is dependent upon the block under construction. A table relating the variables, the blocks, and the in plane stiffness terms is shown in figure 4.13b. The same approach may be applied



$$\begin{bmatrix} r_1 \\ \phi_{p_1} \\ \phi_{q_1} \\ r_2 \\ \phi_{p_2} \\ \phi_{q_2} \\ r_3 \\ \phi_{p_3} \\ \phi_{q_3} \\ r_4 \\ \phi_{p_4} \\ \phi_{q_4} \end{bmatrix} = \begin{bmatrix} L_R & M_R & N_R \\ L_P & M_P & N_P \\ L_Q & M_Q & N_Q \\ \dots & L_R & M_R & N_R \\ & L_P & M_P & N_P \\ & L_Q & M_Q & N_Q \\ & \dots & L_R & M_R & N_R \\ & & L_P & M_P & N_P \\ & & L_Q & M_Q & N_Q \end{bmatrix} \times \begin{bmatrix} X_1 \\ Y_1 \\ Z_1 \\ \theta X_1 \\ \theta Y_1 \\ \theta Z_1 \\ \vdots \\ X_2 \\ Y_2 \\ Z_2 \\ \theta X_2 \\ \theta Y_2 \\ \theta Z_2 \\ \vdots \\ X_3 \\ Y_3 \\ Z_3 \\ \theta X_3 \\ \theta Y_3 \\ \theta Z_3 \\ \vdots \\ X_4 \\ Y_4 \\ Z_4 \\ \theta X_4 \\ \theta Y_4 \\ \theta Z_4 \end{bmatrix}$$

$$\underline{Z}_0 = \underline{A}_0 \cdot \underline{X}$$

OUT OF PLANE DISPLACEMENT TRANSFORMATION MATRIX FOR A RECTANGULAR PLATE

FIGURE 4.10

$$\begin{bmatrix} p_1 \\ q_1 \\ p_2 \\ q_2 \\ p_3 \\ q_3 \\ p_4 \\ q_4 \end{bmatrix} = \begin{bmatrix} L_P & M_P & N_P \\ L_Q & M_Q & N_Q \\ \dots & L_P & M_P & N_P \\ \dots & L_Q & M_Q & N_Q \\ \dots & L_P & M_P & N_P \\ \dots & L_Q & M_Q & N_Q \end{bmatrix} \times \begin{bmatrix} X_1 \\ Y_1 \\ Z_1 \\ \theta X_1 \\ \theta Y_1 \\ \theta Z_1 \\ \vdots \\ X_2 \\ Y_2 \\ Z_2 \\ \theta X_2 \\ \theta Y_2 \\ \theta Z_2 \\ \vdots \\ X_3 \\ Y_3 \\ Z_3 \\ \theta X_3 \\ \theta Y_3 \\ \theta Z_3 \\ \vdots \\ X_4 \\ Y_4 \\ Z_4 \\ \theta X_4 \\ \theta Y_4 \\ \theta Z_4 \end{bmatrix}$$

$$\underline{Z_I} = \underline{A_I} \cdot \underline{X}$$

IN PLANE DISPLACEMENT TRANSFORMATION MATRIX FOR A RECTANGULAR PLATE

FIGURE 4.11

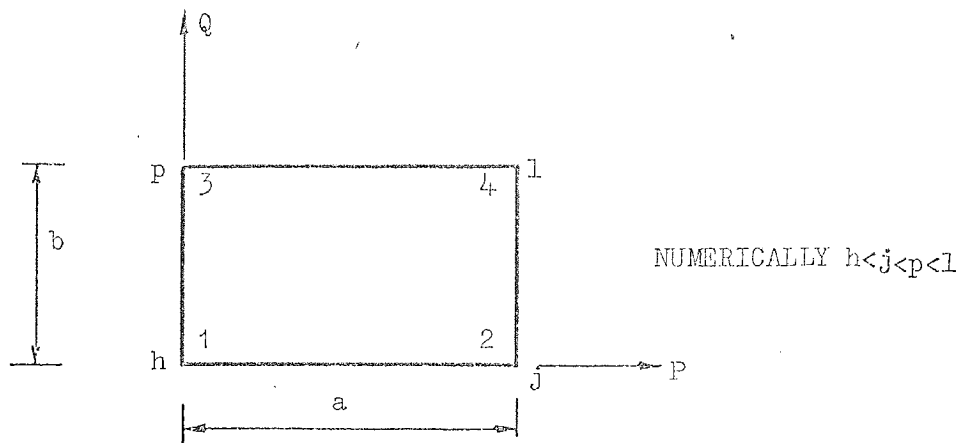
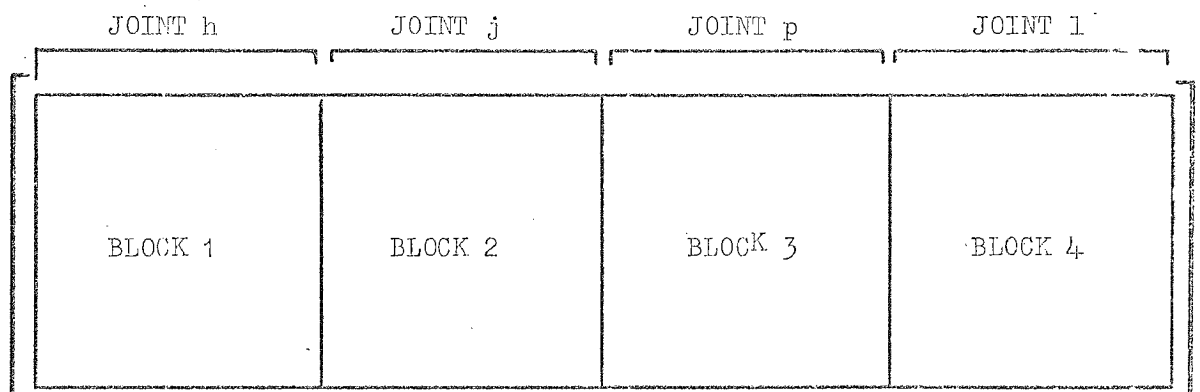
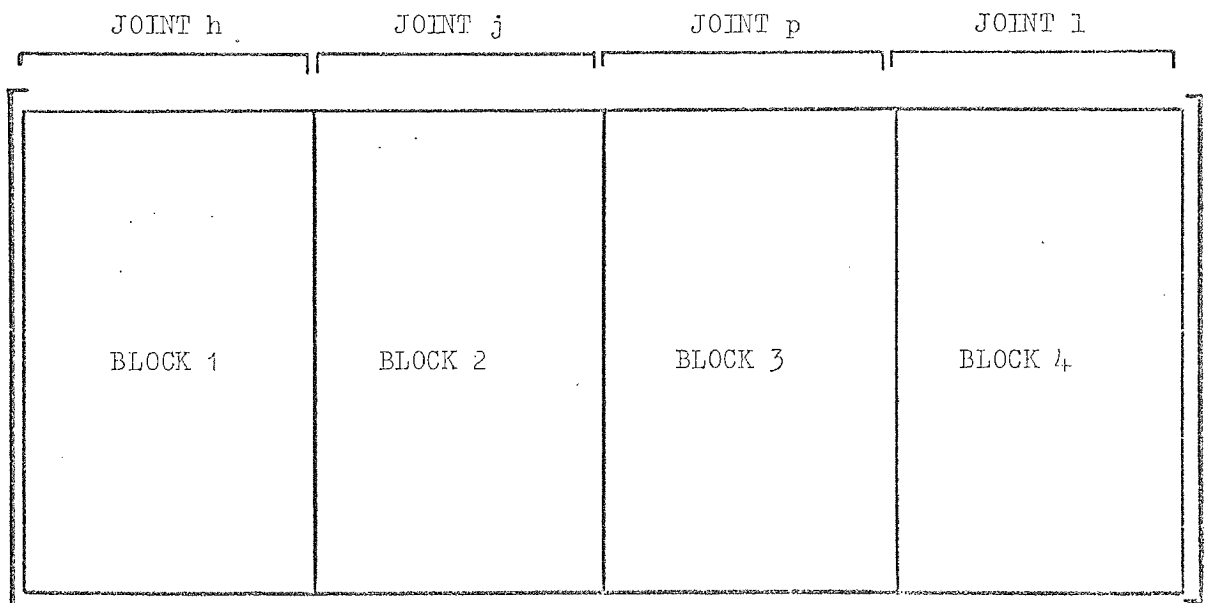


FIGURE 4.12a



IN PLANE FORCE MATRIX FOR A RECTANGULAR PLATE

FIGURE 4.12b



OUT OF PLANE FORCE MATRIX FOR A RECTANGULAR PLATE

FIGURE 4.12c

FIGURE 4.12

X	Y	Z	$\theta_x$	$\theta_y$	$\theta_z$
$L_P \cdot A$ +	$M_P \cdot A$ +	$N_P \cdot A$ +	0	0	0
$L_Q \cdot B$	$M_Q \cdot B$	$N_Q \cdot B$			
$L_P \cdot C$ +	$M_P \cdot C$ +	$N_P \cdot C$ +	0	0	0
$L_Q \cdot D$	$M_Q \cdot D$	$N_Q \cdot D$			
$L_P \cdot E$ +	$M_P \cdot E$ +	$N_P \cdot D$ +	0	0	0
$L_Q \cdot F$	$M_Q \cdot F$	$N_Q \cdot F$			
$L_P \cdot G$ +	$M_P \cdot G$ +	$N_P \cdot G$ +	0	0	0
$L_Q \cdot H$	$M_Q \cdot H$	$N_Q \cdot H$			
$L_P \cdot I$ +	$M_P \cdot I$ +	$N_P \cdot I$ +	0	0	0
$L_Q \cdot J$	$M_Q \cdot J$	$N_Q \cdot J$			
$L_P \cdot K$ +	$M_P \cdot K$ +	$N_P \cdot K$ +	0	0	0
$L_Q \cdot L$	$M_Q \cdot L$	$N_Q \cdot L$			
$L_P \cdot M$ +	$M_P \cdot M$ +	$N_P \cdot M$ +	0	0	0
$L_Q \cdot N$	$M_Q \cdot N$	$N_Q \cdot N$			
$L_P \cdot O$ +	$M_P \cdot O$ +	$N_P \cdot O$ +	0	0	0
$L_Q \cdot P$	$M_Q \cdot P$	$N_Q \cdot P$			

GENERAL IN PLANE FORCE MATRIX FOR A RECTANGULAR PLATE

FIGURE 4.13a

CODE	BLOCK			
	1	2	3	4
A	1,1	1,3	1,5	1,7
B	1,2	1,4	1,6	1,8
C	2,1	2,3	2,5	2,7
D	2,2	2,4	2,6	2,8
E	3,1	3,3	3,5	3,7
F	3,2	3,4	3,6	3,8
G	4,1	4,3	4,5	4,7
H	4,2	4,4	4,6	4,8

CODE	BLOCK			
	1	2	3	4
I	5,1	5,3	5,5	5,7
J	5,2	5,4	5,6	5,8
K	6,1	6,3	6,5	6,7
L	6,2	6,4	6,6	6,8
M	7,1	7,3	7,5	7,7
N	7,2	7,4	7,6	7,8
O	8,1	8,3	8,5	8,7
P	8,2	8,4	8,6	8,8

KEY TO TERMS WITHIN THE GENERAL BLOCK. ELEMENTS REFER TO TERMS  
WITHIN THE IN PLANE STIFFNESS MATRIX

FIGURE 4.13b

FIGURE 4.13



to the out of plane blocks. The general block is shown in figure 4.14, and the table relating the variables, the blocks, and the out of plane stiffness terms is given in figure 4.15. Consequently any one of the blocks may be generated from consideration of the relevant general block and the associated table.

(4.4.3) Rectangular plate stresses. In order that the stresses within a finite element may be computed, the  $\underline{D} \underline{B} \underline{A} \underline{X}$  multiplication must be performed for each element. Clearly the  $\underline{DBA}$  matrix for each rectangular plate has to be constructed. Figure 4.16b gives the in plane stress matrix and figure 4.16c the out of plane stress matrix. Both of these yield stresses at the centre of gravity of a rectangular plate. When each of the matrices is multiplied by the relevant  $\underline{A}$  matrix the resulting matrix is of the layout illustrated in figure 4.16d. As with the  $\underline{kA}$  matrix, four distinct blocks exist for both the in and out of plane cases, each one corresponding to one corner of the plate shown in figure 4.16a.

One general block may be used to represent all of the in plane  $\underline{DBA}$  blocks and is illustrated in figure 4.17a. When this block is used in conjunction with the table shown in figure 4.17b each of the four in plane  $\underline{DBA}$  blocks can be formed. An identical method is adopted in the case of the out of plane  $\underline{DBA}$  blocks, the general block being shown in figure 4.18a, and the table relating it to the individual out of plane  $\underline{DBA}$  blocks is in figure 4.18b.

The assumed stress distribution across the depth of a rectangular plate due to the action of out of plane forces is shown in figure 4.19a, and due to in plane forces in figure 4.19b. The resultant of these two diagrams is illustrated in figure 4.19c. From the figures it can be appreciated that the stress variation across the depth of the section is assumed to be linear, this condition is imposed by the basic assumptions (6).

(4.4.4) Direct Evaluation of the  $\underline{A' k A}$  contribution. It was stated



	X	Y	Z	$\theta_x$	$\theta_y$	$\theta_z$
A	$L_R \cdot A$	$M_R \cdot A$	$N_R \cdot A$	$L_P \cdot B$ $L_Q \cdot C$	$M_P \cdot B$ $M_Q \cdot C$	$N_P \cdot B$ $N_Q \cdot C$
B	$L_R \cdot D$	$M_R \cdot D$	$N_R \cdot D$	$L_P \cdot E$ $L_Q \cdot F$	$M_P \cdot E$ $M_Q \cdot F$	$N_P \cdot E$ $N_Q \cdot F$
C	$L_R \cdot G$	$M_R \cdot G$	$N_R \cdot G$	$L_P \cdot H$ $L_Q \cdot I$	$M_P \cdot H$ $M_Q \cdot I$	$N_P \cdot H$ $N_Q \cdot I$
D	$L_R \cdot J$	$M_R \cdot J$	$N_R \cdot J$	$L_P \cdot K$ $L_Q \cdot L$	$M_P \cdot K$ $M_Q \cdot L$	$N_P \cdot K$ $N_Q \cdot L$
E	$L_R \cdot M$	$M_R \cdot M$	$N_R \cdot M$	$L_P \cdot N$ $L_Q \cdot O$	$M_P \cdot N$ $M_Q \cdot O$	$N_P \cdot N$ $N_Q \cdot O$
F	$L_R \cdot P$	$M_R \cdot P$	$N_R \cdot P$	$L_P \cdot Q$ $L_Q \cdot R$	$M_P \cdot Q$ $M_Q \cdot R$	$N_P \cdot Q$ $N_Q \cdot R$
G	$L_R \cdot S$	$M_R \cdot S$	$N_R \cdot S$	$L_P \cdot T$ $L_Q \cdot U$	$M_P \cdot T$ $M_Q \cdot U$	$N_P \cdot T$ $N_Q \cdot U$
H	$L_R \cdot V$	$M_R \cdot V$	$N_R \cdot V$	$L_P \cdot W$ $L_Q \cdot X$	$M_P \cdot W$ $M_Q \cdot X$	$N_P \cdot W$ $N_Q \cdot X$
I	$L_R \cdot Y$	$M_R \cdot Y$	$N_R \cdot Y$	$L_P \cdot Z$ $L_Q \cdot AA$	$M_P \cdot Z$ $M_Q \cdot AA$	$N_P \cdot Z$ $N_Q \cdot AA$
J	$L_R \cdot AB$	$M_R \cdot AB$	$N_R \cdot AB$	$L_P \cdot AC$ $L_Q \cdot AD$	$M_P \cdot AC$ $M_Q \cdot AD$	$N_P \cdot AC$ $N_Q \cdot AD$
K	$L_R \cdot AE$	$M_R \cdot AE$	$N_R \cdot AE$	$L_P \cdot AF$ $L_Q \cdot AG$	$M_P \cdot AF$ $M_Q \cdot AG$	$N_P \cdot AF$ $N_Q \cdot AG$
L	$L_R \cdot AH$	$M_R \cdot AH$	$N_R \cdot AH$	$L_P \cdot AI$ $L_Q \cdot AJ$	$M_P \cdot AI$ $M_Q \cdot AJ$	$N_P \cdot AI$ $N_Q \cdot AJ$

GENERAL OUT OF PLANE FORCE MATRIX FOR A RECTANGULAR PLATE

FIGURE 4.14

Code	Block			
	1	2	3	4
A	1,1	1,4	1,7	1,10
B	1,2	1,5	1,8	1,11
C	1,3	1,6	1,9	1,12
D	2,1	2,4	2,7	2,10
E	2,2	2,5	2,8	2,11
F	2,3	2,6	2,9	2,12
G	3,1	3,4	3,7	3,10
H	3,2	3,5	3,8	3,11
I	3,3	3,6	3,9	3,12
J	4,1	4,4	4,7	4,10
K	4,2	4,5	4,8	4,11
L	4,3	4,6	4,9	4,12
M	5,1	5,4	5,7	5,10
N	5,2	5,5	5,8	5,11
O	5,3	5,6	5,9	5,12
P	6,1	6,4	6,7	6,10
Q	6,2	6,5	6,8	6,11
R	6,3	6,6	6,9	6,12

Code	Block			
	1	2	3	4
S	7,1	7,4	7,7	7,10
T	7,2	7,5	7,8	7,11
U	7,3	7,6	7,9	7,12
V	8,1	8,4	8,7	8,10
W	8,2	8,5	8,8	8,11
X	8,3	8,6	8,9	8,12
Y	9,1	9,4	9,7	9,10
Z	9,2	9,5	9,8	9,11
AA	9,3	9,6	9,9	9,12
AB	10,1	10,4	10,7	10,10
AC	10,2	10,5	10,8	10,11
AD	10,3	10,6	10,9	10,12
AE	11,1	11,4	11,7	11,10
AF	11,2	11,5	11,8	11,11
AG	11,3	11,6	11,9	11,12
AH	12,1	12,4	12,7	12,10
AI	12,2	12,5	12,8	12,11
AJ	12,3	12,6	12,9	12,12

KEY TO TERMS WITHIN THE GENERAL OUT OF PLANE BLOCK ELEMENTS REFER  
TO TERMS WITHIN THE OUT OF PLANE STIFFNESS MATRIX.

FIGURE 4.15

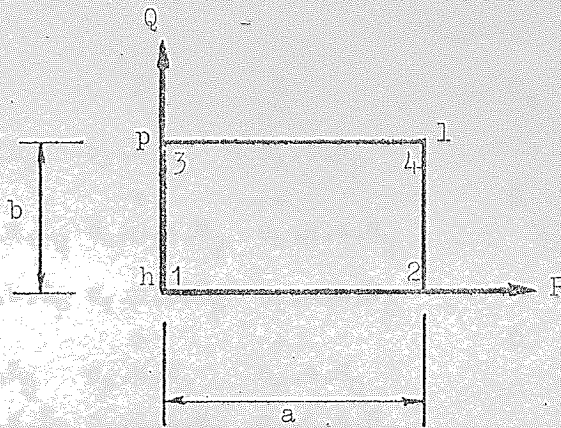


FIGURE 4.16a

$$\frac{E}{2ab(1-\mu^2)} \begin{bmatrix} -b & -\mu \cdot b & b & -\mu \cdot a & b & \mu \cdot a & b & \mu \cdot a \\ -\mu \cdot b & -a & \mu \cdot b & -a & -\mu \cdot b & a & \mu \cdot b & a \\ -a \cdot a & -a \cdot b & -a \cdot a & a \cdot b & a \cdot a & -a \cdot b & a \cdot a & a \cdot b \end{bmatrix} \alpha = \frac{1-\mu}{2}$$

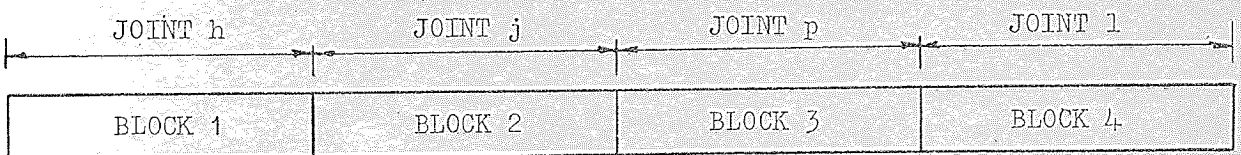
IN PLANE STRESS MATRIX FOR A RECTANGULAR PLATE. RESULTING STRESSES ARE  
COMPUTED AT THE CENTRE OF GRAVITY OF THE PLATE

FIGURE 4.16b

$$\frac{Et}{4ab(1-\mu^2)} \begin{bmatrix} 0 & -\mu \cdot a & b & 0 & -\mu \cdot a & -b & 0 & \mu \cdot a & b & 0 & \mu \cdot a & -b \\ 0 & -a & \mu b & 0 & a & -\mu \cdot b & 0 & a & \mu b & 0 & a & -\mu \cdot b \\ 8 \cdot a & b \cdot a & -a \cdot a & -8 \cdot a & -b \cdot a & -a \cdot a & -8 \cdot a & b \cdot a & a \cdot a & 8 \cdot a & -b \cdot a & a \cdot a \end{bmatrix} \alpha = \frac{1-\mu}{2}$$

OUT OF PLANE STRESS MATRIX FOR A RECTANGULAR PLATE. RESULTING STRESSES ARE  
COMPUTED AT THE CENTRE OF GRAVITY OF THE PLATE

FIGURE 4.16c



LAYOUT OF THE IN PLANE OR OUT OF PLANE DBA MATRIX FOR A RECTANGULAR PLATE

FIGURE 4.16d

FIGURE 4.16



$$\frac{E}{2ab(1-\mu^2)} \begin{bmatrix} \begin{matrix} X & Y & Z \end{matrix} \\ \begin{matrix} c_1 \cdot b \cdot L_P & c_1 \cdot b \cdot M_P & c_1 \cdot b \cdot N_P \\ + & + & + \\ c_2 \cdot \mu \cdot a \cdot L_Q & c_2 \cdot \mu \cdot a \cdot M_Q & c_2 \cdot \mu \cdot a \cdot N_Q \\ c_1 \cdot \mu \cdot b \cdot L_P & c_1 \cdot \mu \cdot b \cdot M_P & c_1 \cdot \mu \cdot b \cdot N_P \\ + & + & + \\ c_2 \cdot a \cdot L_Q & c_2 \cdot a \cdot M_Q & c_2 \cdot a \cdot N_Q \\ c_2 \cdot a \cdot a \cdot L_P & c_2 \cdot a \cdot a \cdot M_P & c_2 \cdot a \cdot a \cdot N_P \\ + & + & + \\ c_1 \cdot a \cdot b \cdot L_Q & c_1 \cdot a \cdot b \cdot M_Q & c_1 \cdot a \cdot b \cdot N_Q \end{matrix} \end{bmatrix} \begin{bmatrix} \theta_x & \theta_y & \theta_z \\ 0 & 0 & 0 \\ 0 & 0 & 0 \\ 0 & 0 & 0 \end{bmatrix}$$

$$a = \frac{1-\mu}{2}$$

GENERAL IN PLANE DBA BLOCK FOR A RECTANGULAR PLATE. RESULTING STRESSES  
ARE COMPUTED AT THE CENTRE OF GRAVITY OF THE PLATE

FIGURE 4.17a

		BLOCK CODE			
		1	2	3	4
SIGN	$c_1$	-1	+1	-1	+1
CODE	$c_2$	-1	-1	+1	+1

KEY TO TERMS WITHIN THE GENERAL IN PLANE DBA BLOCK

FIGURE 4.17b

FIGURE 4.17

$$\frac{Et}{4ab(1-\mu^2)} \begin{bmatrix} X & Y & Z & \theta_x & \theta_y & \theta_z \\ 0 & 0 & 0 & s_1 \cdot \mu \cdot a \cdot L_P & s_1 \cdot \mu \cdot a \cdot M_P & s_1 \cdot \mu \cdot a \cdot N_P \\ & & & + & + & + \\ & & & s_2 \cdot b \cdot L_Q & s_2 \cdot b \cdot M_Q & s_2 \cdot b \cdot N_Q \\ 0 & 0 & 0 & s_1 \cdot a \cdot L_P & s_1 \cdot a \cdot M_P & s_1 \cdot a \cdot N_P \\ & & & + & + & + \\ & & & s_2 \cdot \mu \cdot b \cdot L_Q & s_2 \cdot \mu \cdot b \cdot M_Q & s_2 \cdot \mu \cdot b \cdot N_Q \\ s_3 \cdot 8 \cdot a \cdot L_R & s_3 \cdot 8 \cdot a \cdot M_R & s_3 \cdot 8 \cdot a \cdot N_R & s_2 \cdot b \cdot a \cdot L_P & s_2 \cdot b \cdot a \cdot M_P & s_2 \cdot b \cdot a \cdot N_P \\ & & & + & + & + \\ & & & s_1 \cdot a \cdot a \cdot L_Q & s_1 \cdot a \cdot a \cdot M_Q & s_1 \cdot a \cdot a \cdot N_Q \end{bmatrix}$$

$$\alpha = \frac{1-\mu}{2}$$

GENERAL OUT OF PLANE DBA BLOCK FOR A RECTANGULAR PLATE.

FINAL STRESSES ARE COMPUTED AT THE CENTRE OF GRAVITY OF THE PLATE

FIGURE 4.18a

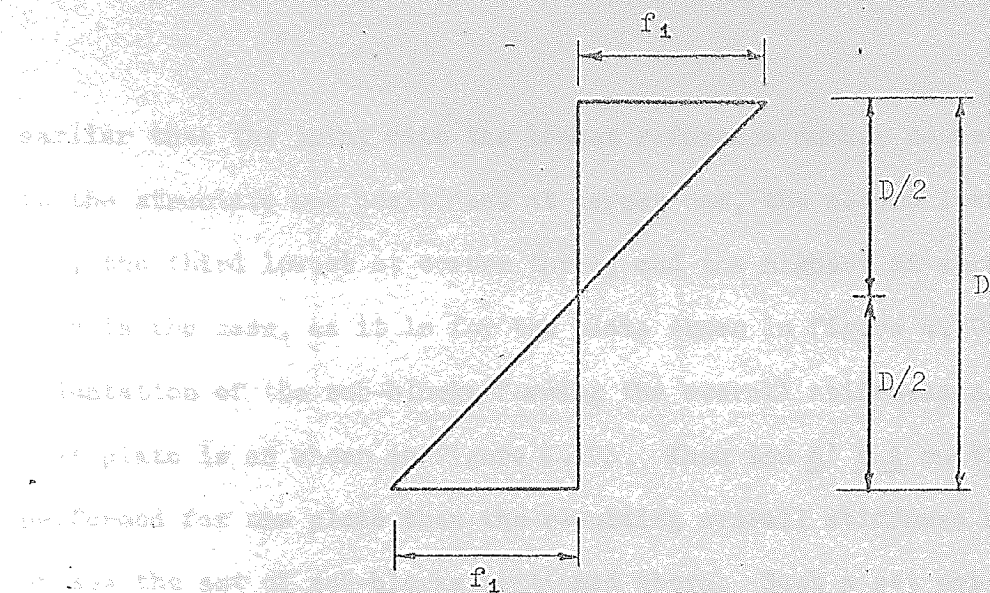
		BLOCK CODE			
		1	2	3	4
SIGN CODE	$s_1$	-1	-1	+1	+1
	$s_2$	+1	-1	+1	-1
	$s_3$	+1	-1	-1	+1

KEY TO TERMS WITHIN THE GENERAL OUT OF PLANE BLOCK

FIGURE 4.18b

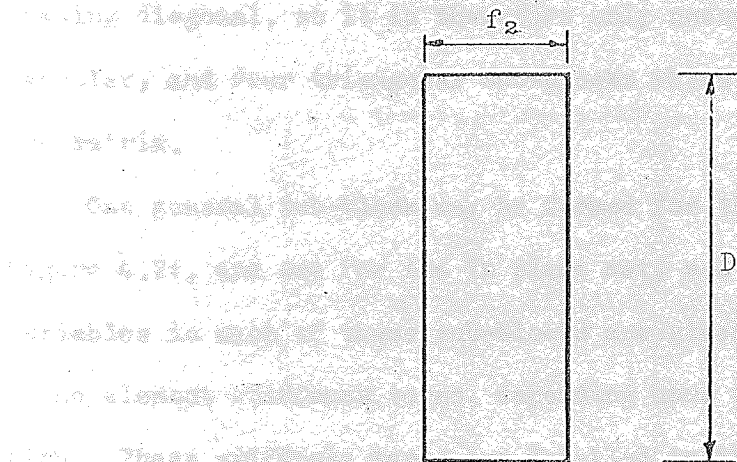
FIGURE 4.18





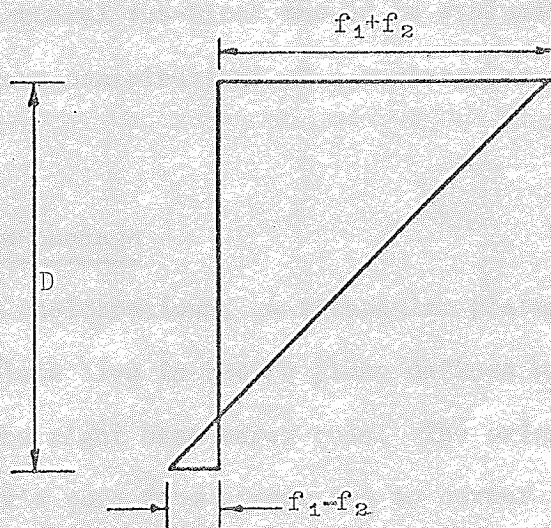
ASSUMED STRESS DISTRIBUTION DUE TO OUT OF PLANE FORCES

FIGURE 4.19a



ASSUMED STRESS DISTRIBUTION DUE TO IN PLANE FORCES

FIGURE 4.19b



ASSUMED RESULTANT STRESS DISTRIBUTION

FIGURE 4.19c

FIGURE 4.19

earlier that the joint with the lowest reference number connecting the plate to the structure was positioned at corner one, the second lowest at corner two, the third lowest at corner three, and the highest at corner four. When this is the case, as it is for the plate shown in figure 4.20a, then the orientation of the sub-blocks forming the overall stiffness contribution of that plate is as shown in figure 4.20b. When the  $\underline{A}' \underline{k} \underline{A}$  multiplication is performed for one plate then the resulting overall stiffness matrix comprises the set of sub-blocks mentioned above. Such a set exists for both in and out of plane cases. Both of these sets are symmetrical about their leading diagonal, so it is therefore only necessary to consider the six rectangular, and four triangular sub-blocks which form the lower triangle of the matrix.

One general sub-block may be formed for the out of plane set, see figure 4.21, and one for the in plane set, see figure 4.22. The unassigned variables in each of these sub-blocks are given the relevant in or out of plane element stiffness terms, depending upon the sub-block under construction. These stiffness terms are detailed in the table given in figure 4.23. In the case of triangular sub-blocks only the on diagonal and lower triangle terms of the relevant general sub-block should be evaluated. In this manner all the overall stiffness contributions of a rectangular plate may be generated.

#### (4.5) Triangular plate package

(4.5.1) General Considerations. A triangular plate element is shown in figure 4.24. The plate lies in the PQ plane defined by its local axes P, Q, R which conform to the right hand screw rule. The origin of these axes is at corner one, the P axis runs from corner one to corner two, the Q axis is orthogonal to the side between corners one and two and runs in the direction of corner three. Each corner may experience both local in plane displacements  $u$  and  $v$  as well as local out of plane displacements  $a_P$ ,  $a_Q$  and  $w$ . Such



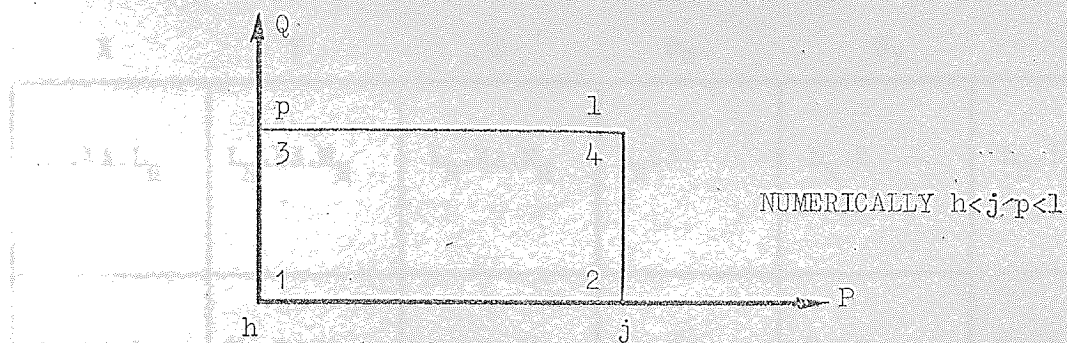


FIGURE 4.20a.

	h	j	p	l
h	hh	hj	hp	hl
j	jh	jj	jp	jl
p	ph	pj	pp	pl
l	lh	lj	lp	ll

THE ORIENTATION OF THE SIXTEEN SUB-BLOCKS FORMED BY A RECTANGULAR PLATE

FIGURE 4.20b

FIGURE 4.20



	X	Y	Z	$\theta_x$	$\theta_y$	$\theta_z$
X	$L_R \cdot XA \cdot L_R$	$L_R \cdot XA \cdot M_R$	$L_R \cdot XA \cdot N_R$	$L_R \cdot J$	$L_R \cdot K$	$L_R \cdot L$
Y	$M_R \cdot XA \cdot L_R$	$M_R \cdot XA \cdot M_R$	$M_R \cdot XA \cdot N_R$	$M_R \cdot J$	$M_R \cdot K$	$M_R \cdot L$
Z	$N_R \cdot XA \cdot L_R$	$N_R \cdot XA \cdot M_R$	$N_R \cdot XA \cdot N_R$	$N_R \cdot J$	$N_R \cdot K$	$N_R \cdot L$
$\theta_x$	$L_R \cdot A$	$M_R \cdot A$	$N_R \cdot A$	$L_P \cdot B$ + $L_Q \cdot C$	$M_P \cdot B$ + $M_Q \cdot C$	$N_P \cdot B$ + $N_Q \cdot C$
$\theta_y$	$L_R \cdot D$	$M_R \cdot D$	$N_R \cdot D$	$L_P \cdot E$ + $L_Q \cdot F$	$M_P \cdot E$ + $M_Q \cdot F$	$N_P \cdot E$ + $N_Q \cdot F$
$\theta_z$	$L_R \cdot G$	$M_R \cdot G$	$N_R \cdot G$	$L_P \cdot H$ + $L_Q \cdot I$	$M_P \cdot H$ + $M_Q \cdot I$	$N_P \cdot H$ + $N_Q \cdot I$

$$A = (L_P \cdot XB + L_Q \cdot XC) ;$$

$$B = (L_P \cdot XF + L_Q \cdot XG) ;$$

$$C = (L_P \cdot XH + L_Q \cdot XI) ;$$

$$D = (M_P \cdot XB + M_Q \cdot XC) ;$$

$$E = (M_P \cdot XF + M_Q \cdot XG) ;$$

$$F = (M_P \cdot XH + M_Q \cdot XI) ;$$

$$G = (N_P \cdot XB + N_Q \cdot XC) ;$$

$$H = (N_P \cdot XF + N_Q \cdot XG) ;$$

$$I = (N_P \cdot XH + N_Q \cdot XI) ;$$

$$J = (L_P \cdot XD + L_Q \cdot XE) ;$$

$$K = (M_P \cdot XD + M_Q \cdot XE) ;$$

$$L = (N_P \cdot XD + N_Q \cdot XE) ;$$

GENERAL RECTANGULAR AND TRIANGULAR SUB-BLOCK FOR THE OUT OF  
PLANE OVERALL STIFFNESS CONTRIBUTION OF A RECTANGULAR PLATE

FIGURE 4.21

	X	Y	Z	$\theta_x$	$\theta_y$	$\theta_3$
X	$L_P \cdot A$ +	$M_P \cdot A$ +	$N_P \cdot A$ +	0	0	0
	$L_Q \cdot B$	$M_Q \cdot B$	$N_Q \cdot B$			
Y	$L_P \cdot C$ +	$M_P \cdot C$ +	$N_P \cdot C$ +	0	0	0
	$L_Q \cdot D$	$M_Q \cdot D$	$N_Q \cdot D$			
Z	$L_P \cdot E$ +	$M_P \cdot E$ +	$N_P \cdot E$ +	0	0	0
	$L_Q \cdot F$	$M_Q \cdot F$	$N_Q \cdot F$			
$\theta_x$	0	0	0	0	0	0
$\theta_y$	0	0	0	0	0	0
$\theta_3$	0	0	0	0	0	0

$$A = (L_P \cdot ZA + L_Q \cdot ZB) ; \quad C = (M_P \cdot ZA + M_Q \cdot ZB) ; \quad E = (N_P \cdot ZA + N_Q \cdot ZB) ;$$

$$B = (L_P \cdot ZC + L_Q \cdot ZD) ; \quad D = (M_P \cdot ZC + M_Q \cdot ZD) ; \quad F = (N_P \cdot ZC + N_Q \cdot ZD) ;$$

GENERAL RECTANGULAR AND TRIANGULAR SUB-BLOCK FOR THE IN PLANE  
OVERALL STIFFNESS CONTRIBUTION OF A RECTANGULAR PLATE

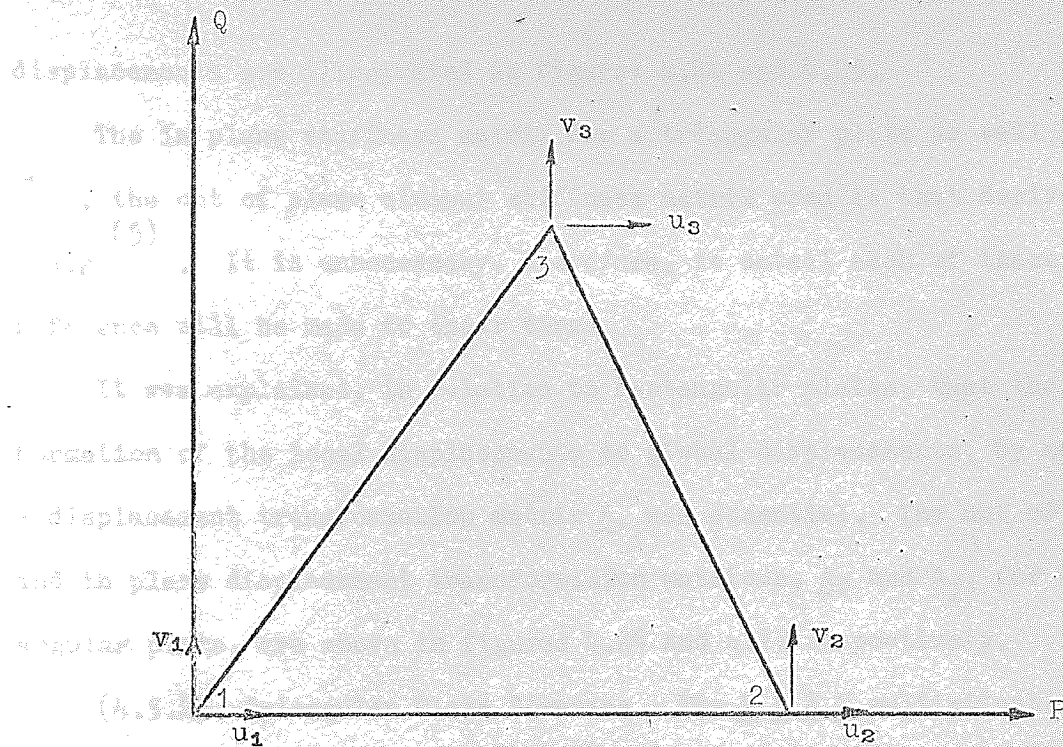
FIGURE 4.22



		Triangular Sub-Blocks				Rectangular Sub-Blocks					
		hh	jj	pp	ll	jh	ph	pj	lh	lj	lp
OUT OF PLANE CODES	XA	1,1	4,4	7,7	10,10	4,1	7,1	7,4	10,1	10,4	10,7
	XB	2,1	5,4	8,7	11,10	5,1	8,1	8,4	11,1	11,4	11,7
	XC	3,1	6,4	9,7	12,10	6,1	9,1	9,4	12,1	12,4	12,7
	XD	1,2	4,5	7,8	10,11	4,2	7,2	7,5	10,2	10,5	10,8
	XE	1,3	4,6	7,9	10,12	4,3	7,3	7,6	10,3	10,6	10,9
	XF	2,2	5,5	8,8	11,11	5,2	8,2	8,5	11,2	11,5	11,8
	XG	3,2	6,5	9,8	12,11	6,2	9,2	9,5	12,2	12,5	12,8
	XH	2,3	5,6	8,9	11,12	5,3	8,3	8,6	11,3	11,6	11,9
	XI	3,3	6,6	9,9	12,12	6,3	9,3	9,6	12,3	12,6	12,9
IN PLANE CODES	ZA	1,1	3,3	5,5	7,7	3,1	5,1	5,3	7,1	7,3	7,5
	ZB	2,1	4,3	6,5	8,7	4,1	6,1	6,3	8,1	8,3	8,5
	ZC	1,2	3,4	5,6	7,8	3,2	5,2	5,4	7,2	7,4	7,6
	ZD	2,2	4,4	6,6	8,8	4,2	6,2	6,4	8,2	8,4	8,6

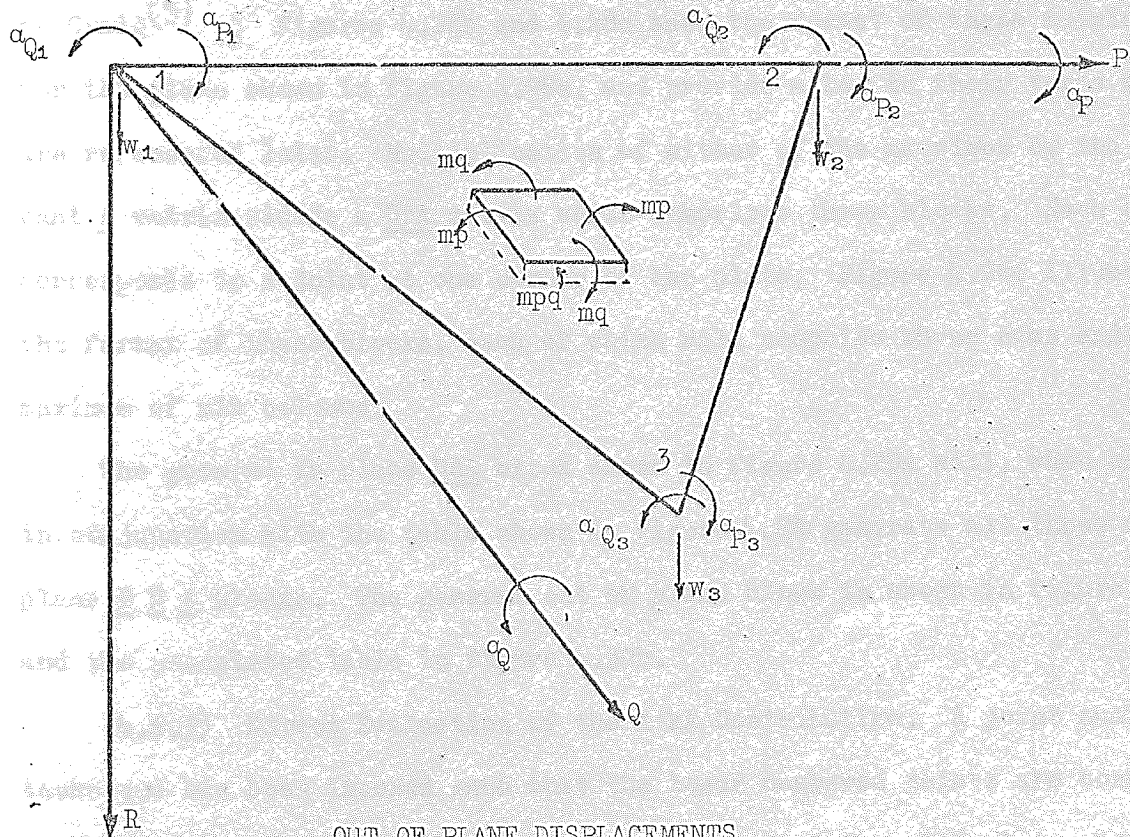
TABLE RELATING THE CODES FOR THE GENERAL IN AND OUT OF PLANE SUB-BLOCKS.  
 OUT OF PLANE CODE REFER TO ELEMENTS OF THE OUT OF PLANE STIFFNESS MATRIX.  
 IN PLANE CODE REFER TO ELEMENTS OF THE OUT OF PLANE STIFFNESS MATRIX.

FIGURE 4.23



IN PLANE DISPLACEMENTS

FIGURE 4.24



OUT OF PLANE DISPLACEMENTS

FIGURE 4.25



displacements are illustrated in figures 4.24 and 4.25.

The in plane stiffness matrix for a triangular plate is well documented<sup>(27, 1)</sup>, the out of plane element stiffness matrix used is that derived by Craig<sup>(5)</sup>. It is unnecessary, therefore, to detail each of these although reference will be made to their terms.

It was explained, in relation to rectangular plates, that the transformation of the local displacements to global displacements, by means of a displacement transformation matrix  $\underline{A}$ , was essential. The out of plane and in plane displacement transformation matrices,  $\underline{A}_0$  and  $\underline{A}_I$ , for a triangular plate, are shown in figures 4.26 and 4.27 respectively.

(4.5.2) Triangular Plate Stresses. The  $\underline{D} \underline{B} \underline{A} \underline{X}$  multiplication for each element yields the stresses at a point within that element. In order that this multiplication may be carried out it is necessary to form the  $\underline{DBA}$  matrix for each element. The out of plane and in plane  $\underline{D} \underline{B}$  matrices for stresses at the centre of gravity of a triangular plate have been detailed by Craig<sup>(5)</sup>. Figures 4.28b and 4.28c show the format of these matrices for the plate shown in figure 4.28a, and provide a key to their terms which are referenced later. Multiplication of either of the matrices by the relevant  $\underline{A}$  matrix yields a  $\underline{DBA}$  matrix which comprises three blocks. Each block corresponds to a joint at one corner of the plate. Figure 4.28d illustrates the format of these blocks, each of which will comprise three rows and a maximum of six columns.

The general in plane  $\underline{DBA}$  block shown in figure 4.29a will, when used in conjunction with the table shown in figure 4.29b generate all three in plane  $\underline{D} \underline{B} \underline{A}$  blocks. The general out of plane block is shown in figure 4.30a and the associated table in figure 4.30b.

(4.5.3) Direct Evaluation of the  $A'kA$  Contribution. A joint numbering technique has been imposed such that the lower numbered joints are connected to the lower numbered corners, this is so for the triangular plate shown in figure 4.31a. A consequence of this is that the orientation of the nine

$$\begin{bmatrix} w_1 \\ \alpha_{P1} \\ \alpha_{Q1} \\ w_2 \\ \alpha_{P2} \\ \alpha_{Q2} \\ w_3 \\ \alpha_{P3} \\ \alpha_{Q3} \end{bmatrix} = \begin{bmatrix} L_R & M_R & N_R \\ & L_P & M_P & N_P \\ & L_Q & M_Q & N_Q \\ & & \dots & L_R & M_R & N_R \\ & & & L_M & M_P & N_P \\ & & & L_Q & M_Q & N_Q \\ & & & & \dots & L_R & M_R & N_R \\ & & & & & L_P & M_P & N_P \\ & & & & & L_Q & M_Q & N_Q \end{bmatrix} \times \begin{bmatrix} X_1 \\ Y_1 \\ Z_1 \\ \theta_{X1} \\ \theta_{Y1} \\ \theta_{Z1} \\ \vdots \\ X_2 \\ Y_2 \\ Z_2 \\ \theta_{X2} \\ \theta_{Y2} \\ \theta_{Z2} \\ \vdots \\ X_3 \\ Y_3 \\ Z_3 \\ \theta_{X3} \\ \theta_{Y3} \\ \theta_{Z3} \end{bmatrix}$$

$$\underline{Z} = \underline{A_0} \underline{X}$$

OUT OF PLANE DISPLACEMENT TRANSFORMATION MATRIX FOR A TRIANGULAR PLATE

FIGURE 4.26

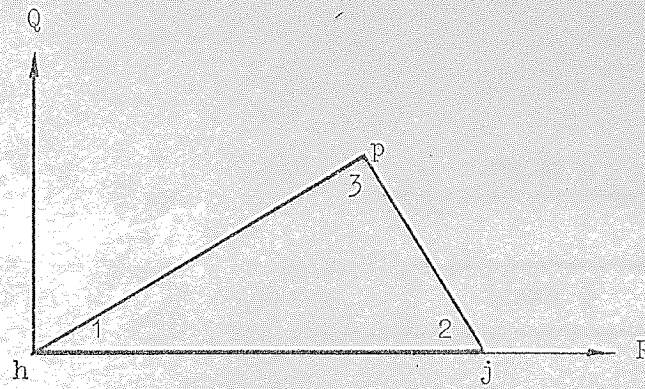


$$\begin{bmatrix} u_1 \\ v_1 \\ u_2 \\ v_2 \\ u_3 \\ v_3 \end{bmatrix} = \begin{bmatrix} L_P & M_P & N_P \\ L_Q & M_Q & N_Q \\ \dots & L_P & M_P & N_P \\ & L_Q & M_Q & N_Q \\ & \dots & L_P & M_P & N_P \\ & & L_Q & M_Q & N_Q \end{bmatrix} \times \begin{bmatrix} X_1 \\ Y_1 \\ Z_1 \\ \theta X_1 \\ \theta Y_1 \\ \theta Z_1 \\ \vdots \\ X_2 \\ Y_2 \\ Z_2 \\ \theta X_2 \\ \theta Y_2 \\ \theta Z_2 \\ \vdots \\ X_3 \\ Y_3 \\ Z_3 \\ \theta X_3 \\ \theta Y_3 \\ \theta Z_3 \end{bmatrix}$$

$$\underline{Z} = \underline{A}^{-1} \underline{X}$$

IN PLANE DISPLACEMENT TRANSFORMATION MATRIX FOR A TRIANGULAR PLATE

FIGURE 4.27



NUMERICALLY  $h < j < p$

FIGURE 4.28a

$$\begin{bmatrix} \sigma_P \\ \sigma_Q \\ \tau_{PQ} \end{bmatrix} = \begin{bmatrix} 1,1 & 1,2 & 1,3 & 1,4 & 1,5 & 1,6 & 1,7 & 1,8 & 1,9 \\ 2,1 & 2,2 & 2,3 & 2,4 & 2,5 & 2,6 & 2,7 & 2,8 & 2,9 \\ 3,1 & 3,2 & 3,3 & 3,4 & 3,5 & 3,6 & 3,7 & 3,8 & 3,9 \end{bmatrix} \times \begin{bmatrix} w_1 \\ a_{P_1} \\ a_{Q_1} \\ w_2 \\ a_{P_2} \\ a_{Q_2} \\ w_3 \\ a_{P_3} \\ a_{Q_3} \end{bmatrix}$$

$$\underline{\sigma}_o = \underline{DB}_o \underline{Z}_o$$

KEY TO THE TERMS COMPRISING THE OUT OF PLANE STRESS MATRIX FOR A  
TRIANGULAR PLATE

FIGURE 4.28b

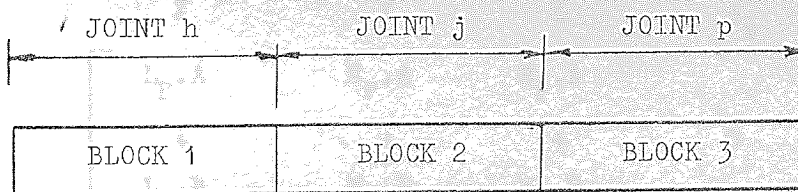
$$\begin{bmatrix} \sigma_P \\ \sigma_Q \\ \tau_{PQ} \end{bmatrix} = \begin{bmatrix} 1,1 & 1,2 & 1,3 & 1,4 & 1,5 & 1,6 \\ 2,1 & 2,2 & 2,3 & 2,4 & 2,5 & 2,6 \\ 3,1 & 3,2 & 3,3 & 3,4 & 3,5 & 3,6 \end{bmatrix} \times \begin{bmatrix} u_1 \\ v_1 \\ u_2 \\ v_2 \\ u_3 \\ v_3 \end{bmatrix}$$

$$\underline{\sigma}_I = \underline{DB}_I \underline{Z}_I$$

KEY TO THE TERMS COMPRISING THE IN PLANE STRESS MATRIX FOR A TRIANGULAR  
PLATE

FIGURE 4.28c





FORMAT FOR THE IN PLANE AND OUT OF PLANE DBA MATRIX FOR A TRIANGULAR PLATE

FIGURE 4.28a

FIGURE 4.28

$$\begin{array}{c}
 \begin{array}{ccccc}
 X & Y & Z & \theta_x & \theta_y & \theta_z
 \end{array} \\
 \left[ \begin{array}{ccccc}
 L_P \cdot A & M_P \cdot A & N_P \cdot A & & \\
 + & + & + & 0 & 0 & 0 \\
 L_Q \cdot B & M_Q \cdot B & N_Q \cdot B & & & \\
 + & + & + & 0 & 0 & 0 \\
 L_P \cdot C & M_P \cdot C & N_P \cdot C & & & \\
 + & + & + & 0 & 0 & 0 \\
 L_Q \cdot D & M_Q \cdot D & N_Q \cdot D & & & \\
 + & + & + & 0 & 0 & 0 \\
 L_P \cdot E & M_P \cdot E & N_P \cdot E & & & \\
 + & + & + & 0 & 0 & 0 \\
 L_Q \cdot F & M_Q \cdot F & N_Q \cdot F & & & 
 \end{array} \right]
 \end{array}$$

GENERAL IN PLANE DBA BLOCK FOR A TRIANGULAR PLATE. STRESSES AT THE CENTRE OF GRAVITY OF THE PLATE

FIGURE 4.29a

BLOCK NUMBER	ARRAY CODES					
	A	B	C	D	E	F
1	1,1	1,2	1,3	1,4	1,5	1,6
2	2,1	2,2	2,3	2,4	2,5	2,6
3	3,1	3,2	3,3	3,4	3,5	3,6

KEY TO TERMS WITHIN THE GENERAL IN PLANE DBA BLOCK

ARRAY CODES REFER TO ELEMENTS OF THE IN PLANE ELEMENT STIFFNESS MATRIX

FIGURE 4.29b

FIGURE 4.29



X	Y	Z	$\theta_x$	$\theta_y$	$\theta_z$
$L_R \cdot A$	$M_R \cdot A$	$N_R \cdot A$	$L_P \cdot B$ +	$M_P \cdot B$ +	$N_P \cdot B$ +
			$L_Q \cdot C$	$M_Q \cdot C$	$N_Q \cdot C$
$L_R \cdot D$	$M_R \cdot D$	$N_R \cdot D$	$L_P \cdot E$ +	$M_P \cdot E$ +	$N_P \cdot E$ +
			$L_Q \cdot F$	$M_Q \cdot F$	$N_Q \cdot F$
$L_R \cdot G$	$M_R \cdot G$	$N_R \cdot G$	$L_P \cdot H$ +	$M_P \cdot H$ +	$N_P \cdot H$ +
			$L_Q \cdot I$	$M_Q \cdot I$	$N_Q \cdot I$

GENERAL OUT OF PLANE DBA BLOCK FOR A TRIANGULAR PLATE

STRESSES AT THE CENTRE OF GRAVITY OF THE PLATE

FIGURE 4.30a

BLOCK NUMBER	ARRAY CODE								
	A	B	C	D	E	F	G	H	I
1	1,1	1,2	1,3	2,1	2,2	2,3	3,1	3,2	3,3
2	1,4	1,5	1,6	2,4	2,5	2,6	3,4	3,5	3,6
3	1,7	1,8	1,9	2,7	2,8	2,9	3,7	3,8	3,9

KEY TO TERMS WITHIN THE GENERAL OUT OF PLANE DBA BLOCK

ARRAY CODES REFER TO ELEMENTS OF THE OUT OF PLANE ELEMENT STIFFNESS  
MATRIX

FIGURE 4.30b

FIGURE 4.30

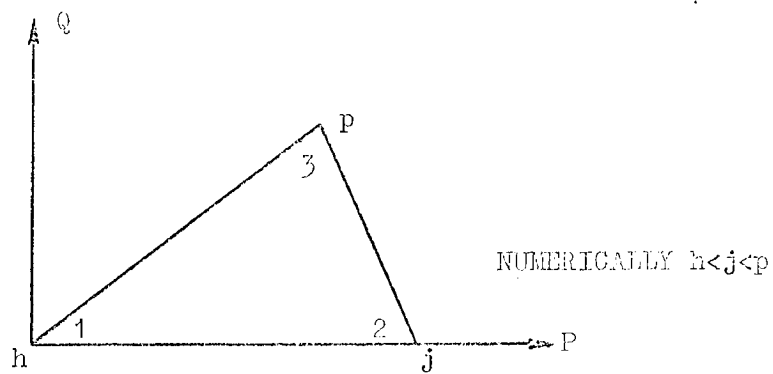
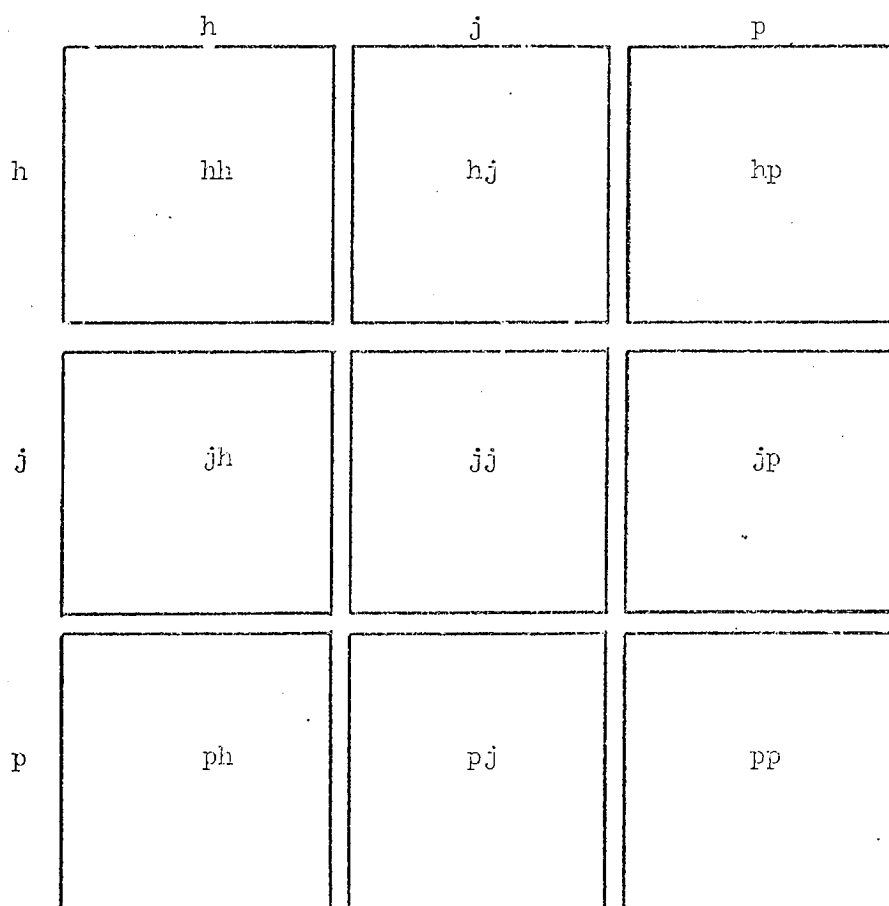


FIGURE 4.31 a



THE ORIENTATION OF THE NINE SUB-BLOCKS FORMED BY A TRIANGULAR PLATE

FIGURE 4.31 b

FIGURE 4.31

sub-blocks forming the contribution of such a triangular plate to the overall stiffness matrix is that shown in figure 4.31b. There are two such sets of sub-blocks, one for the in plane and one for the out of plane case. Since each set is symmetrical about its leading diagonal then it is only necessary to consider the three triangular and the three rectangular sub-blocks comprising the lower triangle of figure 4.31b.

The general out of plane sub-block is illustrated in figure 4.32 and when used in conjunction with the table given in figure 4.34 yields the required out of plane sub-blocks. Similarly the in plane sub-blocks may be formed by consideration of the general sub-block shown in figure 4.33 and the table in figure 4.34.

#### (4.6) Prismatic member package

(4.6.1) General considerations. Figure 4.35 shows a prismatic member with its local axes P, Q, R. The origin of these axes is at the arbitrarily defined end A of a member, the P axis runs from end A to end B, and the Q axis, which is orthogonal to the P axis, lies in the PQ plane. This plane is defined by the joints at the members ends along with a third, in plane, joint. If the right hand screw rule is used then the direction of the R axis is fixed.

Each end of the member may experience three rotations and three translations; these are illustrated in figure 4.36. The result of these movements is a vector, comprising eight displacements, which is shown in figure 4.37. This figure gives the terms comprising the element stiffness matrix of a member <sup>(2)</sup>. Each of these terms has been assigned a code value to be used in subsequent tables, these code values are given in figure 4.38. The inclusion of the product moment of inertia in the matrix permits the analysis of structures containing members having no axis of symmetry.

Member displacements have been relative to the local axes, and the displacement transformation matrix,  $A_F$ , is required to reconcile such

	X	Y	Z	$\theta_x$	$\theta_y$	$\theta_z$
X	$XA \cdot L_R \cdot L_R$	$XA \cdot M_R \cdot L_R$	$XA \cdot N_R \cdot L_R$	$L_R \cdot G$	$L_R \cdot H$	$L_R \cdot I$
Y	$XA \cdot M_R \cdot L_R$	$XA \cdot M_R \cdot M_R$	$XA \cdot M_R \cdot N_R$	$M_R \cdot G$	$M_R \cdot H$	$M_R \cdot I$
Z	$XA \cdot N_R \cdot L_R$	$XA \cdot N_R \cdot M_R$	$XA \cdot N_R \cdot N_R$	$N_R \cdot G$	$N_R \cdot H$	$N_R \cdot I$
$\theta_x$	$L_R \cdot J$	$M_R \cdot J$	$N_R \cdot J$	$L_P \cdot A$ + $L_Q \cdot B$	$L_P \cdot C$ + $L_Q \cdot D$	$L_P \cdot E$ + $L_Q \cdot F$
$\theta_y$	$L_R \cdot K$	$M_R \cdot K$	$N_R \cdot K$	$M_P \cdot A$ + $M_Q \cdot B$	$M_P \cdot C$ + $M_Q \cdot D$	$M_P \cdot E$ + $M_Q \cdot F$
$\theta_z$	$L_R \cdot L$	$M_R \cdot L$	$N_R \cdot L$	$N_P \cdot A$ + $N_Q \cdot B$	$N_P \cdot C$ + $N_Q \cdot D$	$N_P \cdot E$ + $N_Q \cdot F$

$$A = XF \cdot L_P + XG \cdot L_Q ;$$

$$B = XH \cdot L_P + XI \cdot L_Q ;$$

$$C = XF \cdot M_P + XG \cdot M_Q ;$$

$$D = XH \cdot M_P + XI \cdot M_Q ;$$

$$E = XF \cdot N_P + XG \cdot N_Q ;$$

$$F = XH \cdot N_P + XI \cdot N_Q ;$$

$$G = XB \cdot L_P + XC \cdot L_Q ;$$

$$H = XB \cdot M_P + XC \cdot N_Q ;$$

$$I = XB \cdot N_P + XC \cdot N_Q ;$$

$$J = XD \cdot L_P + XE \cdot L_Q ;$$

$$K = XD \cdot M_P + XE \cdot M_Q ;$$

$$L = XD \cdot N_P + XE \cdot N_Q ;$$

GENERAL RECTANGULAR AND TRIANGULAR SUB-BLOCK FOR THE OUT OF PLANE

OVERALL STIFFNESS CONTRIBUTION OF A TRIANGULAR PLATE

FIGURE 4.32

	X	Y	Z	$\theta_x$	$\theta_y$	$\theta_3$
X	$L_P \cdot A$ + $L_Q \cdot B$	$L_P \cdot C$ + $L_Q \cdot D$	$L_P \cdot E$ + $L_Q \cdot F$	0	0	0
Y	$M_P \cdot A$ + $M_Q \cdot B$	$M_P \cdot C$ + $M_Q \cdot D$	$M_P \cdot E$ + $M_Q \cdot F$	0	0	0
Z	$N_P \cdot A$ + $N_Q \cdot B$	$N_P \cdot C$ + $N_Q \cdot D$	$N_P \cdot E$ + $N_Q \cdot F$	0	0	0
$\theta_x$	0	0	0	0	0	0
$\theta_y$	0	0	0	0	0	0
$\theta_3$	0	0	0	0	0	0

$$A = Y_A \cdot L_P + Y_B \cdot L_Q ;$$

$$B = Y_C \cdot L_P + Y_D \cdot L_Q ;$$

$$C = Y_A \cdot M_P + Y_B \cdot M_Q ;$$

$$D = Y_C \cdot M_P + Y_D \cdot M_Q ;$$

$$E = Y_A \cdot N_P + Y_B \cdot N_Q ;$$

$$F = Y_C \cdot N_P + Y_D \cdot N_Q ;$$

GENERAL RECTANGULAR AND TRIANGULAR SUB-BLOCK FOR THE IN PLANE OVERALL  
STIFFNESS CONTRIBUTION OF A TRIANGULAR PLATE

FIGURE 4.33

		TRIANGULAR SUB-BLOCKS			RECTANGULAR SUB-BLOCKS		
		hh	jj	pp	jh	ph	pj
OUT OF PLANE CODES	XA	1,1	4,4	7,7	4,1	7,1	7,4
	XB	-	-	-	4,2	7,2	7,5
	XC	-	-	-	4,3	7,3	7,6
	XD	2,1	5,4	8,7	5,1	8,1	8,4
	XE	3,1	6,4	9,7	6,1	9,1	9,4
	XF	2,2	5,5	8,8	5,2	8,2	8,5
	XG	2,3	5,6	8,9	5,3	8,3	8,6
	XH	3,2	6,5	9,8	6,2	9,2	9,5
	XI	3,3	6,6	9,9	6,3	9,3	9,6
IN PLANE CODES	YA	1,1	3,3	5,5	3,1	5,1	5,3
	YB	1,2	3,4	5,6	3,2	5,2	5,4
	YC	2,1	4,3	6,5	4,1	6,1	6,3
	YD	2,2	4,4	6,6	4,2	6,2	6,4

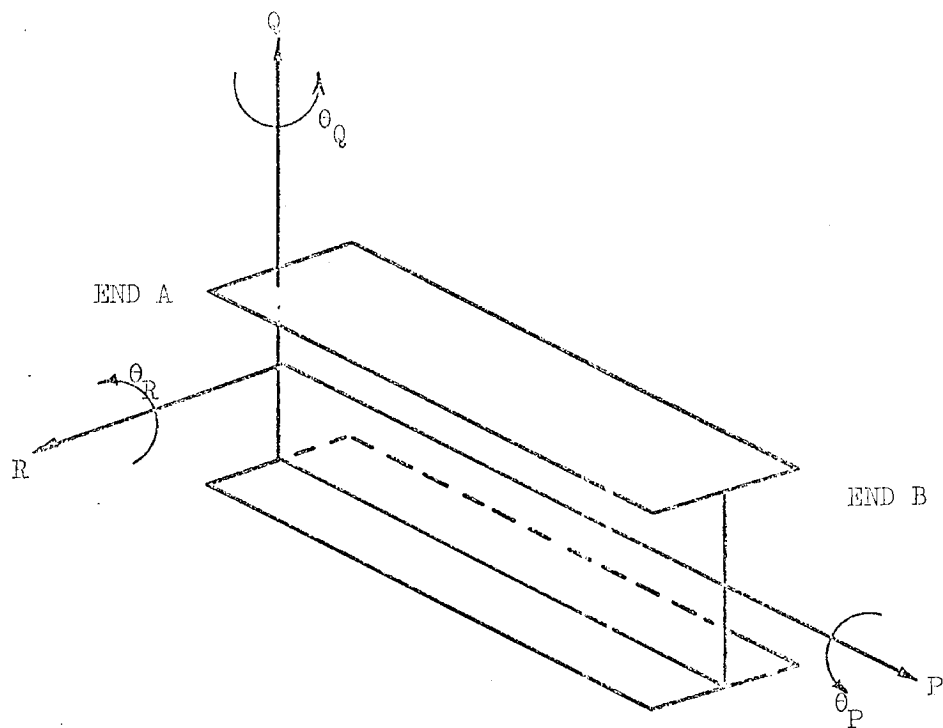
TABLE RELATING THE CODES IN FIGURES 4.32 AND 4.33 TO TERMS IN THE  
RELEVANT ELEMENT STIFFNESS MATRIX

IN PLANE CODES REFER TO TERMS IN THE IN PLANE STIFFNESS MATRIX

OUT OF PLANE CODES REFER TO TERMS IN THE OUT OF PLANE STIFFNESS  
MATRIX

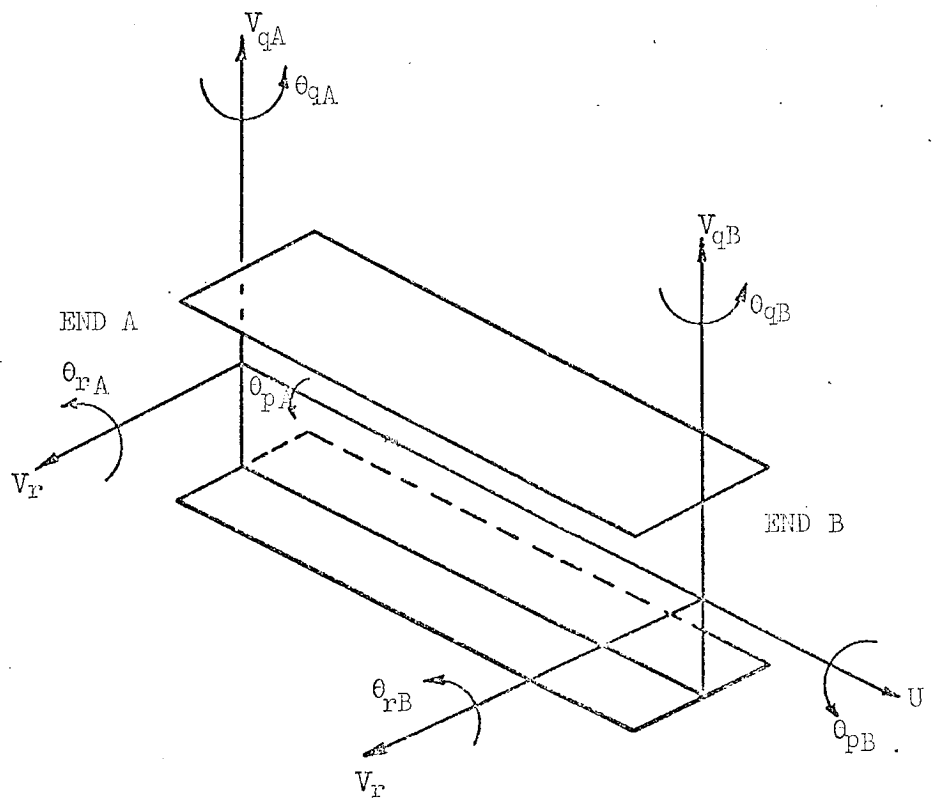
FIGURE 4.34





MEMBER REFERENCE AXES

FIGURE 4.35



MEMBER DEFLECTIONS AT EACH END

FIGURE 4.36

$$\begin{bmatrix} P \\ S_q \\ M_{rA} \\ M_{rB} \\ T \\ S_r \\ M_{qA} \\ M_{qB} \end{bmatrix} = \begin{bmatrix} \frac{E \cdot A \cdot \epsilon}{l} \\ 0 & \frac{12E \cdot I_r}{l^3} \\ 0 & \frac{-6E \cdot I_r}{l^2} & \frac{4E \cdot I_r}{l} \\ 0 & \frac{-6E \cdot I_r}{l^2} & \frac{2E \cdot I_r}{l} & \frac{4E \cdot I_r}{l} & \text{SYMMETRICAL} \\ 0 & \frac{12E \cdot A_1}{l^3} & \frac{-6E \cdot A_1}{l^2} & \frac{-6E \cdot A_1}{l^2} & D \\ 0 & \frac{12E \cdot I_{qr}}{l^3} & \frac{-6E \cdot I_{qr}}{l^2} & \frac{-6E \cdot I_{qr}}{l^2} & \frac{12E \cdot A_2}{l^3} & \frac{12E \cdot I_q}{l^3} \\ 0 & \frac{-6E \cdot I_{qr}}{l^2} & \frac{4E \cdot I_{qr}}{l} & \frac{2E \cdot I_{qr}}{l} & \frac{-6E \cdot A_2}{l^2} & \frac{-6E \cdot I_q}{l^2} & \frac{4E \cdot I_q}{l} \\ 0 & \frac{-6E \cdot I_{qr}}{l^2} & \frac{2E \cdot I_{qr}}{l} & \frac{4E \cdot I_{qr}}{l} & \frac{-6E \cdot A_2}{l^2} & \frac{-6E \cdot I_q}{l^2} & \frac{2E \cdot I_q}{l} & \frac{4E \cdot I_q}{l} \end{bmatrix} \times \begin{bmatrix} u \\ v_q \\ \theta_{rA} \\ \theta_{rB} \\ \alpha \\ v_r \\ \theta_{qA} \\ \theta_{qB} \end{bmatrix}$$

$$A_1 = I_{qr} \cdot q_s - I_r \cdot r_s$$

$$A_2 = I_q \cdot q_s - I_{qr} \cdot r_s$$

$$D = \frac{GJ}{l} + \frac{12E}{l^3} (q_s^2 \cdot I_q - 2q_s \cdot r_s \cdot I_{qr} + r_s^2 \cdot I_r)$$

THE ELEMENT STIFFNESS MATRIX OF A MEMBER

FIGURE 4.37

XA							
0	XB	SYMMETRIC					
0	XC	XD					
0	XE	XF	XG				
0	XH	XI	XJ	XK			
0	XL	XM	XN	XO	XP		
0	XQ	XR	XS	XT	XU	XV	
0	XW	XY	XZ	XAA	XAB	XAC	XAD

KEY TO TERMS WITHIN THE STIFFNESS MATRIX OF ONE MEMBER

FIGURE 4.38

$$\begin{bmatrix} u \\ v_q \\ \theta_{rA} \\ \theta_{rB} \\ \alpha \\ v_r \\ \theta_{qA} \\ \theta_{qB} \end{bmatrix} = \begin{bmatrix} -L_P & -M_P & -N_P & L_{QR} & M_{QR} & N_{QR} & -- & L_P & M_P & N_P & L_{RQ} & M_{RQ} & N_{RQ} \\ -L_Q & -M_Q & -N_Q & L_{PRa} & M_{PRa} & N_{PRa} & -- & L_Q & M_Q & N_Q & L_{PRb} & M_{PRb} & N_{PRb} \\ 0 & 0 & 0 & L_R & M_R & N_R & -- & 0 & 0 & 0 & 0 & 0 & 0 \\ 0 & 0 & 0 & 0 & 0 & 0 & -- & 0 & 0 & 0 & L_R & M_R & N_R \\ 0 & 0 & 0 & -L_P & -M_P & -N_P & -- & 0 & 0 & 0 & L_P & M_P & N_P \\ -L_R & -M_R & -N_R & L_{PQa} & M_{PQa} & N_{PQa} & -- & L_R & M_R & N_R & L_{PQb} & M_{PQb} & N_{PQb} \\ 0 & 0 & 0 & -L_Q & -M_Q & -N_Q & -- & 0 & 0 & 0 & 0 & 0 & 0 \\ 0 & 0 & 0 & 0 & 0 & 0 & -- & 0 & 0 & 0 & -L_Q & -M_Q & -N_Q \end{bmatrix} \begin{bmatrix} X_i \\ Y_i \\ Z_i \\ \theta_{X_i} \\ \theta_{Y_i} \\ \theta_{Z_i} \\ \vdots \\ X_j \\ Y_j \\ Z_j \\ \theta_{X_j} \\ \theta_{Y_j} \\ \theta_{Z_j} \end{bmatrix}$$

$$\underline{Z} = \underline{A_f} \underline{X}$$

$$\begin{aligned}
 L_{RQ} &= R_c * L_Q - Q_c * L_R \\
 M_{RQ} &= R_c * M_Q - Q_c * M_R \\
 N_{RQ} &= R_c * N_Q - Q_c * N_R \\
 L_{QR} &= -L_Q * R_c + L_R * Q_c \\
 M_{QR} &= -M_Q * R_c + M_R * Q_c \\
 N_{QR} &= -N_Q * R_c + N_R * Q_c \\
 L_{PRa} &= R_c * L_P - P_{ca} * L_R \\
 M_{PRa} &= R_c * M_P - P_{ca} * M_R \\
 N_{PRa} &= R_c * N_P - P_{ca} * N_R
 \end{aligned}$$

$$\begin{aligned}
 L_{PRb} &= -R_c * L_P + P_{cb} * L_R \\
 M_{PRb} &= -R_c * M_P + P_{cb} * M_R \\
 N_{PRb} &= -R_c * N_P + P_{cb} * N_R \\
 L_{PQa} &= -Q_c * L_P + P_{ca} * L_Q \\
 M_{PQa} &= -Q_c * M_P + P_{ca} * M_Q \\
 N_{PQa} &= -Q_c * N_P + P_{ca} * N_Q \\
 L_{PQR} &= Q_c * L_P - P_{cb} * L_Q \\
 M_{PQR} &= Q_c * M_P - P_{cb} * M_Q \\
 N_{PQR} &= Q_c * N_P - P_{cb} * N_Q
 \end{aligned}$$

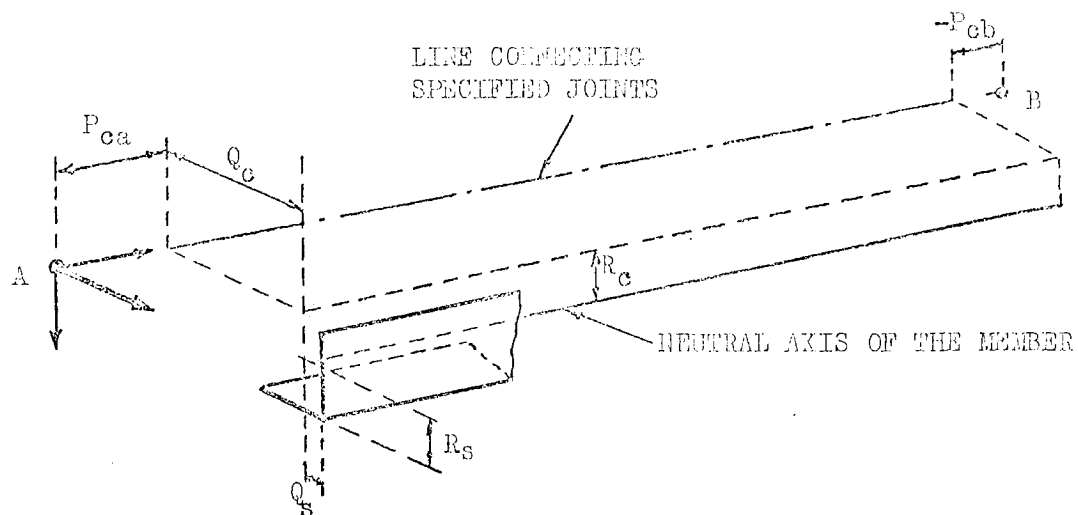
THE DISPLACEMENT TRANSFORMATION MATRIX

FIGURE 4.39

displacements to a set of global axes. In order that the various irregularities, which are common in civil engineering structures, might be coped with, Jennings and Majid <sup>(2)</sup> have modified the  $\underline{A}_1$  matrix to give the one shown in figure 4.39. In this matrix  $p_{ca}$  and  $p_{cb}$  are the lengths of the rigid portions, such as gusset plates or haunches at either end of the member. The offsets, of the centroid of the member from the joint to which it is connected, are given by  $Q_c$ ,  $R_c$ ,  $Q_s$  and  $R_s$ . Such rigid portions and offsets are illustrated in figure 4.40.

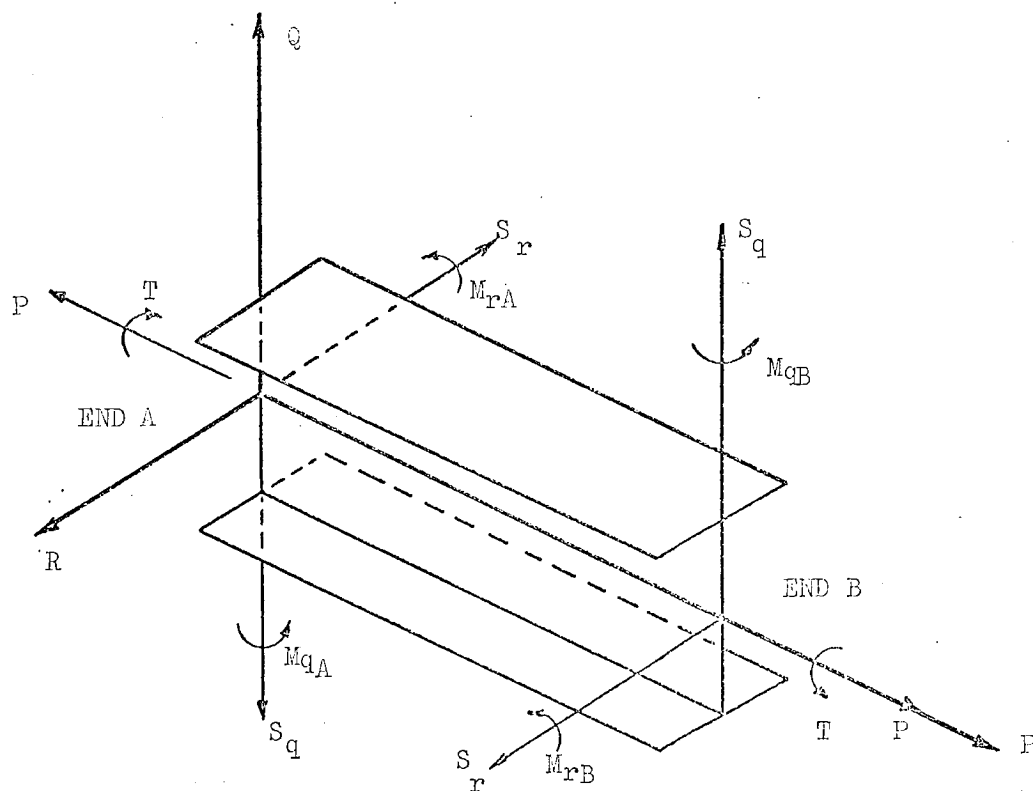
(4.6.2) Member forces. The eight resultant forces and moments acting on each member are shown in figure 4.41. In order that they may be evaluated it is necessary to carry out the  $\underline{kAX}$  multiplication for each member, consequently each member's  $\underline{kA}$  matrix has to be computed. The format of a typical  $\underline{kA}$  matrix is shown in figure 4.42. It comprises two blocks, each one corresponding to an end of the member, with eight rows and up to six columns. If this multiplication is carried out in general terms for one member, then the result may be used to construct directly the matrix for specific members. The six columns corresponding to the three joint translations at each end of the member can be formed from figure 4.43. The general expression for each of the eight rows of one such column is given in figure 4.43a. All of the columns may be formed when this figure is used in conjunction with figure 4.43b. The three columns corresponding to rotations at end A of the member may be formed from the tables given in figure 4.44. The general expression for one of these columns is given in figure 4.44a, which when used with figure 4.44b permits the computation of each of the columns. The three columns corresponding to rotations at end B of the member may be formed from the tables given in figure 4.45. If figures 4.45a and 4.45b are used together then the three required columns will be generated.

(4.6.3) Direct Evaluation of the  $\underline{A'kA}$  Contribution. When end A of a



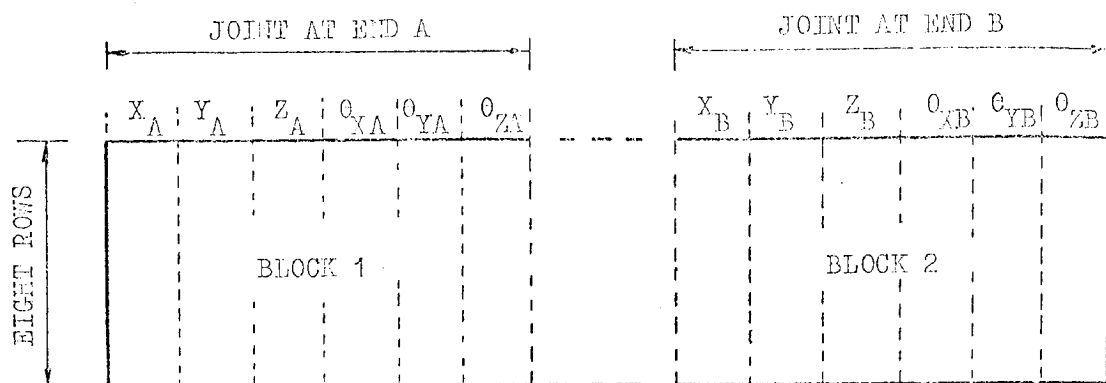
RIGID PORTIONS AND OFFSETS OF A MEMBER'S ENDS FROM THE SPECIFIED JOINTS

FIGURE 4.40



MEMBER FORCES ON EACH MEMBER

FIGURE 4.41



GENERAL  $k_A$  MATRIX FOR A MEMBER

FIGURE 4.42

-A.XA
-B.XB-C.XL
-B.XC-C.XM
-B.XE-C.XN
-B.XH-C.XO
-B.XL-C.XP
-B.XQ-C.XU
-B.XW-C.XAB

CODE	COLUMN					
	$X_A$	$Y_A$	$Z_A$	$X_B$	$Y_B$	$Z_B$
A	$L_P$	$M_P$	$N_P$	$-L_P$	$-M_P$	$-N_P$
B	$L_Q$	$M_Q$	$N_Q$	$-L_Q$	$-M_Q$	$-N_Q$
C	$L_R$	$M_R$	$N_R$	$-L_R$	$-M_R$	$-N_R$

KEY TO TERMS WITHIN EACH TRANSLATIONAL COLUMN

FIGURE 4.43b

GENERAL COLUMN FOR A TRANSLATIONAL DEGREE OF FREEDOM

FIGURE 4.43a

FIGURE 4.43

F.XA
$G.XB + C.XC - A.XH + E.XL - B.XQ$
$G.XC + C.XD - A.XI + E.XM - B.XR$
$G.XE + C.XF - A.XJ + E.XN - B.XS$
$G.XH + C.XI - A.XK + E.XO - B.XT$
$G.XL + C.XM - A.XO + E.XP - B.XU$
$G.XQ + C.XR - A.XT + E.XU - B.XV$
$G.XW + C.XY - A.XAA + E.XAB - B.XAC$

GENERAL COLUMN FOR A ROTATIONAL  
DEGREE OF FREEDOM AT END A OF  
A MEMBER

FIGURE 4.44a

CODE	COLUMN		
	$\theta_{xA}$	$\theta_{yA}$	$\theta_{zA}$
A	$L_P$	$M_P$	$N_P$
B	$L_Q$	$M_Q$	$N_Q$
C	$L_R$	$M_R$	$N_R$
E	$L_{PRa}$	$M_{PRa}$	$N_{PRa}$
F	$L_{PQa}$	$M_{PQa}$	$N_{PQa}$
G	$L_{QR}$	$M_{QR}$	$N_{QR}$

KEY TO TERMS WITHIN EACH  
ROTATIONAL COLUMN FOR END A OF  
A MEMBER

FIGURE 4.44b

FIGURE 4.44

F.XA
$G.XB + C.XE - A.XH + E.XL - B.XW$
$G.XC + C.XF - A.XI + E.XM - B.XY$
$G.XE + C.XG - A.XJ + E.XN - B.XZ$
$G.XH + C.XJ - A.XK + E.XO - B.XAA$
$G.XL + C.XN - A.XO + E.XP - B.XAB$
$G.XQ + C.XS - A.XT + E.XLL - B.XAC$
$G.XW + C.XZ - A.XAA + E.XAB - B.XAD$

GENERAL COLUMN FOR A ROTATIONAL  
DEGREE OF FREEDOM AT END B OF  
A MEMBER

FIGURE 4.45a

CODE	COLUMN		
	$\theta_{xB}$	$\theta_{yB}$	$\theta_{zB}$
A	$-L_P$	$-M_P$	$-N_P$
B	$L_Q$	$M_Q$	$N_Q$
C	$L_R$	$M_R$	$N_R$
D	$L_{PRb}$	$M_{PRb}$	$N_{PRb}$
F	$L_{PQb}$	$M_{PQb}$	$N_{PQb}$
G	$L_{RQ}$	$M_{RQ}$	$N_{RQ}$

KEY TO TERMS WITHIN EACH  
ROTATIONAL COLUMN FOR END B  
OF A MEMBER

FIGURE 4.45b

FIGURE 4.45

member is connected to a lower numbered joint than end B, as is the case in figure 4.46a, then the orientation of the four sub-blocks is that shown in figure 4.46b. These sub-blocks are the contribution made by a member to the overall stiffness matrix of a structure. Such a set of sub-blocks is symmetrical about its leading diagonal, consequently the sub-blocks which form the lower triangle of the set, namely the two on-diagonal triangular sub-blocks and one rectangular sub-block, need only be considered. Only three sub-blocks need construction consequently it is unnecessary to adopt the approach used for plate elements. Each of the sub-blocks has been detailed explicitly. The expressions forming the terms of sub-block hh are given in figure 4.47. The integer on the left of each expression gives the term's location within the sub-block. Similarly the terms of sub-block jh are given in figure 4.48 and those forming sub-block jj in figure 4.49. For a complete interpretation these figures should be read in conjunction with figures 4.38 and 4.39.



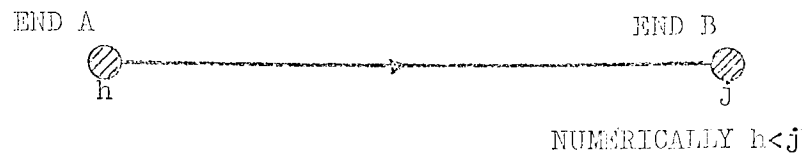
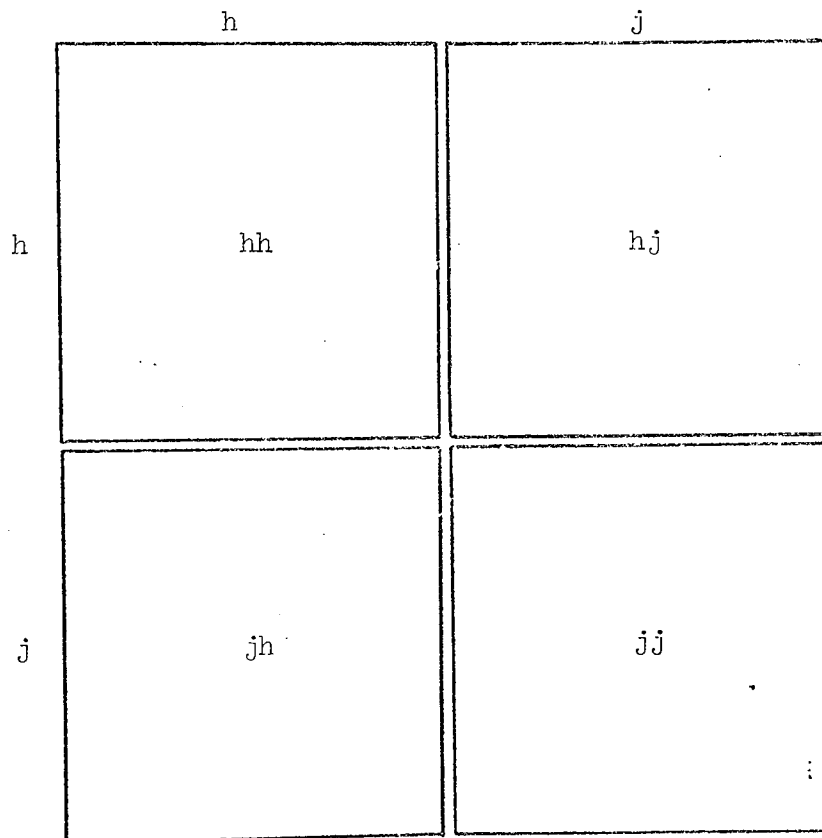


FIGURE 4.46a



THE ORIENTATION OF THE FOUR SUB-BLOCKS FORMED BY A PRISMATIC MEMBER

FIGURE 4.46b

FIGURE 4.46

- 21  $\#NP^*LP^*XA^*NQ^*LQ^*XB^*XL^*(HQ^*LR^*NR^*LO)^*NR^*LR^*XP$
- 22  $\#NP^*HP^*XA^*MQ^*HQ^*XB^*XL^*(HQ^*HR^*NR^*HQ)^*NR^*HR^*XP$
- 31  $\#NP^*LP^*XA^*NQ^*LQ^*XB^*XL^*(NQ^*LR^*NR^*LO)^*NR^*LR^*XP$
- 32  $\#NP^*MP^*XA^*NQ^*MQ^*XB^*XL^*(NQ^*HR^*NR^*HQ)^*NR^*HR^*XP$
- 33  $\#NP^*NP^*XA^*NQ^*NQ^*XB^*XL^*(NR^*NQ^*NR^*NQ)^*NR^*NR^*XP$
- 41  $\#-LP^*LQR^*XA-LPRA^*(LQ^*XB+LR^*XL)-LR^*(LQ^*XC+LR^*XH)^*LP^*(LQ^*XH+LR^*XO)-LPQA^*(LQ^*XL+LR^*XP)+LQ^*(LQ^*XO+LR^*XU)$
- 42  $\#-LQR^*HP^*XA-LPRA^*(HQ^*XB+HR^*XL)-LR^*(HQ^*XC+HR^*XH)^*LP^*(HQ^*XH+HR^*XO)-LPQA^*(HQ^*XL+HR^*XP)+LQ^*(HQ^*XO+HR^*XU)$
- 43  $\#-LQR^*NP^*XA-LPRA^*(NQ^*XB+NR^*XL)-LR^*(NQ^*XC+NR^*XH)^*LP^*(NQ^*XH+NR^*XO)-LPQA^*(NQ^*XL+NR^*XP)+LQ^*(NQ^*XO+NR^*XU)$
- 44  $\#LQR^*LQR^*XA+LPRA^*(LPRA^*XB+LR^*XC-LP^*XH+LPQA^*XL-LQ^*XO)^*LR^*(LPRA^*XC+LR^*XD-LF^*XI+LPQA^*XM-LQ^*XR)-LP^*(LPRA^*XH+LR^*XI-LP^*XK+LPQA^*XO-LQ^*XT)+LFQA^*(LPRA^*XL+LR^*XH-LP^*XO+LPQA^*XP-LQ^*XU)-LQ^*(LPRA^*XO+LR^*XR-LF^*XT+LPQA^*XU-LQ^*XV)$
- 51  $\#-MQR^*LP^*XA-MPRA^*(LQ^*XB+LR^*XL)-MR^*(LQ^*XC+LR^*XH)^*MP^*(LQ^*XH+LR^*XO)-MPQA^*(LQ^*XL+LR^*XP)+MQ^*(LQ^*XO+LR^*XU)$
- 52  $\#-MQR^*MP^*XA-MPRA^*(HQ^*XB+MR^*XL)-MR^*(HQ^*XC+MR^*XH)^*MP^*(HQ^*XH+MR^*XO)-MPQA^*(HQ^*XL+MR^*XP)+MQ^*(HQ^*XO+MR^*XU)$
- 53  $\#-MQR^*NP^*XA-MPRA^*(NQ^*XB+NR^*XL)-MR^*(NQ^*XC+NR^*XH)^*MP^*(NQ^*XH+NR^*XO)-MPQA^*(NQ^*XL+NR^*XP)+MQ^*(NQ^*XO+NR^*XU)$
- 54  $\#MQR^*LQR^*XA+MPRA^*(LPRA^*XB+LR^*XC-LP^*XH+LPQA^*XL-LQ^*XO)^*MR^*(LPRA^*XC+LR^*XD-LF^*XI+LPQA^*XM-LQ^*XR)-MP^*(LPRA^*XH+LR^*XI-LP^*XK+LPQA^*XO-LQ^*XT)+MFQA^*(LPRA^*XL+LR^*XH-LP^*XO+LPQA^*XP-LQ^*XU)-MQ^*(LPRA^*XO+LR^*XR-LF^*XT+LPQA^*XU-LQ^*XV)$
- 55  $\#MQR^*MQR^*XA+MPRA^*(MPRA^*XB+MR^*XC-MP^*XH+MPQA^*XL-MQ^*XO)^*MR^*(MPRA^*XC+MR^*XD-MF^*XI+MPQA^*XM-MQ^*XR)-MP^*(MPRA^*XH+MR^*XI-MP^*XK+MPQA^*XO-MQ^*XT)+MFQA^*(MPRA^*XL+MR^*XH-MP^*XO+MPQA^*XP-MQ^*XU)-MQ^*(MPRA^*XO+MR^*XR-MF^*XT+MPQA^*XU-MQ^*XV)$
- 61  $\#-NQR^*LP^*XA-NPRA^*(LQ^*XB+LR^*XL)-NR^*(LQ^*XC+LR^*XH)^*NP^*(LQ^*XH+LR^*XO)-NPQA^*(LQ^*XL+LR^*XP)+NQ^*(LQ^*XO+LR^*XU)$
- 62  $\#-NQR^*MP^*XA-NPRA^*(HQ^*XB+MR^*XL)-NR^*(HQ^*XC+MR^*XH)^*NP^*(HQ^*XH+MR^*XO)-NPQA^*(HQ^*XL+MR^*XP)+NQ^*(HQ^*XO+MR^*XU)$
- 63  $\#-NQR^*NP^*XA-NPRA^*(NQ^*XB+NR^*XL)-NR^*(NQ^*XC+NR^*XH)^*NP^*(NQ^*XH+NR^*XO)-NPQA^*(NQ^*XL+NR^*XP)+NQ^*(NQ^*XO+NR^*XU)$
- 64  $\#NQR^*LQR^*XA+NPRA^*(LPRA^*XB+LR^*XC-LP^*XH+LPQA^*XL-LQ^*XO)^*NR^*(LPRA^*XC+LR^*XD-LF^*XI+LPQA^*XM-LQ^*XR)-NP^*(LPRA^*XH+LR^*XI-LP^*XK+LPQA^*XO-LQ^*XT)+NFQA^*(LPRA^*XL+LR^*XH-LP^*XO+LPQA^*XP-LQ^*XU)-NQ^*(LPRA^*XO+LR^*XR-LP^*XT+LPQA^*XU-LQ^*XV)$
- 65  $\#NQR^*MQR^*XA+NPRA^*(MPRA^*XB+MR^*XC-MP^*XH+MPQA^*XL-MQ^*XO)^*NR^*(MPRA^*XC+MR^*XD-MF^*XI+MPQA^*XM-MQ^*XR)-NP^*(MPRA^*XH+MR^*XI-MP^*XK+MPQA^*XO-MQ^*XT)+NFQA^*(MPRA^*XL+MR^*XH-MP^*XO+MPQA^*XP-MQ^*XU)-NQ^*(MPRA^*XO+MR^*XR-MF^*XT+MPQA^*XU-MQ^*XV)$
- 66  $\#NQR^*NQR^*XA+NPRA^*(NPRA^*XB+NR^*XC-NP^*XH-NPQA^*XL-NQ^*XO)^*NR^*(NPRA^*XC+NR^*XD-NP^*XI+NPQA^*XM-NQ^*XR)-NP^*(NPRA^*XH+NR^*XI-NP^*XK+NPQA^*XO-NQ^*XT)+NPQA^*(NPRA^*XL+NR^*XH-NP^*XO+NPQA^*XP-NQ^*XU)-NQ^*(NPRA^*XO+NR^*XR-NP^*XT+NPQA^*XU-NQ^*XV)$

TRIANGULAR SUB-BLOCK hh

FIGURE 4.47

- 11  $\square - LP * LP * XA * LC * (LQ * XB * LR * XL) * LR * (LQ * XL * LR * XP)$
- 12  $\square - LP * MP * XA * LC * (MQ * XB * MR * XL) * LR * (MQ * XL * MR * XP)$
- 13  $\square - LP * NP * XA * LC * (NQ * XB * NR * XL) * LR * (NQ * XL * NR * XP)$
- 14  $\square LP * LQR * XA * LC * (LPRA * XB * LR * XC - LP * XH * LPQA * XL - LQ * XQ) * LR * (LPRA * XL * LR * XH - LP * XO * LPQA * XP - LQ * XU)$
- 15  $\square LP * MQR * XA * LC * (MPRA * XB * MR * XC - MP * XH * MPQA * XL - MQ * XQ) * LR * (MPRA * XL * MR * XH - MP * XO * MPQA * XP - MQ * XU)$
- 16  $\square LP * NQR * XA * LC * (NPRA * XB * NR * XC - NP * XH * NPQA * XL - NQ * XQ) * LR * (NPRA * XL * NR * XH - NP * XO * NPQA * XP - NQ * XU)$
- 21  $\square - MP * LP * XA * MC * (LQ * XB * LR * XL) * MR * (LQ * XL * LR * XP)$
- 22  $\square - MP * MP * XA * MC * (MQ * XB * MR * XL) * MR * (MQ * XL * MR * XP)$
- 23  $\square - MP * NP * XA * MC * (NQ * XB * NR * XL) * MR * (NQ * XL * NR * XP)$
- 24  $\square MP * LQR * XA * MC * (LPRA * XB * LR * XC - LP * XH * LPQA * XL - LQ * XQ) * MR * (LPRA * XL * LR * XH - LP * XO * LPQA * XP - LQ * XU) +$
- 25  $\square MP * MQR * XA * MC * (MPRA * XB * MR * XC - MP * XH * MPQA * XL - MQ * XQ) * MR * (MPRA * XL * MR * XH - MP * XO * MPQA * XP - MQ * XU)$
- 26  $\square MP * NQR * XA * MC * (NPRA * XB * NR * XC - NP * XH * NPQA * XL - NQ * XQ) * MR * (NPRA * XL * MR * XH - NP * XO * NPQA * XP - NQ * XU)$
- 31  $\square - NP * LP * XA * NC * (LQ * XB * LR * XL) * NR * (LQ * XL * LR * XP)$
- 32  $\square - NP * MP * XA * NC * (MQ * XB * MR * XL) * NR * (MQ * XL * MR * XP)$
- 33  $\square - NP * NP * XA * NC * (NQ * XB * NR * XL) * NR * (NQ * XL * NR * XP)$
- 34  $\square NP * LQR * XA * NC * (LPRA * XB * LR * XC - LP * XH * LPQA * XL - LQ * XQ) * NR * (LPRA * XL * LR * XH - LP * XO * LPQA * XP - LQ * XU)$
- 35  $\square NP * MQR * XA * NC * (MPRA * XB * MR * XC - MP * XH * MPQA * XL - MQ * XQ) * NR * (MPRA * XL * MR * XH - MP * XO * MPQA * XP - MQ * XU)$
- 36  $\square NP * NQR * XA * NC * (NPRA * XB * NR * XC - NP * XH * NPQA * XL - NQ * XQ) * NR * (NPRA * XL * NR * XH - NP * XO * NPQA * XP - NQ * XU)$
- 41  $\square - LRQ * LP * XA * LPRB * (LQ * XB * LR * XL) * LR * (LQ * XE * LR * XN) * LP * (LQ * XH * LR * XO) * LPQB * (LQ * XL * LR * XP) + LQ * (LQ * XW * LR * XAB)$
- 42  $\square - LRQ * MP * XA * LPRB * (MQ * XB * MR * XL) * LR * (MQ * XE * MR * XN) * LP * (MQ * XH * MR * XO) * LPQB * (MQ * XL * MR * XP) + LQ * (MQ * XW * MR * XAB)$
- 43  $\square - LRQ * NP * XA * LPRB * (NQ * XB * NR * XL) * LR * (NQ * XE * NR * XN) * LP * (NQ * XH * NR * XO) * LPQB * (NQ * XL * NR * XP) + LQ * (NQ * XW * NR * XAB)$
- 44  $\square LRQ * LQR * XA * LPRB * (LPRA * XB * LR * XC - LP * XH * LPQA * XL - LQ * XQ) * LR * (LPRA * XE * LR * XF - LP * XJ * LPQA * XH - LQ * XS) * LP * (LPRA * XH * LR * XI - LP * XK * LPQA * XO - LQ * XT) + LPQB * (LPRA * XL * LR * XH - LP * XO * LPQA * XP - LQ * XU) * LQ * (LPRA * XH * LR * XY - LP * XAA * LPQA * XAB - LQ * XAC)$

.... CONTINUED

FIGURE 4.48

- 45  $\square LRQ * MQR * XA + LPRB * (MPRA * XB + MR * XC - MP * XH + MPQA * XL - MQ * XO) + LR * (MPRA * XE + MR * XF - MP * XJ + MPQA * XN - MQ * XS) + LP * (MPRA * XH + MR * XI - MP * XK + MPQA * XO - MQ * XT) + LPQB * (MPRA * XL + MR * XM - MP * XO + MPQA * XP - MQ * XU) - LQ * (MPRA * XW + MR * XY - MP * XAA + MPQA * XAB - MQ * XAC)$
- 46  $\square LRQ * NQR * XA + LPRB * (NPRA * XB + NR * XC - NP * XH + NPQA * XL - NQ * XO) + LR * (NPRA * XE + NR * XF - NP * XJ + NPQA * XN - NQ * XS) + LP * (NPRA * XH + NR * XI - NP * XK + NPQA * XO - NQ * XT) + LPQB * (NPRA * XL + NR * XM - NP * XO + NPQA * XP - NQ * XU) - LQ * (NPRA * XW + NR * XY - NP * XAA + NPQA * XAB - NQ * XAC)$
- 51  $\square - MRQ * LP * XA - MPRB * (LQ * XB + LR * XL) - MR * (LQ * XE + LR * XN) - MP * (LQ * XH + LR * XO) - MPQB * (LQ * XL + LR * XP) + MQ * (LQ * XW + LR * XAB)$
- 52  $\square - MRQ * MP * XA - MPRB * (MQ * XB + MR * XL) - MR * (MQ * XE + MR * XN) - MP * (MQ * XH + MR * XO) - MPQB * (MQ * XL + MR * XP) + MQ * (MQ * XW + MR * XAB)$
- 53  $\square - MRQ * NP * XA - MPRB * (NQ * XB + NR * XL) - MR * (NQ * XE + NR * XN) - MP * (NQ * XH + NR * XO) - MPQB * (NQ * XL + NR * XP) + MQ * (NQ * XW + NR * XAB)$
- 54  $\square MRQ * LQR * XA + MPRB * (LPRA * XB + LR * XC - LP * XH + LPQA * XL - LQ * XO) + MR * (LPRA * XE + LR * XF - LP * XJ + LPQA * XN - LQ * XS) + MP * (LPRA * XH + LR * XI - LP * XK + LPQA * XO - LQ * XT) + MPQB * (LPRA * XL + LR * XM - LP * XO + LPQA * XP - LQ * XU) - MQ * (LPRA * XW + LR * XY - LP * XAA + LPQA * XAB - LQ * XAC)$
- 55  $\square MRQ * MQR * XA + MPRB * (MPRA * XB + MR * XC - MP * XH + MPQA * XL - MQ * XO) + MR * (MPRA * XE + MR * XF - MP * XJ + MPQA * XN - MQ * XS) + MP * (MPRA * XH + MR * XI - MP * XK + MPQA * XO - MQ * XT) + MPQB * (MPRA * XL + MR * XM - MP * XO + MPQA * XP - MQ * XU) - MQ * (MPRA * XW + MR * XY - MP * XAA + MPQA * XAB - MQ * XAC)$
- 56  $\square MRQ * NQR * XA + MPRB * (NPRA * XB + NR * XC - NP * XH + NPQA * XL - NQ * XO) + MR * (NPRA * XE + NR * XF - NP * XJ + NPQA * XN - NQ * XS) + MP * (NPRA * XH + NR * XI - NP * XK + NPQA * XO - NQ * XT) + MPQB * (NPRA * XL + NR * XM - NP * XO + NPQA * XP - NQ * XU) - MQ * (NPRA * XW + NR * XY - NP * XAA + NPQA * XAB - NQ * XAC)$
- 61  $\square - NRQ * LP * XA - NPRB * (LQ * XB + LR * XL) - NR * (LQ * XE + LR * XN) - NP * (LQ * XH + LR * XO) - NPQB * (LQ * XL + LR * XP) + NQ * (LQ * XW + LR * XAB)$
- 62  $\square - NRQ * MP * XA - NPRB * (MQ * XB + MR * XL) - NR * (MQ * XE + MR * XN) - NP * (MQ * XH + MR * XO) - NPQB * (MQ * XL + MR * XP) + NQ * (MQ * XW + MR * XAB)$
- 63  $\square - NRQ * NP * XA - NPRB * (NQ * XB + NR * XL) - NR * (NQ * XE + NR * XN) - NP * (NQ * XH + NR * XO) - NPQB * (NQ * XL + NR * XP) + NQ * (NQ * XW + NR * XAB)$
- 64  $\square NRQ * LQR * XA + NPRB * (LPRA * XB + LR * XC - LP * XH + LPQA * XL - LQ * XO) + NR * (LPRA * XE + LR * XF - LP * XJ + LPQA * XN - LQ * XS) + NP * (LPRA * XH + LR * XI - LP * XK + LPQA * XO - LQ * XT) + NPQB * (LPRA * XL + LR * XM - LP * XO + LPQA * XP - LQ * XU) - NQ * (LPRA * XW + LR * XY - LP * XAA + LPQA * XAB - LQ * XAC)$
- 65  $\square NRQ * MQR * XA + NPRB * (MPRA * XB + MR * XC - MP * XH + MPQA * XL - MQ * XO) + NR * (MPRA * XE + MR * XF - MP * XJ + MPQA * XN - MQ * XS) + NP * (MPRA * XH + MR * XI - MP * XK + MPQA * XO - MQ * XT) + NPQB * (MPRA * XL + MR * XM - MP * XO + MPQA * XP - MQ * XU) - NQ * (MPRA * XW + MR * XY - MP * XAA + MPQA * XAB - MQ * XAC)$
- 66  $\square NRQ * NQR * XA + NPRB * (NPRA * XB + NR * XC - NP * XH + NPQA * XL - NQ * XO) + NR * (NPRA * XE + NR * XF - NP * XJ + NPQA * XN - NQ * XS) + NP * (NPRA * XH + NR * XI - NP * XK + NPQA * XO - NQ * XT) + NPQB * (NPRA * XL + NR * XM - NP * XO + NPQA * XP - NQ * XU) - NQ * (NPRA * XW + NR * XY - NP * XAA + NPQA * XAB - NQ * XAC)$

RECTANGULAR SUB-BLOCK jh

FIGURE 4.48

- 11  $=LP*LP*XA*LO*(LO*XB+LR*XL)+LR*(LO*XL+LR*XP)$
- 21  $=MP*LP*XA+MQ*(LO*XB+LR*XL)+NR*(LO*XL+LR*XP)$
- 22  $=MP*MP*XA+MQ*(MQ*XB+MR*XL)+MR*(MQ*XL+MR*XP)$
- 31  $=NP*LP*XA+NQ*(LO*XB+LR*XL)+NR*(LO*XL+LR*XP)$
- 32  $=NP*MP*XA+NQ*(MQ*XB+MR*XL)+NR*(MQ*XL+MR*XP)$
- 33  $=NP*NP*XA+NQ*(NQ*XB+NR*XL)+NR*(NQ*XL+NR*XP)$
- 41  $=LRQ*LP*XA+LFRD*(LO*XB+LR*XL)+LR*(LO*XF+LR*XN)+LP*(LO*XH+LR*  
XO)+LPQB*(LO*XL+LR*XP)-LQ*(LO*XW+LR*XAB)$
- 42  $=LRO*MP*XA+LFRB*(MQ*XB+MR*XL)+LR*(MQ*XE+MR*XN)+LP*(MQ*XH+MR*  
XO)+LPQB*(MQ*XL+MR*XP)-LQ*(MQ*XW+MR*XAB)$
- 43  $=LRO*NP*XA+LFRB*(NQ*XB+NR*XL)+LR*(NQ*XE+NR*XN)+LP*(NQ*XH+NR*  
XO)+LPQB*(NQ*XL+NR*XP)-LQ*(NQ*XW+NR*XAB)$
- 44  $=LRO*LRQ*XA+LPRB*(LPRB*XB+LR*XE+LP*XH+LPQB*XL-LQ*XW)+LR*(LPRB*  
XE+LR*XG+LP*XJ+LPQB*XN-LQ*XZ)+LP*(LPRB*XH+LR*XJ+LP*XK+LPQB*XO-LQ*  
XAA)+LPQB*(LFRB*XL+LR*XN+LP*XO+LPQB*XP-LQ*XAB)-LQ*(LPRB*XW+LR*XZ+  
LP*XAA+LPQB*XAB-LQ*XAD)$
- 51  $=HRQ*LP*XA+MFRD*(LO*XB+LR*XL)+MR*(LO*XE+LR*XN)+MP*(LO*XH+LR*  
XO)+MPQB*(LO*XL+LR*XP)-MQ*(LO*XW+LR*XAB)$
- 52  $=HRQ*MP*XA+MFRB*(MQ*XB+MR*XL)+MR*(MQ*XE+MR*XN)+MP*(MQ*XH+MR*  
XO)+MPQB*(MQ*XL+MR*XP)-MQ*(MQ*XW+MR*XAB)$
- 53  $=HRQ*NP*XA+MFRB*(NQ*XB+NR*XL)+MR*(NQ*XE+NR*XN)+MP*(NQ*XH+NR*  
XO)+MPQB*(NQ*XL+NR*XP)-MQ*(NQ*XW+NR*XAB)$
- 54  $=HRQ*LRQ*XA+MPRB*(LPRB*XB+LR*XE+LP*XH+LPQB*XL-LQ*XW)+MR*(LPRB*  
XE+LR*XG+LP*XJ+LPQB*XN-LQ*XZ)+MP*(LPRB*XH+LR*XJ+LP*XK+LPQB*XO-LQ*  
XAA)+MPQB*(LFRB*XL+LR*XN+LP*XO+LPQB*XP-LQ*XAB)-MQ*(LPRB*XW+LR*XZ+  
LP*XAA+LPQB*XAB-LQ*XAD)$
- 55  $=HRQ*HRQ*XA+MPQB*(MPRB*XB+MR*XE+MP*XH+MPQB*XL-MQ*XW)+MR*(MPRB*  
XE+MR*XG+MP*XJ+MPQB*XN-MQ*XZ)+MP*(MPRB*XH+MR*XJ+MP*XK+MPQB*XO-MQ*  
XAA)+MPQB*(MPRB*XL+MR*XN+MP*XO+MPQB*XP-MQ*XAB)-MQ*(MPRB*XW+MR*XZ+  
MP*XAA+MPQB*XAB-MQ*XAD)$
- 61  $=NRQ*LP*XA+NFRD*(LO*XB+LR*XL)+NR*(LO*XE+LR*XN)+NP*(LO*XH+LR*  
XO)+NPQB*(LO*XL+LR*XP)-NQ*(LO*XW+LR*XAB)$
- 62  $=NRQ*MP*XA+NFRB*(MQ*XB+MR*XL)+NR*(MQ*XE+MR*XN)+NP*(MQ*XH+MR*  
XO)+NPQB*(MQ*XL+MR*XP)-NQ*(MQ*XW+MR*XAB)$
- 63  $=NRQ*NP*XA+NFRB*(NQ*XB+NR*XL)+NR*(NQ*XE+NR*XN)+NP*(NQ*XH+NR*  
XO)+NPQB*(NQ*XL+NR*XP)-NQ*(NQ*XW+NR*XAB)$
- 64  $=NRQ*LRQ*XA+APRB*(LPRB*XB+LR*XE+LP*XH+LPQB*XL-LQ*XW)+NR*(LPRB*  
XE+LR*XG+LP*XJ+LPQB*XN-LQ*XZ)+NP*(LPRB*XH+LR*XJ+LP*XK+LPQB*XO-LQ*  
XAA)+NPQB*(LFRB*XL+LR*XN+LP*XO+LPQB*XP-LQ*XAB)-NQ*(LPRB*XW+LR*XZ+  
LP*XAA+LPQB*XAB-LQ*XAD)$
- 65  $=NRQ*MRQ*XA+APRB*(MPRB*XB+MR*XE+MP*XH+MPQB*XL-MQ*XW)+NR*(MPRB*  
XE+MR*XG+MP*XJ+MPQB*XN-MQ*XZ)+NP*(MPRB*XH+MR*XJ+MP*XK+MPQB*XO-MQ*  
XAA)+NPQB*(MPRB*XL+MR*XN+MP*XO+MPQB*XP-MQ*XAB)-NQ*(MPRB*XW+MR*XZ+  
MP*XAA+MPQB*XAB-MQ*XAD)$
- 66  $=NRQ*NRO*XA+APRB*(NPRB*XB+NR*XE+NP*XH+NPQB*XL-LQ*XW)+NR*(NPRB*  
XE+NR*XG+NP*XJ+NPQB*XN-LQ*XZ)+NP*(NPRB*XH+NR*XJ+NP*XK+NPQB*XO-MQ*  
XAA)+NPQB*(NPRB*XL+NR*XN+NP*XO+NPQB*XP-LQ*XAB)-NQ*(NPRB*XW+NR*XZ+  
NP*XAA+NPQB*XAB-LQ*XAD)$

TRIANGULAR SUB-BLOCK jj

FIGURE 4.49

## CHAPTER 5

### FORMATION OF THE STIFFNESS MATRICES FOR A CURVED PLATE ELEMENT

#### (5.1) Introduction

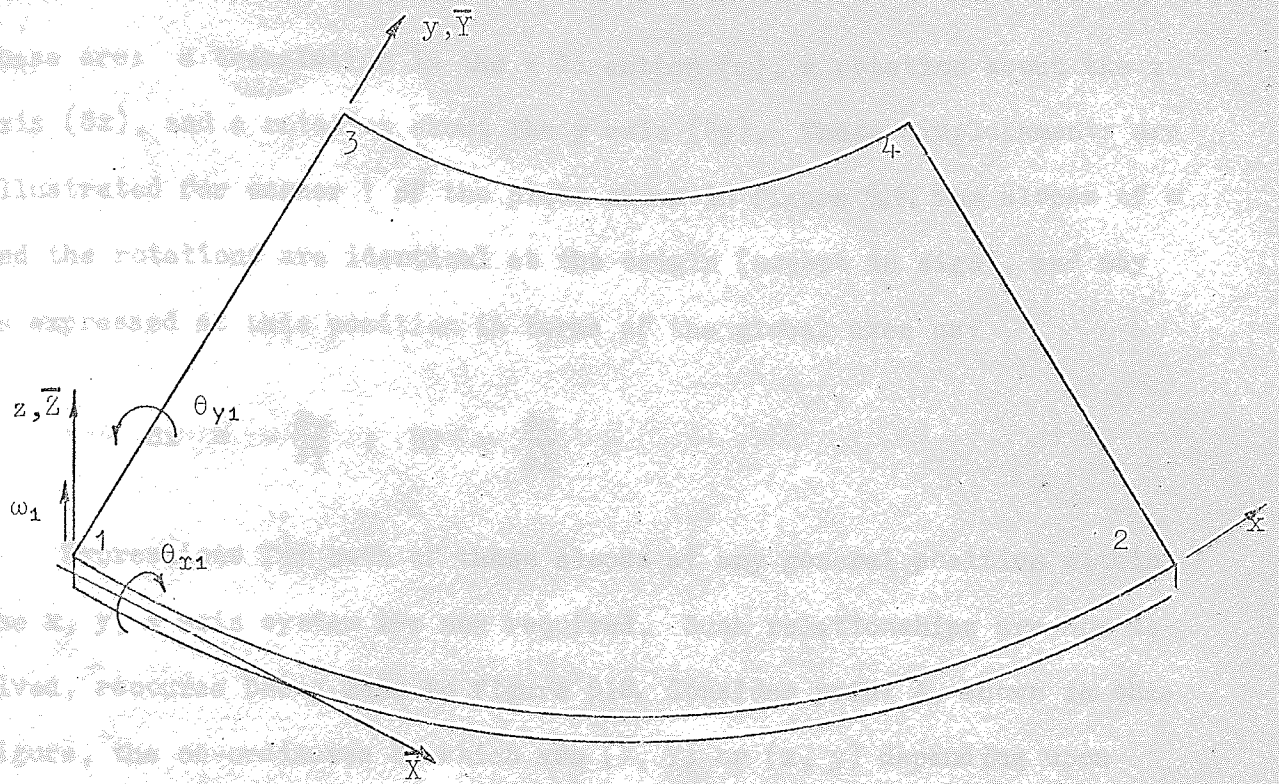
In order that the programme might be as flexible as possible it is essential that many element types should be included. The consideration of structures involving some degree of curvature suggests a further element not previously considered, namely an annular segment. Approximations to the annular shape have been employed<sup>(6)</sup> where a curve was split into a series of straight lines, thus permitting the use of triangular or rectangular plates to simulate the true shape. Such approximations are unsatisfactory for all but the finest mesh.

To enable the incorporation of an annular plate element to the programme library it is necessary to formulate the in and out of plane stiffness matrices of the element. These matrices are developed in the following text, as are the matrices required during the computation of stresses within such an annular element. Finally the displacement transformation matrices which relate local displacements to global displacements are formed.

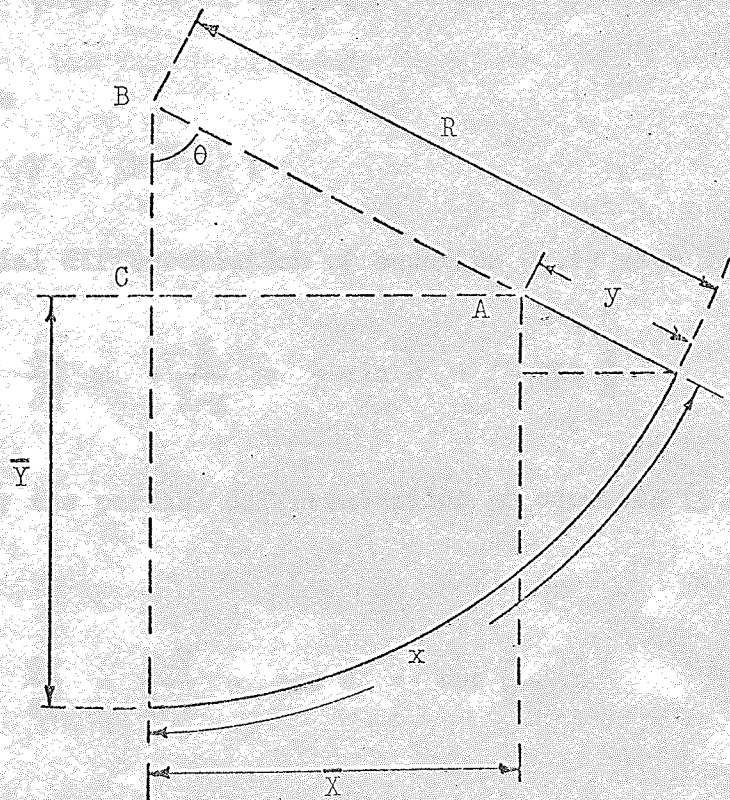
#### (5.2) The out of plane displacement function

Consider the curved plate shown in figure 5.1, with the origin of the local axes  $x, y, z$  at corner 1 of the element. Let the  $x$  axis run along the curved edge of the plate from corner 1 to corner 2, and the  $y$  axis run radially from corner 1 to corner 3. Consider also a further set of axes  $\bar{X}, \bar{Y}, \bar{Z}$  with the same origin as the  $x, y, z$  axes, and in which  $y$  and  $z$  coincide with  $\bar{Y}$  and  $\bar{Z}$  while the  $\bar{X}$  axis is tangential to the element. These axes are also shown in figure 5.1.

Each corner of the plate has three out of plane displacements,



OUT OF PLANE DISPLACEMENTS SHOWN AT CORNER ONE  
FIGURE 5.1 .



LOCAL AND GLOBAL AXES  
FIGURE 5.2



these are: a translation in the z direction ( $\omega$ ), a rotation about the x axis ( $\theta_x$ ), and a rotation about the y axis ( $\theta_y$ ). These displacements are illustrated for corner 1 of the plate shown in figure 5.1. The slopes of  $\omega$  and the rotations are identical at the origin (except in sign), and may be expressed at this position in terms of the global axes as:

$$\theta_x = -\frac{\partial \omega}{\partial \bar{Y}} ; \quad \theta_y = \frac{\partial \omega}{\partial \bar{X}}$$

Expressions for both of these slopes at any general position within the x, y, z axis system are now required. Such relationships are now derived, recourse being made to figure 5.2. Consider point A, shown in this figure, the co-ordinates of which are  $(\bar{X}, \bar{Y})$  or  $(x, y)$  depending upon which of the two co-ordinate systems is used. Applying Pythagoras' theorem to triangle ABC the following expression is obtained:

$$(R-y)^2 = \bar{X}^2 + (R-\bar{Y})^2 \quad \dots (5.1)$$

Now since

$$y = y(\bar{X}, \bar{Y}) ; \quad \dots (5.2)$$

the partial differentiation of equation (5.1) with respect to  $\bar{X}$  gives:

$$\frac{\partial y}{\partial \bar{X}} = -\frac{\bar{X}}{R-y} = -\sin \theta = -\sin \frac{x}{R} \quad \dots (5.3)$$

Similarly the partial differentiation of equation (5.1) with respect to  $\bar{Y}$  gives:

$$\frac{\partial y}{\partial \bar{Y}} = \frac{R-\bar{Y}}{R-y} = \cos \theta = \cos \frac{x}{R} \quad \dots (5.4)$$

Figure 5.2 shows that

$$x = R.\theta \quad \text{and} \quad \tan \theta = \frac{\bar{X}}{R-\bar{Y}} ;$$



Thus  $x$  axis is tangent

$$\frac{x}{R} = \tan^{-1} \left( \frac{\bar{X}}{R-\bar{Y}} \right) \quad \dots (5.5)$$

Hence

$$x = x(\bar{X}, \bar{Y})$$

The partial differentiation of equation (5.5) with respect to  $\bar{X}$  gives

$$\frac{\partial x}{\partial \bar{X}} = \frac{R \cdot (R-\bar{Y})}{(R-\bar{Y})^2 + \bar{X}^2} = \frac{R}{(R-y)} \cdot \cos \frac{x}{R} \quad \dots (5.6)$$

Similarly the partial differentiation of equation (5.5) with respect to  $\bar{Y}$  gives:

$$\frac{\partial x}{\partial \bar{Y}} = \frac{R \cdot \bar{X}}{(R-\bar{Y})^2 + \bar{X}^2} = \frac{R}{(R-y)} \cdot \sin \frac{x}{R} \quad \dots (5.7)$$

Furthermore if  $\omega$  is a function of  $x$  and  $y$  then the 'chain rule' (28) may be used in the following manner to relate  $\omega$  to  $\bar{X}$  and  $\bar{Y}$

$$\frac{\partial \omega}{\partial \bar{X}} = \frac{\partial \omega}{\partial x} \cdot \frac{\partial x}{\partial \bar{X}} + \frac{\partial \omega}{\partial y} \cdot \frac{\partial y}{\partial \bar{X}} \quad \dots (5.8)$$

and

$$\frac{\partial \omega}{\partial \bar{Y}} = \frac{\partial \omega}{\partial x} \cdot \frac{\partial x}{\partial \bar{Y}} + \frac{\partial \omega}{\partial y} \cdot \frac{\partial y}{\partial \bar{Y}} \quad \dots (5.9)$$

Substituting equation (5.6) into equation (5.8) gives

$$\frac{\partial \omega}{\partial \bar{X}} = \frac{\partial \omega}{\partial x} \left[ \frac{R}{R-y} \cdot \cos \frac{x}{R} \right] + \frac{\partial \omega}{\partial y} \left[ - \sin \frac{x}{R} \right] = m \quad \dots (5.10)$$

Similarly substituting equation (5.7) into equation (5.9) gives

$$\frac{\partial \omega}{\partial \bar{Y}} = \frac{\partial \omega}{\partial x} \left[ \frac{R}{R-y} \cdot \sin \frac{x}{R} \right] + \frac{\partial \omega}{\partial y} \left[ \cos \frac{x}{R} \right] = n \quad \dots (5.11)$$

The x axis is tangential when  $x = 0$ , substituting this condition into equations (5.10) and (5.11) gives

$$\frac{\partial \omega}{\partial X} = \left[ \frac{R}{R-y} \right] \cdot \frac{\partial \omega}{\partial x} \quad \dots (5.12)$$

$$\frac{\partial \omega}{\partial Y} = \frac{\partial \omega}{\partial y} \quad \dots (5.13)$$

These are the curvatures in the two principal directions.

Consequently the state of deformation of the plate can be entirely described by the  $\omega$  displacement of the plate. To ensure that the plate remains continuous, conditions of continuity and equilibrium should be imposed at each joint. The selection of a displacement function which will ensure complete continuity between the interfaces of various elements is a complex operation. The selection, however, of a displacement function which preserves continuity of  $\omega$  but does not guarantee slope continuity between the elements is a more straightforward task. If such a function satisfies the 'constant strain' criterion then convergence may still be found<sup>(6)</sup>.

One such suitable function containing twelve parameters corresponding to the twelve nodal displacements is:-

$$\omega = a_1 + a_2x + a_3y + a_4x^2 + a_5xy + a_6y^2 + a_7x^3 + a_8x^2y + a_9xy^2 + a_{10}y^3 + a_{11}x^3y + a_{12}xy^3 \quad (5.14)$$

This is the same function as that used for the rectangular plate and was first stated by Zienkiewicz<sup>(6)</sup>. One advantage of this expression is

that along the element boundaries the displacement  $\omega$  varies as a cubic function. To define this uniquely only four constants are required. If the two end values of slopes and displacements are used, then a continuity of  $\omega$  is also imposed along the boundary. The parabola, however,

defining the gradient of  $\omega$  normal to any of the boundaries is not uniquely specified, and therefore a discontinuity of normal slope will occur.

The constants  $a_1$  to  $a_{12}$  in equation (5.14) may be evaluated by solving the twelve simultaneous equations relating the values of  $\omega$ ,  $\frac{\partial \omega}{\partial y}$  and  $\left[ \frac{R}{R-y} \right] \cdot \frac{\partial \omega}{\partial x}$ , at the joints.

For joint  $j$  substituting its co-ordinates  $(x_j, y_j)$  into equation (5.14) and carrying out the partial differentiations mentioned above gives

$$\begin{aligned} \omega_j = & a_1 + a_2 x_j + a_3 y_j + a_4 x_j^2 + a_5 x_j y_j + a_6 y_j^2 + a_7 x_j^3 + \\ & a_8 x_j^2 y_j + a_9 x_j y_j^2 + a_{10} y_j^3 + a_{11} x_j^3 y_j + a_{12} x_j y_j^3 \end{aligned} \quad (5.15)$$

$$\begin{aligned} \left( \frac{\partial \omega}{\partial y} \right)_j = \theta x_j = & -a_3 - a_5 x_j - 2a_6 y_j - a_8 x_j^2 - 2a_9 x_j y_j - \\ & 3a_{10} y_j^2 - a_{11} x_j^3 - 3a_{12} x_j y_j^2 \end{aligned} \quad (5.16)$$

$$\begin{aligned} \frac{\partial \omega}{\partial x} \left[ \frac{R}{R-y} \right] = \theta y_j = & \left[ \frac{R}{R-y} \right] \left( a_2 + 2a_4 x_j + a_5 y_j + 3a_7 x_j^2 + \right. \\ & \left. 2a_8 x_j y_j + a_9 y_j^2 + 3a_{11} x_j^2 y_j + a_{12} y_j^3 \right) \end{aligned} \quad (5.17)$$

If these expressions are formed for corners one, two, three and four of the curved plate then the resulting equations may be written in matrix form as:

$$\{\underline{\delta}\} = \underline{C} \{\underline{a}\} \quad \dots \quad (5.18)$$

This relationship is shown in full in figure 5.3. Here the  $x$  and  $y$  co-ordinates appear as  $X$  and  $Y$ , this is so because for a given plate the co-ordinates of its corners are constant. In the following text  $x$  and  $y$  will be used as variables denoting any general position within the plate. It is convenient at this stage to express the  $\{\underline{a}\}$  vector as the subject of the equation, thus equation (5.18) becomes

$$\{\underline{a}\} = \underline{C}^{-1} \{\underline{\delta}\} \quad \dots \quad (5.19)$$



$$\begin{bmatrix} \omega_1 \\ \theta_{x1} \\ \theta_{y1} \\ \omega_2 \\ \theta_{x2} \\ \theta_{y2} \\ \omega_3 \\ \theta_{x3} \\ \theta_{y3} \\ \omega_4 \\ \theta_{x4} \\ \theta_{y4} \end{bmatrix} = \begin{bmatrix} 1 & & & & & & & & & & & \\ & -1 & & & & & & & & & & \\ & e & & & & & & & & & & \\ & X & X^2 & & & & & & & & & \\ & & & -X & & & & & & & & \\ & & & & -X^2 & & & & & & & \\ & & & & & X^3 & & & & & & \\ & & & & & & -X & & & & & \\ & & & & & & & -X^2 & & & & \\ & & & & & & & & X^3 & & & \\ & & & & & & & & & 3eX^2 & & \\ & & & & & & & & & & -X^3 & \\ & & & & & & & & & & & Y^3 \\ & & & & & & & & & & & & -3Y^2 \\ & & & & & & & & & & & & & eY^3 \\ & & & & & & & & & & & & & & eY^2 \\ & & & & & & & & & & & & & & & XY^2 \\ & & & & & & & & & & & & & & & & Y^3 \\ & & & & & & & & & & & & & & & & & -3Y^2 \\ & & & & & & & & & & & & & & & & & & -3XY^2 \\ & & & & & & & & & & & & & & & & & & & 3eX^2Y \\ & eY^3 \end{bmatrix} \begin{bmatrix} a_1 \\ a_2 \\ a_3 \\ a_4 \\ a_5 \\ a_6 \\ a_7 \\ a_8 \\ a_9 \\ a_{10} \\ a_{11} \\ a_{12} \end{bmatrix}$$

$$\{\underline{\delta}\} = \underline{C}\{\underline{a}\} ; \quad e = \frac{R}{R-y} \quad \text{NON-ZERO TERMS ONLY}$$

FIGURE 5.3



Figure 5.4 shows this relationship.

### (5.3) The out of plane stress and strain matrices

The usual 'thin plate' assumptions of linear variation of stress and strain throughout the thickness of the plate will be adopted. Since this assumption has been made the stresses and strains in the element may be defined in terms of the stress resultant internal moments  $\bar{M}_X$ ;  $\bar{M}_Y$ ;  $\bar{M}_{XY}$ ; and the curvatures  $\frac{\partial^2 \omega}{\partial X^2}$ ;  $\frac{\partial^2 \omega}{\partial Y^2}$ ;  $\frac{\partial^2 \omega}{\partial X \partial Y}$ . The direction of action of each of the moments is illustrated in figure 5.5. Actual stresses are related to these moments by the modulus of the section. General expressions for the curvature will now be derived. As curvature is the differential of the slope, equations (5.10) and (5.11) will be used:

$$\text{since } \frac{\partial \omega}{\partial X} = m; \text{ and } m = m(x,y)$$

then  $\frac{\partial^2 \omega}{\partial X^2}$  is obtained from the chain rule by

$$\frac{\partial^2 \omega}{\partial X^2} = \frac{\partial m}{\partial X} = \frac{\partial m}{\partial x} \cdot \frac{\partial x}{\partial X} + \frac{\partial m}{\partial y} \cdot \frac{\partial y}{\partial X} \quad \dots (5.20)$$

Substituting equations (5.3) and (5.6) into equation (5.20) and also substituting the condition  $x = 0$ , which is necessary for the axes to be tangential, the result is:

$$\frac{\partial^2 \omega}{\partial X^2} = \left[ \frac{R}{R-y} \right] \frac{\partial m}{\partial x} \quad \dots (5.21)$$

Finally if equation (5.10) is partially differentiated with respect to  $x$  and the result substituted into equation (5.21) we have

$$\begin{aligned} \frac{\partial^2 \omega}{\partial X^2} = & \left( \frac{R}{R-y} \right) \left[ \frac{\partial^2 \omega}{\partial x^2} \left( \frac{R}{R-y} \cdot \cos \frac{x}{R} \right) + \frac{\partial \omega}{\partial x} \left( - \frac{1}{R-y} \cdot \sin \frac{x}{R} \right) + \right. \\ & \left. \frac{\partial^2 \omega}{\partial x \partial y} \left( - \sin \frac{x}{R} \right) + \frac{\partial \omega}{\partial y} \left( - \frac{1}{R} \cdot \cos \frac{x}{R} \right) \right] \quad (5.22) \end{aligned}$$



Once again

1959

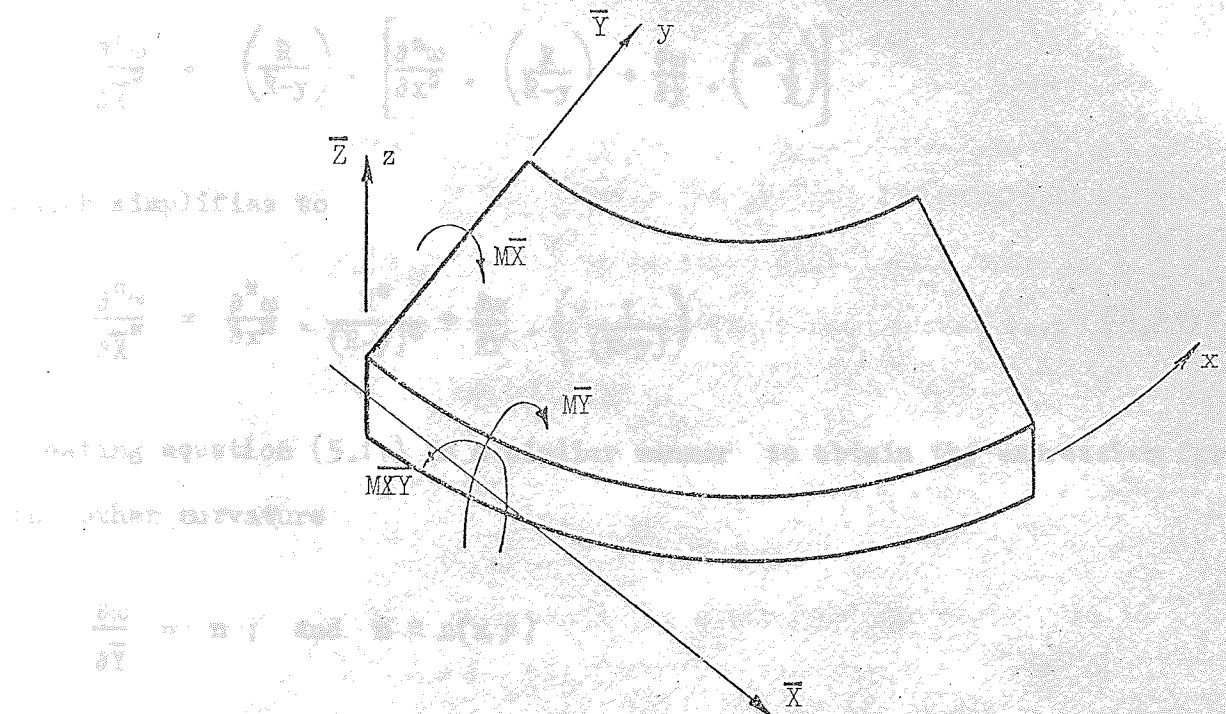


FIGURE 5.5

1,1	1,2	1,3	1,4	1,5	1,6	1,7	1,8	1,9	1,10	1,11	1,12
2,1	2,2	2,3	2,4	2,5	2,6	2,7	2,8	2,9	2,10	2,11	2,12
3,1	3,2	3,3	3,4	3,5	3,6	3,7	3,8	3,9	3,10	3,11	3,12

KEY TO TERMS COMPRISING THE OUT OF PLANE B MATRIX

FIGURE 5.6

Once again substituting in the limiting condition that  $x = 0$  equation (5.22) becomes

$$\frac{\partial^2 \omega}{\partial \bar{X}^2} = \left( \frac{R}{R-y} \right) \cdot \left[ \frac{\partial^2 \omega}{\partial x^2} \cdot \left( \frac{R}{R-y} \right) + \frac{\partial \omega}{\partial y} \cdot \left( -\frac{1}{R} \right) \right] \quad (5.22)$$

which simplifies to

$$\frac{\partial^2 \omega}{\partial \bar{X}^2} = \frac{\partial^2 \omega}{\partial x^2} \cdot \frac{R^2}{(R-y)^2} + \frac{\partial \omega}{\partial y} \cdot \left( -\frac{1}{(R-y)} \right) \quad \dots (5.23)$$

Treating equation (5.11) in a similar manner to obtain the expression for the other curvature

$$\frac{\partial \omega}{\partial \bar{Y}} = n ; \text{ and } n = n(x, y)$$

then  $\frac{\partial^2 \omega}{\partial \bar{Y}^2}$  is obtained from the chain rule by

$$\frac{\partial^2 \omega}{\partial \bar{Y}^2} = \frac{\partial n}{\partial \bar{Y}} = \frac{\partial n}{\partial x} \cdot \frac{\partial x}{\partial \bar{Y}} + \frac{\partial n}{\partial y} \cdot \frac{\partial y}{\partial \bar{Y}} \quad \dots (5.24)$$

Substituting equations (5.4) and (5.7) into equation (5.24) and also the  $x = 0$  condition then result is

$$\frac{\partial^2 \omega}{\partial \bar{Y}^2} = \frac{\partial n}{\partial y} \quad \dots (5.25)$$

Finally if equation (5.11) is partially differentiated with respect to  $y$  and the result substituted into equation (5.25) we have

$$\frac{\partial^2 \omega}{\partial \bar{Y}^2} = \frac{\partial^2 \omega}{\partial x \cdot \partial y} \left( \frac{R}{R-y} \cdot \sin \frac{x}{R} \right) + \frac{\partial \omega}{\partial x} \left( \frac{R}{(R-y)^2} \cdot \sin \frac{x}{R} \right) + \frac{\partial^2 \omega}{\partial y^2} \cdot \cos \frac{x}{R} +$$

$$\frac{\partial \omega}{\partial y} \cdot (0) \quad \dots (5.26)$$



If the limiting condition for the axes to be tangential, when  $x = 0$ , is substituted then equation (5.26) becomes

$$\frac{\partial^2 \omega}{\partial \bar{Y}^2} = \frac{\partial^2 \omega}{\partial y^2} \quad \dots (5.27)$$

Finally to generate  $\frac{\partial^2 \omega}{\partial \bar{X} \cdot \partial \bar{Y}}$  clearly the partial differentiation of equation (5.10) with respect to  $\bar{Y}$  or equation (5.11) with respect to  $\bar{X}$  will give the required result. Selecting the former of these options, which may be expressed mathematically as

$$\frac{\partial^2 \omega}{\partial \bar{X} \cdot \partial \bar{Y}} = \frac{\partial m}{\partial \bar{Y}} \quad \dots (5.28)$$

and since  $m = m(x, y)$  then once again the chain rule has to be used to give

$$\frac{\partial m}{\partial \bar{Y}} = \frac{\partial m}{\partial x} \cdot \frac{\partial x}{\partial \bar{Y}} + \frac{\partial m}{\partial y} \cdot \frac{\partial y}{\partial \bar{Y}} \quad \dots (5.29)$$

Substituting equations (5.4) and (5.7) with the condition of  $x = 0$  into equation (5.29) gives

$$\frac{\partial^2 \omega}{\partial \bar{X} \cdot \partial \bar{Y}} = \frac{\partial m}{\partial \bar{Y}} = \frac{\partial m}{\partial x} \quad \dots (5.30)$$

Hence if equation (5.10) is now partially differentiated with respect to  $x$  and substituted into equation (5.30) the resulting equation is

$$\begin{aligned} \frac{\partial^2 \omega}{\partial \bar{X} \cdot \partial \bar{Y}} = \frac{\partial m}{\partial x} &= \frac{\partial^2 \omega}{\partial x \cdot \partial y} \left( \frac{R}{R-y} \cdot \cos \frac{x}{R} \right) + \frac{\partial \omega}{\partial x} \left( \frac{R}{(R-y)^2} \cdot \cos \frac{x}{R} \right) \\ &+ \frac{\partial \omega}{\partial y^2} \left( -\frac{\sin \frac{x}{R}}{R} \right) + \frac{\partial \omega}{\partial y} \cdot (0) \end{aligned} \quad (5.31)$$

If the condition for tangential axes ( $x = 0$ ) is now substituted into

equation (5.31) the result is

$$\frac{\partial^2 \omega}{\partial \bar{x} \partial \bar{y}} = \frac{\partial^2 \omega}{\partial x \partial y} \cdot \left( \frac{R}{R-y} \right) + \frac{\partial \omega}{\partial x} \left( \frac{R}{(R-y)^2} \right) \quad \dots (5.32)$$

If the polynomial for  $\omega$  given in equation (5.14) is now partially differentiated in accordance with the formats given in equations (5.23), (5.27) and (5.32) the resulting three equations may be written in matrix form as

$$\{\underline{y}\} = \underline{L} \{\underline{a}\} \quad \dots (5.33)$$

These matrices are given in full in figure 5.7 and relate the curvatures to the twelve constants.

If equations (5.19) and (5.33) are combined then the twelve unknown constants in  $\{\underline{a}\}$  are removed and an expression relating the curvatures to the out of plane displacements at each corner is formed; this may be written as

$$\{\underline{y}\} = \underline{L} \cdot \underline{C}^{-1} \cdot \{\underline{\delta}\}$$

and is normally written in the form

$$\{\underline{y}\} = \underline{B} \cdot \{\underline{\delta}\} \quad \dots (5.34)$$

The format of the  $\underline{B}$  matrix is given in figure 5.6 and the individual terms corresponding to the codes in that figure may be formed from figures 5.8, 5.9 and 5.10.

Finally the linear relationship between stress and strain, which is derived in standard texts <sup>(29)</sup> is of the form

$$\{\underline{\sigma}\} = \underline{D} \{\underline{\epsilon}\}$$

and for an isotropic plate  $\underline{D}$  is given by

$$\begin{bmatrix} \gamma_X \\ \gamma_Y \\ 2\gamma_{XY} \end{bmatrix} = \begin{bmatrix} 0 & 0 & -\frac{1}{A} & \frac{2R^2}{A^2} & -\frac{x}{A} & -\frac{2y}{A} & \frac{6xR^2}{A^2} & \frac{2yR^2}{A^2} & -\frac{x^2}{A} & -\frac{2xy}{A} & -\frac{3y^2}{A} & \frac{6xyR^2}{A^2} & -\frac{x^3}{A} & -\frac{3xy^2}{A} \\ 0 & 0 & 0 & 0 & 0 & 2 & 0 & 0 & 0 & 2x & 6y & 0 & 6xy & 0 \\ 0 & \frac{2R}{A^2} & 0 & \frac{4yR}{A^2} & \frac{2R^2}{A^2} & 0 & \frac{6x^2R}{A^2} & \frac{4xR^2}{A^2} & \frac{4yR^2-2y^2R}{A^2} & 0 & 0 & \frac{6x^3R^2}{A^2} & \frac{6y^2R^2-4y^3R}{A^2} & 0 \end{bmatrix} \begin{bmatrix} a_1 \\ a_2 \\ a_3 \\ a_4 \\ a_5 \\ a_6 \\ a_7 \\ a_8 \\ a_9 \\ a_{10} \\ a_{11} \\ a_{12} \end{bmatrix}$$

$$\{\bar{\gamma}\} = \bar{L}\{a\}$$

where  $A = R-y$

FIGURE 5.7



VALUE OF m CORRESPONDING TO EACH COLUMN												
FUNCTION	1	2	3	4	5	6	7	8	9	10	11	12
1		$\frac{1}{R}$										
x	$\frac{1}{XYR}$	$-\frac{1}{XR}$	$\frac{1}{WYR}$	$-\frac{1}{RXY}$	$\frac{1}{XR}$		$-\frac{1}{XYR}$		$-\frac{1}{WYR}$	$\frac{1}{XYR}$		
y	$\frac{6}{Y^2R}$	$-\frac{4}{YR}$					$-\frac{6}{Y^2R}$	$-\frac{2}{RY}$				
xy	$-\frac{6}{XY^2R}$	$\frac{4}{XYR}$		$\frac{6}{Y^2XR}$	$-\frac{4}{XYR}$		$\frac{6}{XY^2R}$	$\frac{2}{XYR}$		$-\frac{6}{XY^2R}$	$-\frac{2}{XYR}$	
xy <sup>2</sup>	$\frac{6}{Y^3XR}$	$-\frac{3}{XY^2R}$		$-\frac{6}{XY^3R}$	$\frac{3}{XY^2R}$		$-\frac{6}{XY^3R}$	$-\frac{3}{XY^2R}$		$\frac{6}{Y^3XR}$	$\frac{3}{XY^2R}$	
y <sup>2</sup>	$-\frac{6}{Y^3R}$	$\frac{3}{Y^2R}$					$\frac{6}{Y^3R}$	$\frac{3}{Y^2R}$				
x <sup>2</sup>	$-\frac{3}{X^2YR}$		$-\frac{2}{WXYR}$	$\frac{3}{X^2YR}$		$-\frac{1}{WXYR}$	$\frac{3}{X^2YR}$		$\frac{2}{WXYR}$	$-\frac{3}{X^2YR}$		$\frac{1}{WXYR}$
x <sup>3</sup>	$\frac{2}{X^3YR}$		$\frac{1}{WX^2YR}$	$-\frac{2}{X^3YR}$		$\frac{1}{WX^2YR}$	$-\frac{2}{X^3YR}$		$-\frac{1}{WX^2YR}$	$\frac{2}{X^3YR}$		$-\frac{1}{WX^2YR}$
$\frac{1}{A}$	$-\frac{6R}{X^2}$		$-\frac{4R}{WX}$	$\frac{6R}{X^2}$		$-\frac{2R}{WX}$						
$\frac{x}{A}$	$\frac{12R}{X^3}$		$\frac{6R}{X^2W}$	$-\frac{12R}{X^3}$		$\frac{6R}{WX^2}$						
$\frac{y}{A}$	$\frac{6R}{X^2Y}$		$\frac{4R}{WXY}$	$-\frac{6R}{X^2Y}$		$\frac{2R}{WXY}$	$-\frac{6R}{X^2Y}$		$-\frac{4R}{WXY}$	$\frac{6R}{X^2Y}$		$-\frac{2R}{WXY}$
$\frac{xy}{A}$	$-\frac{12R}{X^3Y}$		$-\frac{6R}{WX^2Y}$	$\frac{12R}{YX^3}$		$-\frac{6R}{WX^2Y}$	$\frac{12R}{X^3Y}$		$\frac{6R}{WX^2Y}$	$-\frac{12R}{X^3Y}$		$\frac{6R}{WX^2Y}$

PRIME AREA ONE  $B_{1,m}$  TERMS

$W = R/(R-Y)$ ;  $A = R-Y$

FIGURE 5.8

NON-ZERO TERMS ONLY

FUNCTION	VALUE OF $m$ CORRESPONDING TO EACH COLUMN											
	1	2	3	4	5	6	7	8	9	10	11	12
1	$\frac{-6}{Y^2}$	$\frac{4}{Y}$					$\frac{6}{Y^2}$	$\frac{2}{Y}$				
x	$\frac{6}{XY^2}$	$\frac{-4}{XY}$		$\frac{-6}{Y^2X}$	$\frac{4}{XY}$		$\frac{-6}{XY^2}$	$\frac{-2}{XY}$	$\frac{6}{XY^2}$		$\frac{2}{XY}$	
y	$\frac{6}{Y^2R} + \frac{12}{Y^3}$	$\frac{-4}{YR} - \frac{6}{Y^2}$					$\frac{-6}{Y^2R} - \frac{12}{Y^3}$	$\frac{-2}{YR} - \frac{6}{Y^2}$				
xy	$\frac{-6}{XY^2R} - \frac{12}{XY^3}$	$\frac{4}{XYR} + \frac{6}{XY^2}$		$\frac{6}{Y^2XR} + \frac{12}{Y^3X}$	$\frac{-4}{XYR} - \frac{6}{XY^2}$		$\frac{6}{XY^2R} + \frac{12}{Y^3X}$	$\frac{2}{XYR} + \frac{6}{XY^2}$	$\frac{-6}{XY^2R} - \frac{12}{Y^3X}$	$\frac{-2}{XYR} - \frac{6}{XY^2}$		
$xy^2$	$\frac{12}{XY^3R}$	$\frac{-6}{XY^2R}$		$\frac{-12}{Y^3XR}$	$\frac{6}{XY^2R}$		$\frac{-12}{Y^3XR}$	$\frac{-6}{XY^2R}$	$\frac{12}{Y^3XR}$		$\frac{6}{XY^2R}$	
$y^2$	$\frac{-12}{Y^3R}$	$\frac{6}{Y^2R}$					$\frac{12}{Y^3R}$	$\frac{6}{Y^2R}$				

PRIME AREA TWO  $B_{2,m}$  TERMS

NON-ZERO TERMS ONLY

FIGURE 5.9

FUNCTION	VALUE OF m CORRESPONDING TO EACH COLUMN											
	1	2	3	4	5	6	7	8	9	10	11	12
$\frac{1}{A}$	$-\frac{2R}{XY}$	$\frac{2R}{X}$	$\frac{2}{\omega} - \frac{2R}{\omega Y}$	$\frac{2R}{XY}$	$-\frac{2R}{X}$		$\frac{2R}{XY}$		$\frac{2R}{\omega Y}$	$-\frac{2R}{XY}$		
$\frac{x}{A}$	$-\frac{12}{X^2} + \frac{12R}{X^2 Y}$		$-\frac{8}{\omega X} + \frac{8R}{\omega XY}$	$\frac{12}{X^2} - \frac{12R}{X^2 Y}$		$-\frac{4}{\omega X} + \frac{4R}{\omega XY}$	$-\frac{12R}{X^2 Y}$		$-\frac{8R}{\omega XY}$	$\frac{12R}{X^2 Y}$		$-\frac{4R}{\omega XY}$
$\frac{x^2}{A}$	$\frac{12}{X^3} - \frac{12R}{X^3 Y}$		$\frac{6}{\omega X^2} - \frac{6R}{\omega X^2 Y}$	$-\frac{12}{X^3} + \frac{12R}{X^3 Y}$		$\frac{6}{\omega X^2} - \frac{6R}{\omega X^2 Y}$	$\frac{12R}{X^3 Y}$		$\frac{6R}{\omega X^2 Y}$	$-\frac{12R}{X^3 Y}$		$\frac{6R}{\omega X^2 Y}$
$\frac{y}{A}$	$\frac{12R}{XY^2}$	$-\frac{8R}{XY}$		$-\frac{12R}{XY^2}$	$\frac{8R}{XY}$		$-\frac{12R}{XY^2}$	$-\frac{4R}{XY}$		$\frac{12R}{XY^2}$	$\frac{4R}{XY}$	
$\frac{y^2}{A}$	$-\frac{6}{XY^2} - \frac{12R}{XY^3}$	$\frac{4}{XY} + \frac{6R}{XY^2}$		$\frac{6}{XY^2} + \frac{12R}{XY^3}$	$-\frac{4}{XY} - \frac{6R}{XY^2}$		$\frac{6}{XY^2} - \frac{12R}{XY^3}$	$\frac{2}{XY} + \frac{6R}{XY^2}$		$-\frac{6}{XY^2} - \frac{12R}{XY^3}$	$-\frac{2}{XY} - \frac{6R}{XY^2}$	
$\frac{y^3}{A}$	$\frac{8}{XY^3}$	$-\frac{4}{XY^2}$		$-\frac{8}{XY^3}$	$\frac{4}{XY^2}$		$-\frac{8}{XY^3}$	$-\frac{4}{XY^2}$		$\frac{8}{XY^3}$	$\frac{4}{XY^2}$	

PRICE AREA THREE B<sub>3,m</sub> TERMS

NON-ZERO TERMS ONLY

$$A=R-Y; \quad \omega=R/(R-Y);$$

FIGURE 5.10

$$\underline{D} = \frac{E \cdot t^3}{12(1-\mu^2)} \begin{bmatrix} 1 & \mu & 0 \\ \mu & 1 & 0 \\ 0 & 0 & \frac{1}{2}(1-\mu) \end{bmatrix} \quad \dots (5.35)$$

#### (5.4) The out of plane element stiffness matrix

Application of the principles of virtual work <sup>(6)</sup> result in the well known expression for the stiffness of an element

$$\underline{k} = \int_0^V \underline{B}^T \cdot \underline{D} \cdot \underline{B} \cdot dv \quad \dots (5.36)$$

Since the plate is of constant thickness the integration is carried out over its area only.

Figure 5.11 shows a small element of area  $\delta A$  within a curved plate where it is noticed that:

$$\delta A = (\pi \cdot (R-Y)^2 - \pi \cdot ((R-Y) - \delta y)^2) \frac{\delta \theta}{2\pi} \quad \dots (5.37)$$

$$\text{and } \delta \theta = \frac{\delta x}{R} \quad \dots (5.38)$$

Substituting equation (5.38) into equation (5.37) and simplifying we obtain

$$\delta A = \left(1 - \frac{Y}{R} - \frac{\delta y}{2R}\right) \delta x \cdot \delta y \quad \dots (5.39)$$

In the limit as  $\delta x$  and  $\delta y$  tend to zero equation (5.39) becomes:

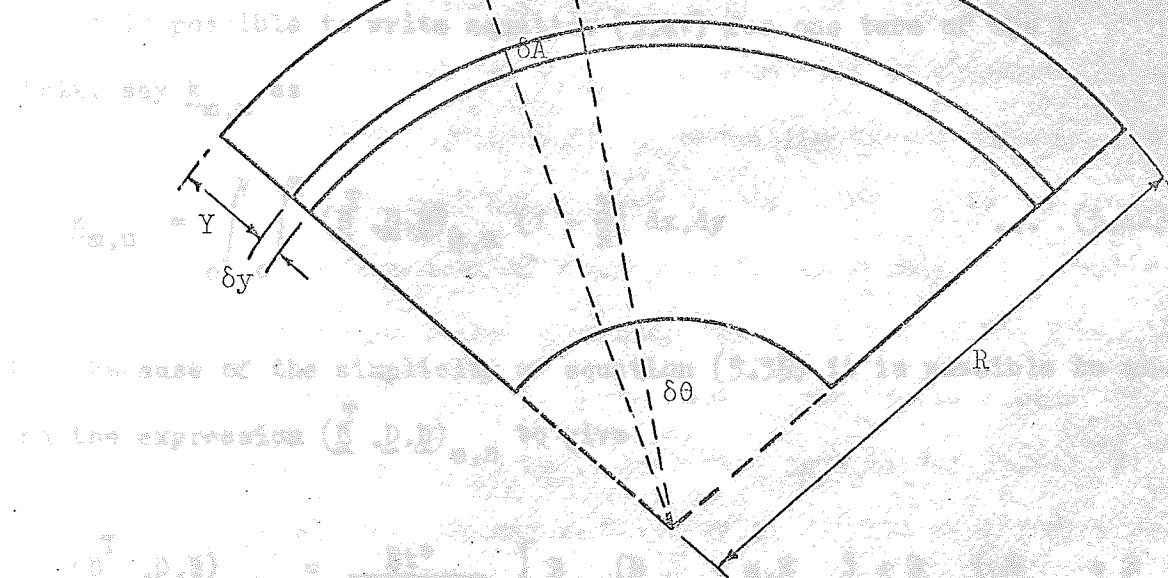
$$dA = \left(1 - \frac{Y}{R}\right) dx \cdot dy \quad \dots (5.40)$$

If equation (5.40) is now substituted into equation (5.36) the result is

$$\underline{k} = \int_0^Y \int_0^X (\underline{B}^T \cdot \underline{D} \cdot \underline{B}) \cdot \left(1 - \frac{Y}{R}\right) \cdot dx \cdot dy \quad \dots (5.41)$$



Because of the complexity of the stiffness matrix, it is, in general, unnecessary to produce an explicit matrix, since the operations and manipulations required to generate the stiffness matrix are so involved, these may be programmed and a computer will execute the operations as required.



GENERAL POSITION OF AN ELEMENTAL STRIP  
WITHIN A CURVED PLATE

FIGURE 5.11

Finally to form  $k_{m,n}$  it is necessary to substitute the values of  $k_{m,n}$  into the expression, perform the multiplication and sum the resulting terms over the limits indicated in equation (5.10). Each term of the  $k_{m,n}$  expression contains several functions of  $x$  and  $y$  the result of the multiplication is a function of  $x$  and  $y$  the result of the summation is a function of  $x$  and  $y$ .

To carry out this process efficiently for computer solution it is necessary to carry out the following operations. Firstly consider the  $k_{m,n}$  expression the summation of three different terms is all required to produce each of these terms individually.

Because of the complexity of the B matrix the explicit derivation of the element stiffness matrix is not a feasible proposition. It is, however, unnecessary to produce an explicit matrix, once the algebraic and matrix manipulations required to generate the stiffness matrix are determined, these may be programmed and a computer will execute the various stages as required.

It is possible to write equation (5.41) for one term of the k matrix, say k<sub>m,n</sub> as

$$\underline{k}_{m,n} = \int_0^Y \int_0^X (\underline{B}^T \cdot \underline{D} \cdot \underline{B})_{m,n} \left(1 - \frac{Y}{R}\right) dx \cdot dy \quad \dots (5.42)$$

Also, because of the simplicity of equation (5.35) it is possible to expand the expression  $(\underline{B}^T \cdot \underline{D} \cdot \underline{B})_{m,n}$  to give

$$(\underline{B}^T \cdot \underline{D} \cdot \underline{B})_{m,n} = \frac{Et^3}{12(1-\mu^2)} \left[ B_{1,m}(B_{1,n} + \mu \cdot B_{2,n}) + B_{2,m}(\mu B_{1,n} + B_{2,n}) + B_{3,m} \cdot B_{3,n} \left(\frac{1-\mu}{2}\right) \right] \quad (5.43)$$

Clearly to form k<sub>m,n</sub> it is necessary to substitute the relevant terms of the B matrix into the expression, perform the multiplications, then integrate the resulting terms over the limits indicated in equation (5.42). Since each term of the B matrix contains several functions of the variables x and y the result of the multiplication is to generate further functions.

To make this process suitable for computer solution it is necessary to carry out the following operations. Firstly equation (5.43) comprises the summation of three distinct terms, it is convenient to consider each of these terms individually. If each of the terms is called a 'prime area' then the three 'prime areas' formed from equation (5.43) are

$$\text{Prime area 1} = B_{1,m}(B_{1,n} + \mu B_{2,n}) \quad \dots (5.44)$$

$$\text{Prime area 2} = B_{2,m}(\mu B_{1,n} + B_{2,n}) \quad \dots (5.45)$$

$$\text{Prime area 3} = B_{3,m} \cdot B_{3,n}\left(\frac{1-\mu}{2}\right) \quad \dots (5.46)$$

Consider at this stage any one of these 'prime areas', say, 'prime area 1'. For each row of the  $\underline{k}$  matrix the  $B_{1,m}$  term, appearing in equation (5.44), is constant, and a table may be drawn up comprising twelve columns, one for each row of the stiffness matrix, and  $\alpha$  rows. Where  $\alpha$  is the maximum number of unique functions of  $x$  and  $y$  appearing in any row. Such a table has previously been drawn up to give the first row of the  $\underline{B}$  matrix and is shown in figure 5.8. Similarly for each of the twelve columns of the  $\underline{k}$  matrix the  $(B_{1,n} + \mu B_{2,n})$  term, appearing in equation (5.44), is constant. Once again a table may be drawn up in which  $n$  varies from one to twelve. This table is shown in figure 5.12. In addition to the twelve columns the table has  $\gamma$  rows, where  $\gamma$  is the maximum number of unique functions in  $x$  and  $y$  occurring in any column. Thus to form the 'prime area 1' contribution to the term  $\underline{k}_{m,n}$  of the stiffness matrix, each term in the  $m^{\text{th}}$  column of the table in figure 5.8 has to be multiplied by every element in the  $n^{\text{th}}$  column of the table in figure 5.12. The result is a different set of terms comprising new functions in  $x$  and  $y$ , and integration of these terms must now be carried out.

Since the positions and forms of all of the functions occurring in both the tables is known, as is the order of multiplication, it is possible to predict the position and character of the resulting functions. Such functions are integrated generally, and the expression for each is stored in a further table, in such a manner that its position may be related to the relevant term generated in the manner described previously.

FUNCTION	VALUE OF n											
	1	2	3	4	5	6	7	8	9	10	11	12
1	$-\frac{6\mu}{Y^3}$	$\frac{4\mu}{Y}$					$\frac{6\mu}{Y^3}$	$\frac{2\mu}{Y}$				
x	$\frac{6\mu}{XY^2}$	$-\frac{4\mu}{XY}$		$-\frac{6\mu}{Y^2X}$	$\frac{4\mu}{XY}$		$-\frac{6\mu}{X^2}$	$-\frac{2\mu}{XY}$		$\frac{6\mu}{XY^2}$	$\frac{2\mu}{XY}$	
y	$\frac{12\mu}{Y^3}$	$-\frac{6\mu}{Y^2}$					$-\frac{12\mu}{Y^3}$	$-\frac{6\mu}{Y^2}$				
xy	$-\frac{12\mu}{XY^3}$	$\frac{6\mu}{XY^2}$		$\frac{12\mu}{Y^3X}$	$-\frac{6\mu}{XY^2}$		$\frac{12\mu}{XY^3}$	$\frac{6\mu}{XY^2}$		$-\frac{12\mu}{XY^3}$	$-\frac{6\mu}{XY^2}$	
$\frac{1}{A}$		1										
$\frac{x}{A}$	$\frac{1}{XY}$	$-\frac{1}{X}$	$\frac{1}{Y\omega}$	$-\frac{1}{XY}$	$\frac{1}{X}$		$-\frac{1}{XY}$		$-\frac{1}{\omega Y}$	$\frac{1}{XY}$		
$\frac{y}{A}$	$\frac{6}{Y^2}$	$-\frac{4}{Y}$					$-\frac{6}{Y^2}$	$-\frac{2}{Y}$				
$\frac{x^2}{A}$	$-\frac{3}{X^2Y}$		$-\frac{2}{\omega XY}$	$\frac{3}{X^2Y}$		$-\frac{1}{\omega XY}$	$\frac{3}{X^2Y}$		$\frac{2}{\omega XY}$	$-\frac{3}{X^2Y}$		$\frac{1}{\omega XY}$
$\frac{y^2}{A}$	$-\frac{6}{Y^3}$	$\frac{3}{Y^2}$					$\frac{6}{Y^3}$	$\frac{3}{Y^2}$				
$\frac{xy}{A}$	$-\frac{6}{XY^2}$	$\frac{4}{XY}$		$\frac{6}{Y^2X}$	$-\frac{4}{XY}$		$\frac{6}{XY^2}$	$\frac{2}{XY}$		$-\frac{6}{XY^2}$	$-\frac{2}{XY}$	
$\frac{xy^2}{A}$	$\frac{6}{Y^3X}$	$-\frac{3}{XY^2}$		$-\frac{6}{XY^3}$	$\frac{3}{XY^2}$		$-\frac{6}{XY^3}$	$-\frac{3}{XY^2}$		$\frac{6}{XY^3}$	$\frac{3}{XY^2}$	

FIGURE 5.12

.../... continued



FUNCTION	1	2	3	4	5	6	7	8	9	10	11	12
$\frac{x^3}{A}$	$\frac{2}{X^3Y}$		$\frac{1}{\omega X^2Y}$	$\frac{-2}{X^3Y}$		$\frac{1}{\omega X^2Y}$	$\frac{-2}{X^3Y}$		$\frac{-1}{\omega X^2Y}$	$\frac{2}{X^3Y}$		$\frac{-1}{\omega X^2Y}$
$\frac{1}{A}$	$\frac{-6R^2}{X^2}$		$\frac{-4R^2}{\omega X}$	$\frac{6R^2}{X^2}$		$\frac{-2R^2}{\omega X}$						
$\frac{x}{A}$	$\frac{12R^2}{X^3}$		$\frac{6R^2}{\omega X^2}$	$\frac{-12R^2}{X^3}$		$\frac{6R^2}{\omega X^2}$						
$\frac{y}{A}$	$\frac{6R^2}{X^2Y}$		$\frac{4R^2}{\omega XY}$	$\frac{-6R^2}{X^2Y}$		$\frac{2R^2}{\omega XY}$	$\frac{-6R^2}{X^2Y}$		$\frac{-4R^2}{\omega XY}$	$\frac{6R^2}{X^2Y}$		$\frac{-2R^2}{\omega XY}$
$\frac{xy}{A}$	$\frac{-12R^2}{X^3Y}$		$\frac{-6R^2}{\omega X^2Y}$	$\frac{12R^2}{X^3Y}$		$\frac{-6R^2}{\omega X^2Y}$	$\frac{12R^2}{X^3Y}$		$\frac{6R^2}{\omega X^2Y}$	$\frac{-12R^2}{X^3Y}$		$\frac{6R^2}{\omega X^2Y}$

PRIME AREA ONE ( $B_{1,n} + \mu B_{2,n}$ )  $\omega = \frac{R}{(R-Y)}$ ;  $A = R - Y$

TO OBTAIN PRIME AREA TWO ( $\mu B_{1,n} + B_{2,n}$ ) FROM THIS TABLE:

- (i) ALL TERMS CONTAINING  $\mu$  SHOULD BE DIVIDED BY  $\mu$
- (ii) ALL REMAINING TERMS SHOULD BE MULTIPLIED BY  $\mu$

NON-ZERO TERMS ONLY

FIGURE 5.12 (continued)

FUNCTION	VALUE OF n											
	1	2	3	4	5	6	7	8	9	10	11	12
$\frac{1}{A^2}$	$\frac{-2R^2}{XY}$	$\frac{2R^2}{X}$	$\frac{2R}{\omega} - \frac{2R^2}{\omega Y}$	$\frac{2R^2}{XY}$	$\frac{-2R^2}{XY}$		$\frac{2R^2}{XY}$		$\frac{2R^2}{\omega Y}$	$\frac{-2R^2}{XY}$		
$\frac{x}{A^2}$	$\frac{-12R}{X^2} + \frac{12R^2}{X^2 Y}$		$\frac{-8R}{\omega X} + \frac{8R^2}{\omega XY}$	$\frac{12R}{X^2} - \frac{12R^2}{X^2 Y}$		$\frac{-4R}{\omega X} + \frac{4R^2}{\omega XY}$	$\frac{-12R^2}{X^2 Y}$		$\frac{-8R^2}{\omega XY}$	$\frac{12R^2}{X^2 Y}$		$\frac{-4R^2}{\omega XY}$
$\frac{y}{A^2}$	$\frac{12R^2}{XY^2}$	$\frac{-8R^2}{XY}$		$\frac{-12R^2}{XY^2}$	$\frac{8R^2}{XY}$		$\frac{-12R^2}{XY^2}$	$\frac{-4R^2}{XY}$		$\frac{12R^2}{XY^2}$	$\frac{4R^2}{XY}$	
$\frac{x^2}{A^2}$	$\frac{12R}{X^3} - \frac{12R^2}{X^3 Y}$		$\frac{6R}{\omega X^2} - \frac{6R}{\omega X^2 Y}$	$\frac{-12R}{X^3} + \frac{12R^2}{X^3 Y}$	$\frac{6R}{\omega X^2} - \frac{6R^2}{\omega X^2 Y}$		$\frac{12R^2}{X^3 Y}$		$\frac{6R^2}{\omega X^2 Y}$	$\frac{-12R^2}{X^3 Y}$		$\frac{6R^2}{\omega X^3 Y}$
$\frac{y^2}{A^2}$	$\frac{-12R^2}{XY^3} - \frac{6R}{XY^2}$	$\frac{4R}{XY} + \frac{6R^2}{XY^2}$		$\frac{6R}{XY^2} + \frac{12R^2}{XY^3}$	$\frac{-4R}{XY} - \frac{6R^2}{XY^2}$		$\frac{6R}{XY^2} + \frac{12R^2}{XY^3}$	$\frac{2R}{XY} + \frac{6R^2}{XY^2}$		$\frac{-6R}{XY^2} - \frac{12R^2}{XY^3}$	$\frac{-2R}{XY} - \frac{6R^2}{XY^2}$	
$\frac{y^3}{A^2}$	$\frac{8R}{XY^3}$	$\frac{-4R}{XY^2}$		$\frac{-8R}{XY^3}$	$\frac{4R}{XY^2}$		$\frac{-8R}{XY^3}$	$\frac{-4R}{XY^2}$		$\frac{8R}{XY^3}$	$\frac{4R}{XY^2}$	

PRIME AREA THREE  $E_{3,n}$

$$\omega = R/(R-Y) ; A = R-Y$$

NON-ZERO TERMS ONLY

MULTIPLY ALL TERMS BY  $\left[ \frac{1-L}{2} \right]$

FIGURE 5.13

It is thus possible to

TO CONSTRUCT ELEMENT  $k_{i,j}$

Figure 5.14

From this process is repeated for each of the prime areas

Each of the three results give the value of element

may be

Figure 5.14

Flow diagram

Flow diagram showing the method of construction of term  $k_{i,j}$

The in

curved

displacement

The occurrence of

of a four

of eight

displacement

of eight

displacement

of eight

displacement

of eight

FLOW DIAGRAM SHOWING THE METHOD OF CONSTRUCTION OF TERM  $k_{i,j}$

FIGURE 5.14



It is thus possible to evaluate the relevant integral as its term is formed.

When this process is repeated for each of the prime areas then the summation of the three results gives the value of element  $k_{m,n}$ . This process may be expressed mathematically as

$$k_{m,n} = \left[ \sum_{J=1}^{J=3} \left( \sum_{l=1}^{l=a} M_{m,l} * \left( \sum_{h=1}^{h=\gamma} N_{h,n} * \int_0^Y \int_0^X f(x,y) dx dy \right) \right) \right]$$

where

$J$  = prime area number

$M$  = table of row constants for prime area  $J$

$N$  = table of column constants for prime area  $J$

$a$  = number of different functions of  $x,y$  in table  $M$

$\gamma$  = number of different functions of  $x,y$  in table  $N$

A flow diagram given in figure 5.14 illustrates the computational approach adopted.

The  $M$  and  $N$  tables for each of the prime areas are given in figures 5.8, 5.9, 5.10, 5.12, 5.13.

#### (5.5) The in plane displacement function

A curved plate with the same corner numbering and axes described during the presentation of the out of plane displacement function is shown in figure 5.15. Each corner of such an element has two in plane displacements,  $u$  parallel to the  $x$  axis, and  $v$  parallel to the  $y$  axis. The occurrence of eight displacements, two at each corner, permits the use of a four termed polynomial to represent the variation of displacement of each component.

Since continuity is desirable between adjacent elements it is neces-



sary for each component to vary in a linear manner along the sides of the element. If this is so then the coincidence of displacements at the joints will automatically ensure coincidence at all intermediate points. Consequently the polynomial becomes limited to terms exhibiting such linear variations; such displacement functions are:

$$u = a_1 + a_2 \cdot x + a_3 \cdot y + a_4 \cdot x \cdot y ; \quad \dots (5.47)$$

$$v = a_5 + a_6 \cdot x + a_7 \cdot y + a_8 \cdot x \cdot y ; \quad \dots (5.48)$$

These are the same functions as those normally used for a rectangular plate and were first stated by Zienkiewicz<sup>(6)</sup>. If the co-ordinates of the four corners of the plate are substituted into each of the expressions the eight resulting simultaneous equations relate the displacements to the constants  $a_1$  to  $a_8$ . These equations may be written in matrix form as

$$\{\underline{\delta}\} = \underline{C}\{\underline{a}\} \quad \dots (5.49)$$

The matrices forming this relationship are given in full in figure 5.16. As with the equivalent out of plane expression it is convenient at this stage to express the  $\{\underline{a}\}$  vector as the subject, thus equation (5.49) becomes

$$\{\underline{a}\} = \underline{C}^{-1}\{\underline{\delta}\} \quad \dots (5.50)$$

Figure 5.17 gives this relationship in full which is identical to that achieved when considering a rectangular plate.

#### (5.6) The in plane stress and strain matrices

When considering the plane stress condition the in plane strains are defined in terms of the displacements by the well known relationship

$$\begin{bmatrix} u_1 \\ u_2 \\ u_3 \\ u_4 \\ v_1 \\ v_2 \\ v_3 \\ v_4 \end{bmatrix} = \begin{bmatrix} 1 & & & & & & & \\ & 1 & X & & & & & \\ & & & Y & & & & \\ & & & & & & & \\ & 1 & X & Y & XY & & & \\ & & & & & 1 & & \\ & & & & & & 1 & X \\ & & & & & & & 1 & Y \\ & & & & & & & & 1 & X & Y & XY \end{bmatrix} \times \begin{bmatrix} a_1 \\ a_2 \\ a_3 \\ a_4 \\ a_5 \\ a_6 \\ a_7 \\ a_8 \end{bmatrix}$$

$$\{\delta\} = \underline{C} \{a\}$$

NON-ZERO TERMS ONLY

FIGURE 5.16

$$\begin{bmatrix} a_1 \\ a_2 \\ a_3 \\ a_4 \\ a_5 \\ a_6 \\ a_7 \\ a_8 \end{bmatrix} = \begin{bmatrix} 1 & & & & & & & \\ & -\frac{1}{X} & \frac{1}{X} & & & & & \\ & & & -\frac{1}{Y} & \frac{1}{Y} & & & \\ & & & & & \frac{1}{XY} & -\frac{1}{XY} & -\frac{1}{XY} & \frac{1}{XY} \\ & & & & & & 1 & & \\ & & & & & & & -\frac{1}{X} & \frac{1}{X} \\ & & & & & & & & -\frac{1}{Y} & \frac{1}{Y} \\ & & & & & & & & & \frac{1}{XY} & -\frac{1}{XY} & -\frac{1}{XY} & \frac{1}{XY} \end{bmatrix} \times \begin{bmatrix} u_1 \\ u_2 \\ u_3 \\ u_4 \\ v_1 \\ v_2 \\ v_3 \\ v_4 \end{bmatrix}$$

$$\{a\} = \underline{C}^{-1} \{\delta\}$$

NON-ZERO TERMS ONLY

FIGURE 5.17



$$\begin{bmatrix} \varepsilon_{\bar{X}} \\ \varepsilon_{\bar{Y}} \\ \gamma_{\bar{X}\bar{Y}} \end{bmatrix} = \begin{bmatrix} \partial u / \partial \bar{X} \\ \partial v / \partial \bar{Y} \\ \partial u / \partial \bar{Y} + \partial v / \partial \bar{X} \end{bmatrix} \quad \dots (5.51)$$

General expressions will now be derived for these strains, recourse being made to figure 5.2. It is clear that from equation (5.47)

$$u = u(x, y)$$

Consequently to obtain  $\frac{\partial u}{\partial \bar{Y}}$  and  $\frac{\partial u}{\partial \bar{X}}$  the chain rule must be invoked, hence

$$\frac{\partial u}{\partial \bar{Y}} = \frac{\partial u}{\partial x} \cdot \frac{\partial x}{\partial \bar{Y}} + \frac{\partial u}{\partial y} \cdot \frac{\partial y}{\partial \bar{Y}} \quad \dots (5.52)$$

and

$$\frac{\partial u}{\partial \bar{X}} = \frac{\partial u}{\partial x} \cdot \frac{\partial x}{\partial \bar{X}} + \frac{\partial u}{\partial y} \cdot \frac{\partial y}{\partial \bar{X}} \quad \dots (5.53)$$

Similarly equation (5.48) makes it clear that

$$v = v(x, y)$$

So to obtain  $\frac{\partial v}{\partial \bar{Y}}$  and  $\frac{\partial v}{\partial \bar{X}}$  the chain rule must once again be used, hence

$$\frac{\partial v}{\partial \bar{Y}} = \frac{\partial v}{\partial x} \cdot \frac{\partial x}{\partial \bar{Y}} + \frac{\partial v}{\partial y} \cdot \frac{\partial y}{\partial \bar{Y}} \quad \dots (5.54)$$

and

$$\frac{\partial v}{\partial \bar{X}} = \frac{\partial v}{\partial x} \cdot \frac{\partial x}{\partial \bar{X}} + \frac{\partial v}{\partial y} \cdot \frac{\partial y}{\partial \bar{X}} \quad \dots (5.55)$$

Now substituting equations (5.7) and (5.4) into equation (5.54) and imposing the condition that  $x = 0$  which is essential for the axes to be tangential the following expression is obtained

$$\frac{\partial v}{\partial \bar{Y}} = \frac{\partial v}{\partial y} = \epsilon_{\bar{Y}} \quad \dots (5.56)$$

Similarly if equations (5.6) and (5.3) are substituted into equation (5.53) and with x put equal to zero then

$$\frac{\partial u}{\partial \bar{X}} = \left[ \frac{R}{R-y} \right] \cdot \frac{\partial u}{\partial x} = \epsilon_{\bar{X}} \quad \dots (5.57)$$

Finally if equations (5.55) and (5.52) are summated and the results of equation (5.3), (5.4), (5.6) and (5.7) are substituted, then the result, once the condition  $x = 0$  is imposed, is

$$\frac{\partial v}{\partial \bar{X}} + \frac{\partial u}{\partial \bar{Y}} = \left[ \frac{R}{R-y} \right] \cdot \frac{\partial v}{\partial x} + \frac{\partial u}{\partial y} = \gamma_{\bar{X} \bar{Y}} \quad \dots (5.58)$$

Partial differentiation of equations (5.47) and (5.48) (which are the in plane displacement functions), in accordance with the formats given in equations (5.56), (5.57) and (5.58), results in three equations which may be written in matrix form as

$$\{\underline{\epsilon}\} = \underline{L} \{\underline{a}\} \quad \dots (5.59)$$

These matrices are given in full in figure 5.18 and relate the three strains to the eight constants.

If equations (5.50) and (5.59) are combined then the eight unknown constants in  $\{\underline{a}\}$  are removed and an expression relating the strains to the in plane displacements at each corner may be written

$$\{\underline{\epsilon}\} = \underline{B} \{\underline{\delta}\} \quad \dots (5.60)$$

The  $\underline{B}$  matrix which is formed by the matrix multiplication  $\underline{L} \underline{C}^{-1}$  is given in full in figure 5.19.

For the case of plane stress, three components of stress,

$$\begin{bmatrix} \epsilon_X \\ \epsilon_{XY} \\ \delta_{XY} \end{bmatrix} = \begin{bmatrix} 0 & 0 & 0 & 0 & 0 & 1 & X \\ 0 & \frac{R}{A} & 0 & \frac{RY}{A} & 0 & 0 & 0 \\ 0 & 0 & 1 & X & 0 & \frac{R}{A} & \frac{RY}{A} \end{bmatrix} \times \begin{bmatrix} a_1 \\ a_2 \\ a_3 \\ a_4 \\ a_5 \\ a_6 \\ a_7 \\ a_8 \end{bmatrix}$$

$$\{\underline{\epsilon}\} = \underline{L} \{\underline{a}\}$$

$$A = R - Y$$

FIGURE 5.18

$$\begin{bmatrix} \epsilon_X \\ \epsilon_Y \\ \delta_{XY} \end{bmatrix} = \begin{bmatrix} 0 & 0 & 0 & 0 & -\frac{1}{Y} + \frac{x}{XY} & \frac{-x}{XY} & \frac{1}{Y} \frac{x}{XY} & \frac{x}{XY} \\ \frac{-R}{AX} + \frac{Ry}{AXY} & \frac{R}{AX} - \frac{Ry}{AXY} & \frac{-Ry}{AXY} & \frac{Ry}{AXY} & 0 & 0 & 0 & 0 \\ -\frac{1}{Y} + \frac{x}{XY} & \frac{-x}{XY} & \frac{1}{Y} - \frac{x}{XY} & \frac{x}{XY} & \frac{-R}{AX} + \frac{Ry}{AXY} & \frac{R}{AX} - \frac{Ry}{AXY} & \frac{-Ry}{AXY} & \frac{Ry}{AXY} \end{bmatrix} \times \begin{bmatrix} u_1 \\ u_2 \\ u_3 \\ u_4 \\ v_1 \\ v_2 \\ v_3 \\ v_4 \end{bmatrix}$$

$$\{\underline{\epsilon}\} = \underline{B} \{\underline{\delta}\}$$

$$(A = R - x)$$

FIGURE 5.19



corresponding to the strains already defined, are considered; such stresses are

$$\{\underline{\sigma}\} = \begin{bmatrix} \sigma_{\underline{X}} \\ \sigma_{\underline{Y}} \\ \tau_{\underline{X} \underline{Y}} \end{bmatrix}$$

Finally the stress strain relationship for plane stresses in an isotropic material, derived in standard texts<sup>(29,30)</sup> is given by

$$\{\underline{\sigma}\} = \underline{D} \{\underline{\epsilon}\}$$

where

$$\underline{D} = \frac{E}{1-\mu^2} \begin{bmatrix} 1 & \mu & 0 \\ \mu & 1 & 0 \\ 0 & 0 & \frac{1-\mu}{2} \end{bmatrix} \dots (5.61)$$

#### (5.7) The in plane element stiffness matrix

During the discussion concerning the out of plane stiffness matrix the element stiffness  $\underline{k}$  for a curved plate was given in equation (5.36). Because the in plane  $\underline{B}$  matrix is less complex than the out of plane  $\underline{B}$  matrix it is possible to express the result of equation (5.36) explicitly. The terms of the resulting  $\underline{k}$  matrix for the in plane stiffness of a curved plate are given in figure 5.21 the key to these terms is illustrated in figure 5.20.

If the radius of a curved plate is increased whilst its other dimensions remain fixed, then the shape of the plate tends to a rectangle. Consequently for large values of radius in relation to these other plate

11							
21	22						
31	32	33					
41	42	43	44				
51	52	53	54	55			
61	62	63	64	65	66		
71	72	73	74	75	76	77	
81	82	83	84	85	86	87	88

KEY TO THE TERMS FORMING THE IN PLANE ELEMENT STIFFNESS MATRIX  
OF A CURVED PLATE

FIGURE 5.20

$$(11) = \frac{R}{XY^2} (Y-R)^2 \log_e \left( \frac{R}{R-Y} \right) + \frac{R}{X} \left( \frac{3}{2} - \frac{R}{Y} \right) + \frac{FX}{6} \left( \frac{2}{Y} - \frac{1}{R} \right)$$

$$(21) = \frac{-R}{XY^2} (Y-R)^2 \log_e \left( \frac{R}{R-Y} \right) + \frac{R}{X} \left( -\frac{3}{2} + \frac{R}{Y} \right) + \frac{FX}{12} \left( \frac{2}{Y} - \frac{1}{R} \right)$$

$$(22) = \frac{R}{XY^2} (Y-R)^2 \log_e \left( \frac{R}{R-Y} \right) + \frac{R}{X} \left( \frac{3}{2} - \frac{R}{Y} \right) + \frac{FX}{6} \left( \frac{2}{Y} - \frac{1}{R} \right)$$

$$(31) = \frac{R^2}{XY^2} (Y-R) \log_e \left( \frac{R}{R-Y} \right) + \frac{R}{X} \left( -\frac{1}{2} + \frac{R}{Y} \right) + \frac{FX}{6} \left( \frac{1}{R} - \frac{2}{Y} \right)$$

$$(32) = \frac{-R^2}{XY^2} (Y-R) \log_e \left( \frac{R}{R-Y} \right) + \frac{R}{X} \left( \frac{1}{2} - \frac{R}{Y} \right) + \frac{FX}{12} \left( \frac{1}{R} - \frac{2}{Y} \right)$$

$$(33) = \frac{R^3}{XY^2} \log_e \left( \frac{R}{R-Y} \right) + \frac{R}{X} \left( -\frac{1}{2} - \frac{R}{Y} \right) + \frac{FX}{6} \left( \frac{2}{Y} - \frac{1}{R} \right)$$



$$(41) = \frac{-R^2}{XY^2} (Y-R) \log_e \left( \frac{R}{R-Y} \right) + \frac{R}{X} \left( \frac{1}{2} - \frac{R}{Y} \right) + \frac{FX}{12} \left( \frac{1}{R} - \frac{2}{Y} \right)$$

$$(42) = \frac{R^2}{XY^2} (Y-R) \log_e \left( \frac{R}{R-Y} \right) + \frac{R}{X} \left( \frac{R}{Y} - \frac{1}{2} \right) + \frac{FX}{6} \left( -\frac{2}{Y} + \frac{1}{R} \right)$$

$$(43) = \frac{-R^3}{XY^2} \log_e \left( \frac{R}{R-Y} \right) + \frac{R}{X} \left( \frac{R}{Y} + \frac{1}{2} \right) + \frac{FX}{12} \left( \frac{2}{Y} - \frac{1}{R} \right)$$

$$(44) = \frac{R^3}{XY^2} \log_e \left( \frac{R}{R-Y} \right) + \frac{R}{X} \left( -\frac{1}{2} - \frac{R}{Y} \right) + \frac{FX}{6} \left( \frac{2}{Y} - \frac{1}{R} \right)$$

$$(51) = \frac{1}{4} (F + \mu)$$

$$(52) = \frac{1}{4} (F - \mu)$$

$$(53) = \frac{1}{4} (-F + \mu)$$

$$(54) = -\frac{1}{4} (F + \mu)$$

$$(55) = \frac{RF}{XY^2} (Y-R)^2 \log_e \left( \frac{R}{R-Y} \right) + \frac{R}{X} \left( \frac{3F}{2} - \frac{RF}{Y} \right) + \frac{X}{6} \left( \frac{2}{Y} - \frac{1}{R} \right)$$

$$(61) = \frac{1}{4} (-F + \mu)$$

$$(62) = -\frac{1}{4} (F + \mu)$$

$$(63) = \frac{1}{4} (F + \mu)$$

$$(64) = \frac{1}{4} (F - \mu)$$

$$(65) = \frac{-RF}{XY^2} (Y-R)^2 \log_e \left( \frac{R}{R-Y} \right) + \frac{R}{X} \left( -\frac{3F}{2} + \frac{RF}{Y} \right) + \frac{X}{12} \left( \frac{2}{Y} - \frac{1}{R} \right)$$

$$(66) = \frac{RF}{XY^2} (Y-R)^2 \log_e \left( \frac{R}{R-Y} \right) + \frac{R}{X} \left( \frac{3F}{2} - \frac{RF}{Y} \right) + \frac{X}{6} \left( \frac{2}{Y} - \frac{1}{R} \right)$$

$$(71) = \frac{1}{4} (F - \mu)$$

$$(72) = \frac{1}{4} (F + \mu)$$

$$(73) = -\frac{1}{4} (F + \mu)$$

$$(74) = \frac{1}{4} (-F + \mu)$$

$$(75) = \frac{R^2 F}{XY^2} (Y-R) \log_e \left( \frac{R}{R-Y} \right) + \frac{R}{X} \left( \frac{-F}{2} + \frac{RF}{Y} \right) - \frac{X}{6} \left( \frac{2}{Y} - \frac{1}{R} \right)$$

$$(76) = \frac{-R^2 F}{XY^2} (Y-R) \log_e \left( \frac{R}{R-Y} \right) + \frac{R}{X} \left( \frac{F}{2} - \frac{RF}{Y} \right) + \frac{X}{12} \left( \frac{-2}{Y} + \frac{1}{R} \right)$$

$$(77) = \frac{R^3 F}{XY^2} \log_e \left( \frac{R}{R-Y} \right) + \frac{R}{X} \left( \frac{-F}{2} - \frac{RF}{Y} \right) + \frac{X}{6} \left( \frac{2}{Y} - \frac{1}{R} \right)$$

$$(81) = -\frac{1}{4} (F + \mu)$$

$$(82) = \frac{1}{4} (-F + \mu)$$

$$(83) = \frac{1}{4} (F - \mu)$$

$$(84) = \frac{1}{4} (F + \mu)$$

$$(85) = \frac{-R^2 F}{XY^2} (Y-R) \log_e \left( \frac{R}{R-Y} \right) + \frac{R}{X} \left( \frac{F}{2} - \frac{RF}{Y} \right) + \frac{X}{12} \left( \frac{1}{R} - \frac{2}{Y} \right)$$

$$(86) = \frac{R^2 F}{XY^2} (Y-R) \log_e \left( \frac{R}{R-Y} \right) + \left( \frac{-F}{2} + \frac{RF}{Y} \right) + \frac{X}{6} \left( \frac{1}{R} - \frac{2}{Y} \right)$$

$$(87) = \frac{-R^3 F}{XY^2} \log_e \left( \frac{R}{R-Y} \right) + \frac{R}{X} \left( \frac{F}{2} + \frac{RF}{Y} \right) + \frac{X}{12} \left( \frac{2}{Y} - \frac{1}{R} \right)$$

$$(88) = \frac{R^3 F}{XY^2} \log_e \left( \frac{R}{R-Y} \right) + \frac{R}{X} \left( \frac{-F}{2} - \frac{RF}{Y} \right) + \frac{X}{6} \left( \frac{2}{Y} - \frac{1}{R} \right)$$



where  $F = \frac{1 - \mu}{2}$

ALL TERMS SHOULD BE MULTIPLIED BY  $\left( \frac{Et}{1 - \mu^2} \right)$

TERMS FORMING THE IN PLANE STIFFNESS MATRIX FOR A CURVED PLATE

FIGURE 5.21

dimensions both the in and out of plane element stiffness matrices of the curved plate ought to resemble the equivalent rectangular plate stiffness matrix. This phenomenon is investigated in chapter 7.

#### (5.8) The out of plane displacement transformation matrix

The out of plane element displacements are relative to a set of local axes. It is desirable, however, to express such displacements in terms of a set of global axes. This relationship is usually expressed mathematically as:

$$\underline{Z} = \underline{A} \underline{X} \quad \dots (5.62)$$

A curved plate with local axes  $p, q, r$  is shown in figure 5.22. A further, intermediate, set of axes  $\alpha, \beta, \gamma$  are also shown in the figure, and the displacements will firstly be related to these. Such a relationship is given by

$$\underline{Z} = \underline{u} \cdot \underline{\alpha} \quad \dots (5.63)$$

The matrices comprising this equation are given in figure 5.23. If the intermediate  $\alpha, \beta, \gamma$  axes are related to the global  $X, Y, Z$  axes then the required relationship may be formed. Consider then figure 5.24 which shows the intermediate axes, taking a general orientation within the global space; then for joint 1;

$$\begin{aligned} \theta_{\alpha 1} &= L_{\alpha} \cdot \theta_{x1} + M_{\alpha} \cdot \theta_{y1} + N_{\alpha} \cdot \theta_{z1} ; \\ \theta_{\beta 1} &= L_{\beta} \cdot \theta_{x1} + M_{\beta} \cdot \theta_{y1} + N_{\beta} \cdot \theta_{z1} ; \\ \omega_1 &= L_{\gamma} \cdot x_1 + M_{\gamma} \cdot y_1 + N_{\gamma} \cdot z_1 . \end{aligned}$$

When this is expressed in matrix form for the four corners of the plate the relationship is shown in figure 5.25 and is given by

$$\underline{\alpha} = \underline{V} \cdot \underline{X} \quad \dots (5.64)$$



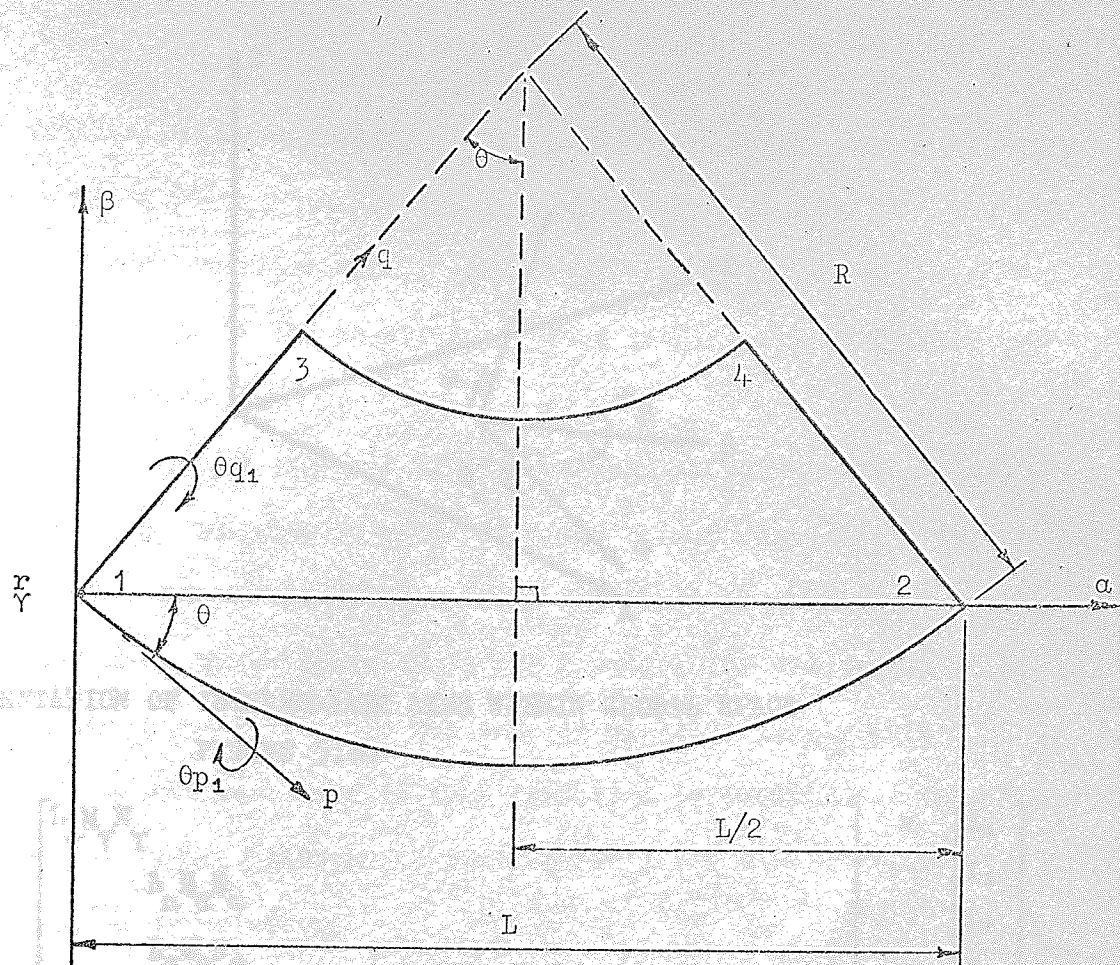


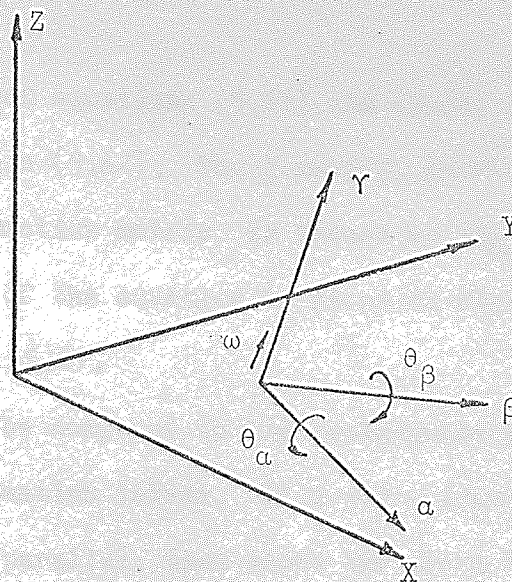
FIGURE 5.22

$$\begin{bmatrix} \omega_1 \\ \theta_{p1} \\ \theta_{q1} \\ \omega_2 \\ \theta_{p2} \\ \theta_{q2} \\ \omega_3 \\ \theta_{p3} \\ \theta_{q3} \\ \omega_4 \\ \theta_{p4} \\ \theta_{q4} \end{bmatrix} = \begin{bmatrix} 1 & & & & & & & & & & & \\ & \cos\theta - \sin\theta & & & & & & & & & & \\ & \sin\theta & \cos\theta & & & & & & & & & \\ & & & 1 & & & & & & & & \\ & & & & \cos\theta & \sin\theta & & & & & & \\ & & & & -\sin\theta & \cos\theta & & & & & & \\ & & & & & & 1 & & & & & \\ & & & & & & & \cos\theta - \sin\theta & & & & \\ & & & & & & & \sin\theta & \cos\theta & & & \\ & & & & & & & & & 1 & & \\ & & & & & & & & & & \cos\theta & \sin\theta \\ & & & & & & & & & & -\sin\theta & \cos\theta \end{bmatrix} \times \begin{bmatrix} \omega_1 \\ \theta_{\alpha 1} \\ \theta_{\beta 1} \\ \omega_2 \\ \theta_{\alpha 2} \\ \theta_{\beta 2} \\ \omega_3 \\ \theta_{\alpha 3} \\ \theta_{\beta 3} \\ \omega_4 \\ \theta_{\alpha 4} \\ \theta_{\beta 4} \end{bmatrix}$$

$$\underline{Z} = \underline{u} \cdot \underline{\alpha}$$

FIGURE 5.23

Thus the displacement vector  
in the form of a column matrix  
displacement vector  
matrix form  
the term is finite  
This matrix  
displacement vector  
and  $\gamma$  and  $\beta$  are  
the local rotation



ORIENTATION OF INTERMEDIATE AXES WITHIN GLOBAL SPACE

FIGURE 5.24

$$\begin{bmatrix} \omega_1 \\ \theta_{\alpha 1} \\ \theta_{\beta 1} \\ \omega_2 \\ \theta_{\alpha 2} \\ \theta_{\beta 2} \\ \omega_3 \\ \theta_{\alpha 3} \\ \theta_{\beta 3} \\ \omega_4 \\ \theta_{\alpha 4} \\ \theta_{\beta 4} \end{bmatrix} = \begin{bmatrix} L & M & N \\ \gamma & \gamma & \gamma \\ & L & M & N \\ & \alpha & \alpha & \alpha \\ & & L & M & N \\ & & \beta & \beta & \beta \\ & & & L & M & N \\ & & & \gamma & \gamma & \gamma \\ & & & & L & M & N \\ & & & & \alpha & \alpha & \alpha \\ & & & & & L & M & N \\ & & & & & \beta & \beta & \beta \\ & & & & & & L & M & N \\ & & & & & & & L & M & N \\ & & & & & & & \alpha & \alpha & \alpha \\ & & & & & & & & L & M & N \\ & & & & & & & & \beta & \beta & \beta \end{bmatrix} \times \begin{bmatrix} X_1 \\ Y_1 \\ Z_1 \\ \theta_{X1} \\ \theta_{Y1} \\ \theta_{Z1} \\ X_2 \\ Y_2 \\ Z_2 \\ \theta_{X2} \\ \theta_{Y2} \\ \theta_{Z2} \\ X_3 \\ Y_3 \\ Z_3 \\ \theta_{X3} \\ \theta_{Y3} \\ \theta_{Z3} \\ X_4 \\ Y_4 \\ Z_4 \\ \theta_{X4} \\ \theta_{Y4} \\ \theta_{Z4} \end{bmatrix}$$

$$\underline{a} = \underline{V} \underline{\bar{X}}$$

FIGURE 5.25



Thus the combination of equations (5.63) and (5.64) gives a relationship in the form of equation (5.62). The A matrix, known as the out of plane displacement transformation matrix is formed by the u.v multiplication. The full matrix form of the equation is given in figure 5.26 with the key to the term in figure 5.27.

This matrix can be compared to the rectangular plate out of plane displacement transformation matrix. If  $p$  and  $\alpha$  (see figure 5.22) are parallel, and  $q$  and  $\beta$  are parallel, then since the plate sides along the axes are the local rectangular plate axes, the A matrix for the curved plate will become the A matrix for the rectangular plate. Clearly this will be so when  $\theta$  equals zero, and if this condition is substituted into the matrix shown in figure 5.26 then the rectangular plate displacement transformation matrix is obtained.

#### (5.9) The in plane displacement transformation matrix

This matrix is formed in a similar manner to that employed in the out of plane case. A curved plate with local axes and in plane displacements is shown in figure 5.28. Once again two transformations are made, the first in the form of equation (5.63), the matrices of which are illustrated in full in figure 5.29. The second transformation from the intermediate  $\alpha, \beta, \gamma$  axes to the global  $X, Y, Z$  axes which are shown in figure 5.30 is of the form already expressed in equation (5.64), figure 5.31 gives the full matrices forming this expression. In a similar manner to that discussed previously equations (5.63) and (5.64) are combined to give an expression conforming to equation (5.62). The matrices comprising this equation are given in figure 5.32 which should be read in conjunction with figure 5.27.

Once again parallels may be drawn between the curved and rectangular plate displacement transformation matrices. If the condition of  $\theta$

$$\begin{bmatrix} \omega_1 \\ \theta_{X1} \\ \theta_{Y2} \\ \omega_2 \\ \theta_{X2} \\ \theta_{Y2} \\ \omega_3 \\ \theta_{X3} \\ \theta_{Y3} \\ \omega_4 \\ \theta_{X4} \\ \theta_{Y4} \end{bmatrix} = \begin{bmatrix} L_1 & M_1 & N_1 & & & & & & & & & \\ & L_2 & M_2 & N_2 & & & & & & & & \\ & L_3 & M_3 & N_3 & & & & & & & & \\ & & L_4 & M_4 & N_4 & & & & & & & \\ & & L_5 & M_5 & N_5 & & & & & & & \\ & & & L_1 & M_1 & N_1 & & & & & & \\ & & & & L_2 & M_2 & N_2 & & & & & \\ & & & & L_3 & M_3 & N_3 & & & & & \\ & & & & & L_4 & M_4 & N_4 & & & & \\ & & & & & & L_5 & M_5 & N_5 & & & \end{bmatrix} \begin{bmatrix} X_1 \\ Y_1 \\ Z_1 \\ \theta_{X1} \\ \theta_{Y1} \\ \theta_{Z1} \\ X_2 \\ Y_2 \\ Z_2 \\ \theta_{X2} \\ \theta_{Y2} \\ \theta_{Z2} \\ X_3 \\ Y_3 \\ Z_3 \\ \theta_{X3} \\ \theta_{Y3} \\ \theta_{Z3} \\ X_4 \\ Y_4 \\ Z_4 \\ \theta_{X4} \\ \theta_{Y4} \\ \theta_{Z4} \end{bmatrix} \times$$

THE OUT OF PLANE DISPLACEMENT TRANSFORMATION MATRIX  $\underline{Z} = \underline{A} \underline{X}$

FIGURE 5.26 READ IN CONJUNCTION WITH FIGURE 5.27



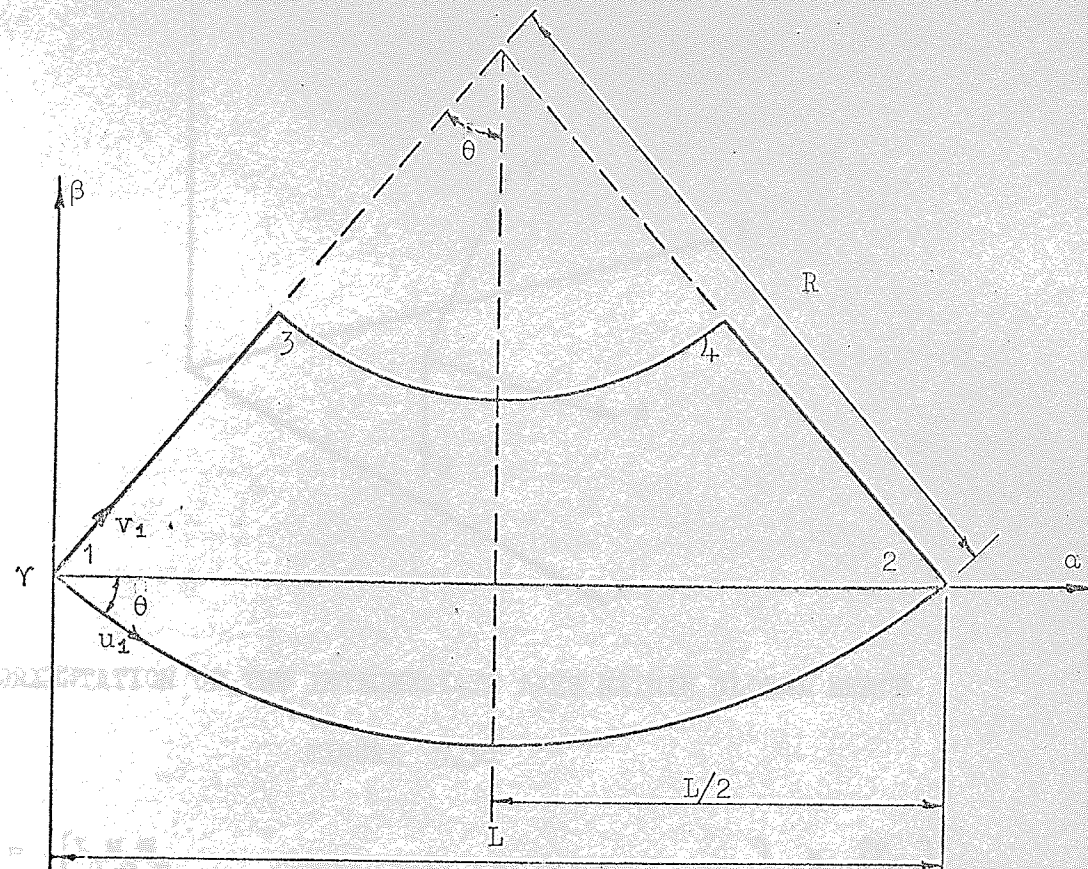
$$L_1 = L_Y; \quad L_2 = L_\alpha \cos \theta - L_\beta \sin \theta; \quad L_3 = L_\alpha \sin \theta + L_\beta \cos \theta; \quad L_4 = L_\alpha \cos \theta + L_\beta \sin \theta; \quad L_5 = -L_\alpha \sin \theta + L_\beta \cos \theta;$$

$$M_1 = M_Y; \quad M_2 = M_\alpha \cos \theta - M_\beta \sin \theta; \quad M_3 = M_\alpha \sin \theta + M_\beta \cos \theta; \quad M_4 = M_\alpha \cos \theta + M_\beta \sin \theta; \quad M_5 = -M_\alpha \sin \theta + M_\beta \cos \theta;$$

$$N_1 = N_Y; \quad N_2 = N_\alpha \cos \theta - N_\beta \sin \theta; \quad N_3 = N_\alpha \sin \theta + N_\beta \cos \theta; \quad N_4 = N_\alpha \cos \theta + N_\beta \sin \theta; \quad N_5 = -N_\alpha \sin \theta + N_\beta \cos \theta;$$

KEY TO VARIABLES IN THE DISPLACEMENT TRANSFORMATION MATRICES

FIGURE 5.27



LOCAL PLATE AXES

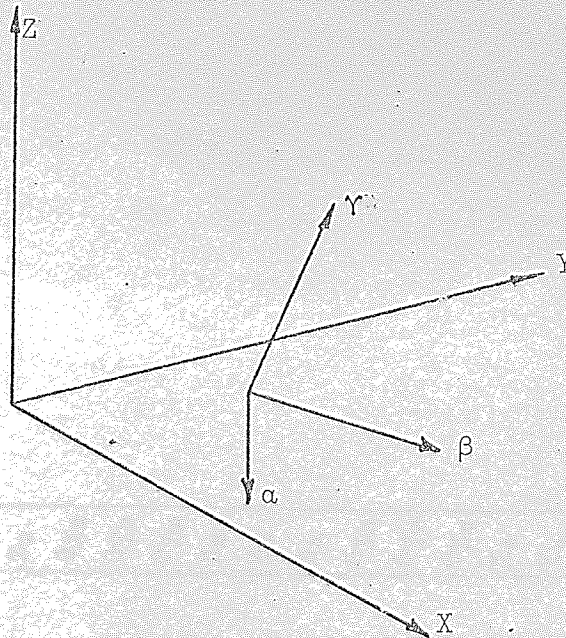
FIGURE 5.28

$$\begin{bmatrix} u_1 \\ u_2 \\ u_3 \\ u_4 \\ v_1 \\ v_2 \\ v_3 \\ v_4 \end{bmatrix} = \begin{bmatrix} \cos \theta & -\sin \theta & & & & & \\ & \cos \theta & \sin \theta & & & & \\ & & \cos \theta & -\sin \theta & & & \\ & & & \cos \theta & \sin \theta & & \\ \sin \theta & \cos \theta & & & & & \\ & & -\sin \theta & \cos \theta & & & \\ & & & \sin \theta & \cos \theta & & \\ & & & & -\sin \theta & \cos \theta & \end{bmatrix} \times \begin{bmatrix} \alpha_1 \\ \beta_1 \\ \alpha_2 \\ \beta_2 \\ \alpha_3 \\ \beta_3 \\ \alpha_4 \\ \beta_4 \end{bmatrix}$$

$$\underline{Z} = \underline{u} \cdot \underline{a}$$

FIGURE 5.29





ORIENTATION OF THE INTERMEDIATE AXES WITHIN GLOBAL SPACE

FIGURE 5.30

$$\begin{bmatrix} \alpha_1 \\ \beta_1 \\ \alpha_2 \\ \beta_2 \\ \alpha_3 \\ \beta_3 \\ \alpha_4 \\ \beta_4 \end{bmatrix} = \begin{bmatrix} L_{\alpha} & M_{\alpha} & N_{\alpha} \\ L_{\beta} & M_{\beta} & N_{\beta} \\ L_{\alpha} & M_{\alpha} & N_{\alpha} \\ L_{\beta} & M_{\beta} & N_{\beta} \\ L_{\alpha} & M_{\alpha} & N_{\alpha} \\ L_{\beta} & M_{\beta} & N_{\beta} \\ L_{\alpha} & M_{\alpha} & N_{\alpha} \\ L_{\beta} & M_{\beta} & N_{\beta} \end{bmatrix} \times \begin{bmatrix} X_1 \\ Y_1 \\ Z_1 \\ \theta_{X_1} \\ \theta_{Y_1} \\ \theta_{Z_1} \\ X_2 \\ Y_2 \\ Z_2 \\ \theta_{X_2} \\ \theta_{Y_2} \\ \theta_{Z_2} \\ X_3 \\ Y_3 \\ Z_3 \\ \theta_{X_3} \\ \theta_{Y_3} \\ \theta_{Z_3} \\ X_4 \\ Y_4 \\ Z_4 \\ \theta_{X_4} \\ \theta_{Y_4} \\ \theta_{Z_4} \end{bmatrix}$$

$$\underline{\alpha} = \underline{V} \cdot \underline{X}$$

FIGURE 5.31

$$\begin{bmatrix} u_1 \\ u_2 \\ u_3 \\ u_4 \\ v_1 \\ v_2 \\ v_3 \\ v_4 \end{bmatrix} = \begin{bmatrix} L_2 & M_2 & N_2 & & & & & \\ & L_4 & M_4 & N_4 & & & & \\ & & L_2 & M_2 & N_2 & & & \\ & & & L_4 & M_4 & N_4 & & \\ L_3 & M_3 & N_3 & & & & & \\ & & & & L_5 & M_5 & N_5 & \\ & & & & & L_3 & M_3 & N_3 \\ & & & & & & L_5 & M_5 & N_5 \end{bmatrix} \times \begin{bmatrix} X_1 \\ Y_1 \\ Z_1 \\ \theta X_1 \\ \theta Y_1 \\ \theta Z_1 \\ X_2 \\ Y_2 \\ Z_2 \\ \theta X_2 \\ \theta Y_2 \\ \theta Z_2 \\ X_3 \\ Y_3 \\ Z_3 \\ \theta X_3 \\ \theta Y_3 \\ \theta Z_3 \\ X_4 \\ Y_4 \\ Z_4 \\ \theta X_4 \\ \theta Y_4 \\ \theta Z_4 \end{bmatrix}$$

$$\underline{Z} = \underline{A} \underline{X}$$

THE IN PLANE DISPLACEMENT TRANSFORMATION MATRIX

FIGURE 5.32



equalling zero, previously discussed, is substituted into the matrix given in figure 5.32 then the resulting matrix is the in plane rectangular plate displacement transformation matrix.

## CHAPTER 6

### CURVED PLATE PROGRAMMING

#### (6.1) Introduction

A general introduction to element packages has been given in chapter 4. In that chapter the auxiliary package as well as the rectangular plate, triangular plate and member packages were detailed. At that stage the curved plate theory, which is an essential prerequisite to the programming of a curved plate package, had not been developed. As a result of that derivation in chapter 5 it is now possible to carry out the programming steps necessary in the formation of such a curved plate package. The contents of this chapter are concerned with the documentation of that package.

#### (6.2) General Considerations

An example of the type of curved plate under consideration is illustrated in figure 6.1. Its four corners are assigned the numbers one to four such that corners one and two occur on the outer edge, and corners three and four on the inner edge. The local co-ordinate axes  $P$ , tangential,  $Q$ , radial and  $R$ , with origin at corner one are also shown in the figure.

When such a plate is subjected to loading out of its plane then the four corners could experience out of plane displacements, such displacements are shown for corner one in figure 6.1. Similarly if an in plane loading system is applied then the displacements shown at corner one in figure 6.2 could occur at the corners of the plate.

In order that such displacements may be calculated it is necessary to have the facility to construct the in plane and out of plane stiffness matrices for such an element. The manner in which this is carried out has already been described in chapter 5.

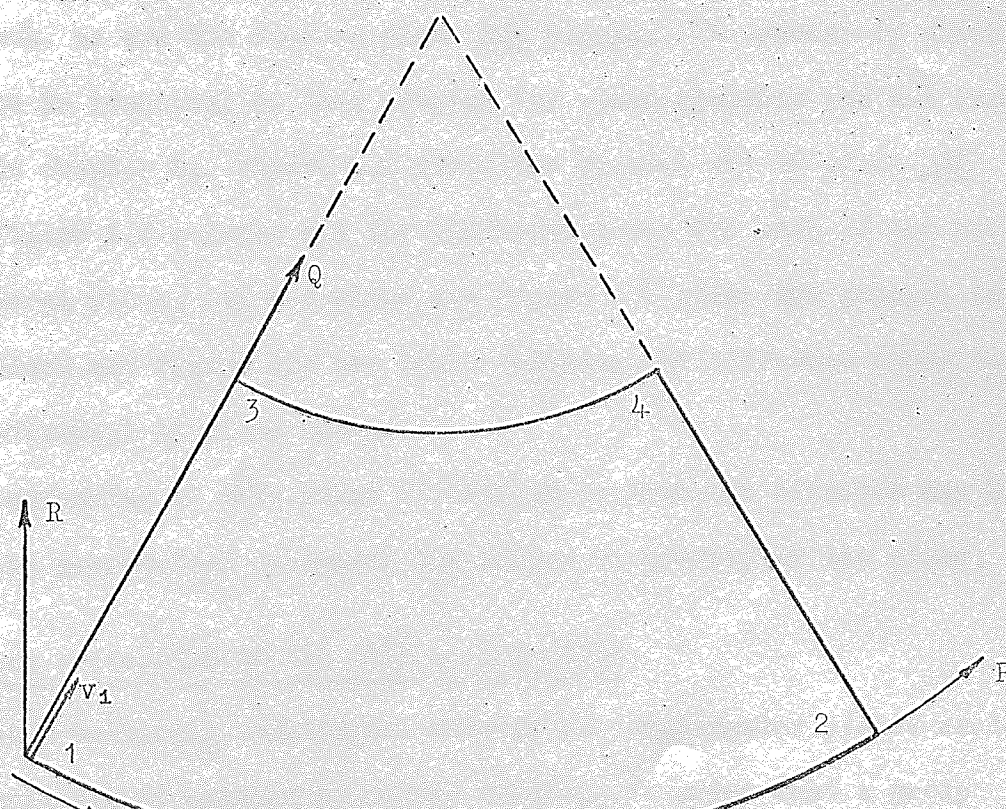
Since it is necessary to relate the local displacements of the plate





THE OUT OF PLANE DISPLACEMENTS RELATIVE TO THE LOCAL AXES FOR CORNER  
ONE OF THE CURVED PLATE

FIGURE 6.1



THE IN PLANE DISPLACEMENTS RELATIVE TO THE LOCAL AXES FOR CORNER  
ONE OF THE CURVED PLATE

FIGURE 6.2

to a set of global axes the displacement transformation matrices need to be available. These matrices for both the in and out of plane cases have been derived in chapter 5 and need not be repeated here.

### (6.3) Curved plate stresses

The stresses within such a plate are calculated by evaluating the DBAX multiplication. Consequently the DB matrix for each plate has to be formed. The in and out of plane B matrices were formed in chapter 5 and will not be expressed explicitly here. The format of these matrices is given in figures 6.3 and 6.4, the code numbers shown in place of the terms are used in later figures. The DBA multiplication for one plate yields four blocks illustrated in figure 6.5. Each of these blocks corresponds to a corner of the plate and comprises a maximum of six columns each corresponding to an unsuppressed degree of freedom. Each row relates to a resulting stress.

Each of the four out of plane DBA blocks are now related to a single general block, as are the four in plane DBA blocks. The manner in which this is done is identical to that adopted for other elements and has been described in chapter 4. Figure 6.6 gives the general out of plane DBA block and figure 6.7 relates all the different codes for each of the blocks to this general block. In a similar way figure 6.8 gives the general in plane DBA block and figure 6.9 the table relating the different codes to the four individual in plane blocks.

The programming of this stage is written so that the stresses may be either at the geometrical centre or the centre of gravity of the plate.

### (6.4) Direct evaluation of the A'kA contribution

The joint numbering constraints adopted for rectangular plates would be too restrictive if applied to curved plates. In order that a group boundary may split a plate either radially or circumferentially two



$$\begin{bmatrix} 1,1 & 1,2 & 1,3 & 1,4 & 1,5 & 1,6 & 1,7 & 1,8 & 1,9 & 1,10 & 1,11 & 1,12 \\ 2,1 & 2,2 & 2,3 & 2,4 & 2,5 & 2,6 & 2,7 & 2,8 & 2,9 & 2,10 & 2,11 & 2,12 \\ 3,1 & 3,2 & 3,3 & 3,4 & 3,5 & 3,6 & 3,7 & 3,8 & 3,9 & 3,10 & 3,11 & 3,12 \end{bmatrix}$$

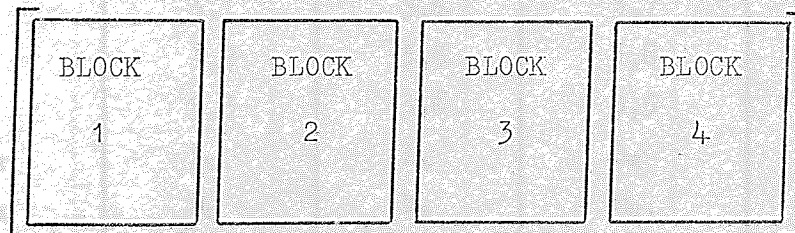
KEY TO TERMS FORMING THE OUT OF PLANE B MATRIX FOR A CURVED PLATE

FIGURE 6.3

$$\begin{bmatrix} 1,1 & 1,2 & 1,3 & 1,4 & 1,5 & 1,6 & 1,7 & 1,8 \\ 2,1 & 2,2 & 2,3 & 2,4 & 2,5 & 2,6 & 2,7 & 2,8 \\ 3,1 & 3,2 & 3,3 & 3,4 & 3,5 & 3,6 & 3,7 & 3,8 \end{bmatrix}$$

KEY TO TERMS FORMING THE IN PLANE B MATRIX FOR A CURVED PLATE

FIGURE 6.4



FORMAT OF BOTH THE IN AND OUT OF PLANE DBA MATRIX FOR A CURVED PLATE.  
EACH BLOCK CORRESPONDS TO ONE NODE OF THE PLATE AND COMPRISES SIX  
COLUMNS AND THREE ROWS.

FIGURE 6.5

$$\begin{array}{c}
 \sigma_P \\
 \sigma_Q \\
 \tau_{PQ}
 \end{array}
 \begin{bmatrix}
 X & Y & Z & \theta_x & \theta_y & \theta_z \\
 L_1 \cdot (A + \mu B) & M_1 \cdot (A + \mu B) & N_1 \cdot (A + \mu B) & L_a \cdot (c + \mu D) & M_a \cdot (c + \mu D) & N_a \cdot (c + \mu D) \\
 L_1 \cdot (\mu A + B) & M_1 \cdot (\mu A + B) & N_1 \cdot (\mu A + B) & L_b \cdot (E) & M_b \cdot (E) & N_b \cdot (E) \\
 L_1 \cdot F \cdot G & M_1 \cdot F \cdot G & N_1 \cdot F \cdot G & L_a \cdot (\mu c + D) & M_a \cdot (\mu c + D) & N_a \cdot (\mu c + D) \\
 & & & L_b \cdot (\mu E) & M_b \cdot (\mu E) & N_b \cdot (\mu E) \\
 & & & L_a \cdot F \cdot H & M_a \cdot F \cdot H & N_a \cdot F \cdot H \\
 & & & L_b \cdot F \cdot R & M_b \cdot F \cdot R & N_b \cdot F \cdot R
 \end{bmatrix}$$

All terms multiplied by  $\frac{E \cdot t^3}{12(1-\mu^2)}$  ;  $F = \left(\frac{1-\mu}{2}\right)$

### GENERAL OUT OF PLANE DBA BLOCK

FIGURE 6.6

CODE	BLOCK NUMBER			
VALUE	1	2	3	4
A	1,1	1,4	1,7	1,10
B	2,1	2,4	2,7	2,10
C	1,2	1,5	1,8	1,11
D	2,2	2,5	2,8	2,11
E	1,3	1,6	1,9	1,12
G	3,1	3,4	3,7	3,10
H	3,2	3,5	3,8	3,11
R	3,3	3,6	3,9	3,12
L <sub>a</sub>	L <sub>2</sub>	L <sub>4</sub>	L <sub>2</sub>	L <sub>4</sub>
M <sub>a</sub>	M <sub>2</sub>	M <sub>4</sub>	M <sub>2</sub>	M <sub>4</sub>
N <sub>a</sub>	N <sub>2</sub>	N <sub>4</sub>	N <sub>2</sub>	N <sub>4</sub>
L <sub>b</sub>	L <sub>3</sub>	L <sub>5</sub>	L <sub>3</sub>	L <sub>5</sub>
M <sub>b</sub>	M <sub>3</sub>	M <sub>5</sub>	M <sub>3</sub>	M <sub>5</sub>
N <sub>b</sub>	N <sub>3</sub>	N <sub>5</sub>	N <sub>3</sub>	N <sub>5</sub>

CODE VALUES REFER TO TERMS WITHIN THE OUT OF PLANE B MATRIX AND TERMS WITHIN THE OUT OF PLANE DISPLACEMENT TRANSFORMATION MATRIX

KEY TO TERMS FORMING EACH OF THE OUT OF PLANE DBA BLOCKS

FIGURE 6.7



$$\begin{array}{ccccc}
 X & Y & Z & \theta_x & \theta_y & \theta_z \\
 \left[ \begin{array}{ccc}
 s_1 \cdot \mu \cdot G \cdot L_a & s_1 \cdot \mu \cdot G \cdot M_a & s_1 \cdot \mu \cdot G \cdot N_a \\
 + & + & + \\
 s_2 \cdot A \cdot L_b & s_2 \cdot A \cdot M_b & s_2 \cdot A \cdot N_b \\
 s_1 \cdot G_1 \cdot L_a & s_1 \cdot G_1 \cdot M_a & s_1 \cdot G_1 \cdot N_a \\
 + & + & + \\
 s_2 \cdot \mu \cdot A \cdot L_b & s_2 \cdot \mu \cdot A \cdot M_b & s_2 \cdot \mu \cdot A \cdot N_b \\
 s_2 \cdot F \cdot A \cdot L_a & s_2 \cdot F \cdot A \cdot M_a & s_2 \cdot F \cdot A \cdot N_a \\
 + & + & + \\
 s_1 \cdot F \cdot G \cdot L_b & s_1 \cdot F \cdot G \cdot M_b & s_1 \cdot F \cdot G \cdot N_b
 \end{array} \right] & \begin{array}{ccc}
 0 & 0 & 0 \\
 0 & 0 & 0 \\
 0 & 0 & 0
 \end{array}
 \end{array}$$

$$F = \frac{(1-\mu)}{2}; \text{ all terms multiplied by } \frac{E}{(1-\mu^2)}$$

GENERAL IN PLANE DBA BLOCK

FIGURE 6.8

CODE VALUE	BLOCK NUMBER			
	1	2	3	4
$s_1$	+1	-1	-1	+1
$s_2$	-1	-1	+1	+1
$L_a$	$L_2$	$L_4$	$L_2$	$L_4$
$M_a$	$M_2$	$M_4$	$M_2$	$M_4$
$N_a$	$N_2$	$N_4$	$N_2$	$N_4$
$L_b$	$L_3$	$L_5$	$L_3$	$L_5$
$M_b$	$M_3$	$M_5$	$M_3$	$M_5$
$N_b$	$N_3$	$N_5$	$N_3$	$N_5$
$G$	2,1	2,1	2,4	2,4
$A$	1,7	1,7	1,7	1,7

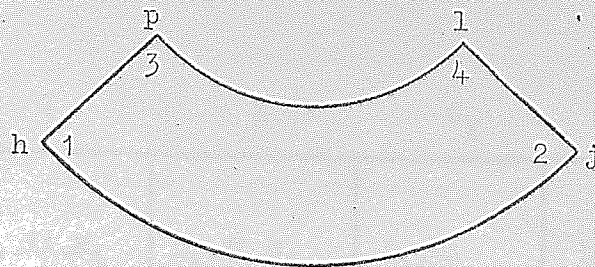
CODE VALUES REFER TO TERMS WITHIN THE IN PLANE B MATRIX AND TERMS WITHIN  
THE IN PLANE DISPLACEMENT TRANSFORMATION MATRIX  
KEY TO TERMS FORMING EACH OF THE OUT OF PLANE DBA BLOCKS

FIGURE 6.9

numbering options have to be permitted. Figure 6.10 shows a curved plate as well as two sets of sub-blocks, each set corresponding to one of the different joint numbering options. When numbering conforms to one of these options then the orientation of the sixteen sub-blocks contributed to the stiffness matrix by the curved plate is as shown in the relevant sub-block set. Such a set of the sub-blocks will exist for both the in and out of plane cases. As each set is symmetrical about its leading diagonal it is only necessary to consider the on-diagonal sub-blocks and those occurring below the leading diagonal.

Once again a general sub-block is used to which all the sub-blocks are related. Figure 6.11 is the general out of plane sub-block, which when used in conjunction with figures 6.12 and 6.13 produces all the required sub-blocks. Similarly figure 6.14 gives the general in plane sub-block and its use in conjunction with figures 6.15 and 6.16 yields the required in plane sub-blocks.





	h	j	p	l
h	hh	hj	hp	hl
j	jh	jj	jp	jl
p	ph	pj	pp	pl
l	lh	lj	lp	ll

SUB-BLOCK ORIENTATION WHEN  $h < j < p < l$  NUMERICALLY

	h	p	j	l
h	hh	hp	hj	hl
p	ph	pp	pj	pl
j	jh	jp	jj	jl
l	lh	lp	lj	ll

SUB-BLOCK ORIENTATION WHEN  $h < p < j < l$  NUMERICALLY

FIGURE 6.10

	X	Y	Z	$\theta_X$	$\theta_Y$	$\theta_Z$
X	$L_1.XA.L_1$	$L_1.XA.M_1$	$L_1.XA.N_1$	$L_1.CA$	$L_1.CB$	$L_1.CC$
Y	$M_1.XA.L_1$	$M_1.XA.M_1$	$M_1.XA.N_1$	$M_1.CA$	$M_1.CB$	$M_1.CC$
Z	$N_1.XA.L_1$	$N_1.XA.M_1$	$N_1.XA.N_1$	$N_1.CA$	$N_1.CB$	$N_1.CC$
$\theta_X$	$L_1.CD$	$M_1.CD$	$N_1.CD$	$L_A.CG$ + $L_B.CH$	$L_A.CI$ + $L_B.CJ$	$L_A.CK$ + $L_B.CL$
$\theta_Y$	$L_1.CE$	$M_1.CE$	$N_1.CE$	$M_A.CG$ + $M_B.CH$	$M_A.CI$ + $M_B.CJ$	$M_A.CK$ + $M_B.CL$
$\theta_Z$	$L_1.CF$	$M_1.CF$	$N_1.CF$	$N_A.CG$ + $N_B.CH$	$N_A.CI$ + $N_B.CJ$	$N_A.CK$ + $N_B.CL$

GENERAL RECTANGULAR AND TRIANGULAR SUB-BLOCK FOR THE OUT OF PLANE OVERALL STIFFNESS CONTRIBUTION OF A CURVED PLATE.

FOR A TRIANGULAR SUB-BLOCK CONSIDER ONLY THE LOWER TRIANGLE TERMS OF THE GENERAL SUB-BLOCK.

FOR INTERPRETATION THIS FIGURE SHOULD BE READ IN CONJUNCTION WITH FIGURES 6.12 AND 6.13.

FIGURE 6.11



	TRIANGULAR SUB-BLOCKS				RECTANGULAR SUB-BLOCKS						
	hh	jj	pp	ll	jh	ph	pj	jp	lh	lj	lp
XA	1,1	4,4	7,7	10,10	4,1	7,1	7,4	4,7	10,1	10,4	10,7
XB	-	-	-	-	4,2	7,2	7,5	4,8	10,2	10,5	10,8
XC	-	-	-	-	4,3	7,3	7,6	4,9	10,3	10,6	10,9
XD	2,1	5,4	8,7	11,10	5,1	8,1	8,4	5,7	11,1	11,4	11,7
XE	3,1	6,4	9,7	12,10	6,1	9,1	9,4	6,7	12,1	12,4	12,7
XF	2,2	5,4	8,8	11,11	5,2	8,2	8,5	5,8	11,2	11,5	11,8
XG	2,3	5,6	8,9	11,12	6,2	8,3	9,5	6,8	11,3	11,6	11,9
XH	3,2	6,5	9,8	12,11	5,3	9,2	8,6	5,9	12,2	12,5	12,8
XI	3,3	6,6	9,9	12,12	6,3	9,3	9,6	6,9	12,3	12,6	12,9
L <sub>A</sub>	L <sub>2</sub>	L <sub>4</sub>	L <sub>2</sub>	L <sub>4</sub>	L <sub>4</sub>	L <sub>2</sub>	L <sub>2</sub>	L <sub>4</sub>	L <sub>4</sub>	L <sub>4</sub>	L <sub>4</sub>
M <sub>A</sub>	M <sub>2</sub>	M <sub>4</sub>	M <sub>2</sub>	M <sub>4</sub>	M <sub>4</sub>	M <sub>2</sub>	M <sub>2</sub>	M <sub>4</sub>	M <sub>4</sub>	M <sub>4</sub>	M <sub>4</sub>
N <sub>A</sub>	N <sub>2</sub>	N <sub>4</sub>	N <sub>2</sub>	N <sub>4</sub>	N <sub>4</sub>	N <sub>2</sub>	N <sub>2</sub>	N <sub>4</sub>	N <sub>4</sub>	N <sub>4</sub>	N <sub>4</sub>
L <sub>B</sub>	L <sub>3</sub>	L <sub>5</sub>	L <sub>3</sub>	L <sub>5</sub>	L <sub>5</sub>	L <sub>3</sub>	L <sub>3</sub>	L <sub>5</sub>	L <sub>5</sub>	L <sub>5</sub>	L <sub>5</sub>
M <sub>B</sub>	M <sub>3</sub>	M <sub>5</sub>	M <sub>3</sub>	M <sub>5</sub>	M <sub>5</sub>	M <sub>3</sub>	M <sub>3</sub>	M <sub>5</sub>	M <sub>5</sub>	M <sub>5</sub>	M <sub>5</sub>
N <sub>B</sub>	N <sub>3</sub>	N <sub>5</sub>	N <sub>3</sub>	N <sub>5</sub>	N <sub>5</sub>	N <sub>3</sub>	N <sub>3</sub>	N <sub>5</sub>	N <sub>5</sub>	N <sub>5</sub>	N <sub>5</sub>
L <sub>C</sub>	-	-	-	-	L <sub>2</sub>	L <sub>2</sub>	L <sub>4</sub>	L <sub>2</sub>	L <sub>2</sub>	L <sub>2</sub>	L <sub>2</sub>
M <sub>C</sub>	-	-	-	-	M <sub>2</sub>	M <sub>2</sub>	M <sub>4</sub>	M <sub>2</sub>	M <sub>2</sub>	M <sub>2</sub>	M <sub>2</sub>
N <sub>C</sub>	-	-	-	-	N <sub>2</sub>	N <sub>2</sub>	N <sub>4</sub>	N <sub>2</sub>	N <sub>2</sub>	N <sub>2</sub>	N <sub>2</sub>
L <sub>D</sub>	-	-	-	-	L <sub>3</sub>	L <sub>3</sub>	L <sub>5</sub>	L <sub>3</sub>	L <sub>3</sub>	L <sub>3</sub>	L <sub>3</sub>
M <sub>D</sub>	-	-	-	-	M <sub>3</sub>	M <sub>3</sub>	M <sub>5</sub>	M <sub>3</sub>	M <sub>3</sub>	M <sub>3</sub>	M <sub>3</sub>
N <sub>D</sub>	-	-	-	-	N <sub>3</sub>	N <sub>3</sub>	N <sub>5</sub>	N <sub>3</sub>	N <sub>3</sub>	N <sub>3</sub>	N <sub>3</sub>

CODE VALUES REFER TO TERMS WITHIN THE OUT OF PLANE ELEMENT STIFFNESS MATRIX  $\underline{k}$ , AND TERMS WITHIN THE OUT OF PLANE DISPLACEMENT TRANSFORMATION MATRIX

KEY TO TERMS FORMING EACH OF THE OUT OF PLANE SUB-BLOCKS

FIGURE 6.12

$$CA = L_A \cdot XB + L_B \cdot XC ;$$

$$CB = M_A \cdot XB + M_B \cdot XC ;$$

$$CC = N_A \cdot XB + N_B \cdot XC ;$$

$$CD = L_C \cdot XD + L_D \cdot XE ;$$

$$CE = M_C \cdot XD + M_D \cdot XE ;$$

$$CF = N_C \cdot XD + N_D \cdot XE ;$$

$$CG = L_C \cdot XF + L_D \cdot XG ;$$

$$CI = M_C \cdot XF + M_D \cdot XG ;$$

$$CK = N_C \cdot XF + N_D \cdot XG ;$$

$$CH = L_C \cdot XH + L_D \cdot XI ;$$

$$CJ = M_C \cdot XH + M_D \cdot XI ;$$

$$CL = N_C \cdot XH + N_D \cdot XI ;$$

KEY FOR OUT OF PLANE SUB-BLOCKS Ph and lj

$$CA = L_C \cdot XB + L_D \cdot XC ;$$

$$CB = M_C \cdot XB + M_D \cdot XC ;$$

$$CC = N_C \cdot XB + N_D \cdot XC ;$$

$$CD = L_A \cdot XD + L_B \cdot XE ;$$

$$CE = M_A \cdot XD + M_B \cdot XE ;$$

$$CF = N_A \cdot XD + N_B \cdot XE ;$$

$$CG = L_A \cdot XF + L_B \cdot XG ;$$

$$CI = M_A \cdot XF + M_B \cdot XG ;$$

$$CK = N_A \cdot XF + N_B \cdot XG ;$$

$$CH = L_A \cdot XH + L_B \cdot XI ;$$

$$CJ = M_A \cdot XH + M_B \cdot XI ;$$

$$CL = N_A \cdot XH + N_B \cdot XI ;$$

KEY FOR ALL OUT OF PLANE SUB-BLOCKS EXCEPT THE TWO DETAILED ABOVE

FIGURE 6.13



	X	Y	Z	$\theta_x$	$\theta_y$	$\theta_3$
X	$L_A \cdot GA$ + $L_B \cdot GB$	$M_A \cdot GA$ + $M_B \cdot GB$	$N_A \cdot GA$ + $N_B \cdot GB$	0	0	0
Y	$L_A \cdot GC$ + $L_B \cdot GD$	$M_A \cdot GC$ + $M_B \cdot GD$	$N_A \cdot GC$ + $N_B \cdot GD$	0	0	0
Z	$L_A \cdot GE$ + $L_B \cdot GF$	$M_A \cdot GE$ + $M_B \cdot GF$	$N_A \cdot GE$ + $N_B \cdot GF$	0	0	0
$\theta_x$	0	0	0	0	0	0
$\theta_y$	0	0	0	0	0	0
$\theta_3$	0	0	0	0	0	0

GENERAL RECTANGULAR AND TRIANGULAR SUB-BLOCK FOR THE IN PLANE OVERALL STIFFNESS CONTRIBUTION OF A CURVED PLATE

FOR A TRIANGULAR SUB-BLOCK CONSIDER ONLY THE LOWER TRIANGLE TERMS OF THE GENERAL SUB-BLOCK

FOR INTERPRETATION THIS FIGURE SHOULD BE READ IN CONJUNCTION WITH FIGURES 6.15 6.16

FIGURE 6.14

$$\begin{aligned}
GA &= L_C \cdot PA + L_D \cdot PB ; & GB &= L_C \cdot PC + L_D \cdot PD ; \\
GC &= M_C \cdot PA + M_D \cdot PB ; & GD &= M_C \cdot PC + M_D \cdot PD ; \\
GE &= N_C \cdot PA + N_D \cdot PB ; & GF &= N_C \cdot PC + N_D \cdot PD ;
\end{aligned}$$

KEY TO VALUES IN FIGURE 6.14

FIGURE 6.15

CODE	TRIANGULAR SUB-BLOCKS				RECTANGULAR SUB-BLOCKS						
	hh	jj	pp	ll	jh	ph	pj	jp	lh	lj	lp
PA	1,1	2,2	3,3	4,4	2,1	3,1	3,2	2,3	4,1	4,2	4,3
PB	5,1	6,2	7,3	8,4	6,1	7,1	7,2	6,3	8,1	8,2	8,3
PC	1,5	2,6	3,7	4,8	2,5	3,5	3,6	2,7	4,5	4,6	4,7
PD	5,5	6,6	7,7	8,8	6,5	7,5	7,6	6,7	8,5	8,6	8,7
$L_A^A$	$L_2$	$L_4$	$L_2$	$L_4$	$L_2$	$L_2$	$L_4$	$L_2$	$L_2$	$L_4$	$L_2$
$M_A$	$M_2$	$M_4$	$M_2$	$M_4$	$M_2$	$M_2$	$M_4$	$M_2$	$M_2$	$M_4$	$M_2$
$N_A$	$N_2$	$N_4$	$N_2$	$N_4$	$N_2$	$N_2$	$N_4$	$N_2$	$N_2$	$N_4$	$N_2$
$L_B$	$L_3$	$L_5$	$L_3$	$L_5$	$L_3$	$L_3$	$L_5$	$L_3$	$L_3$	$L_5$	$L_3$
$M_B$	$M_3$	$M_5$	$M_3$	$M_5$	$M_3$	$M_3$	$M_5$	$M_3$	$M_3$	$M_5$	$M_3$
$N_B$	$N_3$	$N_5$	$N_3$	$N_5$	$N_3$	$N_3$	$N_5$	$N_3$	$N_3$	$N_5$	$N_3$
$L_C$	$L_2$	$L_4$	$L_2$	$L_4$	$L_4$	$L_2$	$L_2$	$L_4$	$L_4$	$L_4$	$L_4$
$M_C$	$M_2$	$M_4$	$M_2$	$M_4$	$M_4$	$M_2$	$M_2$	$M_4$	$M_4$	$M_4$	$M_4$
$N_C$	$N_2$	$N_4$	$N_2$	$N_4$	$N_4$	$N_2$	$N_2$	$N_4$	$N_4$	$N_4$	$N_4$
$L_D$	$L_3$	$L_5$	$L_3$	$L_5$	$L_5$	$L_3$	$L_3$	$L_5$	$L_5$	$L_5$	$L_5$
$M_D$	$M_3$	$M_5$	$M_3$	$M_5$	$M_5$	$M_3$	$M_3$	$M_5$	$M_5$	$M_5$	$M_5$
$N_D$	$N_3$	$N_5$	$N_3$	$N_5$	$N_5$	$N_3$	$N_3$	$N_5$	$N_5$	$N_5$	$N_5$

CODE VALUES REFER TO TERMS WITHIN THE IN PLANE ELEMENT STIFFNESS MATRIX  $\underline{k}$ ,  
AND TERMS WITHIN THE IN PLANE DISPLACEMENT TRANSFORMATION MATRIX

KEY TO TERMS FORMING EACH OF THE IN PLANE SUB-BLOCKS

FIGURE 6.16

## CHAPTER 7

### COMPUTER TESTS ON THE CURVED PLATE ELEMENT

#### (7.1) Introduction

It is essential that the programming of the in and out of plane curved plate stiffness matrices is rigorously checked. In addition to inspecting the logic of the program it is also desirable to investigate the numerical values of individual terms. One way in which this is done is to compare the stiffness matrix of a curved plate to that of a geometrically equivalent rectangular plate.

The approximate nature of the displacement function precludes an exact analysis. Usually the more elements into which the structure is divided the more accurate is the analysis. The subdivision of a plate into several meshes permits the plotting of the relationship between the number of mesh elements and the deflection at a point. It will be shown that this graph follows the accepted trend.

Finally the comparison between a set of independent results, a theoretical series solution and a finite element analysis was carried out.

#### (7.2) Testing the out of plane element stiffness matrix

The programming of the theory developed in Chapter 5, to form the out of plane element stiffness matrix, is a complex operation. It is consequently a difficult task to ensure that such a program is operating free of all errors. Initially, if one considers the on diagonal terms of the matrix, then the two terms corresponding to the translations of the two nodes on the outer arc should be identical, as should those corresponding to the two nodes on the inner arc. In a similar manner comparisons may be made between the terms relating to the two rotations  $\theta_x$  and  $\theta_y$ , (see figure 5.1 Chapter 5).



Once these conditions have been shown to be true then the actual value of such terms may be investigated. If one considers a curved plate with its radius very much larger than its other dimensions, then such a plate will be similar, both geometrically and behaviourally, to a rectangular plate. Consequently the stiffness matrices of each should be comparable. An investigation was made into the behaviour of the on-diagonal terms as the radius of curvature was reduced, as far as possible the other plate dimensions were maintained. Whilst the radial length and the cord length can be retained constant, the length of the plate along the arc will increase as the radius decreases, consequently the curved plate will become less like the rectangular plate.

The ratio of the radius ( $R$ ) to the radial plate dimension ( $Y$ ) gives a non dimensional quantity, which, when plotted against each of the six sets of two unique values of on-diagonal term, for varying radius values, yields the graphs given in figures 7.1, 7.2 and 7.3. Each graph comprises three lines; the unbroken line representing the value of the on-diagonal term for the geometrically equivalent rectangular plate; the broken line represents the two on-diagonal elements corresponding to the nodes on the outside arc of the plate; the chain dotted line is that for the two nodes on the inside arc. It can be seen from these figures that for  $R/Y$  ratios in the order of forty the curved plate very closely simulates the rectangular plate. As the radius is reduced the characteristics of the two plates diverge. For  $R/Y = 1$  the on-diagonal term becomes infinity, it can be seen in all three figures that near this region the curves become asymptotic to the ordinate axis. The nodes on the inside arc of the plate will behave in a different manner to those on the outside arc. This is due to the fact that when the radius is very large both curved faces tend to straight lines, whereas when the radius decreases the inside face becomes relatively more curved than the outside face and consequently will exhibit different

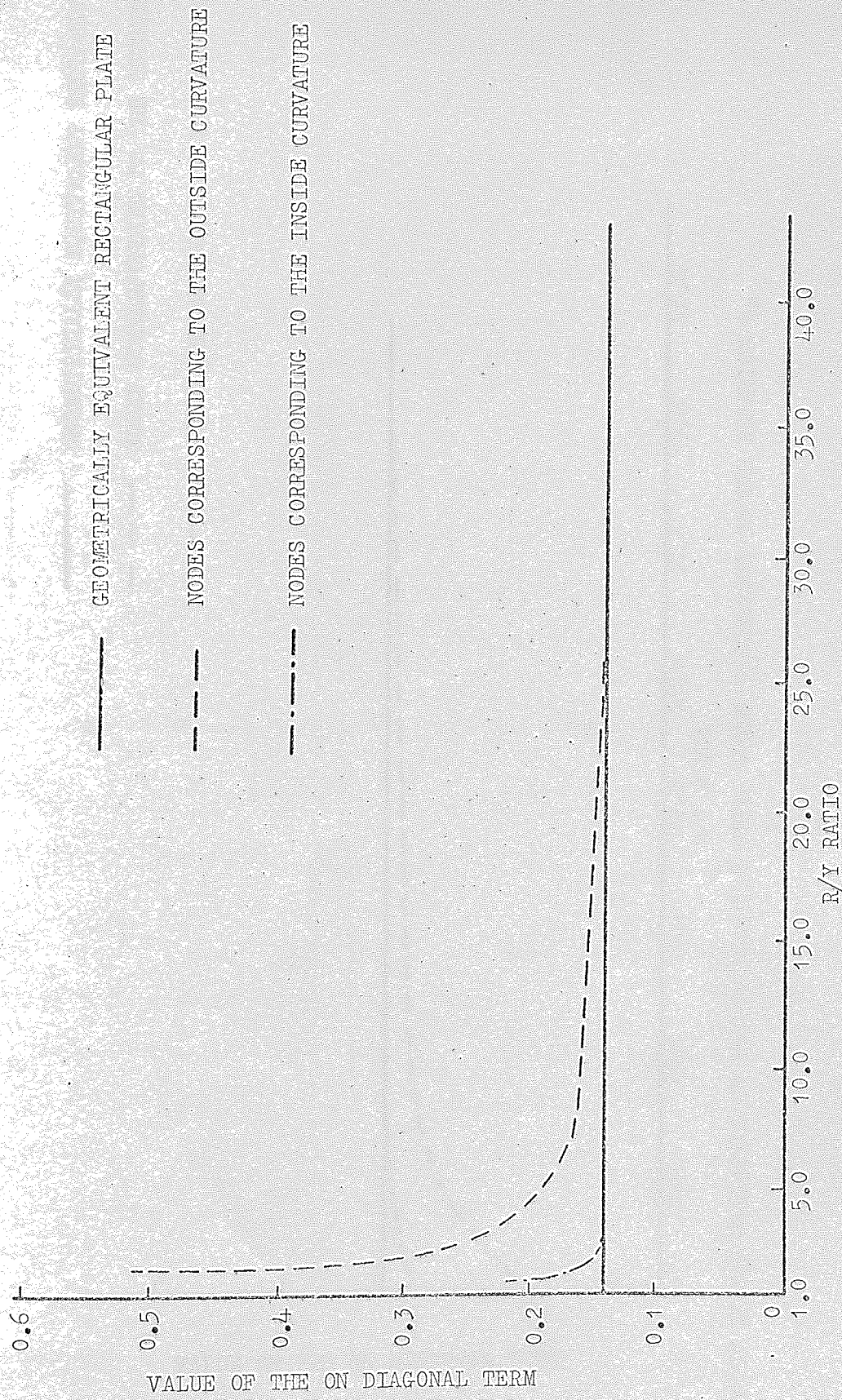


FIGURE 7.1



————— GEOMETRICALLY EQUIVALENT RECTANGULAR PLATE  
 - - - - - NODES CORRESPONDING TO THE OUTSIDE CURVATURE  
 - · - · - · - NODES CORRESPONDING TO THE INSIDE CURVATURE

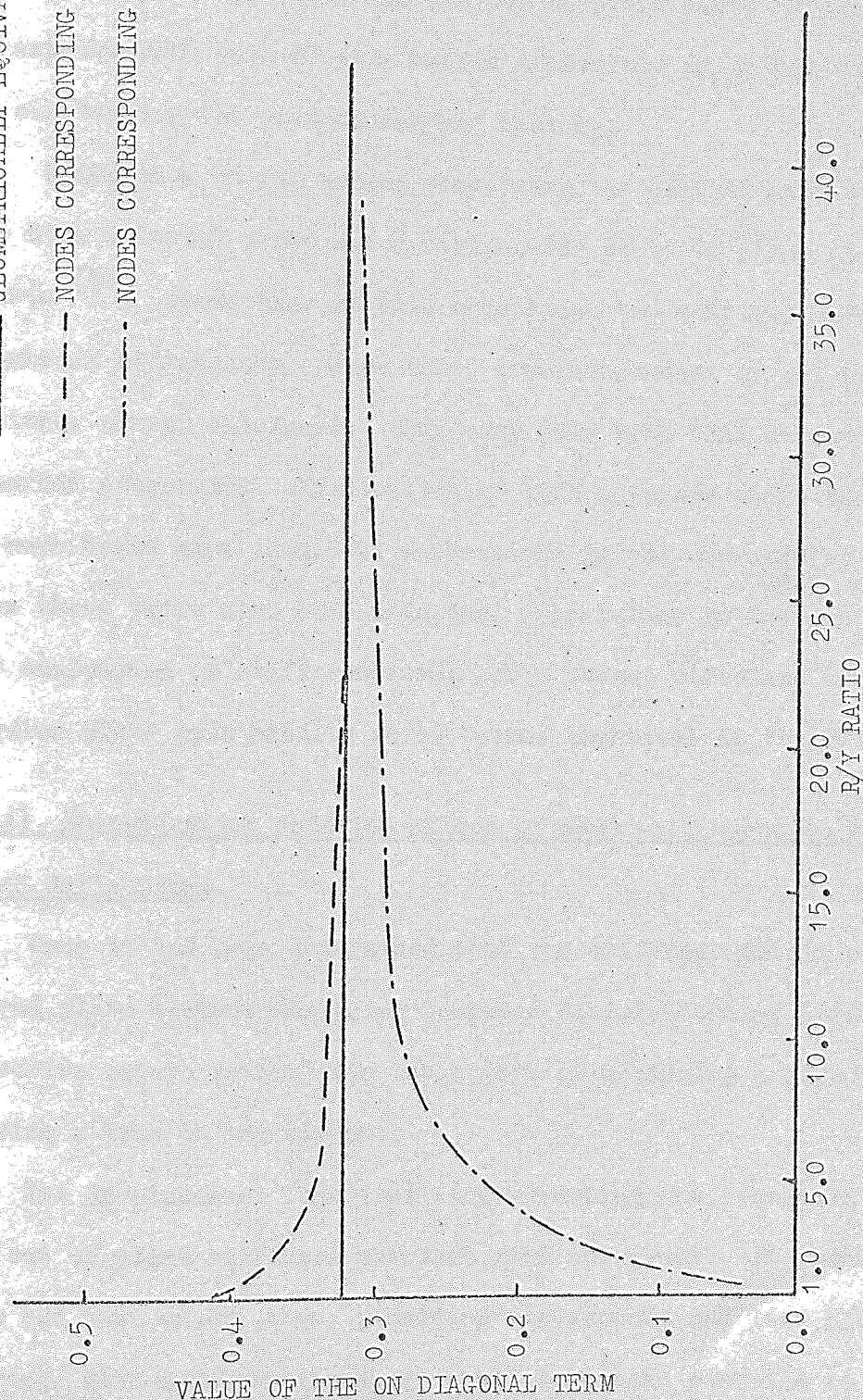


PLOT OF THE VARIATION OF THE ON DIAGONAL TERMS WHICH CORRESPOND TO THE ROTATION  $\theta_r$

FIGURE 7.2



——— GEOMETRICALLY EQUIVALENT RECTANGULAR PLATE  
 - - - - - NODES CORRESPONDING TO THE OUTSIDE CURVATURE  
 - · - · - NODES CORRESPONDING TO THE INSIDE CURVATURE



PLOT OF THE VARIATION OF THE ON DIAGONAL TERMS WHICH CORRESPOND TO THE ROTATION  $\theta_y$

FIGURE 7.3

behavioural characteristics, which will become more marked as the R/Y ratio reduces. Similar investigation has confirmed that the off diagonal terms also converge to the corresponding terms for a rectangular plate.

#### (7.3) Testing the in plane element stiffness matrix

The theory associated with the formation of this matrix is more straightforward than that for the out of plane case. It was feasible to express each term of this matrix explicitly which had the effect of simplifying the programming and testing.

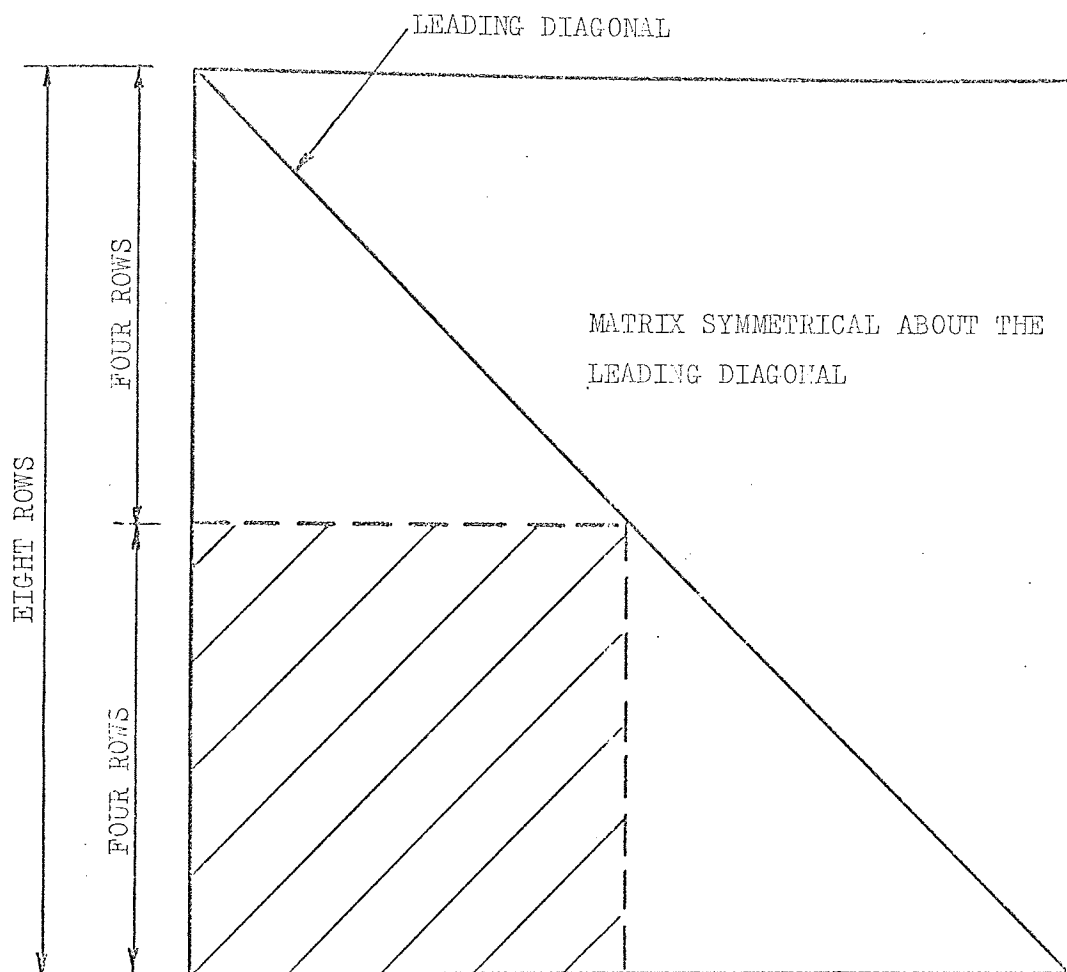
Comparison of the terms, comprising the hatched area in figure 7.4, for both a curved plate and a rectangular plate in plane stiffness matrix <sup>(31)</sup> shows that in this area these two matrices have identical algebraic expressions. Such terms are independent of all plate dimensions, except thickness, they vary only with that dimension and the material properties. Examination of both matrices shows that where two or more terms have identical expressions in the rectangular plate matrix, then these terms also have identical expressions in the curved plate matrix. The evaluation of stiffness terms for a curved plate and an equivalent rectangular plate gave results which became identical as the R/Y ratio increased.

#### (7.4) Investigation into the effect of mesh refinement on the computed deflections

Once it had been determined that the stiffness matrix of a single curved plate element was being computed satisfactorily, then the next objective was to investigate the effect of analysing a structure comprising a mesh of the elements.

The displacement functions adopted during the formation of the in and out of plane stiffness matrices were not exact. If these functions had been exact, then, providing the support and load positions coincided with node positions, it would have been possible to accurately analyse any size curved plate using only one element. As this is not the case it is necessary to employ a mesh of elements to simulate a





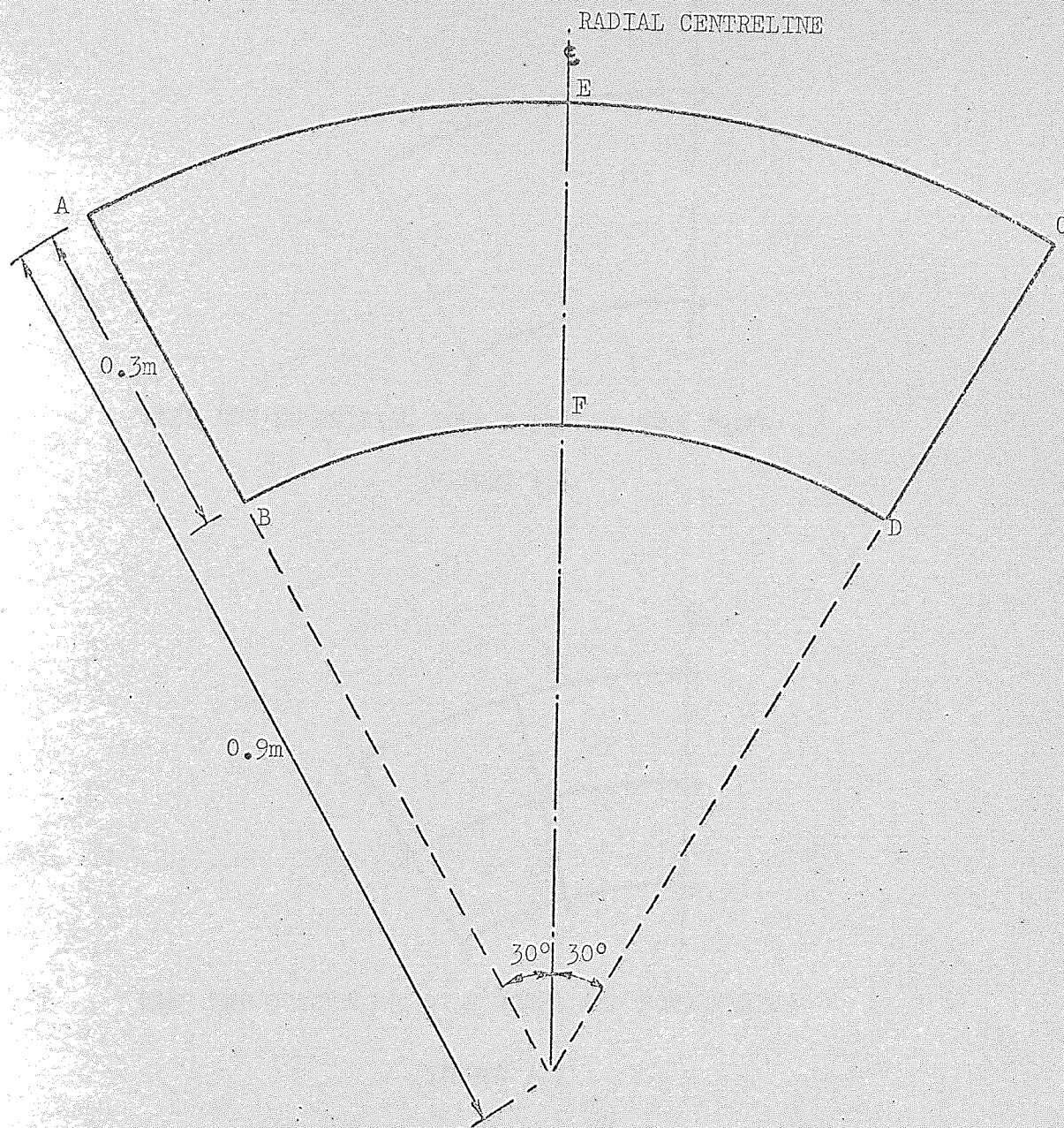
SCHEMATIC REPRESENTATION OF THE EIGHT BY EIGHT IN PLANE ELEMENT STIFFNESS  
 MATRIX OF A CURVED PLATE  
 THE HATCHED BLOCK IS OCCUPIED BY TERMS WHICH ARE IDENTICAL TO THOSE  
 IN THE EQUIVALENT RECTANGULAR PLATE MATRIX

FIGURE 7.4

curved plate structure. The number of mesh elements required to give a good representation of the true function is an indication of the accuracy of the assumed function. The characteristics of this convergence are dependant upon the shape of the mesh elements, thus as mesh refinement progresses the ratio of the side lengths of each element should be maintained constant.

A plate, whose properties and dimensions are shown in figure 7.5, was analysed using five different meshes. The plate was assumed to be rigidly supported at its four corners and loaded on the extremes of its radial centre line. These positions were chosen so that the load and support conditions would be suitable for all meshes. The radial centre line is an axis of symmetry, it is therefore only necessary to analyse one half of the plate providing the applied loading is also symmetrical. The five meshes adopted are shown in figures 7.6, 7.7, 7.8, 7.9 and 7.10 with the elements marked on the left side of the centre line. In each case the number of radial divisions is equal to the number of circumferential divisions.

The vertical deflection of the radial centre line of the plate for each of the meshes has been plotted in figure 7.11. This diagram shows that the coarser meshes give lower deflections than the more refined meshes. These results are presented in a different form in figure 7.12 where the deflection of the node on the outside edge of the centre line is plotted against the number of elements comprising the mesh. From this diagram it can be seen that when the mesh is initially refined there is a significant change in the computed deflection. During continued refinement this change became less pronounced in spite of the fact that with each refinement the number of elements is approximately doubled. The graph shown in figure 7.12 appears to be converging to a solution. It remains to be established whether this is the true deflections as given by a classical solution.



1. THE PLATE WAS ASSUMED TO BE RIGIDLY SUPPORTED AT CORNERS A, B, C AND D.
2. POINT LOADS OF EIGHT NEWTONS ACTING AT RIGHT ANGLES TO THE PLANE OF THE PLATE WERE APPLIED AT E AND F.
3. THE FOLLOWING MATERIAL PROPERTIES WERE ASSUMED;  
 YOUNG'S MODULUS OF ELASTICITY AS  $6.85 \times 10^7 \text{ KN/m}^2$ .  
 POISSON'S RATIO AS 0.33.
4. THE PLATE THICKNESS WAS TAKEN AS  $3.25 \times 10^{-3} \text{ m}$ .

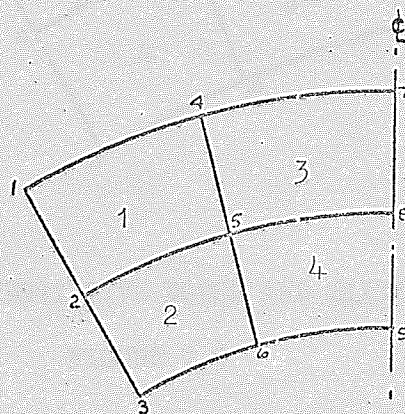
FIGURE 7.5





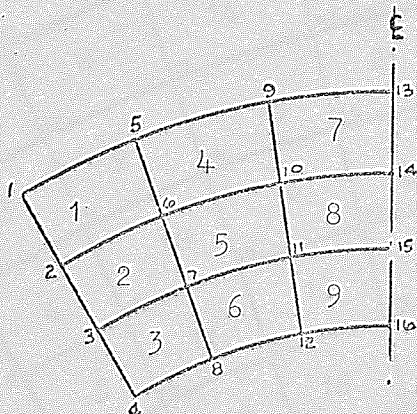
MESH ONE COMPRISING FOUR NODES AND ONE PLATE

FIGURE 7.6



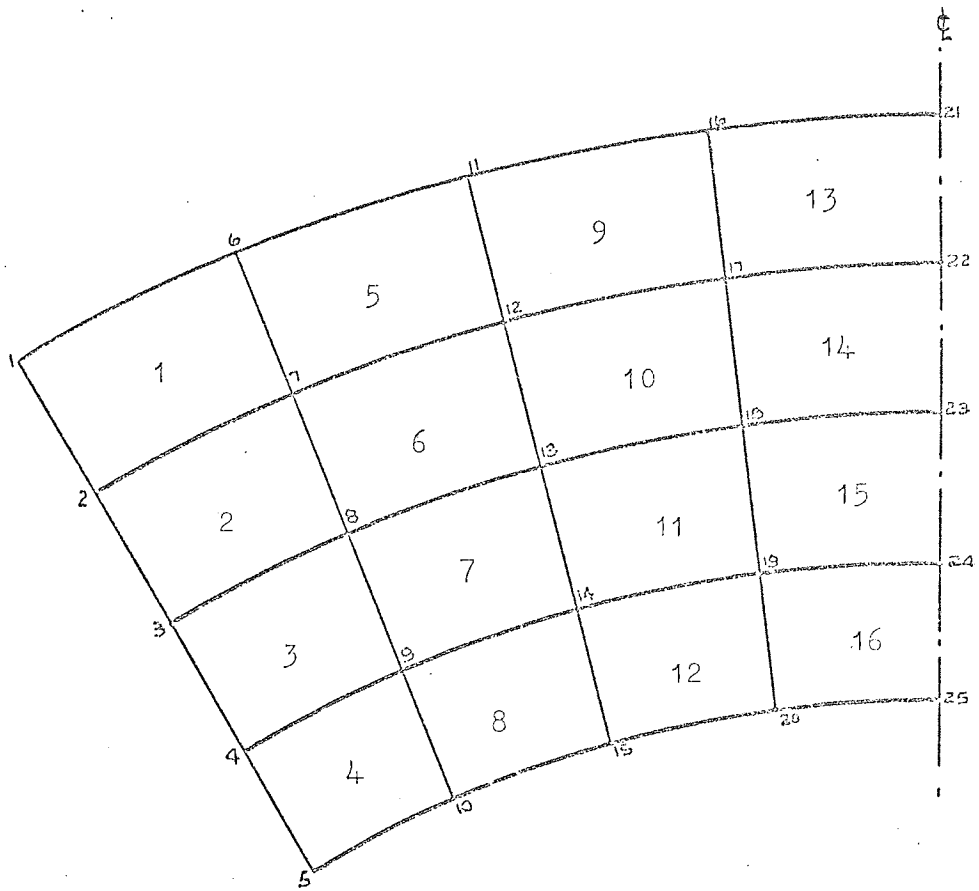
MESH TWO COMPRISING NINE NODES AND FOUR PLATES

FIGURE 7.7



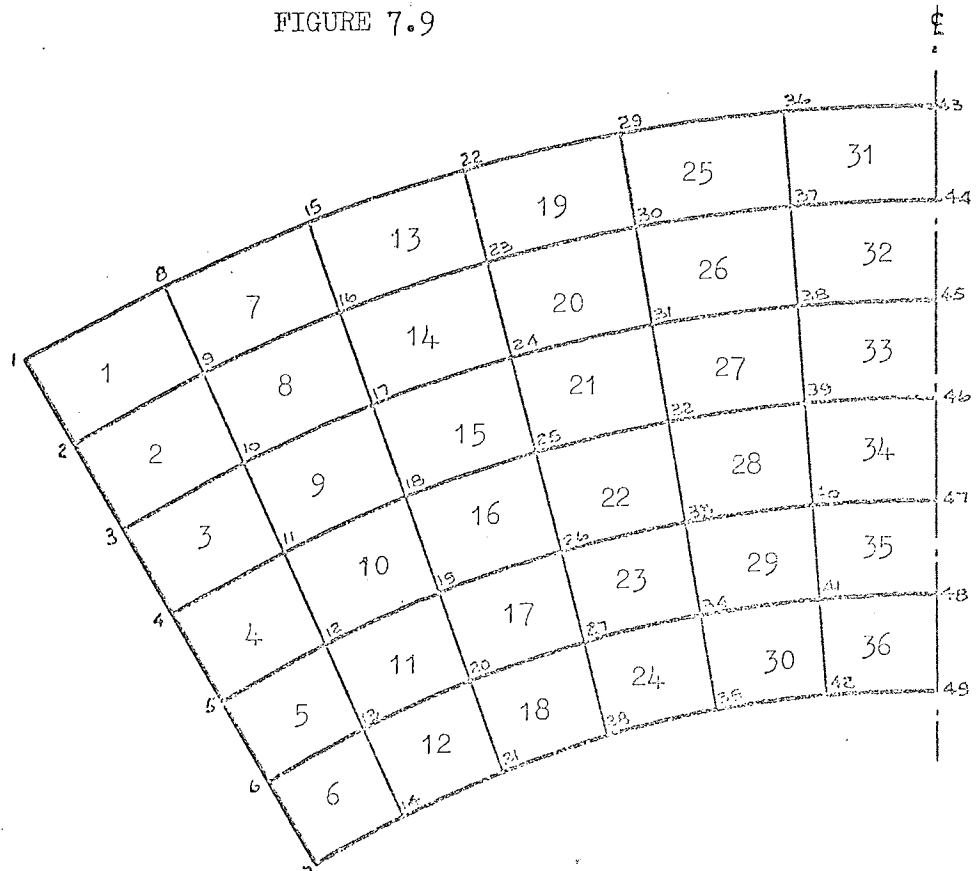
MESH THREE COMPRISING SIXTEEN NODES AND NINE PLATES

FIGURE 7.8



MESH FOUR COMPRISING TWENTY FIVE NODES AND SIXTEEN PLATES

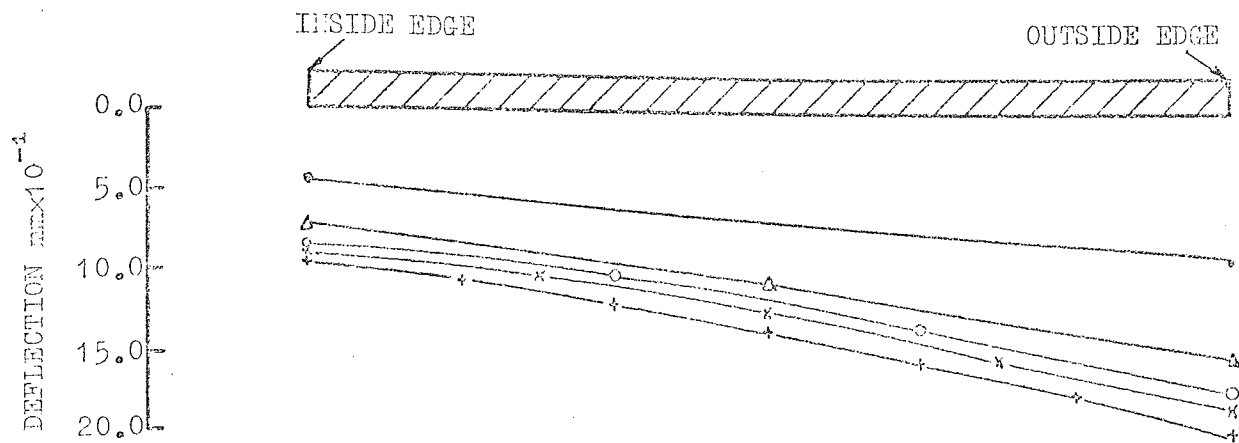
FIGURE 7.9



MESH FIVE COMPRISING FORTY NINE NODES AND THIRTY SIX PLATES

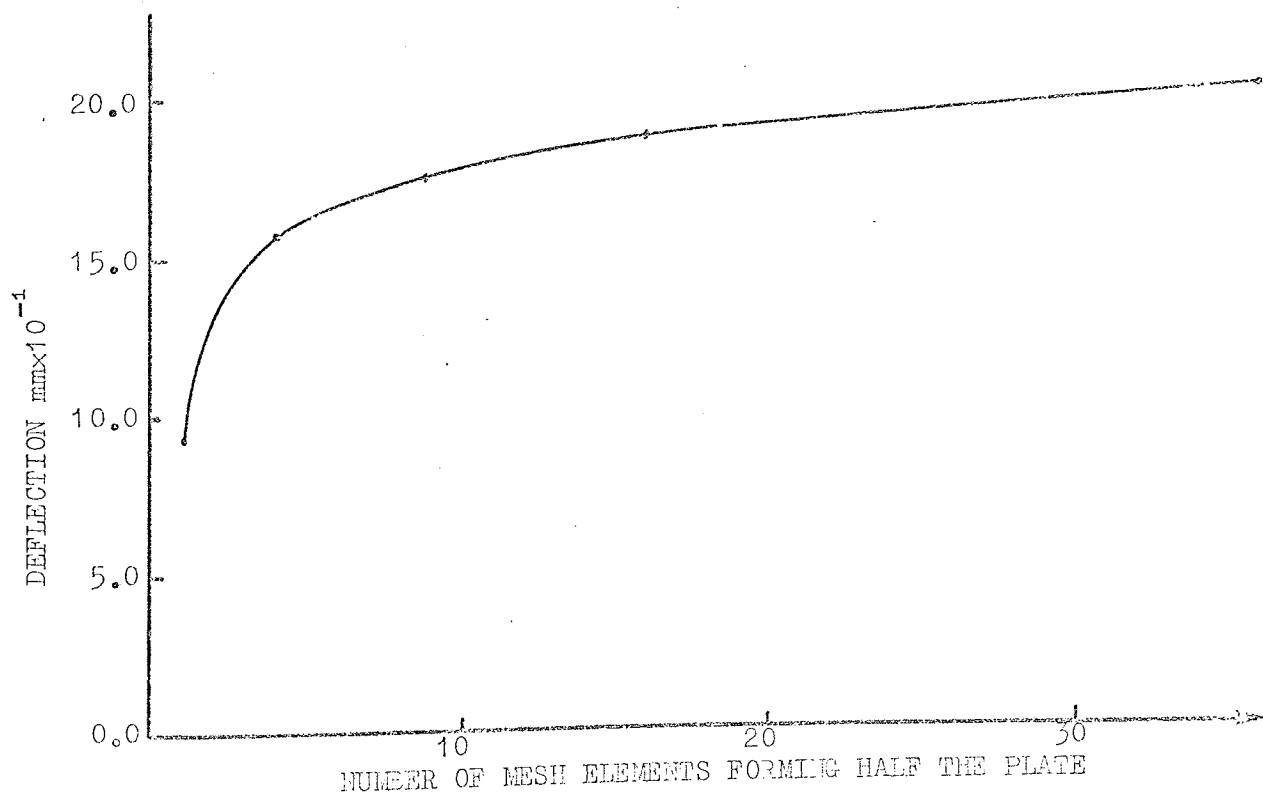
FIGURE 7.10






A PLOT OF THE VERTICAL DEFLECTION OF THE PLATE ALONG ITS RADIAL CENTRE-LINE FOR EACH MESH

FIGURE 7.11



GRAPH SHOWING THE RATE OF CHANGE OF DEFLECTION OF THE NODE ON THE OUTSIDE EDGE OF THE RADIAL CENTRE-LINE AS THE MESH IS REFINED

FIGURE 7.12

 This sort of graph may be used to determine the degree of accuracy being achieved for a given mesh, or to aid the selection of a mesh suitable for an analysis.

One final point on mesh refinement is that the amount of computer time and storage is a function of the number of elements forming a mesh. Therefore as the refinement is carried out a point may be reached at which the increase in accuracy is not enough to justify the increase in computation.

#### (7.5) Comparison between theoretical results and previous experimental work

The testing of the element so far has been predominantly of a qualitative nature. A useful exercise would therefore be to carry out a computational analysis on a problem which has been analysed experimentally.

Coull and Das have presented a paper<sup>(7)</sup> giving an exact solution for the analysis of isotropic curved bridge decks in the form of an infinite Fourier series. They compare this solution with test results obtained from two curved plate tests. One contribution to the discussion of this paper was presented by Jenkins and Siddall<sup>(32)</sup> who adopted a finite element technique to analyse the same problem. The curved element used in their analysis is one detailed by Siddall<sup>(33)</sup>. The formulation of this element makes use of a displacement function obtained by substituting, for  $x$  and  $y$  in terms of polar co-ordinates, in the general out of plane rectangular plate displacement function. This results in the following expression:

$$\begin{aligned} \omega = & A_1 + A_2 r \sin\theta + A_3 r \cos\theta + A_4 r^2 \sin^2\theta + A_5 r^2 \sin\theta \cos\theta \\ & + A_6 r^2 \cos^2\theta + A_7 r^3 \sin^3\theta + A_8 r^3 \sin^2\theta \cos\theta + A_9 r^3 \sin^3\theta \cos^2\theta \\ & + A_{10} r^3 \cos^3\theta + A_{11} r^4 \sin^3\theta \cos\theta + A_{12} r^4 \sin\theta \cos^3\theta \end{aligned}$$

where  $2\theta$  is the angle subtended by the element.

The function is, however, non-conforming in translation, this is because

on any  $\theta$  constant line the displacement curve is a quartic. Complete conformity of translation requires that this curve is cubic as is the case for the author's element detailed in Chapter 5.

The paper<sup>(7)</sup> by Coull and Das concerned with the tests and the theoretical series solution has been reviewed in the introduction to this thesis. A comprehensive description of the tests will not be given here, suffice it to say that two curved plates of different dimensions, one made of asbestos cement and the other perspex were tested in Moire's apparatus. Both radial edges were supported along their length in such a manner that the only permitted movement was a rotation about those edges. Three load cases were considered each comprising a single point load applied perpendicular to the plane of the plate. The three loading positions were at the outer edge, mid-radius and at the inner edge of the plate's radial centre line.

Comparison is made, between the author's finite element solution, Siddall's finite element solution and Coull and Das' series solution, in the table given in figure 7.13. In this table the predicted deflection at the outer edge of the radial centre line is indicated for each theoretical solution. In order that the finite element solutions might be comparable the author adopted the mesh used by Siddall, namely six circumferential divisions and four radial divisions resulting in a twenty four element mesh. The values shown in the table but not calculated by the author have been measured off the graphs presented by Siddall<sup>(33)</sup>. It may be seen from the table that in the case of the asbestos cement model, which had an inner radius of thirteen inches and an outer radius of twenty six inches, that Siddall's results compare very favourably with Coull and Das'. The author's results are consistently below these two set of values. The perspex model, inner radius seven inches outer radius thirteen inches, was the other plate analysed. In this case the author's results and those of Coull and Das are in close agreement especially when the load is applied at either edge of the

	Bray	Jenkins & Siddall	Coull & Das	Load Position
Asbestos Cement Model	1.56	1.80	1.80	a
	0.26	0.36	0.36	b
	0.26	0.36	0.36	c
Perspex Model	74.0	87.0	74.0	a
	37.0	45.0	48.0	b
	16.0	19.0	16.0	c

Deflections are given in inches x  $10^{-3}$

- a. Load at the outer edge of the radial centre line
- b. Load at the mid-radius of the radial centre line
- c. Load at the inner edge of the radial centre line

PREDICTED DEFLECTION AT THE OUTER EDGE OF THE RADIAL CENTRE LINE

FIGURE 7.13

radial centre line. Siddall's solution indicates that the deflections would be larger than those predicted by both of the other methods.

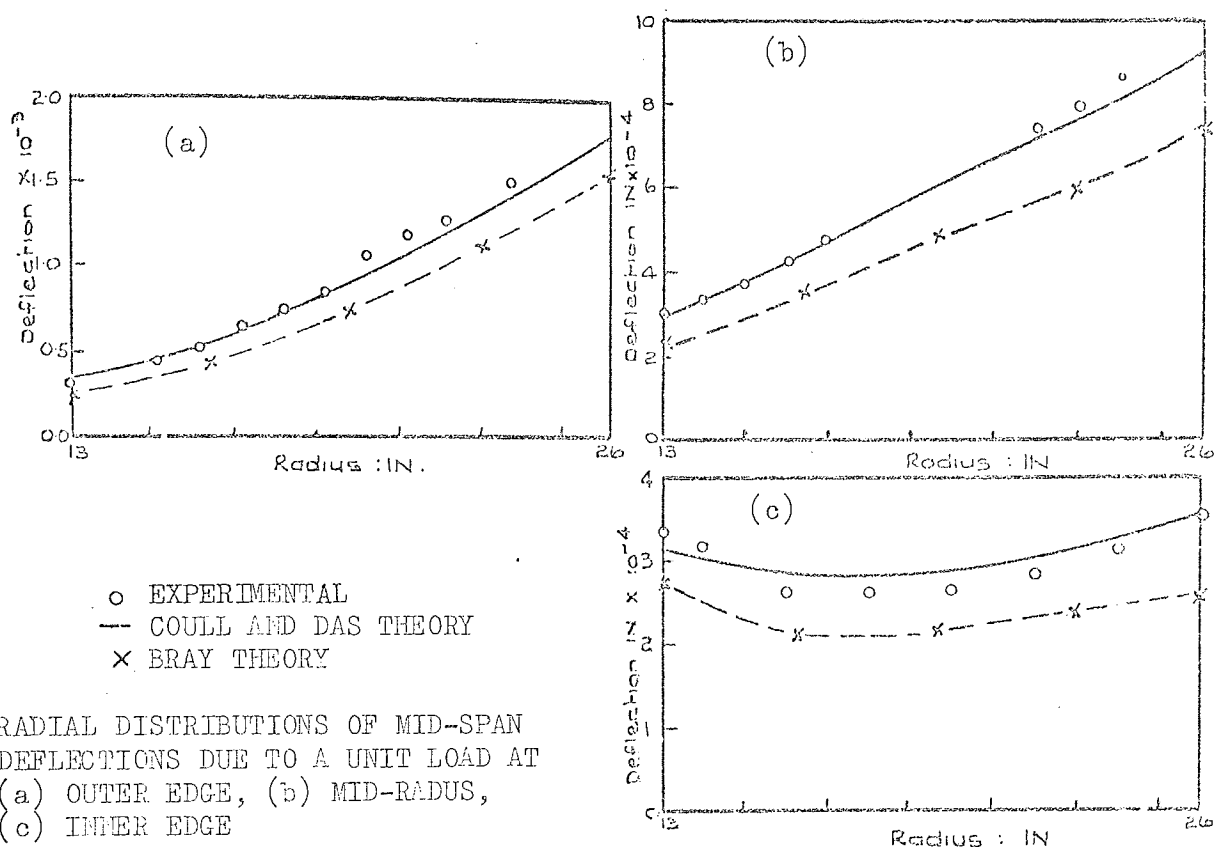
One explanation for some discrepancy in these results is the manner in which the edges of the plates were restrained. In the author's analysis, simulation of the true experimental support conditions would have meant suppression of non-global degrees of freedom. It was therefore decided to permit rotations about two orthogonal axes at each joint on the support line. This would, however, have the effect of permitting a rotation to occur about an axis at right angles to the support line. Coull and Das were able to simulate their experimental conditions, Siddall, however, does not state the support restraints he imposed.

The results obtained from the author's twenty four element mesh are presented graphically in figures 7.14 and 7.15. In these illustrations the author's results are plotted as are Coull and Das' experimental and theoretical lines for both the asbestos cement and the perspex model. The author carried out a further analysis with a seventy two element mesh, six radial and twelve circumferential divisions, the results are presented in figures 7.16 and 7.17.

There would appear to be no significant difference between the results given by the two mesh patterns. The finer of the two meshes being marginally less close to the experimental results.

Generally the results agree more closely in the case of the perspex model, especially when the load is applied at either end of the radial centreline. When the load is at mid-radius the deflection is predicted to be less than the experimentally measured amount, the deflected shape is, however, similar. This similarity in deflected form is also the case for the asbestos cement model where all the load cases under estimate the recorded deflection.

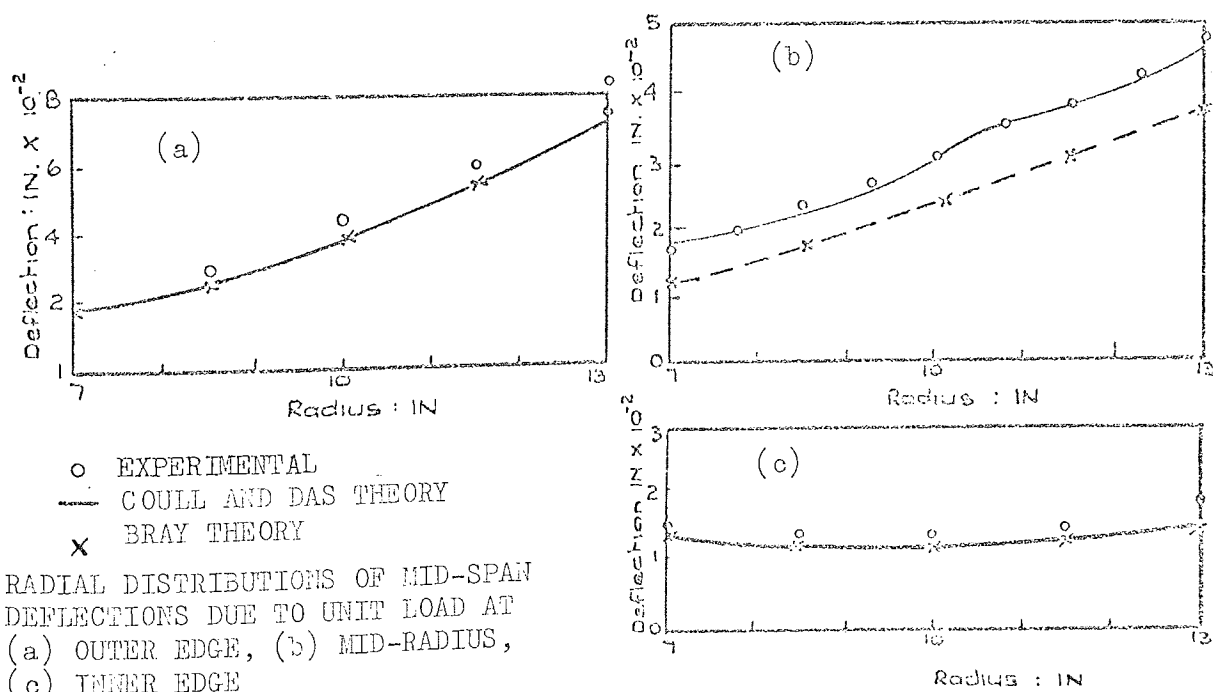




RADIAL DISTRIBUTIONS OF MID-SPAN DEFLECTIONS DUE TO A UNIT LOAD AT  
 (a) OUTER EDGE, (b) MID-RADIUS,  
 (c) INNER EDGE

ASBESTOS-CEMENT MODEL TWENTY FOUR ELEMENT MESH

FIGURE 7.14



RADIAL DISTRIBUTIONS OF MID-SPAN DEFLECTIONS DUE TO UNIT LOAD AT  
 (a) OUTER EDGE, (b) MID-RADIUS,  
 (c) INNER EDGE

PERSPEX MODEL TWENTY FOUR ELEMENT MESH

FIGURE 7.15

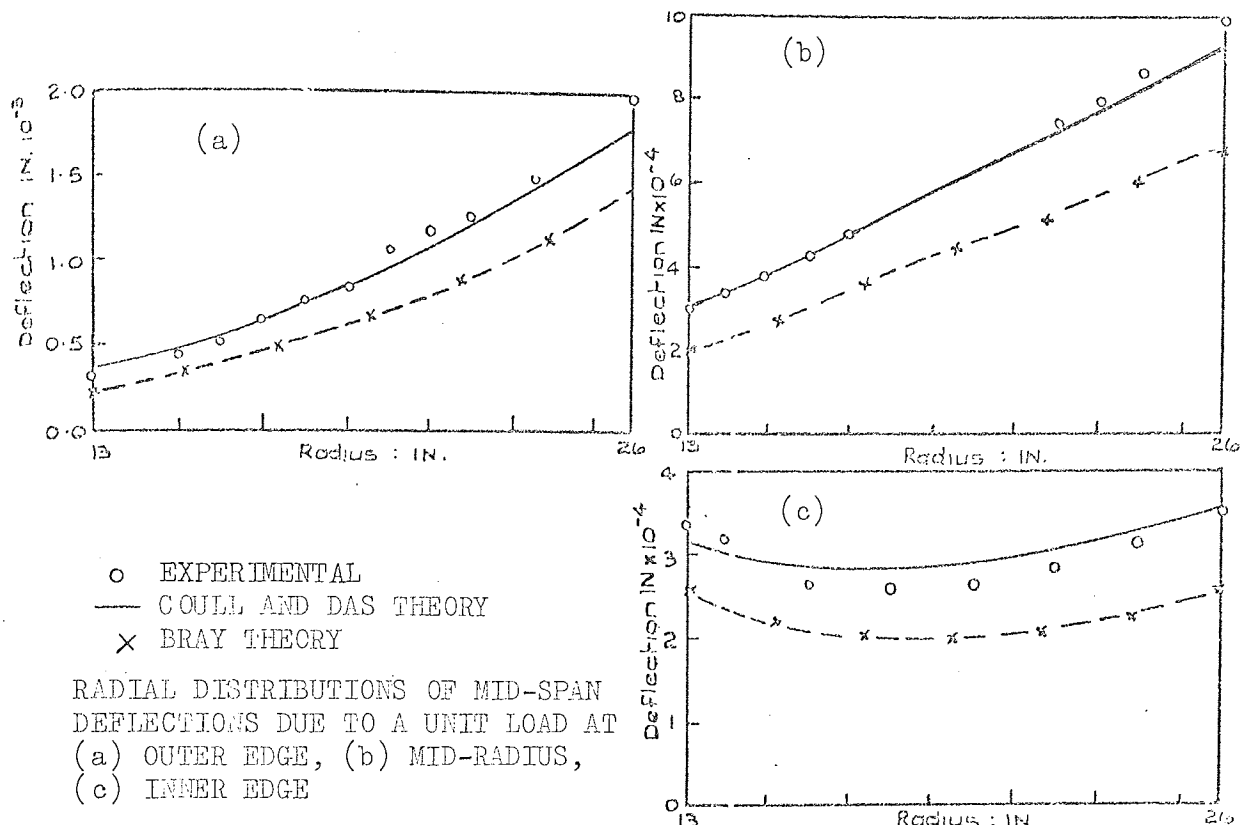


FIGURE 7.16

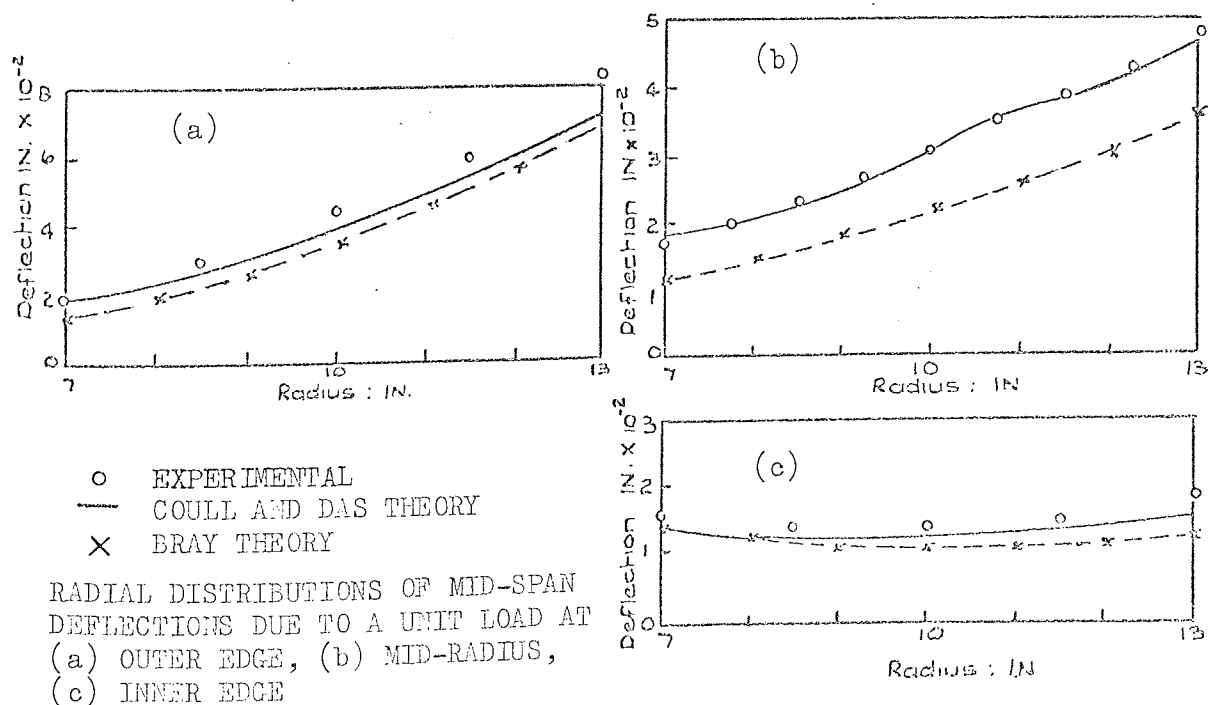


FIGURE 7.17

Further investigation is required to prove the existence of a constant strain criterion in the proposed element. Better simulation of the curved plate should be investigated so that a true comparison can be made with the other solutions.

## CHAPTER 8

### EXPERIMENTAL CURVED PLATE TESTS

#### (8.1) Introduction

It was decided that four tests should be carried out to compare theoretical results with those obtained experimentally. The aim of these tests was to measure deflections and strains at positions within each test plate so that this comparison could be made.

#### (8.2) Material of the plates

The material selection was governed by two criteria. Firstly as two edges of each plate were to be circularly curved a material which could be accurately shaped was essential. Secondly it was decided that the loading would take the form of dead weights, this restricted the maximum load, consequently the plate should not be over stiff.

Three materials were considered, steel, perspex and aluminium. Steel was dismissed on both counts. It would have been difficult to cut to the desired shape and its high Young's Modulus value meant that a very thin section was required. The most attractive material from a stiffness point of view was perspex, cutting it to shape would have been a straightforward operation. It has, however, two disadvantages which finally ruled out its use. It is a poor heat dissipator and it has a tendency to creep. The heat dissipation problem causes complications when using electrical resistance strain gauges, these could have been overcome by using a separate dummy gauge for each active gauge. The third material considered and finally selected was aluminium. With a Young's Modulus value approximately one third that of steel it was deemed to be well suited to the application of dead weights, furthermore cutting it accurately to shape was feasible.

### (8.3) Control tests

These tests were carried out to determine the Young's Modulus and Poisson's ratio value of the material.

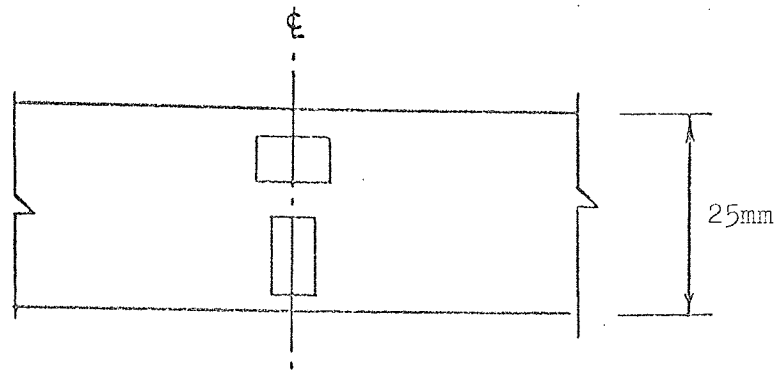
A strip 1 m. long and 25 mm. wide was cut from the same aluminium sheet as the plates. Two electrical resistance gauges were fixed to each face of the strip at its centre line. The orientation of these gauges, identical on each face, is shown in figure 8.1. A bending test was then carried out on the strip in the following manner. The strip was supported on knife edges and subjected to point loads at one third and two thirds span positions, see figure 8.2. Equal load increments were applied, after each increment the four strain gauge readings were recorded. This process was continued during the whole of both the loading and unloading cycle. A graph of the average longitudinal strain plotted against the applied load is given in figure 8.3. The Young's Modulus value was calculated in the manner shown in that figure. A graph of the average longitudinal strain plotted against the average lateral strain is shown in figure 8.4, the slope of this graph gives the value of Poisson's ratio.

### (8.4) Preliminary considerations

It was decided that two plates of different radii but having the same thickness would be tested. The dimensions of these plates are shown in figure 8.5.

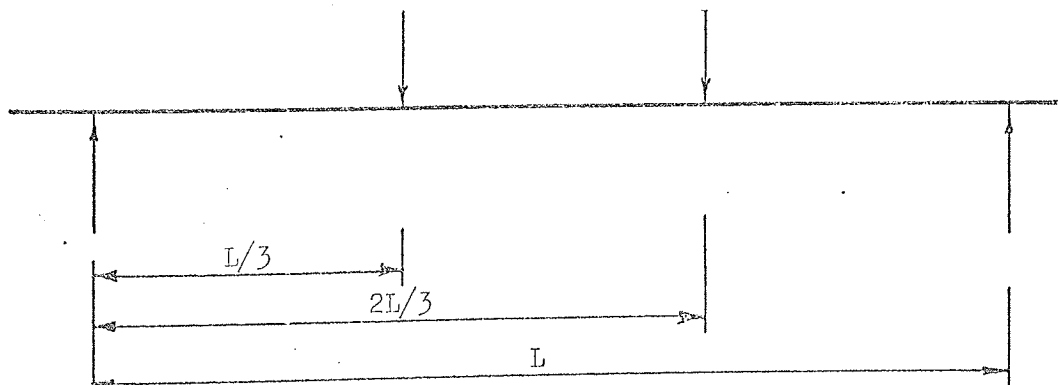
A theoretical finite element analysis restricts the application of loads to nodal points. In order that flexibility of analytical mesh may be maintained a single point load system was adopted. An illustration of the method used to apply such a load is given in figure 8.6. Here it is seen that the weights rest on a load support plate. This plate is rigidly fixed a short distance from one end of a circular rod which is maintained vertical by a collar. The collar is rigidly positioned by a stabilising arm and is a sliding fit on the rod. The load applied





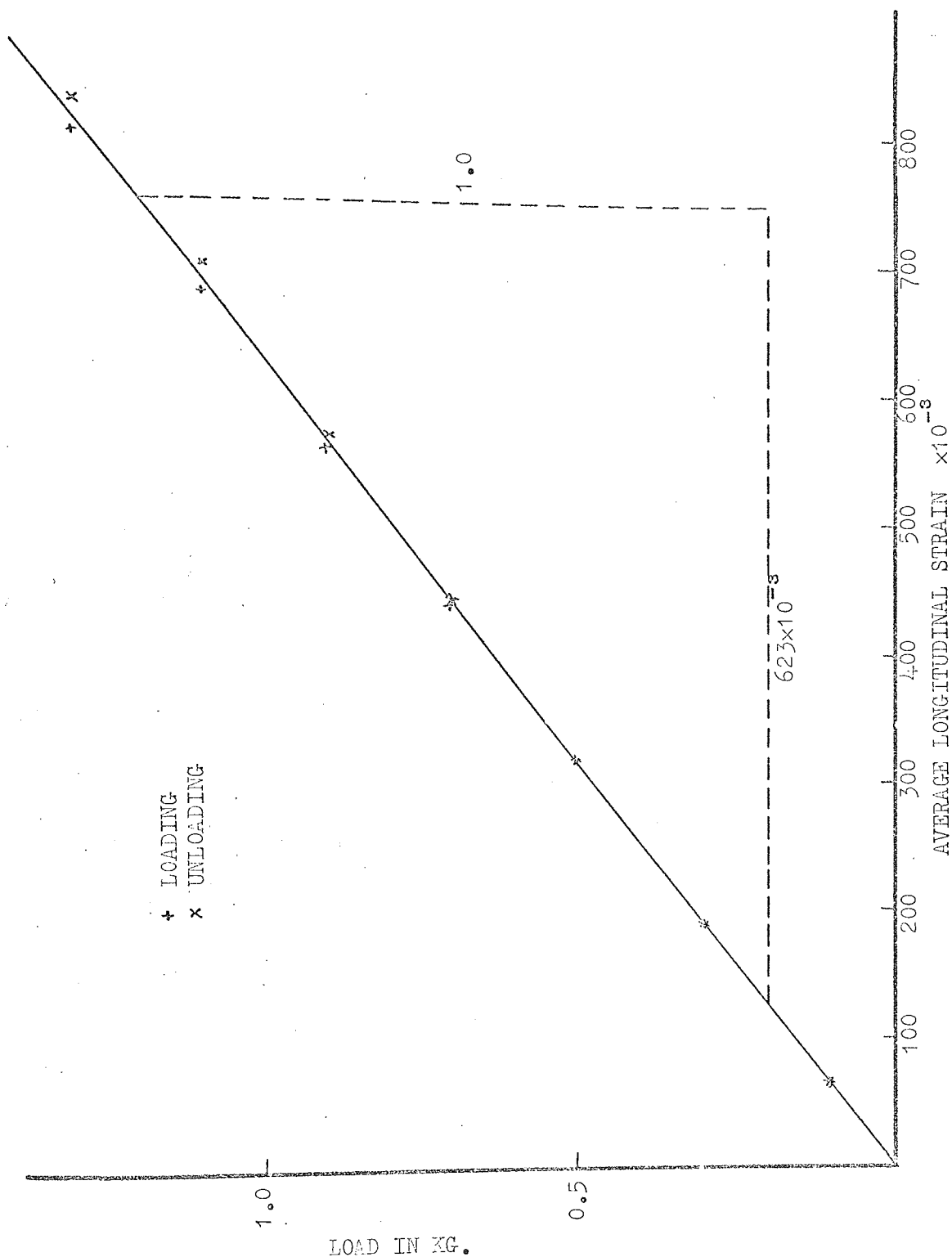
STRAIN GAUGE POSITIONS

FIGURE 8.1



BENDING TEST

FIGURE 8.2



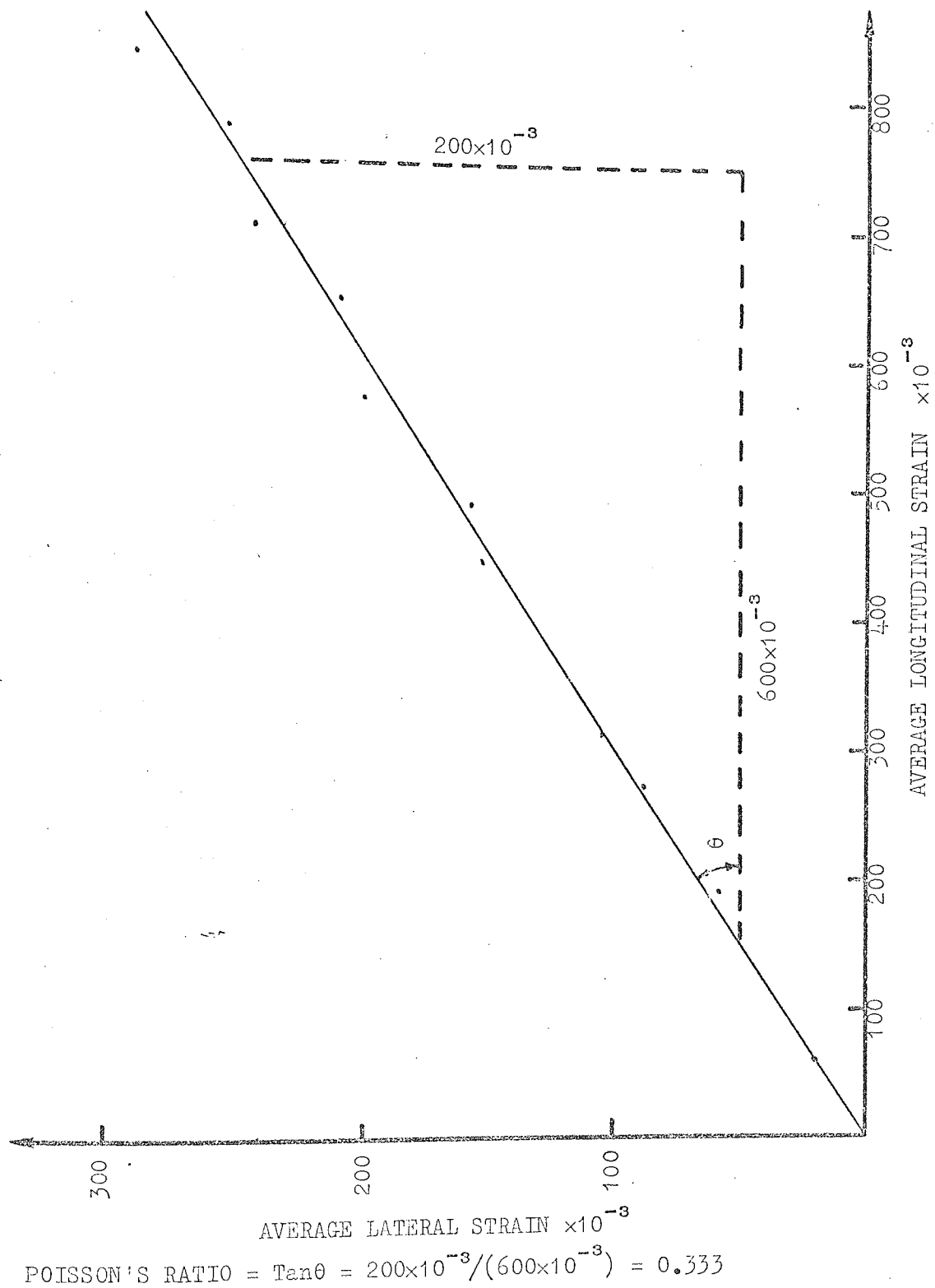
LOAD IN KG.

SLOPE =  $\frac{3EZ}{(gL)}$ ; WHERE L IS THE SPAN  
 E IS THE YOUNG'S MODULUS VALUE  
 Z IS THE SECTION MODULUS

$$\text{SLOPE} = 1.0 / (625 \times 10^{-3}) = E \times 50.63 / (9.81 \times 220.0)$$

$$E = 63.2 \text{ KN/mm}^2$$

FIGURE 8.3



$$\text{POISSON'S RATIO} = \tan \theta = \frac{200 \times 10^{-3}}{(600 \times 10^{-3})} = 0.333$$

FIGURE 8.4

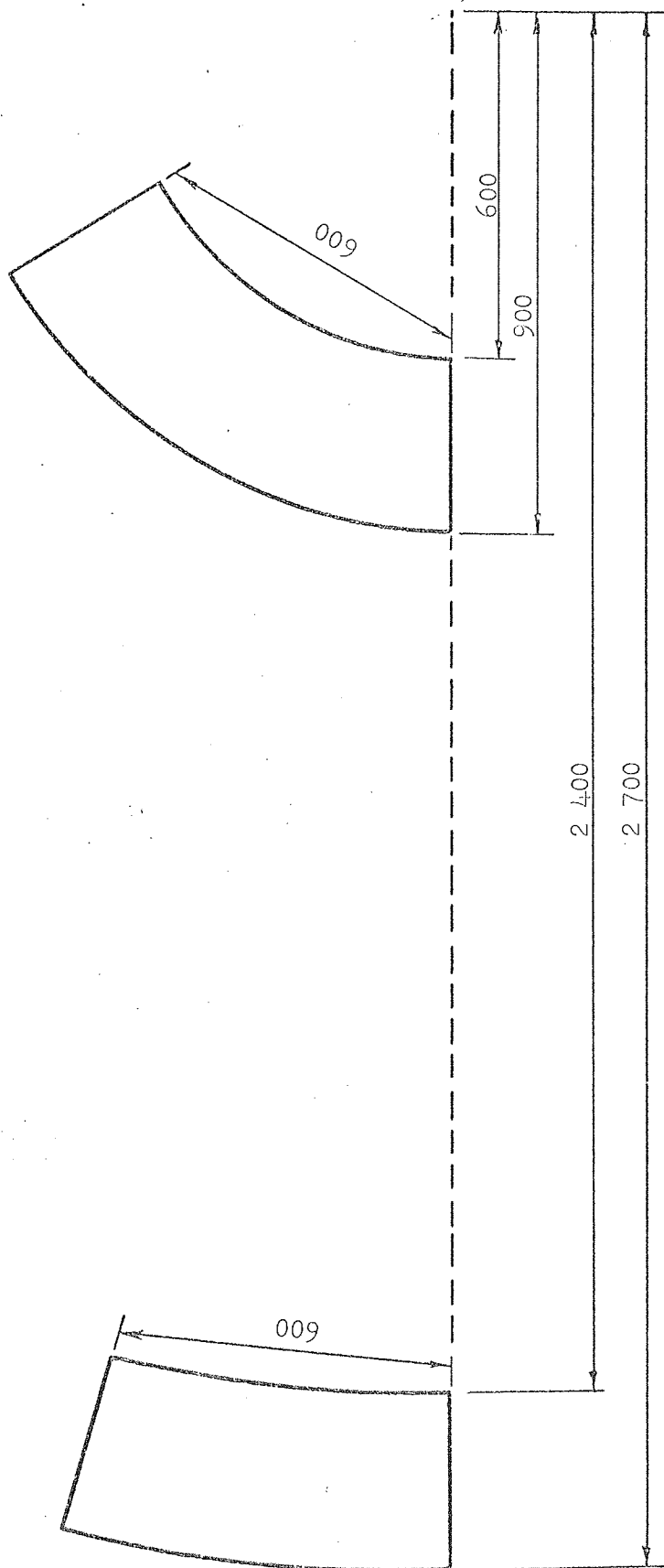
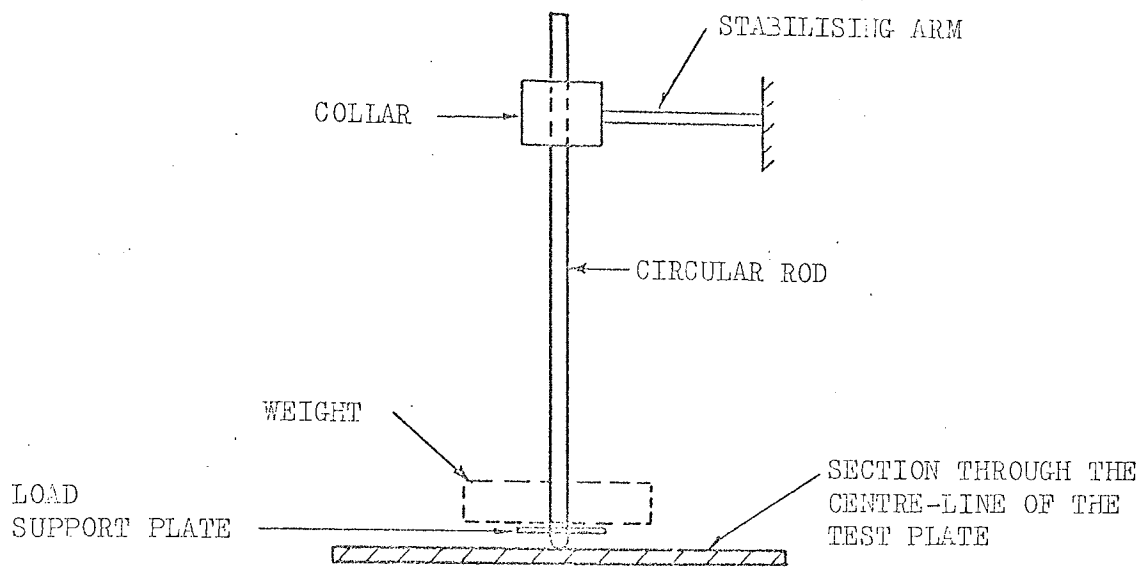


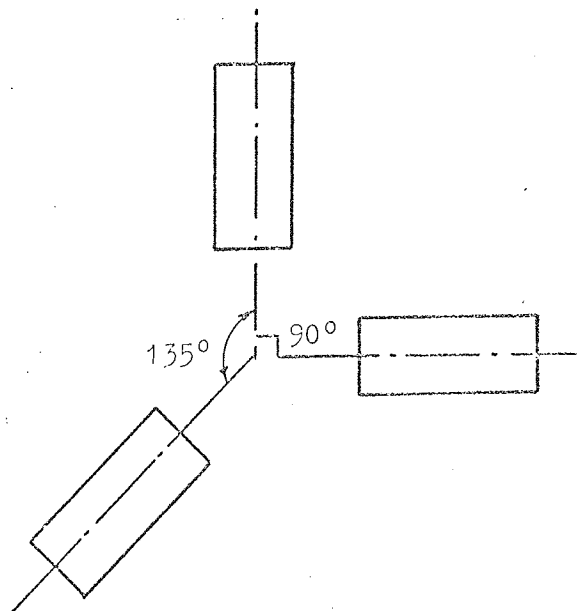
PLATE DIMENSIONS IN mm.  
AVERAGE THICKNESS OF THE PLATES WAS 3.25mm.

FIGURE 8.5



METHOD OF APPLYING A POINT LOAD

FIGURE 8.6



RELATIVE ORIENTATION OF THE THREE GAUGES FORMING A ROSETTE

FIGURE 8.7



to the support plate is transmitted to the curved plate under test through the domed end of the rod.

Experimental deflections were required for later comparison with theoretical deflections and were measured by dial gauges with a sensitivity of 0.01 mm. per division.

Strains were measured by rosettes of three electrical resistance gauges, the relative orientation of these gauges is shown in figure 8.7. The positions of the rosettes on each of the test plates are given in figures 8.10 and 8.11. In each case one gauge of a rosette is tangential whilst another is radial to the test plate. This overall orientation was chosen so that it was compatible with the direction of computed theoretical stresses. Two of the rosettes were placed symmetrically about the plate's centre line thus acting as a check on each other.

Two support conditions were adopted, pinned and fixed. The pinned condition was simulated by supporting the plate on four ball bearings, two on each side as shown in figure 8.8. These ball bearings were countersunk into square steel rods which were rigidly fixed to the testing rig. The fixed supports shown in figure 8.9 were implemented by rigidly bolting two square steel rods together and sandwiching the plate between them. Once again the rods were rigidly fixed to the testing rig.

#### (8.5) Testing the plates

The positions of the support and load points the deflection gauges and the strain rosettes should be related to the theoretical mesh adopted for the analysis. It has been shown in Chapter 7 figure 7.12 that the use of a seventy two element mesh, for this type of structure, will yield results which will not be significantly altered by further mesh refinement. The support condition and loading mode is symmetrical about the radial centre line of each plate therefore, analytically, it is only necessary to consider half of each plate. Figures 8.10 and 8.11 show the meshes, the node numbering and the rosette positions adopted for each plate. A

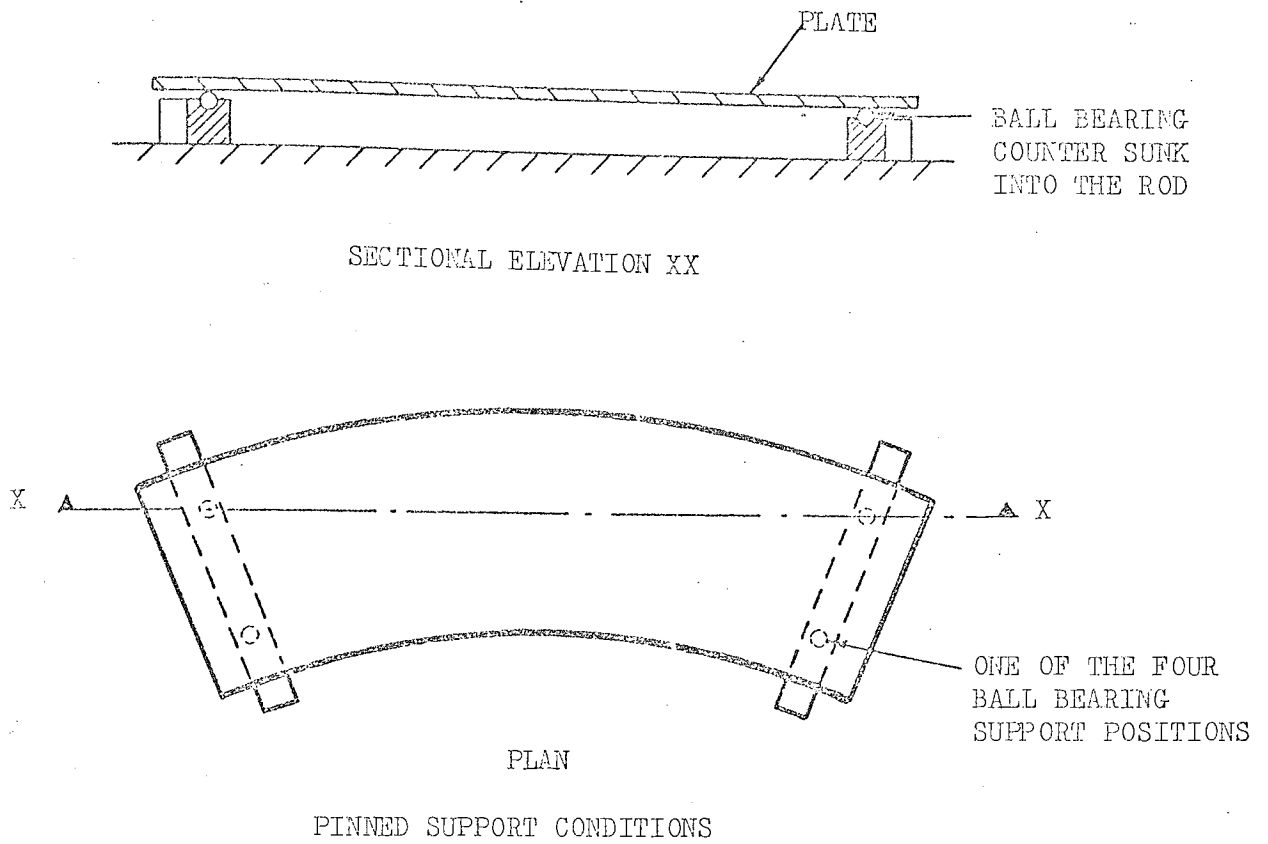


FIGURE 8.8

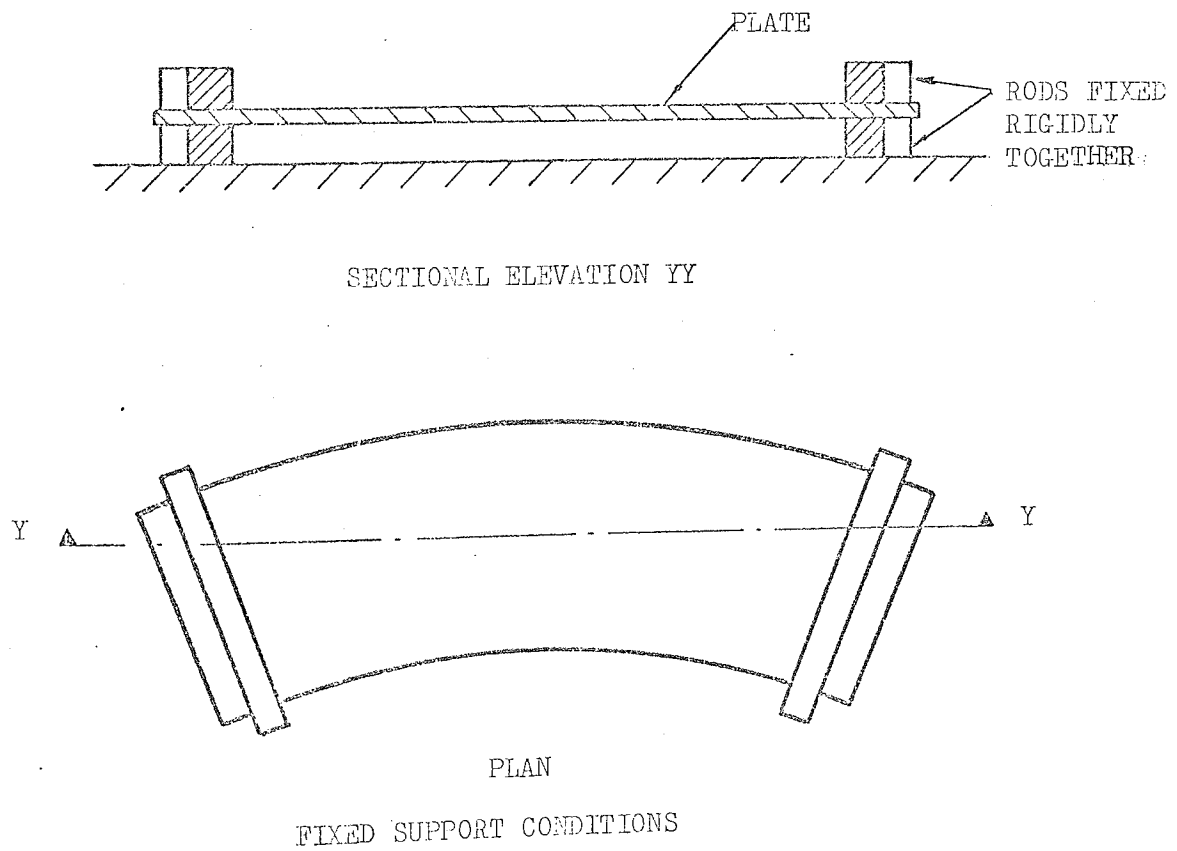
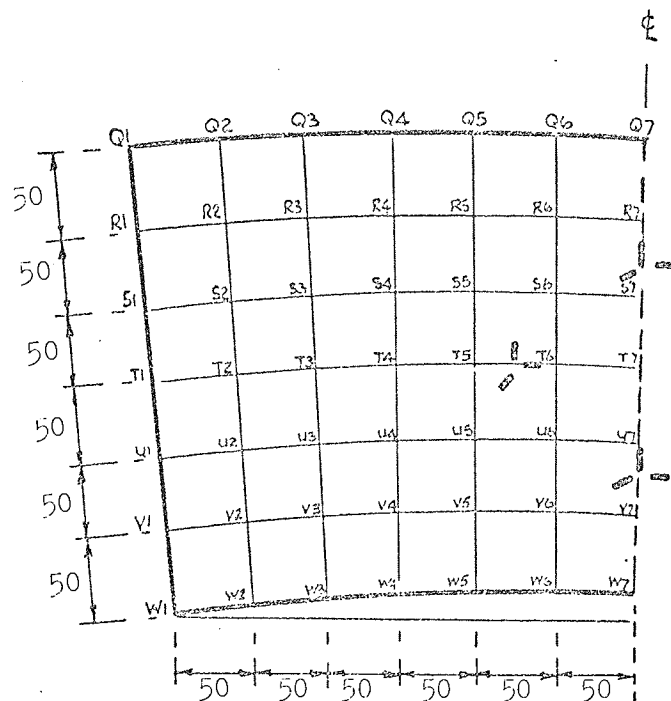
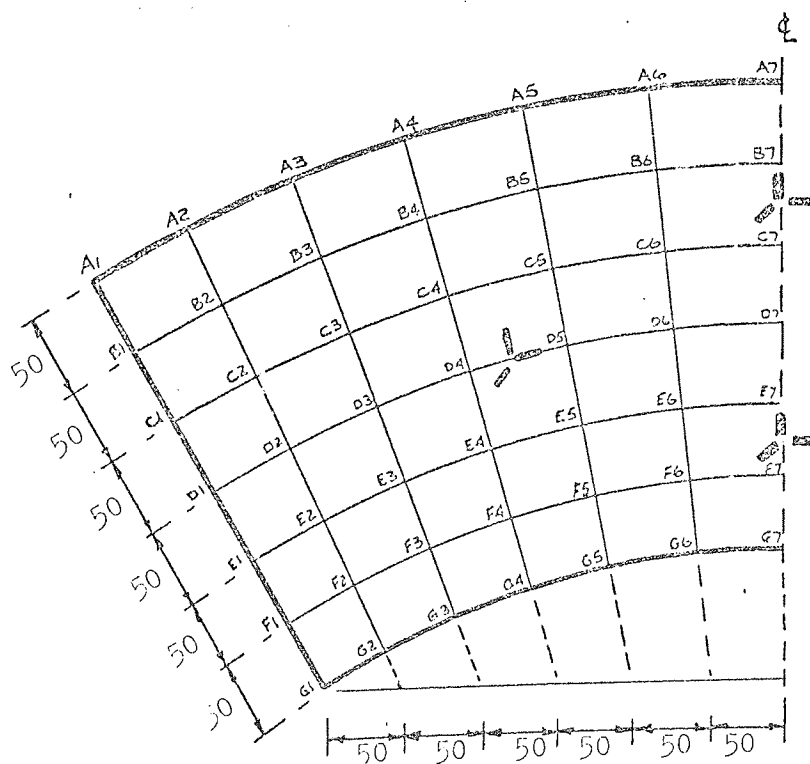


FIGURE 8.9



THEORETICAL MESH AND STRAIN GAUGE ROSETTE POSITIONS FOR HALF OF THE  
LARGE RADIUS PLATE

FIGURE 8.10



THEORETICAL MESH AND STRAIN GAUGE ROSETTE POSITIONS FOR HALF OF THE  
SMALL RADIUS PLATE

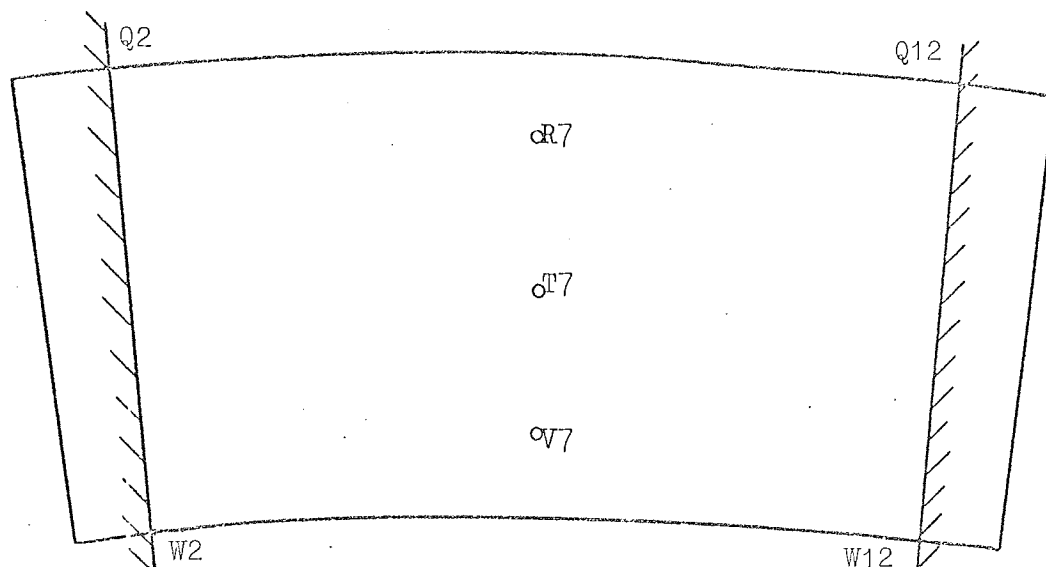
FIGURE 8.11

total of four tests were conducted. Tests one and two were on the large radius plate. The support and load positions for test one are shown in figure 8.12 and for test two in figure 8.13. The support conditions and load position for tests three and four, on the smaller radius plate, are shown in figures 8.14 and 8.15.

It was decided that the maximum permitted deflection should be approximately equal to the thickness of the plate under test. This is desirable because thin plate theory has been the basis of the assumptions made in the theoretical derivation of the curved plate stiffness matrix.

The theoretical mesh was marked on each plate and the plate was positioned on the test rig. Care was taken to ensure that the supports were accurately positioned and in the case of rigid supports that a true fixed condition existed. Initial readings on the deflection and strain gauges were recorded. The loading rod was then positioned on the required node and held in a vertical position by the collar which in turn was located on one end of the stabilising rod (see figure 8.6). To facilitate free movement of the rod through the collar both were oiled and throughout the loading and unloading cycle a constant check was made to ensure that no load was being carried by the collar. With the loading rod positioned the deflection and strain gauge readings were again recorded. It was envisaged that between six and ten equal load increments would be satisfactory. The value of the increment being obtained from a calculation concerning the maximum permissible deflection discussed earlier. After each load had been applied and a check made on the loading collar the system was allowed a short time to react to the load, after which the deflection and strain gauge readings were recorded. This process was repeated during all increments of both the loading and unloading cycle.

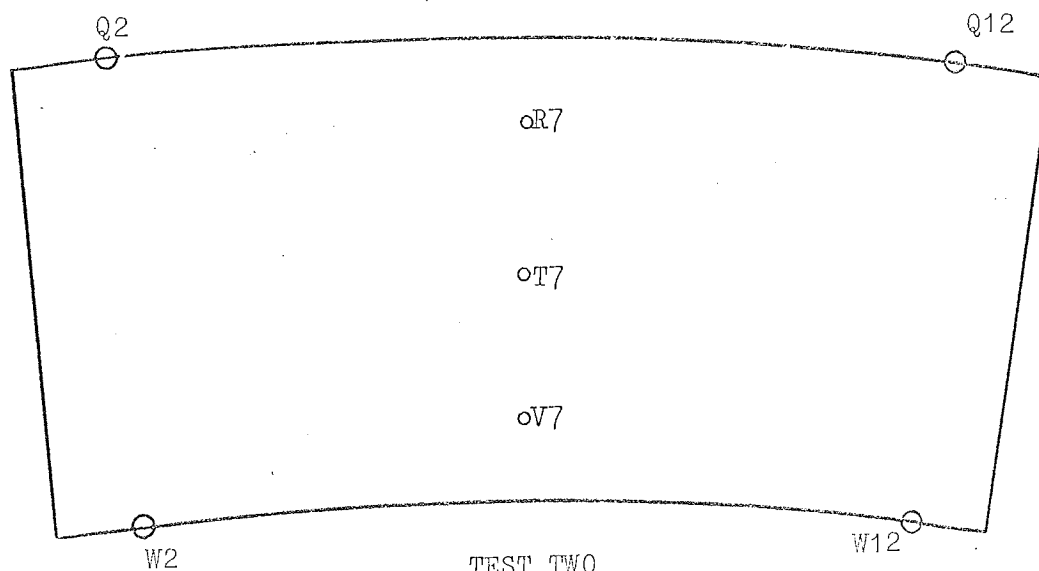
All four tests were conducted in an identical manner.



TEST ONE

○ DIAL GAUGE POSITIONS  
 POINT LOAD APPLIED AT T7  
 CONTINUOUSLY RIGIDLY SUPPORTED ALONG LINES Q2/W2 AND Q12/W12

FIGURE 8.12

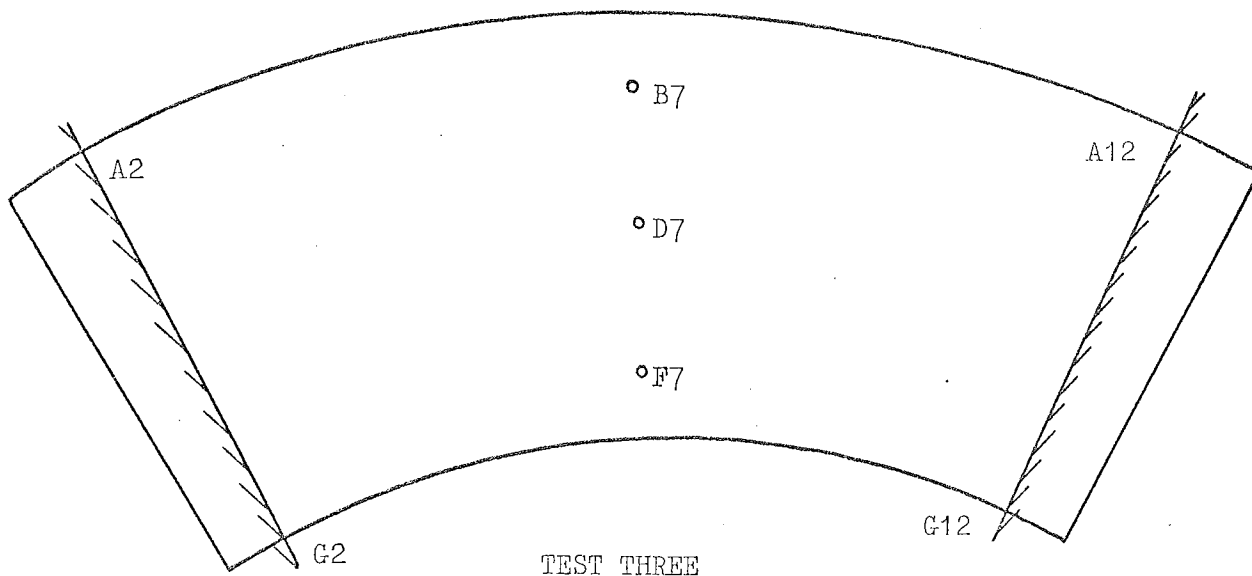


TEST TWO

○ DIAL GAUGE POSITIONS  
 PINNED SUPPORTS AT NODES Q2, W2, Q12, W12  
 POINT LOAD APPLIED AT T7

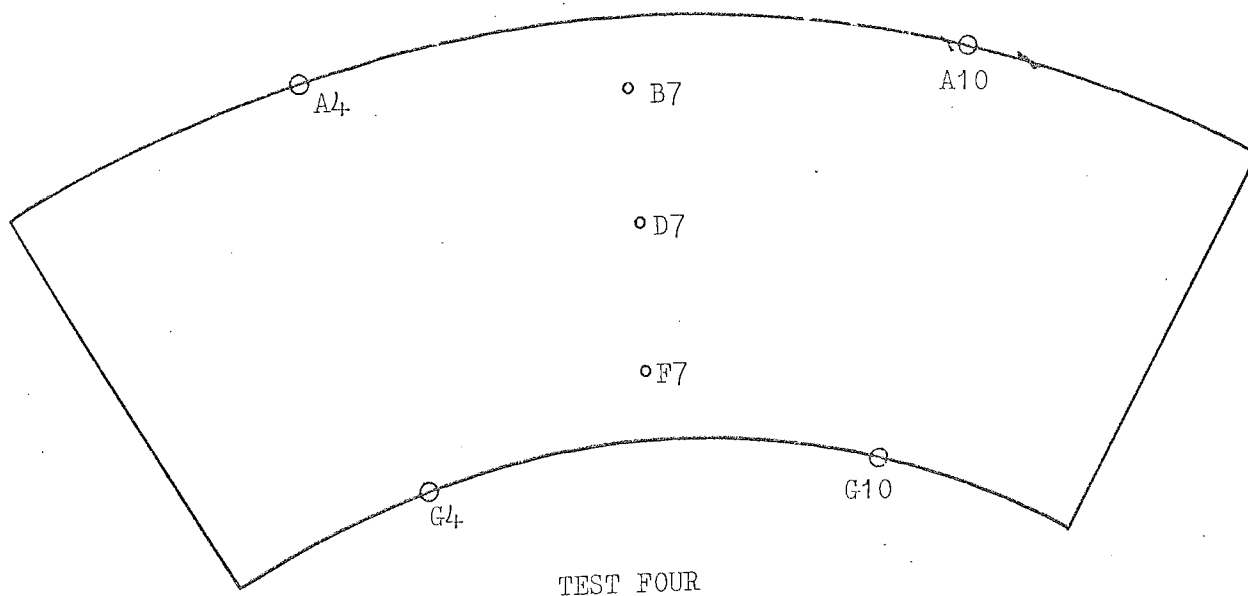
FIGURE 8.13





° DIAL GAUGE POSITIONS  
 POINT LOAD APPLIED AT D7  
 CONTINUOUSLY RIGIDLY SUPPORTED ALONG LINES A2/G2 AND A12/G12

FIGURE 8.14



° DIAL GAUGE POSITIONS  
 POINT LOAD APPLIED AT D7  
 PINNED SUPPORTS AT NODES A4, G4, A10, G10

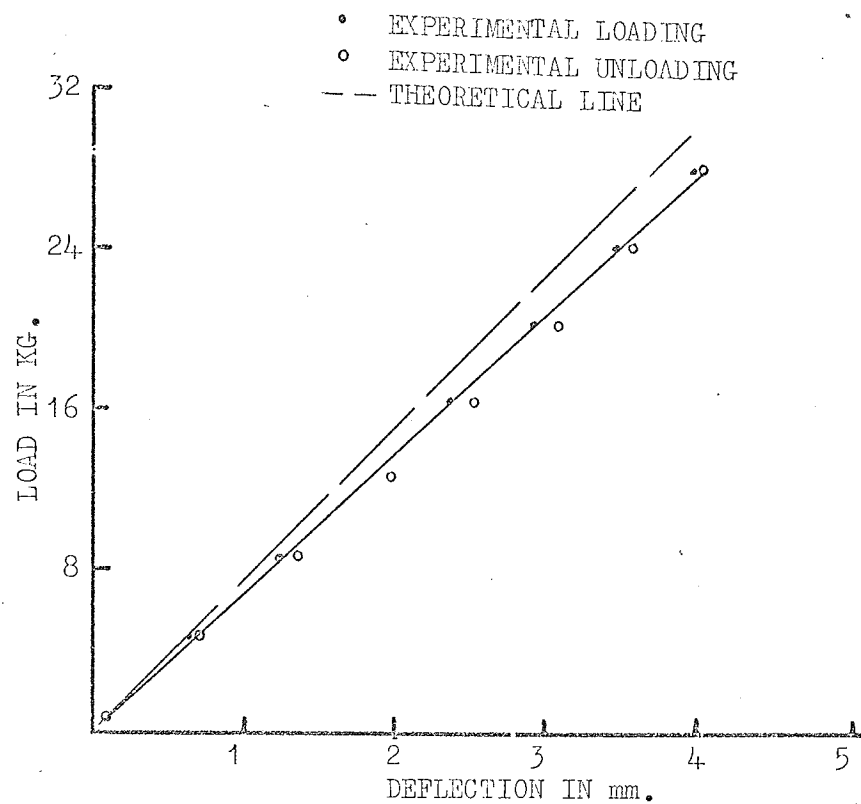
FIGURE 8.15

### (8.6) Comparison between experimental and theoretical results

The meshes shown in figures 8.10 and 8.11 were those used for the analysis of the tests. The plates were loaded in an out of plane manner so for the purposes of the analysis the in plane movements were suppressed.

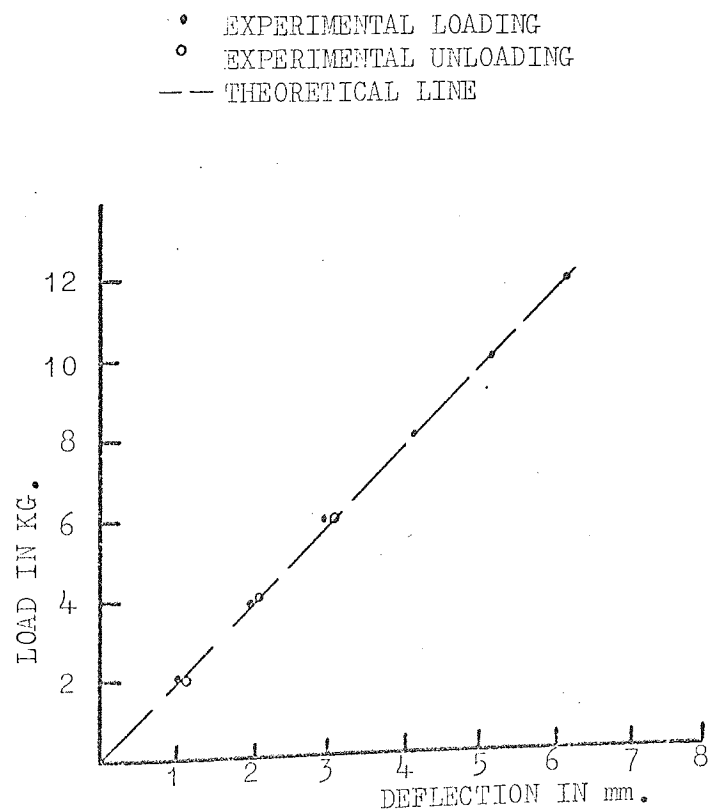
A comparison between independent experimental deflections and theoretical deflections predicted by the author has already been made in Chapter 7. There it was shown (see figures 7.13 to 7.17) that in both the case of the perspex and the asbestos cement plate the poorest agreement was experienced when the load was positioned at the middle of the radial centre line. In order that this discrepancy might be further investigated the load was applied to the author's test plates at the middle of their radial centre lines. One of the deflection gauges was positioned directly beneath the load on the underside of the plate and it is the deflection at this point which will be investigated for all four tests.

Graphs of the deflections under the load for tests one, two, three and four are given in figures 8.16, 8.17, 8.18 and 8.19. In these graphs the measured deflections during the loading and unloading cycles as well as the theoretical deflections have been plotted. Tests two and four produce the best agreement between the experimental and the theoretical deflections, both of these tests have pinned supports. In test two both of the values are identical (see figure 8.17), figure 8.19 shows that in the case of test four the theoretical deflections are ninety eight percent of the experimental. The tests involving fixed supports namely one and three exhibit a greater discrepancy between experimental and theoretical deflections. In the case of test one the theoretical value is ninety one per cent of the experimental whereas in test two this percentage increases to ninety six. One contributing factor to the lack of agreement between these latter results is the fact that the fixed support, although continuous along each side of the plate, could only be theoretically simulated by a fixity at each node along the

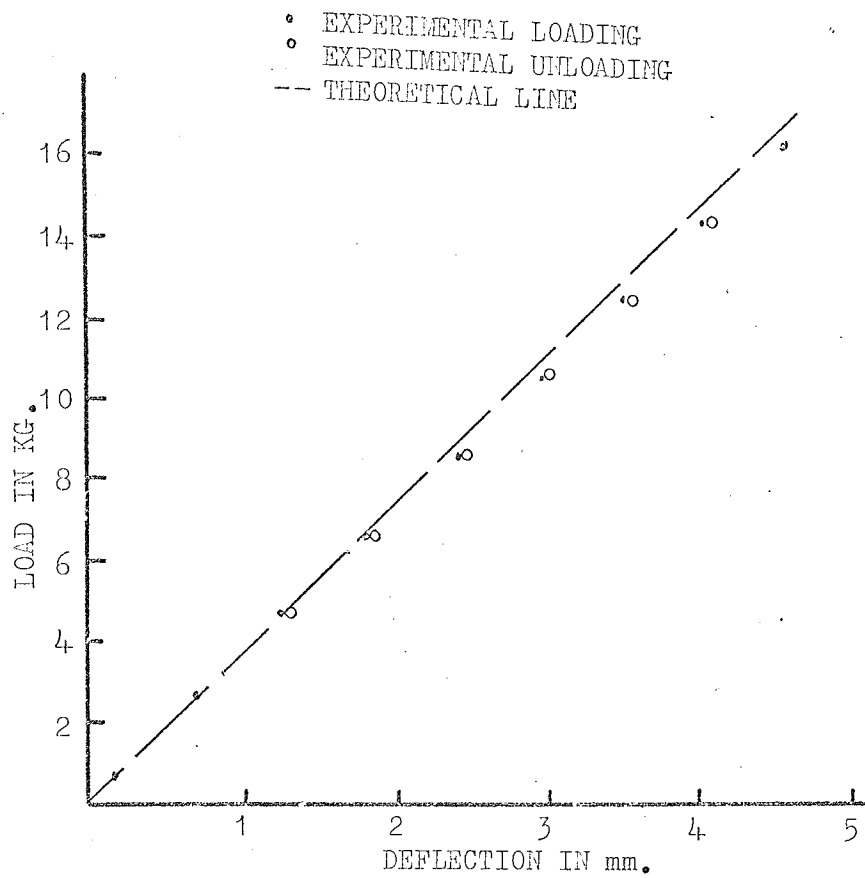


TEST ONE  
DEFLECTION UNDER THE LOAD AT NODE T7

FIGURE 8.16

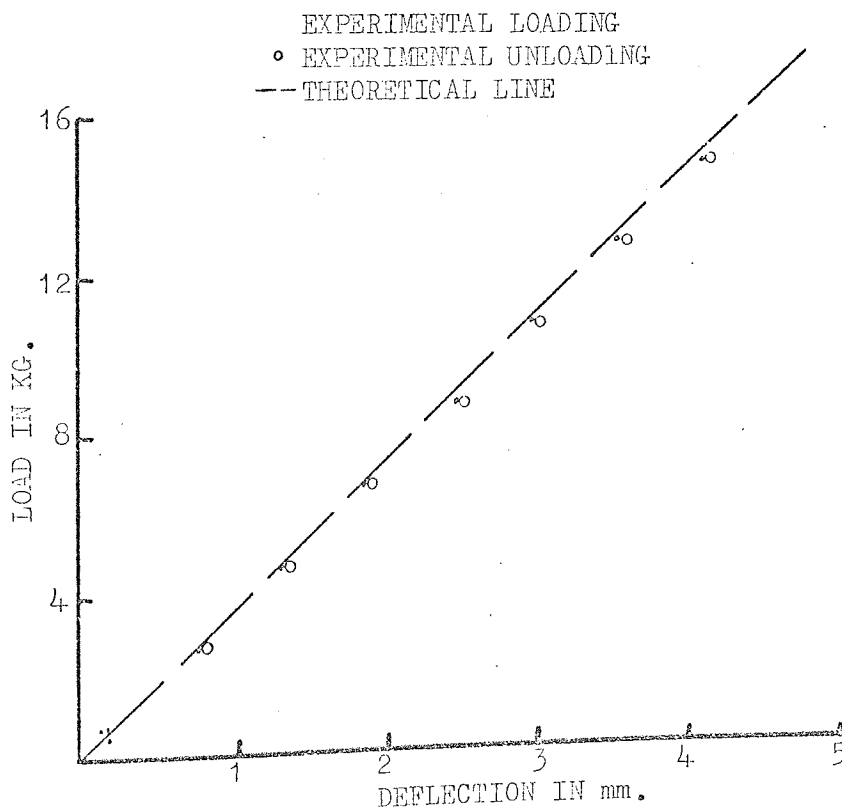


TEST TWO  
DEFLECTION UNDER THE LOAD AT NODE T7  
FIGURE 8.17



TEST THREE  
DEFLECTION UNDER THE LOAD AT NODE D7

FIGURE 8.18



TEST FOUR  
DEFLECTION UNDER THE LOAD AT NODE D7

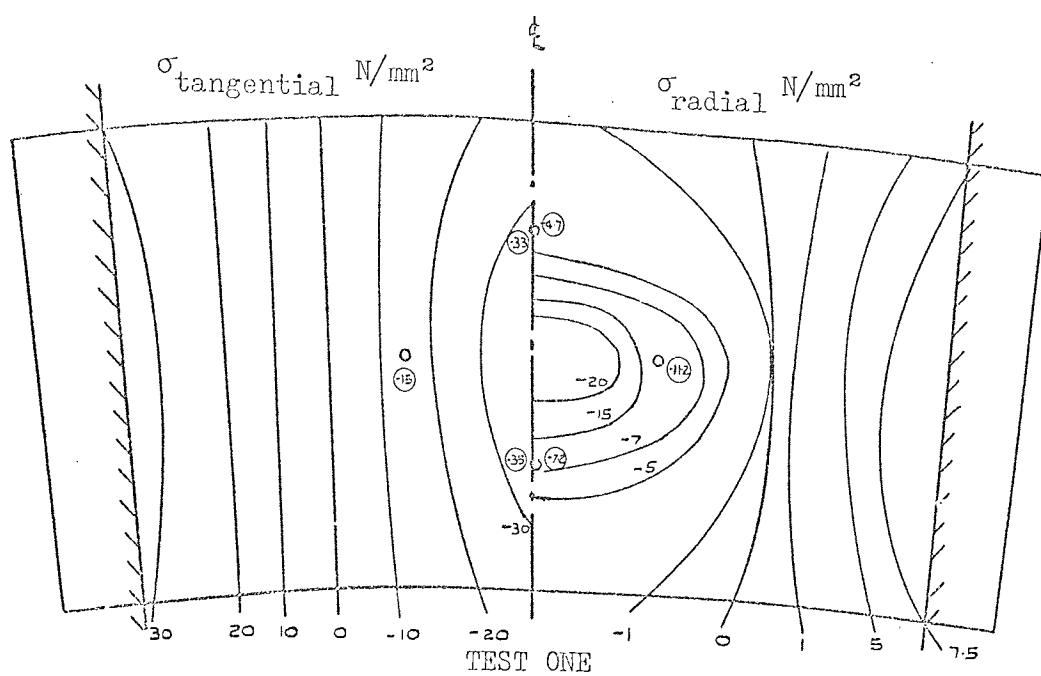
FIGURE 8.19

line of support. In the case of the pinned supports these only existed at nodes and consequently could be accurately simulated. Furthermore, in practice a truly fixed support is harder to create than a pinned support.

The comparisons made in Chapter 7 were solely between deflections, one reason for this experimental work was to investigate the accuracy of the computed stresses within a curved plate element. The theoretical analysis yields three stresses at the geometric centre of each mesh element, one of these stresses is radial and another is tangential to the plate. One way of representing the state of the theoretical radial and tangential stresses in the plate under a given load is to interpolate between the theoretical values obtained for each mesh element and form a graph of stress contours. The symmetry of the plate, supports and load, means that such contours will be identical on each side of the radial centre line. Consequently the contours have been plotted for the radial stresses on one half of the plate and the tangential stresses on the other. These contour graphs for tests one, two, three and four are shown in figures 8.20, 8.21, 8.22 and 8.23. Superimposed in the stress fields are the values of the stresses which have been calculated from the experimental strains. Such experimental strains have been obtained by calculating the best straight line through the strain readings recorded during the test, then using this line, in association with the loading for which the theoretical stresses have been calculated to give the experimental value.

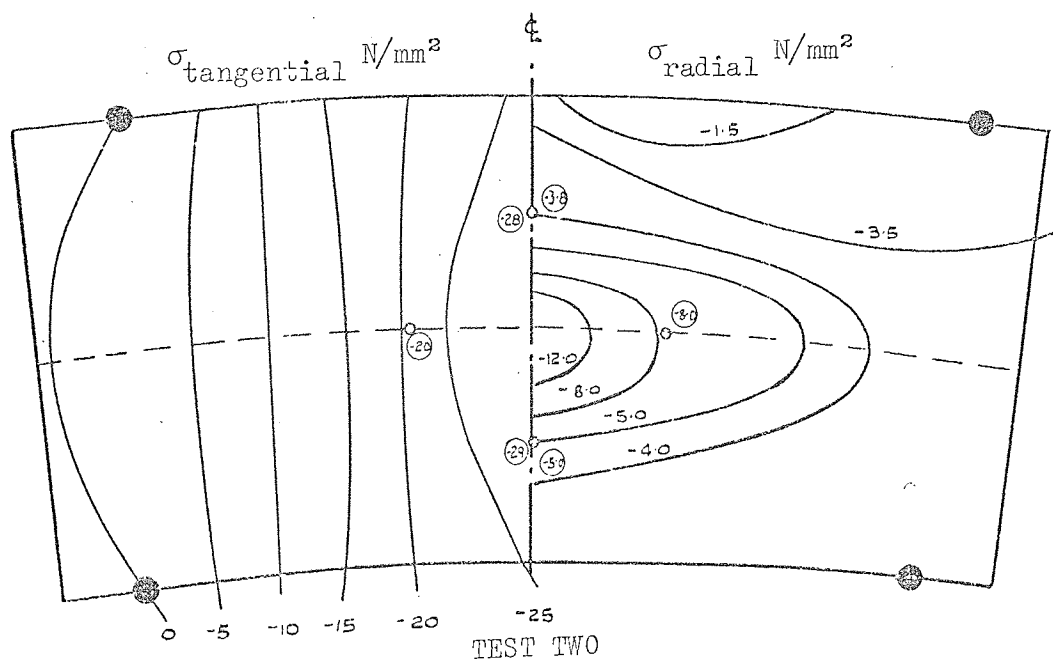
The graphs show in a qualitative way that the experimental stresses and the theoretical contours appear to be in good agreement. These figures do not, however, easily permit a <sup>quantitative</sup> ~~quantitative~~ assessment of the accuracy achieved. Such an assessment may be obtained from the graphs shown in figures 8.24 and 8.25, here tests three and two, representative of each of the two plates and support conditions have been selected for further examination. In each case the stresses on the circumferential centre line have been considered. Figure 8.24 concerning test three shows the tan-





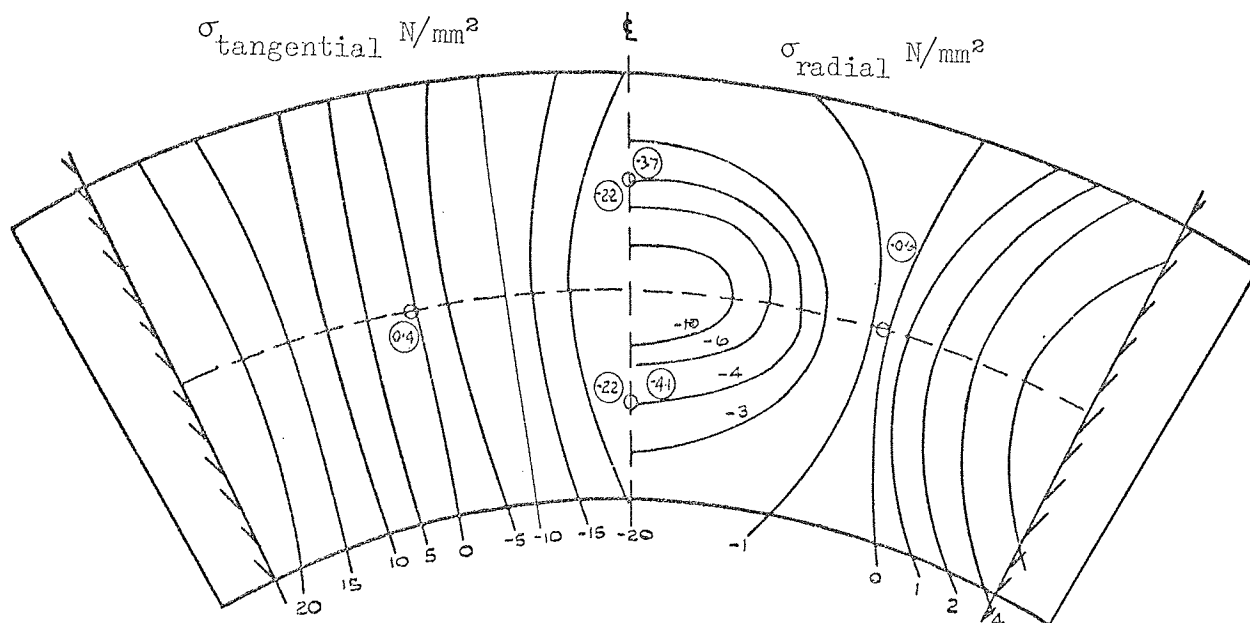
STRESS CONTOURS FOR AN APPLIED POINT LOAD OF 30Kg.  
 ○ ROSETTE POSITIONS WITH THE EXPERIMENTAL VALUES CIRCLED

FIGURE 8.20



STRESS CONTOURS FOR AN APPLIED POINT LOAD OF 12Kg.  
 ○ ROSETTE POSITIONS WITH THE EXPERIMENTAL VALUES CIRCLED

FIGURE 8.21

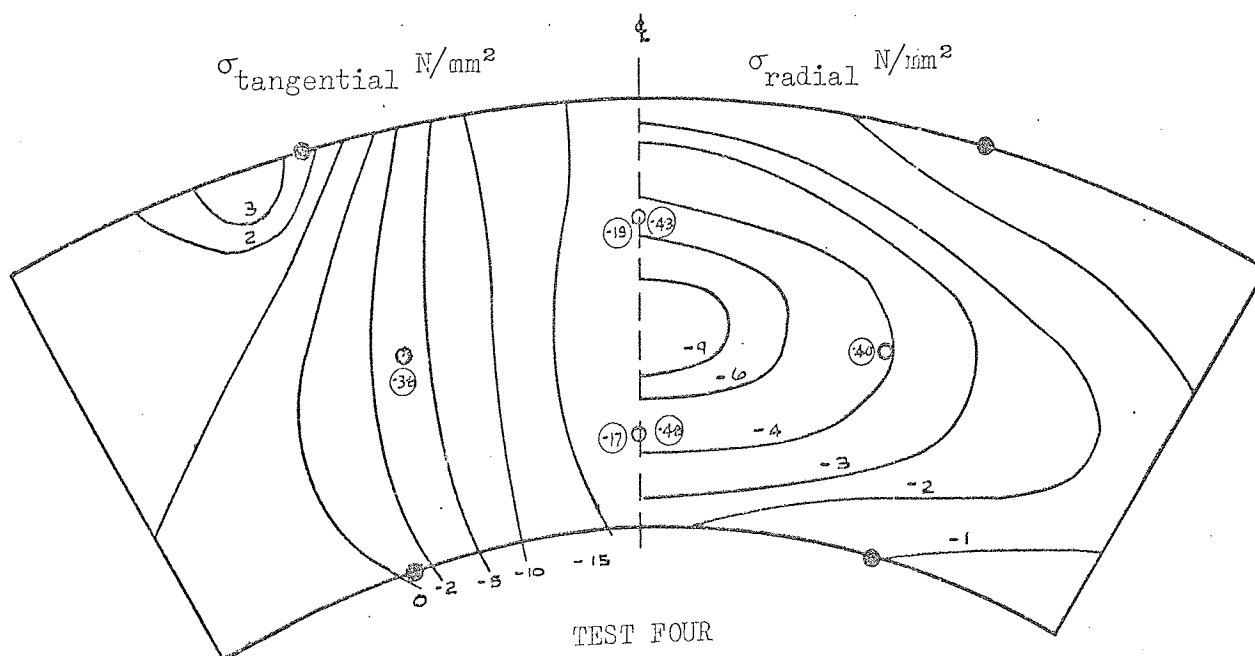


TEST THREE

STRESS CONTOURS FOR AN APPLIED POINT LOAD OF 30Kg.

○ ROSETTE POSITIONS WITH THE EXPERIMENTAL VALUES CIRCLED

FIGURE 8.22



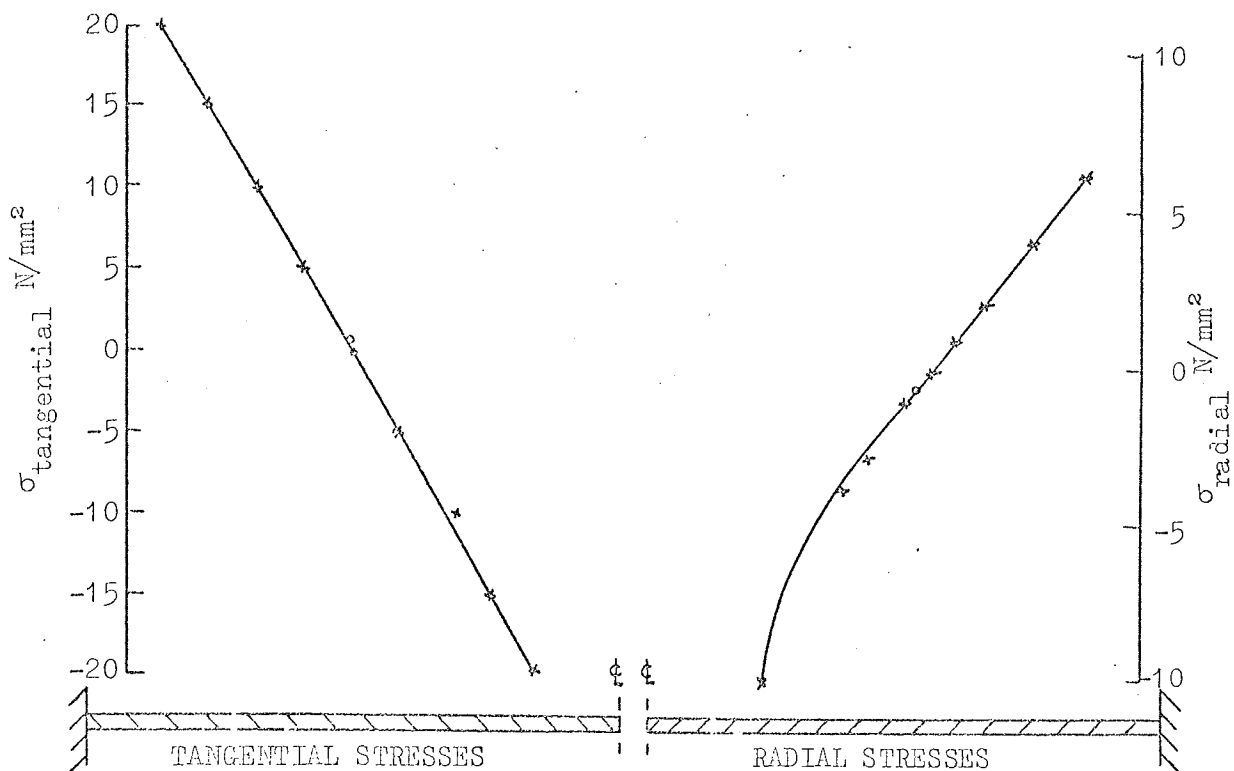
TEST FOUR

STRESS CONTOURS FOR AN APPLIED POINT LOAD OF 10.2Kg.

○ ROSETTE POSITIONS WITH THE EXPERIMENTAL VALUES CIRCLED

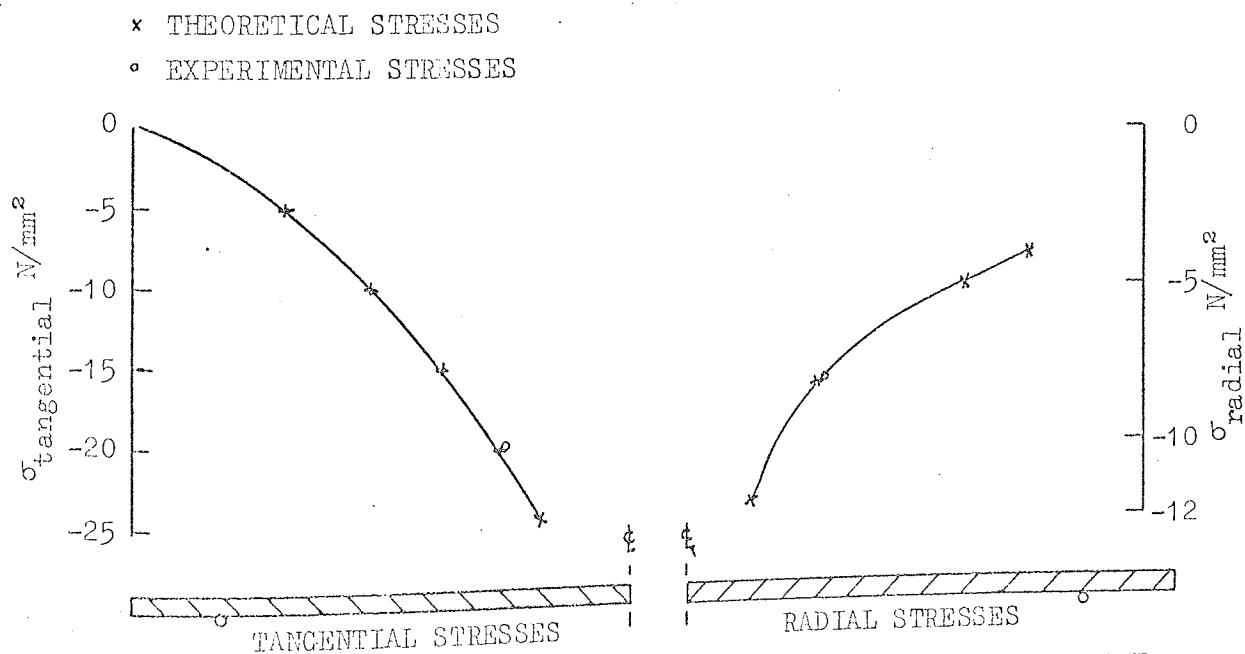
FIGURE 8.23

x THEORETICAL STRESSES  
o EXPERIMENTAL STRESSES



TOP FIBRE STRESSES ALONG THE CIRCUMFERENTIAL CENTRE-LINE OF THE PLATE  
IN TEST THREE

FIGURE 8.24



TOP FIBRE STRESSES ALONG THE CIRCUMFERENTIAL CENTRE-LINE OF THE PLATE  
IN TEST TWO

FIGURE 8.25

gential and radial stresses along this line and figure 8.25 illustrates the same for test two. In each case the stress calculated from the experimental strain is also plotted. It can be seen that the experimental stress shows good agreement with the theoretical stresses.

The stress at a section is a function of the bending moment at that section because the plate is of constant thickness, therefore, the shape of the theoretical stress lines should follow the bending moment distribution across the circumferential centre line of the plate. The graphs therefore follow predictable trends. The close proximity of the experimental points to these theoretical lines precludes a numerical assessment of the accuracy, suffice is to say that in the region of each strain rosette the measured and calculated stresses show good agreement. It would have been advantageous to have several more strain rosettes along the circumferential centre line so that a plot of the experimental stresses along this line could have been made.

In conclusion it is perhaps fair to comment that considering the relatively unsophisticated nature of the tests reasonable agreement is obtained between theoretical and experimental results.

The in plane stiffness matrix requires numerical investigations in order to establish its characteristics.

---

## CHAPTER 9

### THE ANALYSIS OF LARGE STRUCTURES

#### (9.1) Introduction

The shell of an electrical precipitator and a skew concrete road bridge were selected for analysis so that an assessment of the capability and efficiency of the program could be carried out. A previous attempt had been made to analyse these structures by Craig<sup>(5)</sup>, the results obtained were not, however, satisfactory. It was thought that the complexity of the structures had been a contributing factor to this lack of success. The use of these examples also facilitated a comparison of computer time and store requirements and so permitted a quantitative evaluation of the extent of any savings.

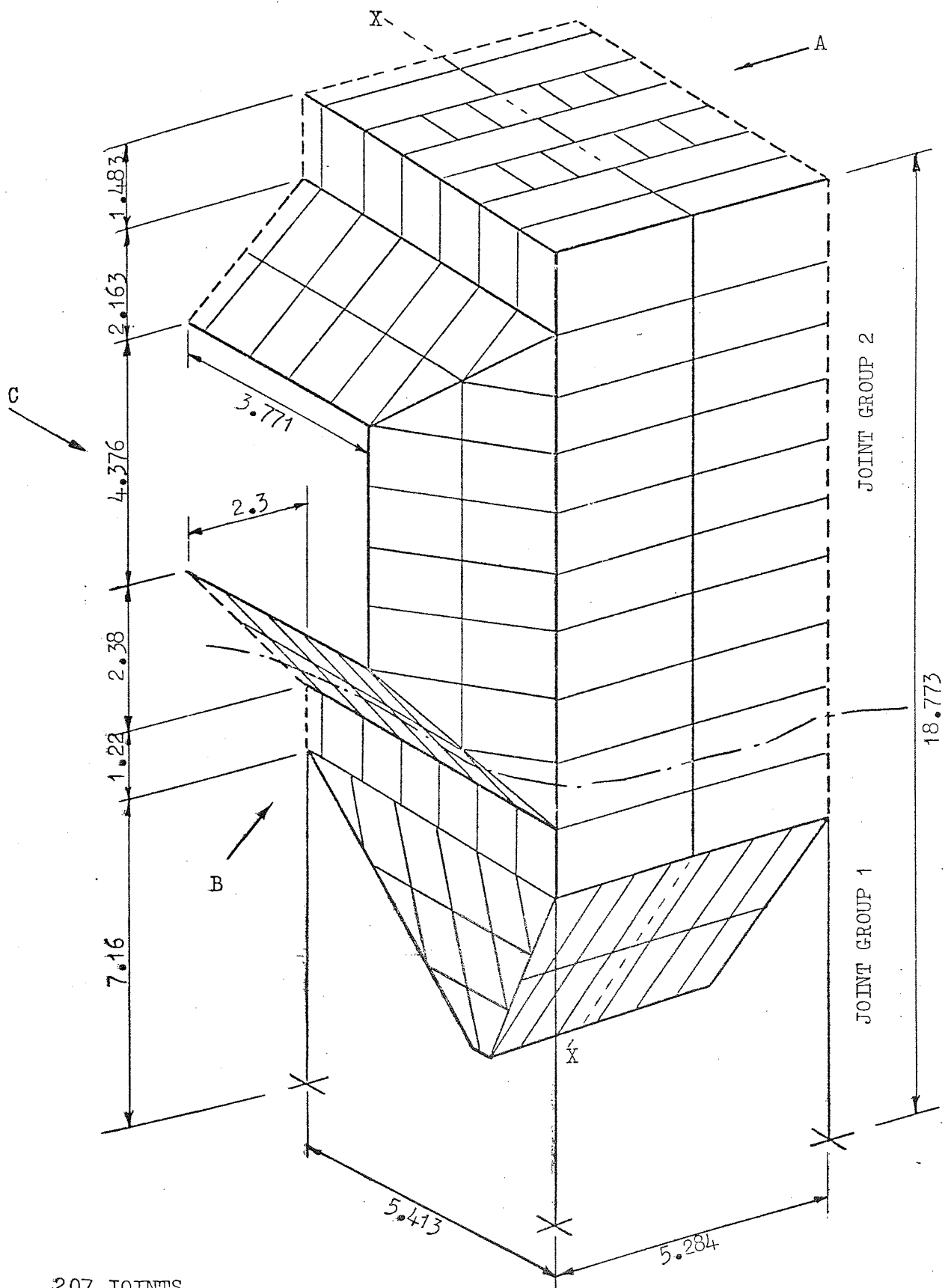
#### (9.2) The electrical precipitator shell

Electrical precipitation is an efficient and versatile method of dust collection which is now commonly used to reduce the emission of quantities of fine fumes generated by various industrial processes. The precipitator's shell or casing is usually constructed in steel or concrete. Although it has the external appearance (see figure 9.1) of a normal building structure it is essentially a low pressure chemical vessel. It is for this reason that design restrictions not applicable to normal structures have to be considered so that the shell can function efficiently. Most important of these are: the negative internal pressure and the internal electrical clearances between the shell and the high voltage discharge system.

#### (9.3) Analysis of the shell

An accurate analysis is desirable so that the structure can be produced as economically as possible. The finite element method is particularly suited to do this because conventional methods cannot accurately estimate





207 JOINTS

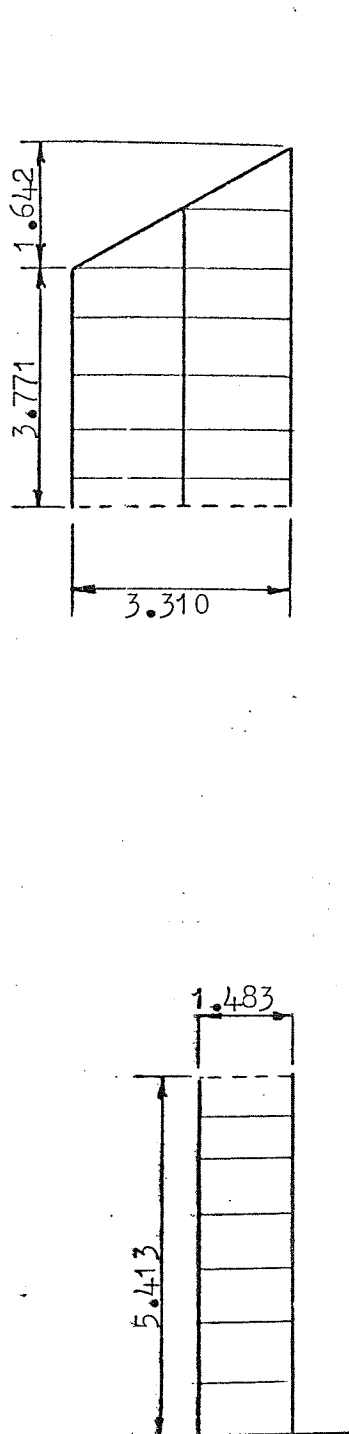
127 RECTANGULAR PLATES

318 PRISMATIC MEMBERS

1029 UNSUPPRESSED DEGREES OF FREEDOM

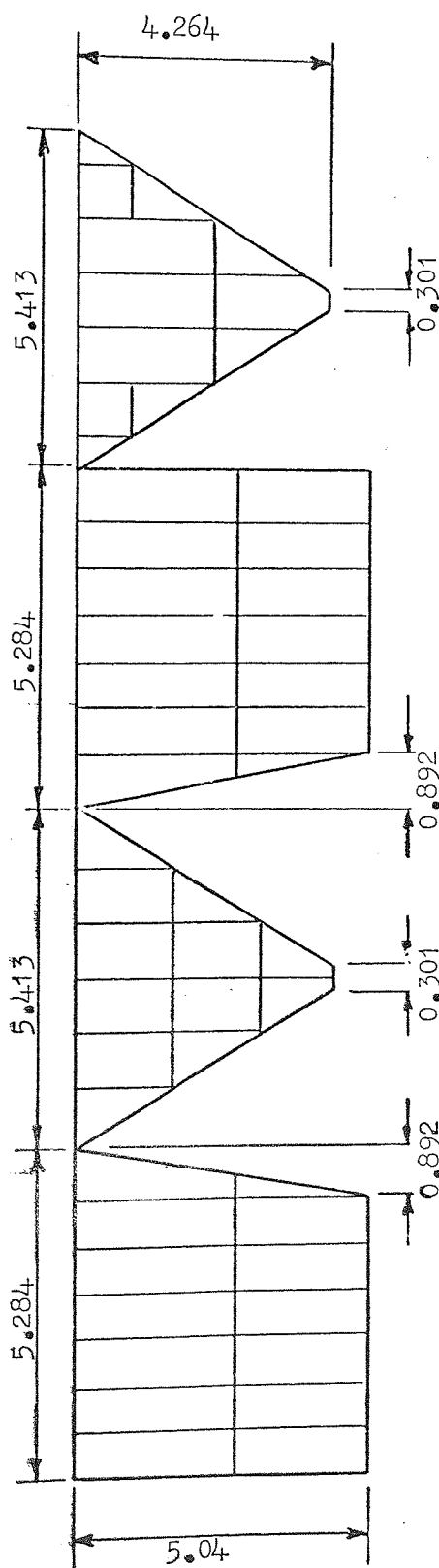
QUARTER SECTION OF THE ELECTRICAL PRECIPITATOR SHELL

FIGURE 9.1



ROOF BEAM ARROW A

UNDERSIDE OF OUTLET ARROW B



HOPPER

DIMENSIONS IN METRES

DETAILS OF THE ELECTRICAL PRECIPITATOR SHELL

FIGURE 9.2

the stiffening effects of the steel sheeting.

The axes of symmetry of the shell as well as the symmetry of the loading permitted the analysis of only one quarter of the structure. The finite element idealisation of this quarter section into prismatic members and rectangular plates is shown in figures 9.1 and 9.2. Subdivision in the manner indicated resulted in 1029 unsuppressed degrees of freedom, thus necessitating the solution of that number of equations. The mesh adopted is almost identical to that used by Craig<sup>(5)</sup>; this is to facilitate the comparisons mentioned earlier. The subdivision of the hopper needed to be fairly fine whereas the wall only required a coarse mesh. A consequence of this is that the larger plates on the wall spanned across several joints on the hopper, this can be seen in figure 9.1.

To prevent overflow of store Craig was restricted to about eighteen joints per group. This made the formation of groups in the region of the hopper difficult. One of the failings of this earlier analysis was overall lack of vertical balance. Craig states that it appeared as though the loads applied to the hopper were being ignored. In an attempt to overcome this he divided the four columns supporting the hopper into several members so that each joint group of the hopper contained part of a column. This did not, however, provide a satisfactory solution. The restriction on the maximum number of joints in a group was not so severe in the case of the author's program. As a result of the problems Craig experienced, it was decided to put all the hopper joints into one group. This group contained 94 joints. The remaining 103 joints formed another group and these two groups replaced the fourteen required by Craig.

The number of locations required to store the overall stiffness matrix of the biggest joint group has a direct bearing on the amount of core store required. The hopper joint group required 43K locations and the other joint group 26K locations. Here it can be seen that although the hopper joint group had less joints it required substantially more core

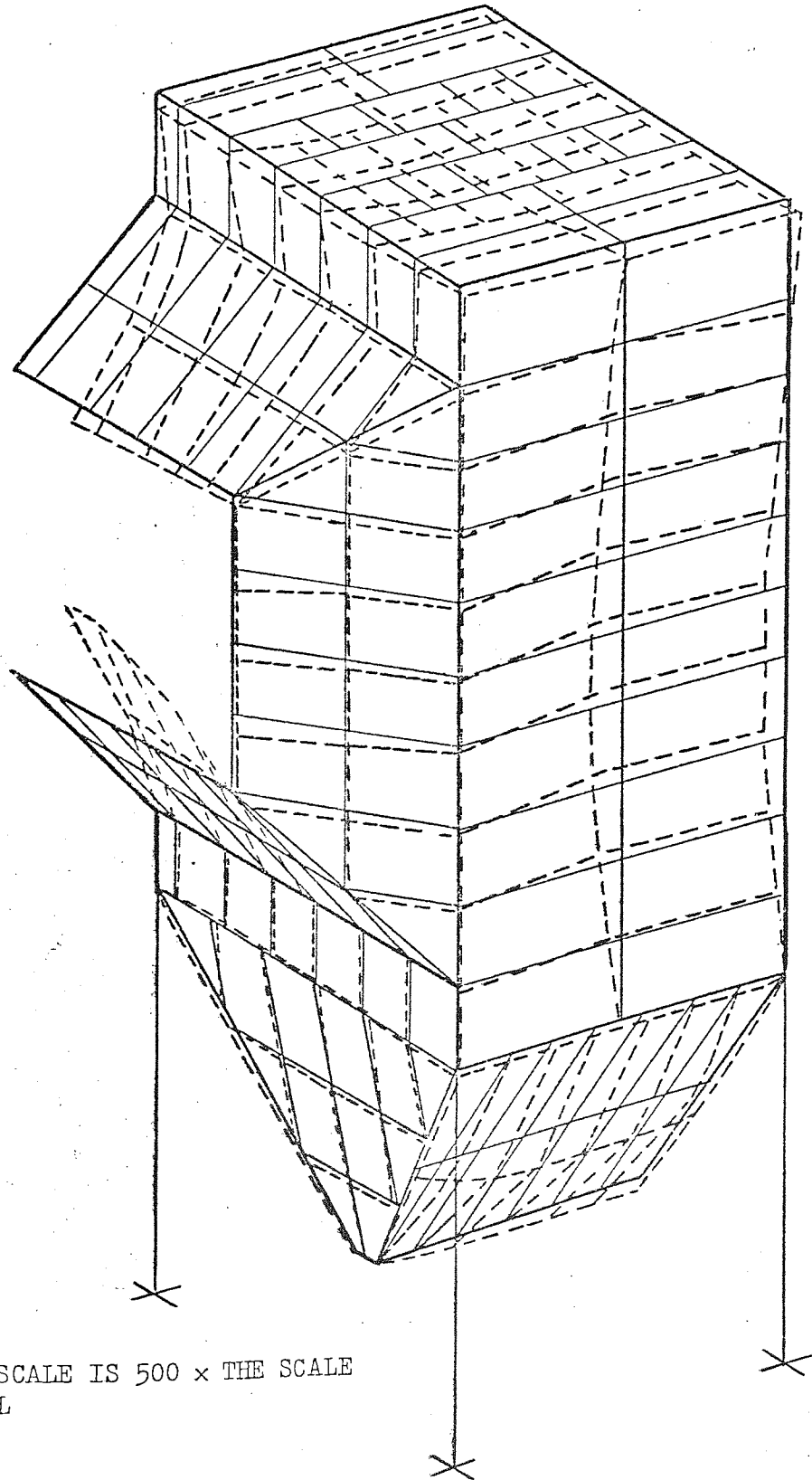
store than the other group. This is so because the interconnectivity of joints is the important factor. The storage requirements could have been significantly reduced had the structure been split into more joint groups. Even with these large joint groups the total execution store required was 83K locations. This compares favourably with Craig's 88K locations requirement for the same problem with less joints per group and less operations performed. (Previously plate stresses had to be computed during a separate run). The amount of central processing unit (cpu) time required by Craig was just under thirty minutes whereas the present analysis required 5.5 minutes. This represents a saving in the order of 80%.

#### (9.4) Results of the shell analysis

Craig states that there were two principal discrepancies in the results he obtained. Firstly the axial forces in the columns did not balance the applied vertical loading and secondly the plate stresses were discontinuous, erratic and often exceeded the permissible. Neither of these discrepancies occurred in the current analysis.

The deflected form of the shell, when subjected to the dead and superimposed loads, is substantially the same as that found by Craig and is shown in figure 9.3. Here it can be seen that the negative internal pressures are causing the main body of the casing to deform inwards. The most significant inward deflections occurring at the mouth and in the main wall. The hopper, in which the precipitated material is held, awaiting disposal, is being deflected outwards, its side wall experiencing larger deflections than its front wall.

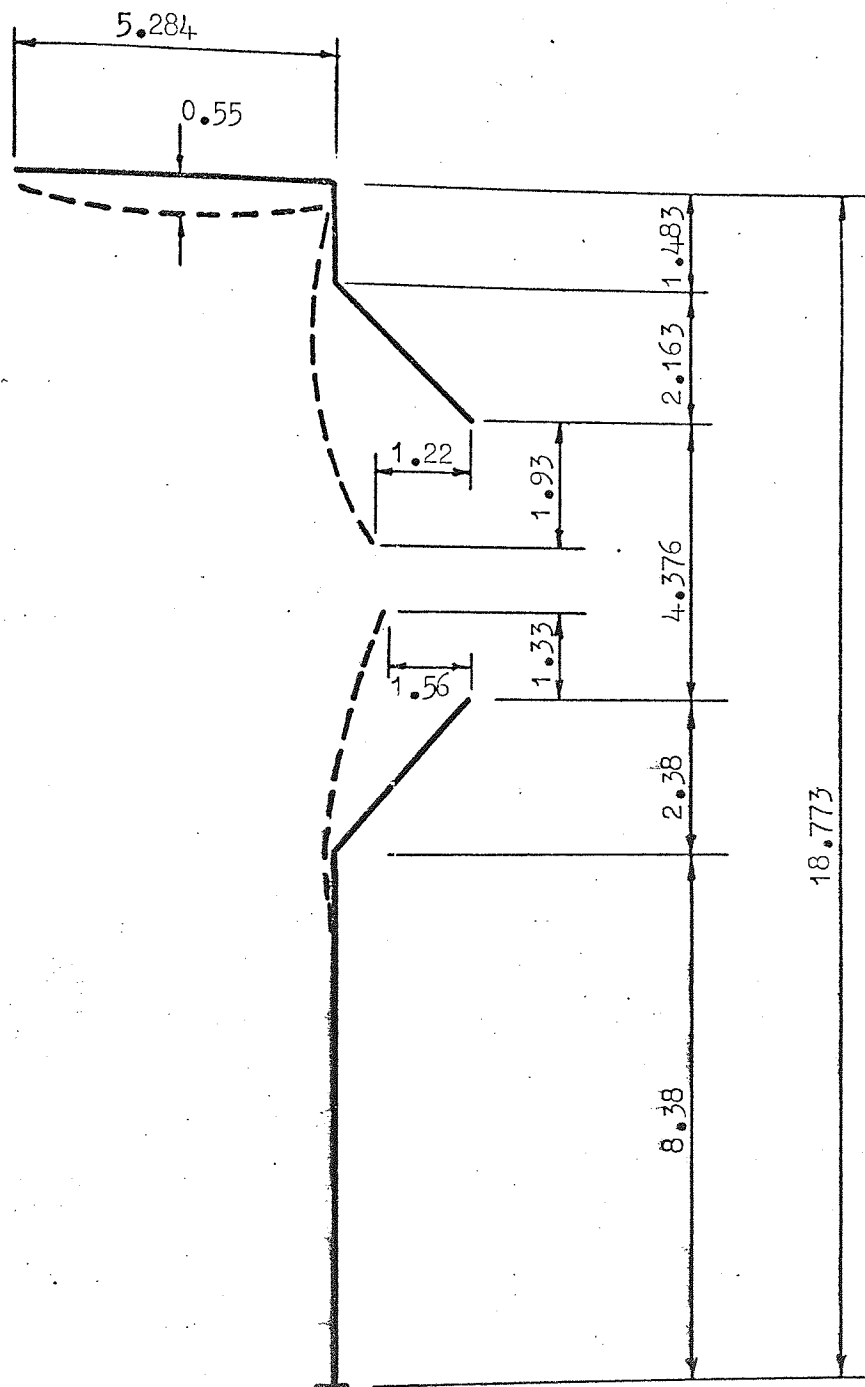
These areas of relatively large displacement will now be considered in more detail. Figure 9.4 illustrates the deformation along the centre-line of half of the shell looking in the direction of arrow C in figure 9.1. Here the deflections of the mouth and the upper edge of the shell are shown. Although these movements are significant when compared to the



DEFLECTION SCALE IS  $500 \times$  THE SCALE  
OF THE SHELL

DEFLECTED FORM OF THE ELECTRICAL PRECIPITATOR SHELL UNDER THE  
INFLUENCE OF THE DEAD AND SUPERIMPOSED LOADS

FIGURE 9.3



DEFLECTIONS IN mm.  
CASING DIMENSIONS IN m.

— ORIGINAL SHAPE  
- - - DEFLECTED FORM

VIEW SHOWING THE DEFLECTION ALONG THE CENTRE LINE OF HALF THE SHELL  
LOOKING IN THE DIRECTION OF ARROW C IN FIGURE 9.1

FIGURE 9.4



deflections of most of the rest of the shell the dimensions given in the figure show that they are in fact very small. The thicknesses of the plates in the region under consideration vary between 0.6 and 0.9 mm. Consequently these maximum deflections represent movements of up to 1.5 times the plate thicknesses.

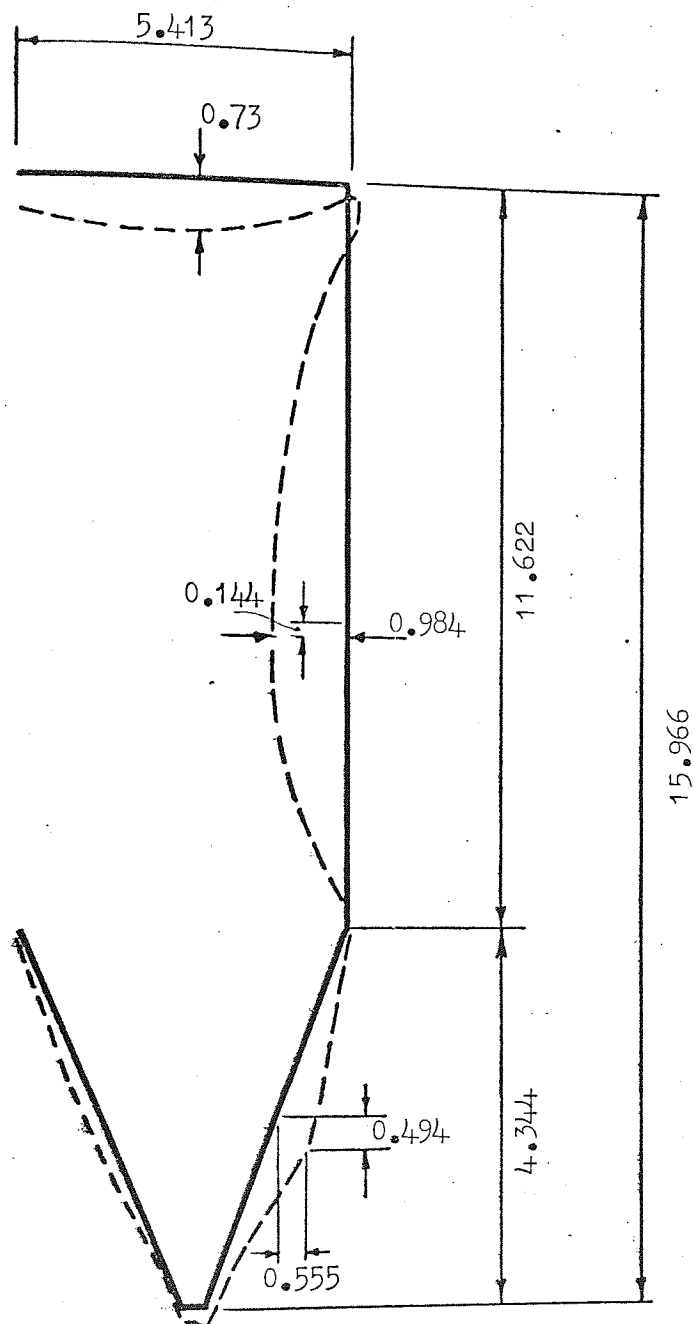
The other location of significant deflection is along the centre of half of the shell. The displacements along this line, given by plane XX in figure 9.1, are shown in figure 9.5. In figure 9.5 the movements caused by the negative internal pressure are shown for the body of the shell, those caused by the residue of precipitated material are shown in the hopper area. Once again the numerical values indicated in the figure illustrate the magnitude of the deflections. The plates in the wall area are 0.9 mm thick and those in the hopper area are 0.6 mm thick. In each case the maximum deflection is of the same order as the plate thickness.

Mention was made of the member forces and plate stresses. One check on the overall equilibrium of the structure is the fact that the axial forces in the four columns should balance the applied vertical loading. In the present analysis this was found to be the case. Examination of the plate stresses indicated that the discontinuous and erratic behaviour experienced by Craig was not present.

The results, therefore, indicate that the program was satisfactorily analysing the shell whilst exhibiting favourable characteristics in respect of computer time and storage requirements.

#### (9.5) Analysis of the road bridge

The bridge was composed of four concrete box beams which supported both carriageways. The structure was symmetrical about its longitudinal centreline and consequently it was only necessary to analyse one side. A typical cross section through one carriageway is given in figure 9.6 where some representative dimensions are also indicated. Further details of the



DEFLECTION IN mm.  
CASING DIMENSIONS IN m.

—— ORIGINAL SHAPE  
- - - - DEFLECTED FORM

VIEW SHOWING THE DEFLECTION ALONG THE CENTRE OF HALF THE SHELL  
GIVEN BY PLANE XX IN FIGURE 9.1

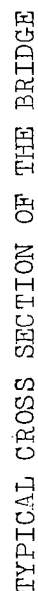
FIGURE 9.5

bridge are given in figure 9.7, where it can be seen that the two sets of columns which support each carriageway are not symmetrically placed. Furthermore the two cross sections illustrate that the depth of the bridge progressively reduces on each side of the columns. The support conditions imposed were such that the ends of the deck were on rollers and the columns were pinned at their bases.

The object of the analysis was to determine the deflections and stresses in the structure due to an imposed load. No comparison to an absolute answer could be made. The results, however, were compared with the results of two other computational analysis programs, one called Strudl which idealises the structure to a space frame and the other by Craig which incorporates plate elements as well as member elements.

In the present analysis the bridge was simulated by rectangular plates, triangular plates and prismatic members in exactly the same way as Craig. The subdivision for part of the bridge is shown in figure 9.8. The total numbers of each of the elements involved were 512 rectangular plates, 58 triangular plates and 86 prismatic members. Rectangular plates were used to represent the box beams which were taken to be one plate in depth. The sides of these beams were, on elevation, trapezoidal but were approximated to a rectangular shape. This approximation is done in the present program by averaging the lengths of opposite sides of each plate. Member elements were used to represent the two sides of the bridge where only little stress was involved. The appropriate offsets of a member from the position of the joint to which it was attached were calculated and these compensated for the thickness of the element.

The box beams were to be of solid construction at either end and under the supports. This was so that they could carry the high stresses which were expected at these positions. Such areas were represented by an assembly of plates, extensive use being made of triangular elements. The plates were positioned vertically and at angles through the thickness of a



- 229 -

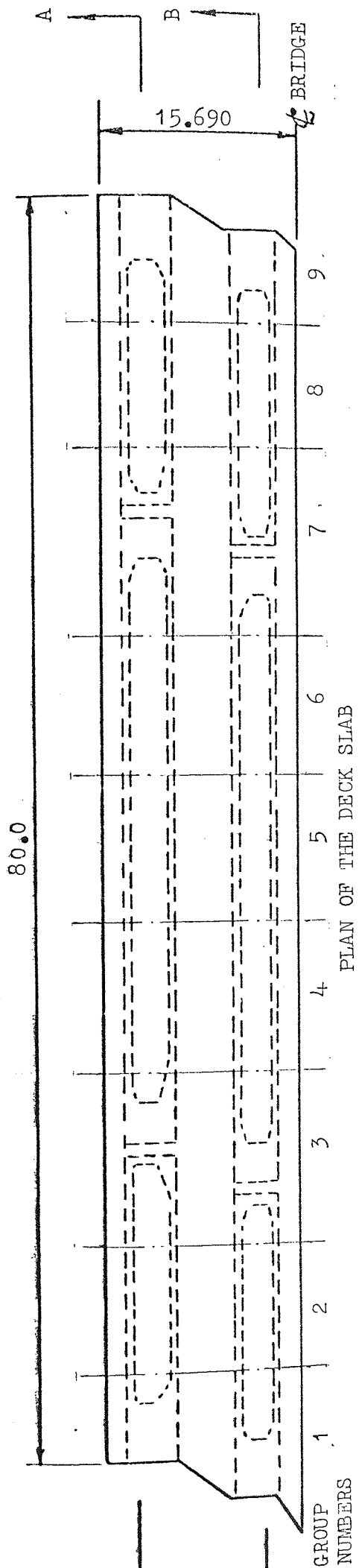
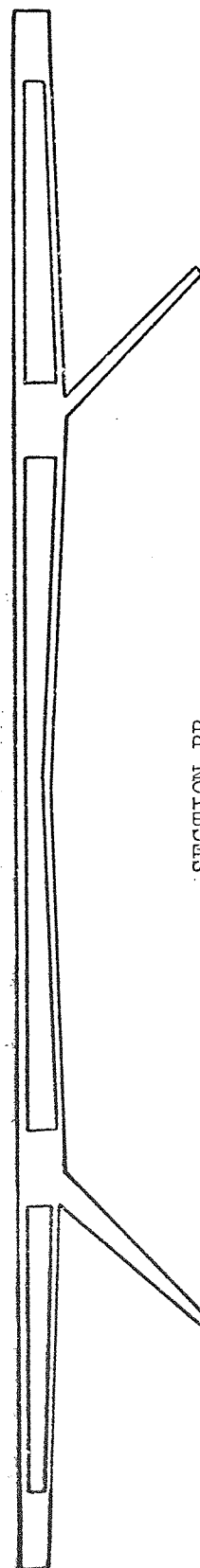
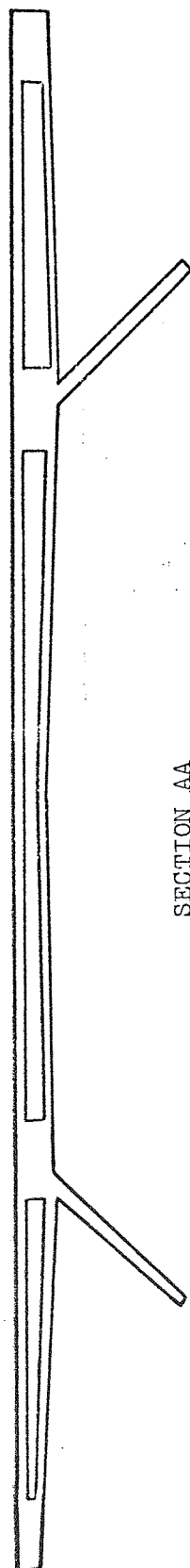
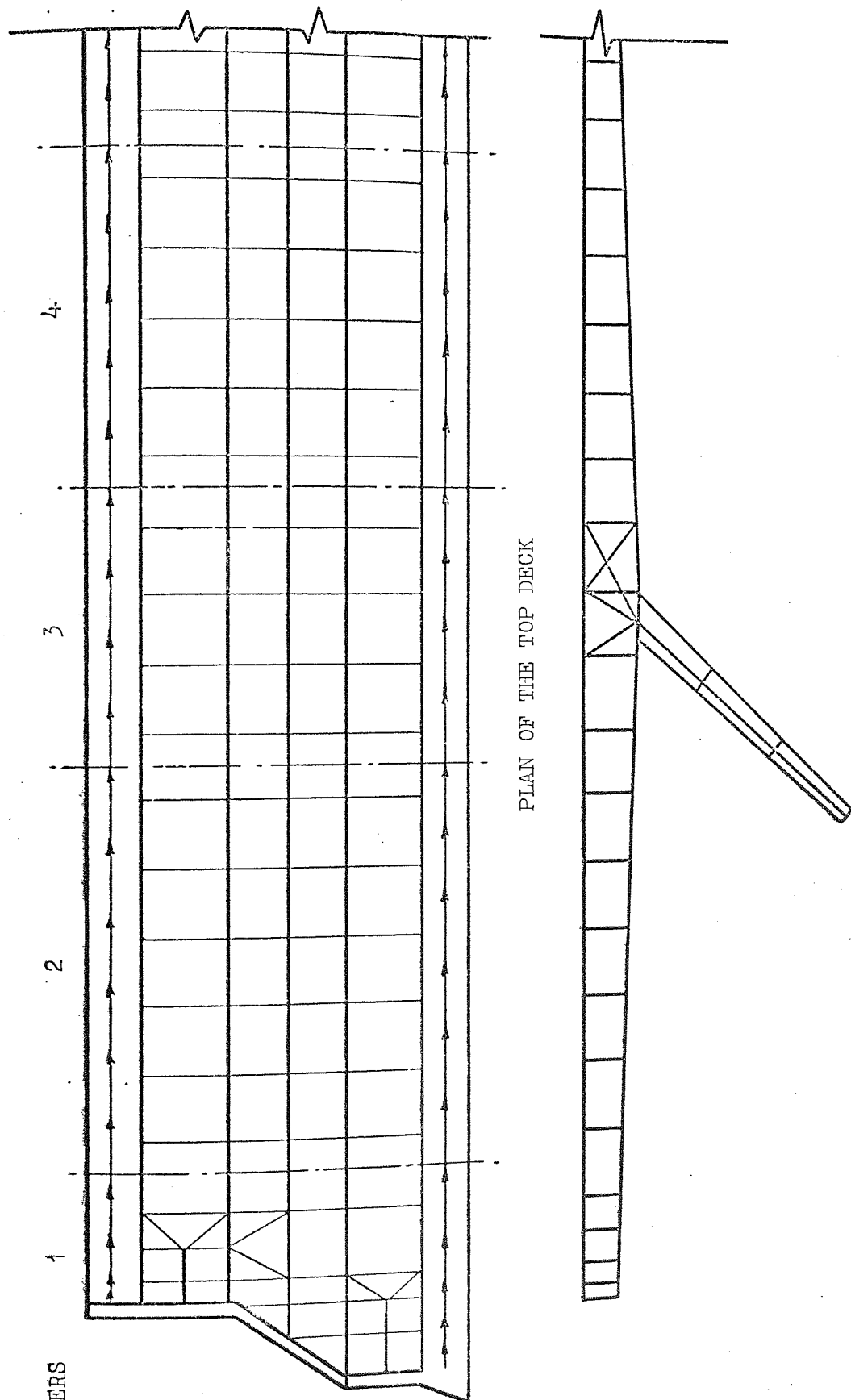


FIGURE 9.7



DIMENSIONS IN METRES

DETAILS OF ROAD BRIDGE



PLAN OF THE TOP DECK

SIDE VIEW OF A TYPICAL BOX BEAM

FINITE ELEMENT REPRESENTATION OF HALF THE BRIDGE

FIGURE 9.8



box and are shown in figure 9.8. The assembly of the plates in this manner catered for the torsional and in plane action of the block. The thicknesses of the plates were arranged so that the total volume of concrete was filled. The column supports were each made up of three rectangular plates.

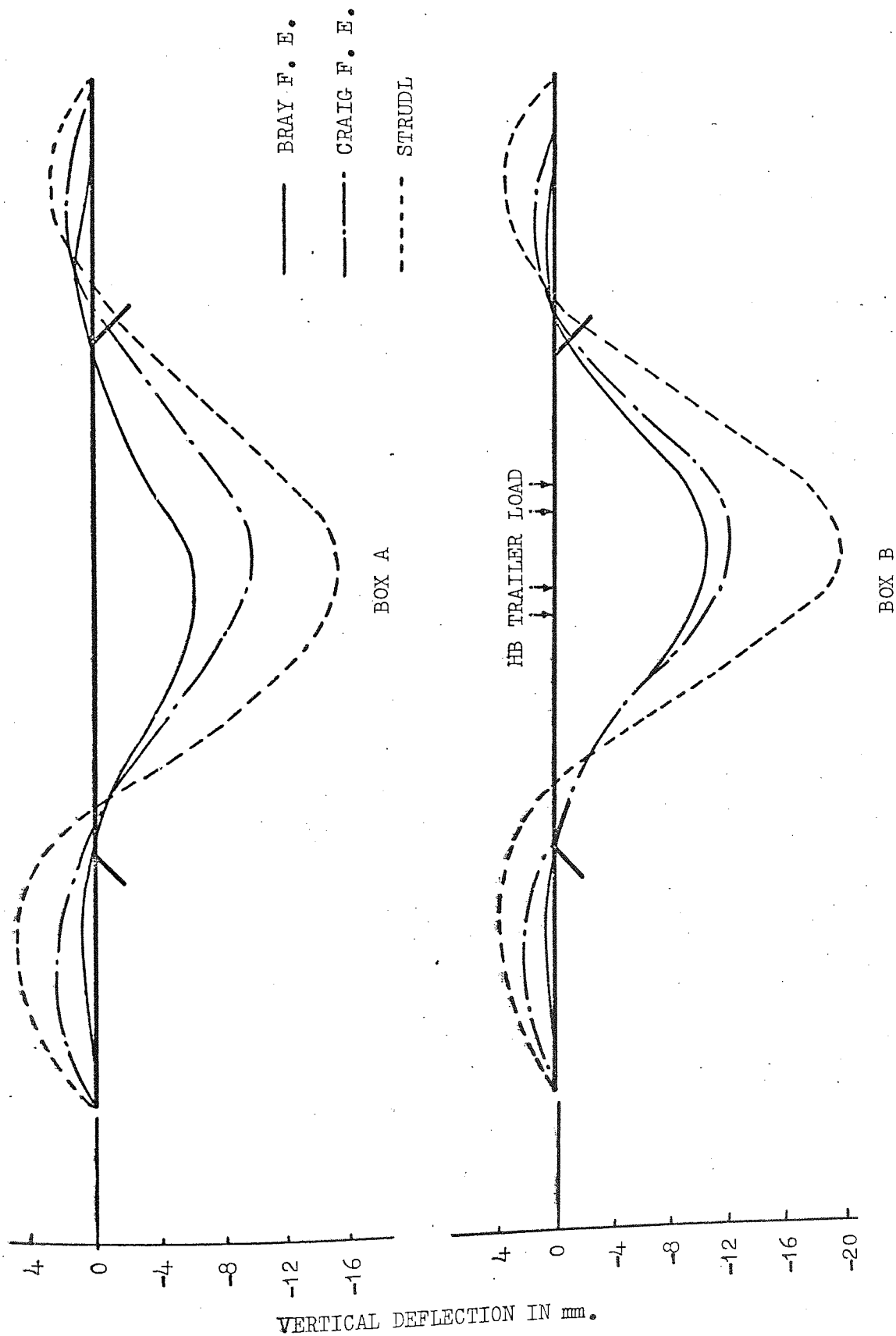
The subdivision used, although apparently rather coarse, especially around the box beams, resulted in 2599 degrees of freedom. Any further refinement of the mesh would have greatly increased this value.

The joints in the structure were divided into 9 groups. Craig found it necessary to use 43 joint groups; this was because the number of joints per group had to be kept low so that there would be no overflow of the core store.

#### (9.6) Results of the bridge analysis

Direct comparisons may be made between the current analysis and that carried out by Craig. Both of these analyses idealised the problem into the same mesh comprising identical finite elements. The Strudl space frame program, however, also used to analyse the structure, represented the two box beams as tapering members. The centre portion of the decking and the four supports were also considered to be members. Finally cross members joining the box beams were used to simulate the torsional stiffness of the assembly.

The loads acting on the bridge were applied to box B at the longitudinal positions indicated in figure 9.9. The vertical deflections of each box along its centre line, when subjected to this loading, is given in figure 9.9. Here it can be seen that in the case of each of the box beams the Strudl results indicate significantly more deflection than that suggested by the finite element solutions. For instance the maximum vertical deflections of the centre span of box B for each analysis are as follows: Strudl 20.0 mm, Craig 12.4 mm, Bray 10.6 mm. These figures indicate that Bray's maximum deflection is only 53% of that given by Strudl and that there is a 15% difference between the two finite element solutions.



VERTICAL DEFLECTIONS ALONG THE CENTRE LINES OF EACH OF THE TWO BOX BEAMS

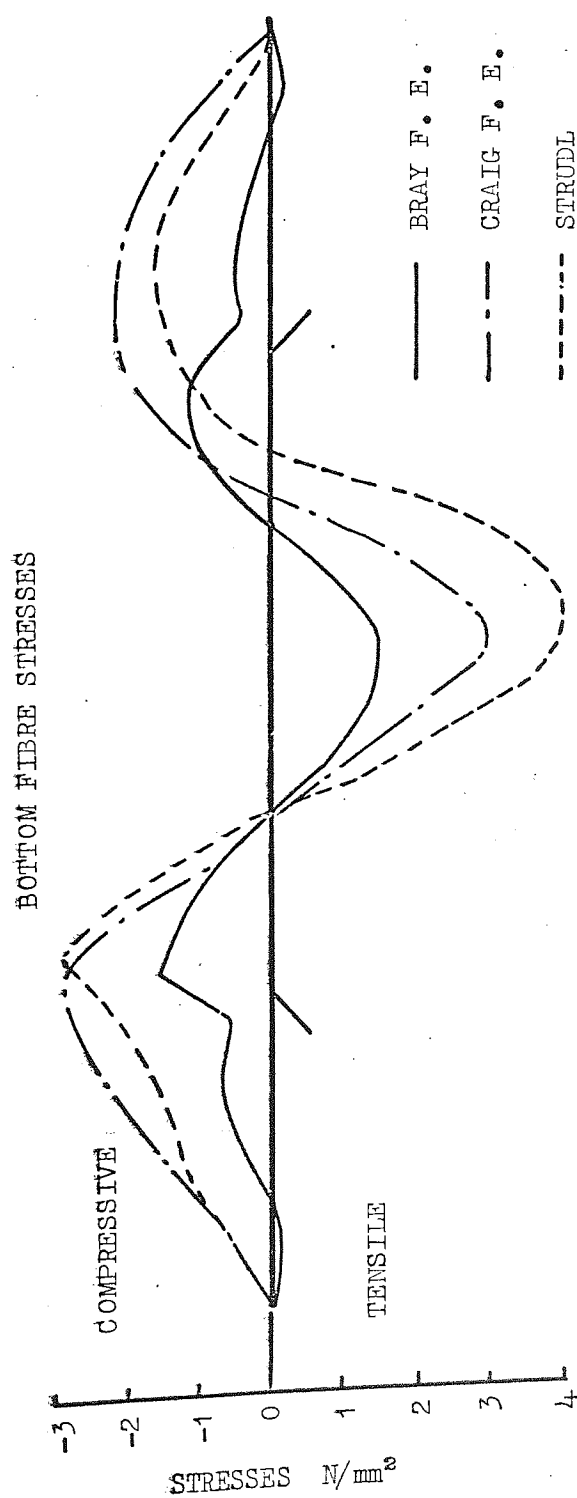
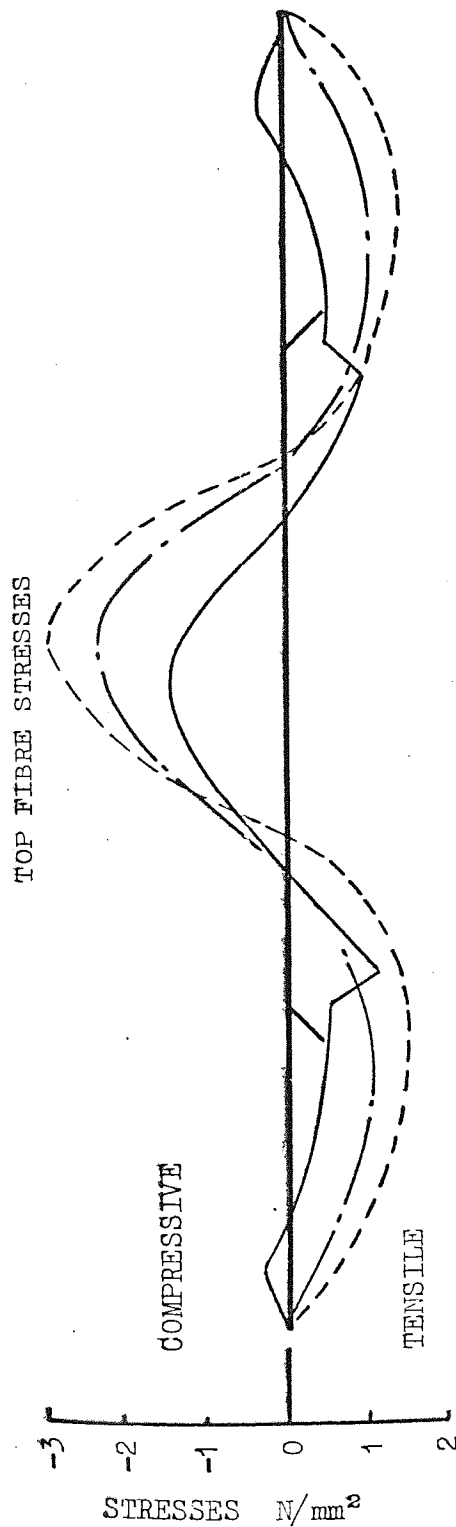
FIGURE 9.9

Inspection of the deflection of the side spans, once again for box B, shows that the maximum deflection in each case was: Strudl 5.0 mm, Craig 2.4 mm, Bray 1.0 mm. In this case Bray's maximum deflection was 20% of Strudl's and there was a 58% difference between the two finite element solutions.

A space frame idealisation, as used by Strudl, would be expected to tend to underestimate the overall stiffness of the structure. The deflections from such an analysis will therefore be larger than those predicted by a more realistic idealisation such as the finite element technique. Some of the numerical differences between the results obtained by Craig and by the present analysis could be attributable to the use of different types of matrix techniques. Craig used a sparse matrix storage method and carried out matrix multiplication to construct  $\underline{K}$  from  $\underline{A}' \underline{k} \underline{A}$ . The present method constructed  $\underline{K}$  directly and made use of the symmetric nature of the overall stiffness matrix.

Graphs of the top and bottom longitudinal stresses in both boxes for each of the analyses are given in figures 9.10 and 9.11. The maximum stresses in both the top and bottom fibres of box B, the loaded box, have been abstracted and are given in figure 9.12. The maximum difference between the two finite element methods is 52% and the minimum is 7%. As was the case for the deflections the results produced by Strudl indicate that the structure is less stiff than predicted by both of the finite element solutions. The maximum difference between Bray's analysis and that of Strudl is 58%, the minimum is 33%. Direct comparisons between the space frame and the finite element idealisation are misleading because of the different assumptions made in each case. The trends in all the analyses are, however, similar.

The most interesting divergence between the two finite element solutions is the difference in the predicted stresses in the region of the supports. These differences are most apparent above the columns, although

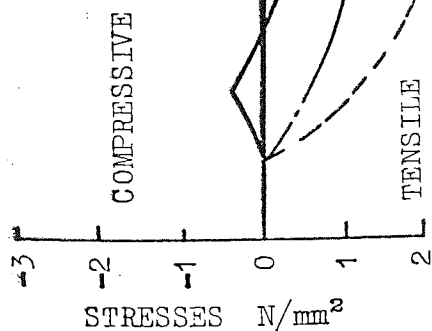


BOX A

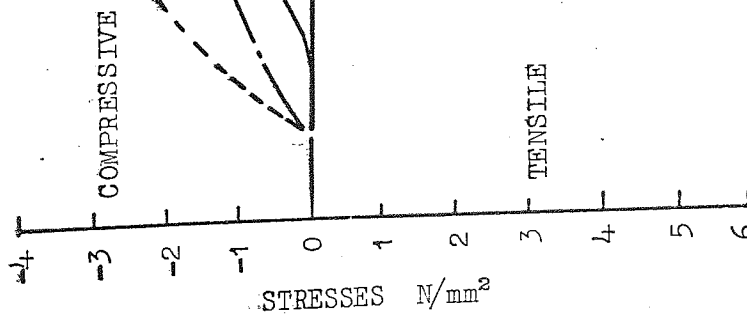
LONGITUDINAL STRESSES AT THE CENTRES OF THE TOP AND BOTTOM PLATES

FIGURE 9.10

TOP FIBRE STRESSES



BOTTOM FIBRE STRESSES



— BRAY F. E.  
 - · - CRAIG F. E.  
 --- STRUDL

BOX B

LONGITUDINAL STRESSES AT THE CENTRES OF THE TOP AND BOTTOM PLATES

FIGURE 9.11

	TOP FIBRE STRESSES		BOTTOM FIBRE STRESSES	
	MID SPAN	END SPAN	MID SPAN	END SPAN
BRAY	2.6 N/mm <sup>2</sup>	1.4 N/mm <sup>2</sup>	2.5 N/mm <sup>2</sup>	1.9 N/mm <sup>2</sup>
CRAIG	2.8	2.2	3.8	4.0
STRUDL	3.9	2.6	5.9	3.4

MAXIMUM VALUES OF THE LONGITUDINAL TOP AND BOTTOM FIBRE STRESSES AT THE  
MID AND END SPANS FOR BOX B

FIGURE 9.12

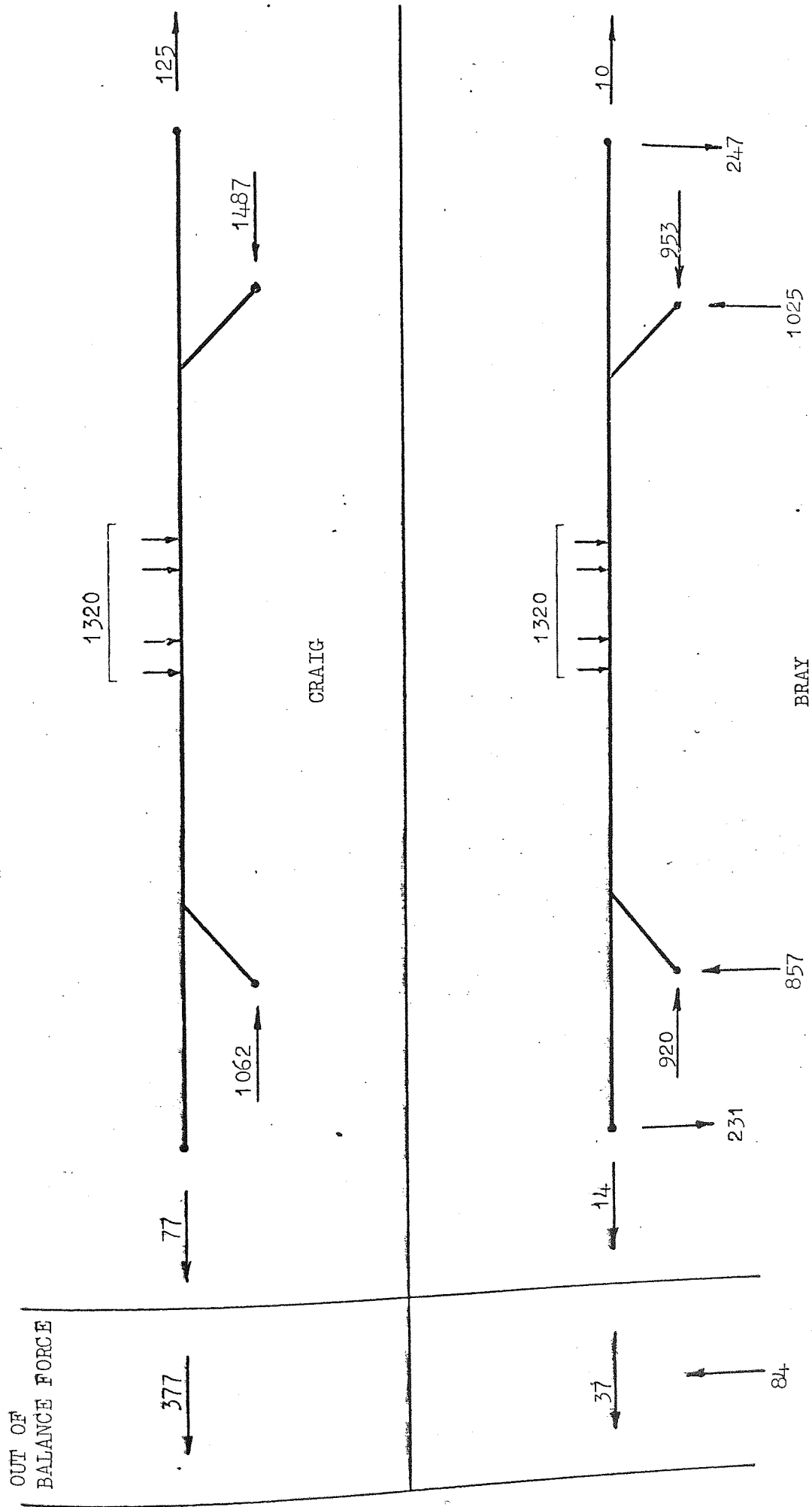


in the regions at the bridge ends, there is a reversal effect not previously indicated. It is noticed that these effects occur in the areas of solid concrete, which have been specifically incorporated to distribute the high stresses, where there is a necessary change in the finite element mesh. The existence of these regions above the columns leads to the inference that the smooth graphs presented by Strudl and Craig's analysis, for the stress in these regions, are less feasible than those by the current analysis. This argument also applies to the solid regions at each end of the bridge. Consequently, a smooth rate of change of stress from each end towards a support would not be expected. In the case of the present analysis it is apparent from the graphs given in figures 9.10 and 9.11 that the stresses are being affected by the existence of the rigid portions.

Possible sources of error in the calculation of the stresses by a finite element technique are the inelastic properties exhibited by concrete as well as the application of a method derived on the bases of a thin plate theory. Some of the plates had thicknesses almost equal to their side lengths, this was particularly so in the solid regions. Similar errors are also inherent in the space frame idealisation which was the other method used.

One problem which Craig had experienced during the analysis of the precipitator shell and also during the analysis of the bridge was a violation of the overall equilibrium equations. In an earlier section of this chapter it was shown that the current analysis overcame that difficulty in respect of the electrical precipitator shell. It is fair to point out, however, that mistakes in Craig's work may have been due purely to data errors. An investigation was made into both the horizontal and vertical equilibrium of the bridge. Figure 9.13 shows the forces calculated to be acting at the supports. As the ends of the bridge were carried on rollers the horizontal reactions at these points should be zero, furthermore since no horizontal load is applied the net horizontal force should also be zero.

FORCES IN KN.



VERTICAL AND HORIZONTAL REACTIONS AT THE BRIDGE SUPPORTS

FIGURE 9.13

The figure indicates that the present analysis was 37 kN out of balance whereas Craig's out of balance force was 377 kN which represents 29% of the applied vertical load. In the case of the vertical reactions the current analysis showed a 6.4% out of balance force. Craig's vertical reactions were not available for comparison. Extensive investigation indicates that the out of balance forces in the case of the present analysis can only be the result of the numerical solution technique adopted.

Finally a comparison was made between the current analysis and Craig's analysis in respect of computer time and core store requirements. The size of the problem prohibited Craig carrying out all of the required calculations in one run. In fact three runs were required - the first calculated the deflections, the second the forces in the members and plates and the third the stresses in the plates. Craig detailed<sup>(5)</sup> many modifications necessary to economise the storage and time requirements of the three programs so that the problem could be run on the Atlas computer. Even with these modifications the values indicated in figure 9.14 show the core storage requirement was at the limit of the Atlas machines capability of 115K. A total central processing unit (cpu) time of 83 minutes was required to run the three jobs. The cpu time for the current analysis was 12 minutes to complete all three major stages of the calculation and this represented a saving of 83% over the previous analysis. A direct comparison between core storage requirements is not possible because of the piecemeal approach Craig was forced to adopt. Furthermore Craig used 43 joint groups whereas in the current analysis only 9 were employed. In spite of this a core store saving of 35% over Craig's maximum requirements is indicated. This figure could have been significantly improved by the use of more joint groups in the current analysis.

The analysis of the electrical precipitator shell and the skew concrete bridge indicate that the results appear to be satisfactory. In addition there are significant savings of both the core store and the cpu

	MINUTES OF CPU TIME		WORDS OF ATLAS CORE STORE	
	CRAIG	BRAY	CRAIG	BRAY
CALCULATION OF JOINT DEFLECTIONS	70	] 12	102K	] 73K
CALCULATION OF ELEMENT STRESSES	9		113K	
CALCULATION OF ELEMENT FORCES	4		59K	

283

CPU TIME AND CORE STORAGE REQUIREMENTS OF THE PROGRAMS USED TO ANALYSE THE  
ROAD BRIDGE

FIGURE 9.14

time for the current system when it is compared with a similar program.

## CHAPTER 10

### GENERAL CONCLUSIONS

This thesis has been concerned with the attainment of two objectives, namely: The writing and development of a set of computer algorithms capable of analysing complex three dimensional structures; and the theoretical derivation of the in and out of plane stiffness matrices for a curved plate element with an investigation into the characteristics of such an element.

When considering the programming section there are two goals which should have been achieved. Firstly does the program have the capability envisaged? Secondly have the objectives relating to the flexibility and versatility of the program, listed in Chapter 1, been attained? The capability of the program has been well tested by the analysis of several different structures. Such structures ranged from the relatively small curved bridge decks up to an electrical precipitator shell and a bridge both of which are detailed in Chapter 9. In that Chapter, comparison was made between the results of the analysis of these large structures as well as computer time and storage requirements for both the proposed program and another comparable system. This showed that the system proposed in this thesis gave favourable results. The computer storage and time requirements of this system indicated that significant savings were being achieved.

With regard to the flexibility and versatility of the program, comment will now be made on the aims set out in Chapter 1. The requirement that the system should be open ended allowing extensions to be made simply, without detailed knowledge of the overall system, has been fully met. Such extensions may be made in any way as long as the result is in the form of additions to the overall stiffness matrix of the structure. This permits the use of isoparametric as well as conven-



tional finite elements. The only interaction between any element package and the rest of the program is the addition of terms to the overall stiffness matrix. When writing a new element package only two facts require to be comprehended. These are the method of storage adopted for the stiffness matrix, which is given in Chapter 1, and the ability to locate the information relating to the joints in the structure, the manner in which this may be done is explained in Chapter 2.

The efficiency of the system in respect of computer storage and time has been found to be very high and comment has been made about this in Chapter 9. The use of subroutines to build up a program means that the system is very flexible. All the subroutines may be stored in compiled form on a magnetic tape and the co-ordinating subroutine for a given analysis will only use those which are relevant to that analysis.

Data preparation probably accounts for the largest part of the cost of any finite element analysis. Any savings here are liable to have just as profound an impact on the economy and range of solutions practicable as corresponding developments in an increased efficiency. The amount of data required varies depending upon the element. For conventional finite elements it is difficult to make a significant amount of data implicit. This is especially true of a general program although a program specifically written to analyse regular structures, such as multi-storey frames, may take advantage of a regular joint pattern and the use of an identical member section throughout. In the case of isoparametric elements it is a straightforward operation to have the data relating to such facts as the co-ordinates of the side nodes calculated within the program. The data for the proposed system has been reduced to a minimum. In spite of this the amount of preparation and checking required when analysing a structure such as the bridge, detailed in Chapter 9, is still significant.

Generally the program is working satisfactorily and the aims have been achieved, consequently there is much scope for the addition of new finite elements to the system.

The analysis of the large structures did bring up some points worthy of comment. The Cholesky triangular factorisation technique, used for the solution of the equations forming the stiffness matrix, worked satisfactorily for the smaller structures analysed with up to around 700 degrees of freedom. During the analysis of the electrical precipitator shell (1029 degrees of freedom) the technique failed to solve the equations. This sort of failure usually indicates a data error which has caused the incorrect construction of the stiffness matrix. An alternative direct solution technique<sup>(34)</sup>, a form of Gaussian elimination, suitable for use with a set of equations stored by a variable band width technique was employed. The results of the analysis of the electrical precipitator shell, using this other solution technique, are those presented in Chapter 9 and appear to be satisfactory. This seems to indicate that the Cholesky method is less suitable for the solution of a large number of equations relating to the sort of structure under consideration. The same anomaly occurred during the analysis of the bridge (2599 degrees of freedom).

Since the efficiency of the Cholesky method is far superior, in respect of both computer store and time, to other techniques it is more attractive for use within the system than these alternative techniques. A useful exercise would therefore be to ascertain the practicability of Cholesky's method when applied to large numbers of equations relating to structural problems.

The size of the inversion units associated with the solution techniques was retained at a maximum of 512 terms. This meant that use could be made of the 'rapid' block transfer facilities available on the Atlas machine. Another advantage was that since only two inversion units were

required to carry out the solution of any number of equations then only 1024 variables would be required in the core store. As a result of the analysis of these large structures it is suggested that the size of these units is increased. The effect of this would be to reduce the number of units (the bridge required 353). The consequential reduction in the number of block transfers would significantly reduce the execution time required by the program. One way of effecting this modification would be to increase the size of an inversion unit up to one half the maximum number of locations required to store the largest stiffness matrix of any joint group. The array in which the stiffness matrix was constructed could then be used during the solution process thus obviating the necessity for an increase in the core store requirements.

One apparent limitation may seem to be the restriction imposed on the numbering of nodes. This technique has been employed to fix the orientation of a set of sub-blocks. In practice this is not a problem, it is, however, a simple enough matter to allow two joint numbering techniques as adopted in the case of the curved plate package, or in fact a random joint numbering method. Random numbering techniques are desirable for some elements such as block elements when used to represent a three dimensional continuum.

A case for the development of a finite element capable of simulating curved structures such as elevated roadways has been made in the introduction. There it was explained that the increased flexibility of the longer outer edge gave rise to stress and deflection characteristics which were quite different from those obtained using elements with straight boundaries. An explicit derivation of both the in and out of plane stiffness matrices for such a curved plate element was carried out and is detailed in Chapter 5 of this thesis. It is recommended that any future work, such as the development of a curved element with thickness variation, should be carried out using a numerical integration technique.

This would be especially advantageous at the implementation stage where a good deal of complex programming could be avoided.

Preliminary testing of the element demonstrated that it exhibited predictable characteristics. One of these being the fact that as the radius was increased to a large value relative to the other plate dimensions the stiffness matrix became identical to that of a geometrically equivalent rectangular plate. Analysis of a curved plate structure with a variety of meshes indicated that the deflection of the joint was seen to converge to a constant value. The existence of a constant strain criterion leads to the assumption that convergence is to the true deflection of the structure.

Three comparisons were made, against an independent experimental test, a theoretical series solution and a finite element solution. Jenkins and Siddall<sup>(32)</sup> had used a finite element, non-conforming in translation, to analyse the experimental results given by Coull and Das<sup>(7)</sup>. The results Jenkins and Siddall obtained showed good agreement with the experimental and theoretical results presented by Coull and Das, although in one case they predicted deflections greater than those recorded, a situation not usual for a finite element solution. The plates tested by Coull and Das were supported along the entire length of each of their radial edges. This represented a support condition which was not coincidental with the author's global axes, consequently an exact simulation was not possible. Jenkins and Siddall do not state the restraints they imposed on their mathematical model. In the author's analysis two orthogonal rotations out of the plane of the plate were permitted. This leads to the analysis of a slightly different structure than the one considered by Jenkins, Siddall, Coull and Das. One way of overcoming this difficulty is to have prismatic member elements along the support lines. Such members could be made to be resistant to rotation about circumferential axis but to offer little resistance to rotation about radial axes. The best solution, however, would be to incorporate facilities for

the suppression of non-global degrees of freedom. In spite of this drawback the author's results showed good agreement with both the theoretical solutions as well as Coull and Das' experimental results.

As a final examination of the element experimental tests were carried out by the author on two curved plates of different radii. Comparisons were made between theoretical and experimental deflections and stresses. One series of tests had fixed ends whilst in the other the plates were simply supported at their four corners, both of these conditions can be simulated by the programme. The experimental and theoretical results indicated that a good agreement was being achieved.

One aspect in which this work could be extended is the formulation of the element stiffness matrices for a curved segment. This would permit the use of a combination of the two curved elements to simulate structures comprising circular plates, such as tank bases. Extensions to the program system should take the form of additional element packages such as conforming triangular plates, shell elements as well as isoparametric solid elements. These additions would greatly increase the scope of solutions which could be carried out by the system. Further development could also take the form of extensions so that the system could deal with non-linear problems. In such problems, however, the reliability of the Cholesky method becomes increasingly questionable. This is because of the progressive loss of stiffness by the structure consequently alternative methods of equation solving would have to be investigated and included in the system.

## REFERENCES

1. TURNER, M. J., R. W. CLOUGH, H. C. MARTIN, and L. J. TOPP, 1956.  
"Stiffness and deflection analysis of complex structures".  
J. Aero. Soc. Vol. 23, pp. 805 - 823.
2. JENNINGS, A., and K. I. MAJID, 1966. "The computer analysis of  
space frames using sparse matrix techniques". Int. Conf. on  
space structures. University of Surrey.
3. JENNINGS, A., 1968. "A sparse matrix storage scheme for the computer  
analysis of structures". Int. J. of Comp. Math. Vol. 2, pp. 1 - 21.
4. MAJID, K. I., and M. WILLIAMSON, 1967. "Linear analysis of complete  
structures by computers". Proc. Instn. Civ. Engrs. Vol. 38, (Oct.).  
pp. 247 - 266.
5. CRAIG, J. S., 1971. "Analysis of linear and non linear civil engineering  
problems using finite element techniques". Ph.D. Thesis. The  
University of Aston in Birmingham.
6. ZIENKIEWICZ, O. C., and Y. K. CHEUNG, 1967. "The finite element method  
in structural and continuum mechanics". McGraw-Hill.
7. COULL, A., and P.C. DAS, 1967. "Analysis of curved bridge decks".  
Proc. Instn. Civ. Engrs. Vol. 37, (May), pp. 75 - 85.
8. JENNINGS, A., and A. D. TUFF, 1970. "A direct method for the solution  
of large sparse symmetric simultaneous equations". I.M.A. Conf.  
on large sparse sets of linear equations. Oxford.
9. LIVESLEY, R. K., 1954. "Analysis of rigid frames by an electronic  
digital computer". Engineering. Vol. 176. p. 230 and 277.
10. LIVESLEY, R. K., 1964. "Matrix methods of structural analysis".  
Pergamon press.
11. ARGYRIS, J. H., 1960. "Energy theorems and structural analysis".  
Butterworth scientific publications.
12. CLOUGH, R. W., 1960. "The finite element method in plane stress  
analysis". Proc. 2nd. Conf. on electronic computation. A.S.C.E.



13. MELOSH, R. J., 1961. "A stiffness matrix for the analysis of thin plates in bending". J. Aero. Soc. Vol. 28. pp. 34 - 42.
14. GALLAGHER, R. H., 1963. "Techniques for the derivation of element stiffness matrices". J.A.I.A.A. Vol. 1.
15. FRAEIJIS DE VEUBEKE, B. M., 1964. "Upper and lower bounds in matrix structural analysis". Matrix methods of structural analysis. Agardograph, 72.
16. MELOSH, R. J., 1963. "Basis for derivation for the direct stiffness method". J.A.I.A.A. Vol. 1.
17. IRONS, B. M. R., and K. J. DRAPER, 1965. "Inadequacy of nodal connections in a stiffness solution for plate bending". J.A.I.A.A. Vol. 3.
18. FRAEIJIS DE VEUBEKE, B. M., 1965. "Displacement and equilibrium models in the finite element method". Stress analysis. Wiley.
19. ZIENKIEWICZ, O. C., and Y. K. CHEUNG, 1964. "The finite element method for the analysis of elastic isotropic and orthotropic slabs". Proc. Instn. Civ. Engrs. Vol. 26.28.
20. IRONS, B. M. R., 1966. "Engineering applications of numerical integration in stiffness methods". J.A.I.A.A. Vol. 4.
21. FAIG, I. C., 1961. "Structural analysis by the displacement method". English electric aviation rept. (S017) unpublished.
22. IRONS, B. M. R., 1966. "Numerical integration applied to the finite element method". Conf. on the use of computer in structural engineering. Newcastle University.
23. IRONS, B. M. R., and O. C. ZIENKIEWICZ, 1968. "The isoparametric finite element system. - A new concept in finite element analysis". Conf. on recent advances in stress analysis. Joint. Brit. Comm. Stress Analysis.

24. MARTIN, R. S., and J. H. WILKINSON, 1965. "Symmetric decomposition of positive definite band matrices". Num. Math., Bd. 7 pp. 355 - 361.
25. FORSYTHE, G. E., and C. B. MOLER, 1967. "Computer solutions of linear algebraic systems". Prentice - Hall.
26. TUFF, A. D., 1970. Private communication.
27. PRZEMIENIECKI, J. S., 1968. "Theory of matrix structural analysis". McGraw - Hill.
28. THOMAS, G. B., 1966. "Calculus and analytic geometry". Addison - Wesley. p. 686.
29. TIMOSHENKO, S., and S. WOINOWSKY - DRIEGER, 1959. "Theory of plates and shells". McGraw - Hill.
30. TIMOSHENKO, S., and J. H. GOODIER, 1951. "Theory of elasticity". McGraw - Hill.
31. JENKINS, W. M., 1969. "Matrix and digital computer methods in structural analysis". McGraw - Hill.
32. JENKINS, W. M., and J. M. SIDDALL, 1967. Contribution to the discussion of reference 7, Proc. Instn. Civ. Engrs., Vol. 33. p. 778.
33. SIDDALL, J. M., 1967. "The Analysis of continuous skew bridge decks by the stiffness method". M.Sc. Thesis. The University of Bradford. Ch. 7, pp. 41 - 46.
34. CROXTON, P. C. L., 1973. "Analysis of complete structures consisting of bare frames and plate components". Ph.D. Thesis. The University of Aston in Birmingham.